DISSERTATION

METFORMIN: A TOOL TO BETTER UNDERSTAND T CELL MEDIATED PROTECTION

AGAINST MYCOBACTERIUM TUBERCULOSIS

Submitted by

Jessica D. Haugen Frenkel

Department of Microbiology, Immunology, and Pathology

In partial fulfillment of the requirements

For the Degree of Doctor of Philosophy

Colorado State University

Fort Collins, Colorado

Fall 2020

Doctoral Committee:

    Advisor: Randall J. Basaraba

    Andrés Obregón-Henao
    Brendan K. Podell
    Adam Chicco
    Anne Avery

ABSTRACT

METFORMIN: A TOOL TO BETTER UNDERSTAND T CELL MEDIATED PROTECTION

AGAINST MYCOBACTERIUM TUBERCULOSIS

Despite over one hundred years of research, Tuberculosis (TB) disease, caused by the bacteria *Mycobacterium tuberculosis* (Mtb), continues to be the leading cause of death by an infectious disease worldwide. This is attributed to socioeconomic factors, slow drug development pipelines and discovery, poor treatment compliance, increasing drug resistance, and the lack of an effective vaccine— predominantly due to our incomplete understanding of an effective immune response against Mtb infection. Novel TB treatment regimens and an advanced understanding of the underlying factors that contribute to TB pathogenesis and host resistance are not only warranted, but essential for the eradication of this disease.

Host-directed therapies, or therapies which target host mediated responses rather than the infectious agent itself, are becoming a novel approach to both treat disease and gain insights into the pathogenesis of many chronic illnesses. In our studies, we sought to evaluate the use of the anti-diabetic drug metformin for these purposes, which was based off its high safety profile, existing approval by the food and drug administration (FDA), and its demonstrated reduction of clinical manifestations associated with other chronic inflammatory illnesses. Moreover, its multi-targeted effects on both systemic and cellular metabolism make it a unique tool to study the role that metabolism plays in disease pathogenesis. In this dissertation, we evaluated the influence of metformin treatment on TB disease outcome and characterized the phenotypic and functional implications of metformin on the T cell response to infection.

Aim 1. Evaluate metformin as a host-directed therapy against *Mycobacterium tuberculosis* infection. In our first, aim we evaluated whether metformin, by normalizing systemic glucose metabolism, could improve clinical TB disease outcome of Mtb infected guinea

pigs. Interest in this study arose from the observation that in both human and animal models, increased systemic blood glucose concentrations highly correspond with TB disease progression and severity. Hyperglycemia, or high blood glucose, and insulin resistance are known risk factors for TB and occur as a consequence of Mtb infection. Patients with underlying metabolic disorders that take metformin display slower disease progression and improved clinical disease outcome, suggesting a role for systemic metabolism in TB disease pathogenesis. Immune cell metabolism, which directly controls cellular fate and function, has also recently been implicated to have profound influences on the outcome of various diseases and is likely to be affected by Mtb infection and metformin treatment alike. Therefore, in addition to evaluating the systemic metabolic implications of metformin treatment on TB disease pathogenesis, our studies also aimed to understand immune cell metabolism in the context of disease and as a mechanism of metformin mediated protection.

In this study, guinea pigs were treated with metformin two weeks prior to or concurrent with aerosol Mtb aerosol infection, which continued throughout the course of infection. During chronic stages of disease, Mtb infected animals displayed significantly reduced Mtb colony forming units and lesion burden in the lungs compared to untreated animals. Improved disease outcome was associated with restored insulin sensitivity, but glucose tolerance was unchanged between groups, suggesting an alternative mechanism of host-mediated protection. Metabolic characterization of PBMC derived T cells by extracellular flux analysis demonstrated that in response to Mtb infection, utilization of the glucose processing pathways, glycolysis and oxidative phosphorylation were both significantly upregulated compared to uninfected animals; treatment with metformin, however, maintained homeostatic metabolic rates. Significant differences in mitochondrial membrane potential and superoxide production, both metabolic indicators of altered cellular function, were also observed between CD4$^+$ T cells from metformin treated and untreated animals. Furthermore,

metformin treatment corresponded to decreased levels of pro-inflammatory cytokines in the lungs.

These data demonstrate that metformin is an effective host-directed therapy against Mtb infection when initiated prior to infection, but this was not due to the maintenance of systemic metabolism. Instead, we provide evidence that metformin elicits protection by directly modulating immune cell metabolism and thus, altering the immune response to Mtb infection. The early treatment timeline required for metformin-induced protection and differences in T cell metabolism further suggest that T cells are directly targeted by metformin and likely play a critical role in enhanced protection against disease.

Aim 2. Characterize T cell differentiation and metabolism in response to metformin treatment. The results obtained from aim 1 align with findings from the literature, which show that T cells with decreased metabolic flux and mitochondrial membrane potential correspond to a memory T cell phenotype. We, therefore, hypothesized that by regulating T cell metabolism, metformin enhances the generation of memory T cells that display decreased pro-inflammatory potential and tissue destruction and promote increased protection against chronic Mtb infection.

To test this hypothesis, we characterized the phenotypic, functional, and metabolic profiles of CD4$^+$ T cells that were differentiated using an *in vitro* model of effector like T cell (T_{EL}) generation, in the presence or absence of metformin. Memory like T cells (T_{ML}) were also generated and the metabolic and functional properties of these cells were characterized and used to define a decreased state of T cell differentiation. Using this model, we found that memory T cell formation was not enhanced by metformin, as originally hypothesized; however, dramatic changes in surface marker expression were observed between cells that did or did not receive metformin. Significant increases in the levels of the cellular migration and tissue adhesion markers CD44 and CD69 and decreased IL-2Rα, or CD25, expression were associated with metformin treated compared to untreated CD4$^+$ T cells. Expression of the terminal differentiation marker KLRG1 and transcription factor Blimp-1 were also significantly decreased by metformin

treatment while the memory associated transcription factor BCL-6 was significantly increased—suggesting that although metformin does not increase memory T cell generation, it does dramatically influence T cell phenotypic development by preventing terminal differentiation. Furthermore, mitochondrial membrane potential and the production of multiple pro-inflammatory cytokines were significantly reduced by metformin treatment, which is consistent with data from our *in vivo* studies in aim 1 and further supports the notion that T cells become less differentiated when treated with metformin.

Metabolic characterization showed that metformin significantly reduced mitochondrial function and increased T_{EL} reliance on glycolytic metabolism, which was in parallel with increased glucose uptake and the maintenance of cellular energy demands as measured by ADP: ATP ratios. These results were unique in comparison to memory T cells and less differentiated subsets, which demonstrate very little reliance on glycolysis for energy. Notably, however, spare respiratory capacity (SRC), a hallmark of memory T cell metabolism, was significantly increased in metformin treated T_{EL}s compared to untreated cells. Most importantly, we show that the generation of non-terminally differentiated CD4+ T cells by metformin resulted in significantly improved cell survival and enhanced proliferation and IL-2 production following secondary antigen challenge.

Together, these data indicate that reduced T cell differentiation by metformin results in a long-lived CD4+ T cell subset that has enhanced survival and superior capacity to respond to antigen re-challenge. Whether or not these cells are responsible for increased protection against Mtb infection is the goal of aim 3 in this dissertation.

Aim 3. Determine whether metformin treated CD4+ T cells confer increased protection against Mtb infection, *in vivo*. In aims 1 and 2 we found that metformin altered T cell metabolism both *in vivo* and *in vitro*, and in in aim 2, we demonstrated that this corresponded to the differentiation of non-terminally differentiated effector CD4+ T cells that have an increased capacity to respond to secondary antigen challenge. The goal of aim 3 was to then determine

whether metformin treated non-terminally differentiated T cells displayed enhanced protection against Mtb challenge *in vivo*. Mtb antigen specific-Ag85b TCR Tg (p25) T cells were either maintained in their naïve state or differentiated *in vitro*, as in aim 2, under T_{EL} or T_{ML} conditions, with or without metformin. Differentiated T cells were then transferred into wild type C57Bl/6 mice, which were exposed to Mtb aerosol infection one day following transfer. On days 15 and 30, disease severity was assessed by quantifying lung Mtb colony forming units (CFUs) and lesion burden. No significant differences were observed between groups at either timepoint. Migratory capacity of adoptively transferred T cells was assessed by quantifying the total number of p25 cells in the vasculature versus lung parenchyma, based on previous studies which describe the dysfunctional migration of terminally differentiated T cells from the blood into tissues where they elicit a protective response. Surprisingly, no differences in the proportion of adoptively transferred CD4$^+$ T cells were observed between metformin treated and untreated subsets. Surface marker expression of molecules known to be associated with differentiation, migration, cell survival, and phenotype were also assessed on adoptively transferred CD4$^+$ T cells 30 days following infection. Interestingly, despite major differences at the time of transfer, only subtle variances were found between T_{EL}, T_{ML}, and naïve (T_N) phenotypes. Furthermore, no significant differences were observed between metformin treated and untreated T_{EL} or T_{ML} cells.

Based on the lack of protection conferred by adoptively transferred T cells in this study, we conclude that pre-differentiated T_{EL} or T_{ML} cells transferred prior to infection do not provide immunological protection against early Mtb infection and acute TB disease. Retrospective evaluation of our study design, however, lead us to believe that under different conditions alternative results will be obtained. Future studies will take into consideration the timing of the cell transfer with respect to infection and other design features, including the use of immunodeficient recipient mice, that may have a large impact on the interpretation of these findings.

Conclusions. In this dissertation we have shown that metformin treatment improves the outcome of TB disease and directly modulates T cell differentiation through metabolic rewiring. Although

the outcome of aim 3 in this study did not turn out as expected, our results shed light on the mechanisms by which metformin impacts T cell differentiation in the general context of disease. These data will be useful for both the application of metformin as a treatment for other diseases and in helping understand the underlying pathogenesis of illnesses for which metformin has proven beneficial. Moreover, further investigation into whether metformin treated T cells provide protection against TB disease when administered during different stages of infection may have implications for the design of vaccines and expand our current understanding of immune failure and protection against disease.

ACKNOWLEDGEMENTS

The completion of this degree would not have been possible without the exceptional mentoring as well as encouragement and support that I have received throughout my PhD journey. First, I would like to thank my advisor Dr. Randall Basaraba for giving me the opportunity to complete my training in his laboratory. I am incredibly grateful to have had a mentor with so much enthusiasm for scientific discovery and creativity, and whom not only allowed, but encouraged exploration of my personal interests within the laboratory. I am also thankful for the confidence and encouragement that Randy has instilled in me throughout my training and for always challenging me to leave my comfort zone to facilitate personal growth.

Thank you to past and present members of the Basaraba lab for their friendship and efforts dedicated to the work described in this dissertation. A special thanks goes out to Forrest Ackart and Alexandra Todd for always providing me with a helping hand, brainstorming experiments and troubleshooting strategies with me, and cheering me up when I encountered failure. Also, thank you to Forrest and Alex for their extreme dedication to the experiments in chapter 2, which would not have been possible without them. In addition, I would like to acknowledge Marissa Quilicci and Amanda Latham for their major contributions to chapters 3 and 4 in this dissertation.

I would also like to thank the members of my graduate committee, Brendan Podell, Andrés Obregón-Henao, Adam Chicco, and Anne Avery for providing me with guidance, suggestions, and support throughout the completion of my studies. Thank you to Andres, for taking the time to personally mentor me through my dissertation and for having countless of meetings with me to analyze data and guide my projects forward. Also, thank you to Brendan and his lab members for willingly sharing laboratory supplies and protocols, helping me prepare for presentations, offering me advice and suggestions, and contributing to the work performed in chapter 2 of this dissertation.

I would like to acknowledge the CSU Flow Cytometry and Experimental Pathology cores for providing instrumentation and technical expertise required for the completion of these studies. In addition, thank you to Barb Andre for providing guidance with biostatistical analyses and laboratories of the Mycobacterial Research Laboratories for sharing supplies, instruments, and technical knowledge that were used to complete these experiments.

In additional to my acquaintances at CSU, I would also like to acknowledge the various teachers and mentors that prepared me to become a scientist long before I was admitted into graduate school. In particular, I would like to thank Jerri Trujillo, Jody Oaks, and Ronna Cochran for giving me the knowledge, experiences, and confidence to pursue a career in science and for always believing in my potential to change the world.

Finally, I would like to thank my family and friends for the immense love and support that they have provided me while pursuing this degree. To my mom, my biggest fan and most enthusiastic supporter, thank you. From science fair in the second grade until now, you have taught me to push through my deepest challenges with grit, turn my failures into success, and follow my dreams. Thank you for your constant support and always believing in me.

Lastly, I would like to give a huge thank you to my incredible husband Daniel—I could not have done this without you. Thank you so much for making sacrifices in your life so that I could pursue my dreams, for enduring every failure and success with me throughout this journey, and for loving me through it all.

TABLE OF CONTENTS

1.1 Tuberculosis: Epidemiology, Transmission, Diagnosis, and Treatments

Epidemiology of Tuberculosis.

In 1882 microbiologist Robert Koch discovered the causative agent of tuberculosis (TB) disease, the bacterium *Mycobacterium tuberculosis* (Mtb) [1]. Attributable to his discovery, we have since gained considerable insights into the pathogenesis of TB disease, leading to the development of therapeutic interventions, strategies for disease prevention, and ultimately, an overall reduction in global TB cases. Despite this progress, however, recent modeling strategies suggest that approximately 23% of the global population is infected with Mtb and have what is referred to as latent tuberculosis [2]. In 2018 alone, the World Health Organization (WHO) estimates that around 10 million people fell ill with TB disease while ~1.45 million individuals died from TB-associated illness [3]. To address the TB global health crisis, the WHO developed the "End TB Strategy", which aims to decrease the incidence of TB deaths by 95% and reduce new cases by 90% between 2015 and 2030 [4]. To meet these targets, a 4-5% reduction in incidence by 2020 and a 10% decline by 2025 must be achieved by adopting the three fundamental pillars for success, which includes 1. integrated patient-centered TB care and prevention, 2. bold policies and supportive systems, and 3. intensified research and innovation [4]. Current reports show that between 2015 and 2018 global TB incidence was reduced by 6.3% and TB deaths decreased by 11%, a step in the right direction, but ultimately failing to meet the desired decreases of 20% and 35% by 2020, respectively [3].

Among the 10 million new cases reported in 2018, South-East Asia accounted for 44%, Africa 24%, and the Western Pacific 18% of all cases [3]. Socioeconomic disparities observed between developed Western civilizations and those areas with high disease burden are undeniably and largely accountable for these high numbers [5, 6, 7]. Studies show that social factors

including living and working conditions, overcrowding, malnutrition, and social habits including smoking and high alcohol consumption are tied to the incidence of TB disease [7, 8, 9, 10]. Decreased access to health care and treatment is also a determinant of disease progression and mortality within these settings, however, studies suggest that even with ample treatment available, countries that rank low on the socioeconomic scale continue to suffer more greatly from TB morbidities [7]. In one epidemiological study, the transmission of TB to children <5 years old was monitored in Cape Town, London, and New York between 1912 and 2012. Despite the introduction of chemotherapy and similar control strategies in the mid-1950's, rates of TB transmission were unequally reduced in Cape Town compared to New York and London [6]. These results suggest the large impact that socioeconomic factors play on TB disease transmission, regardless of treatment availability [6].

Among socioeconomic factors, disease comorbidities, including HIV and diabetes mellitus (DM) significantly increase the susceptibility of TB disease and mortality. Infection with HIV is known to be the single greatest risk factor attributed to the development of active TB, increasing the risk of disease by 20-fold [11, 12]. Although the relationship between HIV and Mtb co-infection is complex, impairment and depletion of the CD4 T cells during HIV infection weakens immune control against Mtb, ultimately leading to increased susceptibility and progression of TB disease [13]. In support of this, HIV-positive patients with diminished CD4 T cell counts are at increased risk for the development of active TB while patients on anti-retroviral therapy (ART), which promotes restoration of the immune response and CD4 T cell numbers, are at significantly decreased risk of succumbing to advanced disease compared to patients not receiving ART [14, 15]. In addition to the effects that HIV has on the advancement of TB disease, Mtb infection increases HIV viral replication, thereby contributing to enhanced viral burden and to the acceleration of AIDS progression [16, 17]. Among people living with HIV/AIDS, TB is currently the leading cause of death and in 2018, HIV/TB co-morbidity accounted for 251,000 deaths [3]. Moreover, 0.8 million TB cases

were attributable to HIV infection, yet it is estimated that nearly 60% of global HIV-related TB cases are not diagnosed or reported [11]. In the TB endemic area of sub-Saharan Africa, an estimated 25 million individuals are infected with HIV, highlighting the importance of controlling both HIV and TB incidence and transmission. To reduce the incidence of TB/HIV co-morbidities a strategy called the "3 I's" has been implemented in high risk regions and includes 1. intensified TB case finding through enhanced screening for TB among HIV-positive persons, 2. isoniazid preventative therapy, and 3. infection control [18]. Moreover, enhancement of TB testing among HIV-positive patients is also performed but poses a challenge due to the decreased presence of bacilli in sputum associated with HIV infection [19].

Persons with uncontrolled diabetes and diabetic complications are also pre-disposed to co-morbidity with TB. Studies that have assessed the association of TB disease in diabetic patients found that diabetes mellitus (DM) increases the risk of developing active TB disease by 1.5 to 4-fold [20, 21, 22, 23]. A systematic review that evaluated the prevalence of latent TB in persons with DM also found a 4.4-fold increased incidence of LTBI [24]. In 2018, it was estimated that DM accounted for 0.4 million cases of TB and that the global prevention of DM could avoid up to 4.1% of all TB cases [20]. Current projections of the impact of DM however, are concerning and estimate that 578 million people will be living with DM by 2030, highlighting the need for increased TB testing and preventative measures among the largely at-risk DM population [25].

Like other risk factors, the relationship between TB and DM is complex and not fully understood. Infection with Mtb alone causes a transient state of elevated blood glucose similar to diabetes (fasting glucose >6.9mmol/L or random glucose >11.1mmol/L), making it difficult to discern whether Mtb-infected individuals possessed undiagnosed underlying DM or if the metabolic alterations are solely due to Mtb infection itself [26]. A meta-analysis published in 2018 showed that after excluding all studies that did not establish DM diagnosis prior to developing TB, DM patients had a 1.5-fold risk of developing active TB compared to non-diabetic counterparts [21].

A dose-like response of disease progression is also observed in patients with poor glycemic control, which have a 2-fold increased risk of developing active TB compared to non-DM persons, while there is no significant difference of disease progression between DM patients with good glycemic control and those without DM [20, 27].

In addition to underlying DM, the influence that TB-associated hyperglycemia has on the pathogenesis and progression of TB is even less clear and is one of the main objectives of our research studies highlighted in this dissertation work. Epidemiological studies in humans as well as studies in guinea pigs show that following successful anti-microbial TB treatment and disease resolution, blood glucose levels return to a normal state [28, 29]. Although more studies are needed to better understand this phenomenon, the transient relationship between TB and hyperglycemia is in accordance with stress hyperglycemia, a condition that has been described in hospital-associated illnesses and occurs due to the intertwined relationship between inflammatory cytokine production and hormones on metabolic regulation [26]. At our current state, a better understanding of the relationship between non-TB associated hyperglycemia and TB-associated hyperglycemia is desperately needed to gain better access and control over testing and treatment of DM patients.

The increasing prevalence of drug resistant Mtb also serves as a key hurdle in controlling the global incidence of TB. Infection with drug-resistant strains currently accounts for about 200,000 deaths each year and are on track to becoming the world's most deadly pathogens [30]. By 2050, estimates predict that approximately a quarter of all TB infections will be drug resistant [30]. Bedaqualine is the newest class of antibiotic approved for use against multidrug-resistant TB and was the first anti-TB drug to be approved in over 40 years, shedding light on the arms race between antibiotic discovery and the evolution of the pathogen [31]. In their most modest forms, strains of antibiotic resistant Mtb carry genes that render them resistant to the front-line TB drugs rifampicin (Rif) or isoniazid (INH). More resistant strains, however, are capable of resisting both Rif and INH, multidrug-resistant TB (MDR-TB), or a combination of both frontline drugs, a second-

line injectable (SLID, kanamycin, amikacin, or capreomycin) and any fluoroquinolone, also known as extensively drug-resistant strains (XDR-TB) [31].

Studies show that the primary reason for the rising incidence of drug resistant TB is not currently due to transmission of drug resistant bacilli, but rather, inappropriate management practices including inadequate treatment regimens and high rates of non-compliance by patients [31]. In India, which accounts for the highest number of patients with drug-resistant TB in the world, infection models suggest that if current TB management practices remain unchanged there will be a 275% increased risk of infection with MDR-TB over the next 20 years [32]. Moreover, these models predict that there will be a shift in the main method of MDR-TB acquisition, which will be predominantly caused by transmission rather than poor TB treatment management [32, 33]. Standardized empirical medical treatment without performing susceptibility testing is associated with increased treatment failure, relapse, and the development of multidrug resistance in patients with INH-resistant Mtb infection [34]. These data, therefore, support a need for modified treatment practices and susceptibility screening in order to combat the further spread of drug-resistant TB.

Transmission of Mtb.

Typically, infection with Mtb causes disease in the lungs, or pulmonary TB. In approximately 15-20% of cases however, the bacteria localize to and infect other tissues of the body causing extrapulmonary TB; although, this generally occurs due to bacterial escape and dissemination from infected cells in the lungs [32]. Infection with Mtb occurs via human-to-human transmission through airborne respiratory droplets caused by coughing, sneezing, singing, shouting or performing other forceful gestures causing respiratory excretion [32]. Of the 1.7 billion people thought to be harboring Mtb, only a subset of these individuals with active pulmonary disease are infectious [2, 32]. An epidemiological study performed on household contacts in Lima, Peru demonstrated that persons with the highest level of infectivity had bacteria that could be positively identified in their sputum (smear) and by culture while those that tested smear negative

and culture positive had decreased risk of infectivity and smear negative culture negative individuals had nearly no risk of transmitting infection [35]. In addition, a recent study assessed the percent of viable bacteria present in respiratory droplets from smear positive culture positive patients and reported that only 43% of respiratory droplets contained viable bacilli. Moreover, only 25% of these had CFU counts greater than 10 bacilli [36].

Diagnosis of Tuberculosis.

Among the quarter of the population that is infected with Mtb, the majority of individuals carry the bacteria in a subclinical latent state, while only 3-5% will develop active disease [2]. There is currently no good way of predicting who will and will not progress to active TB, however, underlying risk factors, such as those previously discussed, are strongly correlated to advanced disease. Identifying infected individuals, as well as their disease state, is important for initiating the appropriate treatment regimen and reducing the transmission of disease. Clinical guidelines have been developed by the WHO for the identification of latent and active TB, however, adoption of these methods varies by region and is largely dependent on the availability of resources.

Currently, there is no single, simple, all-inclusive, and widely available test that is used for the diagnosis of TB [32]. Individuals with symptoms that correspond to TB disease as the suspected diagnosis are typically evaluated for pulmonary lesions by chest x-ray and the presence of bacteria in the sputum by microscopic examination of a sputum smear [37, 38]. Using these methods has led to the identification of millions of cases worldwide, however, the availability of high-quality radiography is often limited and sputum smears lack sensitivity [36, 37]. Limitations with these techniques is especially amplified in high-TB burden areas where money and resources for testing equipment are limited and there is a high incidence of HIV, which is associated with reduced bacteria in the sputum [19]. In one study it was shown that sputum smear microscopy was associated with a sensitivity ranging from 35-80% in HIV-negative patients and only 20% in HIV-positive patients [39]. As an alternative, sputum culturing, which is considered the gold standard for

Mtb identification, may be performed; yet, bacterial culturing and identification can take up to 42 days and requires lab facilities and personnel and so is often not a favorable option [40].

Due to the limitations associated with these testing strategies, research has focused on identifying alternative methods that have higher sensitivity and specificity, require less resources and clinical expertise and are less costly. The identification of biomarkers in the blood or urine of patients has been an attractive strategy that has generated a large amount of interest for the development of new diagnostics [40]. Lipoarabinomannan (LAM) is a mycobacterial glycolipid that is shed from the bacteria during replication in the host and has recently been identified as being detectable in the urine and blood of infected patients [39]. A diagnostic test for the identification of LAM is currently available and is recommended to assist in the diagnosis of TB in HIV-positive patients where bacteria are not readily identified in the sputum [41]. In addition, LAM detection is useful for the identification and diagnosis of extrapulmonary TB, which cannot be done using traditional methods [42]. Although this test provides promise, studies show that LAM tests have varied sensitivities of between 13-51%, and although LAM is suggested to be specific for Mtb, LAM-like glycolipids have been identified in other species of bacteria, which may interfere with testing specificity [39]. Therefore, this testing method is not largely used to diagnose TB in its current state but is a useful alternative resource for TB diagnosis in difficult cases.

On a more positive note, a rapid molecular diagnostic test that detects Mtb-specific amino acid sequences, called the Xpert MTB/RIF Ultra assay was recently developed and approved for TB diagnosis. In 2018, the WHO released an updated compendium of guidelines for the treatment and care of TB recommending the Xpert MTB/RIF Ultra assay as the first line of diagnosis for TB in patients that are capable of producing sputum [4]. The assay is performed in a small cartridge, can be read in 2 hours, and is demonstrated to have an overall sensitivity of 87.5%, including sensitivity of 78.9% on smear-negative samples, and a specificity of 98.7% [43]. When compared to smear microscopy methods, Xpert is estimated to increase TB detection by 23% [44]. Moreover,

in addition to Mtb diagnosis the Xpert assay also identifies the presence of rifampin resistance genes that are responsible for 95% of Mtb RIF resistance [43] . The ease of use and added benefit of resistance identification makes this test a powerful advancement in TB diagnosis and is expected to become a standard TB diagnostic method. However, the high price of manufacturing is a hurdle that will need to be overcome before it is fully adopted by countries around the world.

In addition to active disease testing and diagnosis, testing for LTBI can be performed by tuberculin skin test (TST) or an interferon-gamma release assay (IGRA), though neither of these tests differentiates between active or latent infection. Both tests are immunologically based and depend on re-activation of the cell-mediated immune response following secondary exposure to Mtb antigens [45, 46]. Widespread testing for LTBI is not routinely performed in endemic areas but is rather restricted to persons who are at high risk of developing active TB disease and could benefit from prophylactic treatment [45]. And although immunological tests are beneficial for identifying LTBI in some populations, false positives can occur in persons that have been recently vaccinated with BCG, have been exposed to non-tuberculosis mycobacteria (NTMs), or have previously been infected with and cleared Mtb [47]. Therefore, to minimize the risk of unnecessarily treating people with harsh anti-TB drug regimens that may otherwise cause more harm than good as a result of toxic side effects, only a small population of individuals at high risk of developing disease are routinely tested [48]. The WHO currently recommends systematic LTBI testing for adults, adolescents, and children living with HIV, HIV-negative household contacts, and other at-risk groups including patients initiating anti-TNF treatment, patients receiving dialysis, or patients preparing for organ transplants [48]. WHO does not currently recommend that persons from other high-risk categories including those with diabetes, tobacco smokers, excessive alcohol users, or underweight individuals are systematically tested unless they are included in one of the other recommendations [48].

Treatment of TB Disease.

The treatment of TB is complex and depends on a variety of factors including disease state, Mtb drug susceptibility, and underlying risk factors associated with TB disease progression. Drug regimens are long and often include multiple antibiotics that are associated with harsh side effects including hepatotoxicity, gastrointestinal issues, influenza-like syndrome, dizziness fatigue, and hearing loss [49, 50]. Consequently, poor treatment compliance is common among TB patients and is associated with increased Mtb transmission and the emergence of drug resistance.

In accordance with WHO guidelines, drug regimens have been developed based on disease state for the treatment of LTBI, drug-susceptible TB, and drug-resistant TB. In addition, TST negative individuals with an increased risk of TB disease, such as those living with HIV or household contacts of infected persons, are encouraged to take isoniazid preventative treatment (IPT) [32]. Despite adverse events associated with antibiotic treatment, data shows that preventative treatment for TB reduces the overall risk of active disease by 33% and by 64% in TST-positive individuals [51]. Therefore, the benefit of providing prophylactic treatment is considered to outweigh the risk of side effects and non-compliance.

Table 1. Mtb antibiotic treatment regimens [4, 48].

Treatment Category	Treatment Regimen
Preventive Therapy	• Infants <12 months with HIV that are living in contact with a person with TB should receive 6 months of INH preventive treatment. • In areas with a high TB prevalence, children 12 years or older living with HIV and who do not have contact with a TB infected individual and are considered unlikely to have TB disease should receive IPT for 6 months. • In settings with high TB incidence, adults and adolescents living with HIV who have unknown or positive TST and are unlikely to have active TB should receive at least 36 months of IPT.

	• HIV-negative children <5 years old who are household contact with TB confirmed patients and do not have active TB should be given TB preventive treatment. • In countries with high TB incidence, children older than 5, adolescents, and adults who are household contacts of TB infected individuals and do not have active TB should be given preventive treatment. • In countries with low TB incidence, adults, adolescents, and children who are household contacts of TB-infected individuals should be systematically tested and treated for LTBI.
Treatment of LTBI	• INH monotherapy is recommended for both adults and children in countries with high and low TB incidence. • Rifampicin plus INH daily for 3 months should be offered as an alternative to 6 months of INH monotherapy for children and adolescents aged <15 years in countries with high TB incidence. • Rifapentine and INH weekly for 3 months may be offered as an alternative to 6 months of INH monotherapy as preventative treatment for both adults and children in countries with a high TB incidence. • In countries with low TB incidence, alternatives to 6 months of INH therapy include: 9 months of INH, or a 3-month regimen of a weekly rifapentine plus INH, or 3-4 months of INH plus rifampicin, or 3-4 months of rifampicin alone.
Treatment of Drug Susceptible TB	• The first phase of treatment includes daily dosing for two months with INH, rifampicin, pyrazinamide, and ethambutol followed by four months of daily treatment with INH and rifampicin.
Treatment of Drug Resistant TB	• Rifampicin-susceptible, INH-resistant TB should receive a six-month combination treatment with rifampicin, ethambutol, pyrazinamide, and levofloxacin, with or without INH. • Patients with rifampicin-resistant (RR-TB) or MDR-TB who were not previously treated with sec

TB Vaccination.

In 1921, after 11 years of propagating a virulent strain of *Mycobacterium bovis* through bile, glycerin, and potato medium, scientists Calmette and Gúerin discovered a resulting attenuated strain that provided protection against TB disease [1]. The live attenuated bacilli quickly became the widely administered vaccine, Bacille Calmette-Gúerin (BCG). Today, BCG remains the only approved vaccine for the prevention of TB and is the most widely used vaccine in the world [52]. In TB endemic regions, BCG is administered to infants at birth due to its high protective efficacy against severe forms of disease in infants and children, including meningeal and miliary forms of TB disease. The overall protection by BCG, however, is estimated to be only 50%, resulting in high infection rates in endemic areas despite high vaccine coverage [53]. BCG's efficacy is even more variable in adults (0-80%) and provides poor protection against pulmonary TB, the most common form of disease [54, 55]. It is poorly understood why protection is so variable among individuals, though multiple hypotheses have been proposed.

The original strain of BCG *M. bovis'* loss of virulence is characterized by the deletion of the RD1 locus, which encodes the key virulence factors as well as strong T cell antigens, secretory antigen target 6 (ESAT-6) and culture filtrate protein 10 (CFP-10) [56]. Over the past 100 years, however, BCG has been continuously passaged leading to over 20 genetically distinct substrains [57, 58] There is currently no evidence, however, that the strain of BCG used is associated with increased or decreased protection. The most likely explanation for variable protection is, rather, thought to be due to immune sensitization caused by environmental exposure of NTMs. This hypothesis is supported by data showing that individuals without prior infection to Mtb [55].

To better understand the variable efficacy conferred by BCG, as well as develop novel vaccines with enhanced protection, the identification of correlates of protection is critical. Currently, our understanding of what constitutes vaccine-mediated protection is limited and biomarkers indicative of protection are lacking [59]. Though based on conflicting evidence, there is

a general consensus that IFN-γ-generating CD4 (Th1) and, to a lesser extent, CD8 T cells are central for protection against TB [60, 61, 62]. In animal models of Mtb infection, the depletion of either CD4 or CD8 T cells led to increased pathology and Mtb bacterial burden [15, 63]. Additionally, the lack of IFN-γ production during infection is associated with an inability to restrict Mtb growth and progression to fatal disease [64, 65]. Vaccination with BCG follows the Th1 generating paradigm and is demonstrated to generate effector memory T cells in the lung that produce IFN-γ and other cytokines, including TNF-α and IL-2, which are considered important pro-inflammatory mediators in the response against Mtb [66]. The variable protection provided by BCG alone, however, demonstrates the lack of a fully effective immune response against TB [67, 68].

New vaccines against TB are often designed to amplify the BCG response, either by creating recombinant BCG strains or boosting existing immune populations from previous vaccination [56]. The MVA85A vaccine, a recombinant strain of the Vaccinia Ankara virus expressing the immunodominant Mtb protein antigen 85A, is an example of the prime-boost strategy. In animals, MVA85A was shown to induce a strong antigen specific Th1 response which corresponded to significant protection from Mtb challenge [69, 70, 71]. The results from a clinical trial that included 2,797 infants in South Africa and took nearly two years to complete however, showed no increase in protection following vaccination [72]. The disappointing findings from this study emphasize the importance of identifying correlates of vaccine protection, which can be translated from animal models into humans. Other non-clinical studies also raise caution against relying on the magnitude of the Th1 response as a predictor of protection, and show that the amount of IFN-γ produced by CD4 T cells positively reflects bacterial load and is associated with increased pathology rather than clinical improvement [73]. Other studies demonstrate that IFN-γ production is critical for the early control of Mtb infection, but an ongoing pro-inflammatory response results in pathological damage and dissemination of bacteria to other tissues [59, 74]. Based on these studies it is highly likely that the overall implications of Th1-mediated immunity

depend on a multitude of factors that can either result in benefit or detriment, including the kinetics of this response throughout Mtb infection. The fine tuning of T cell activation, differentiation, and cytokine production during various disease stages must, therefore, be recognized when designing TB vaccines.

Recent studies suggest that rather than cytokine potency, the primary goal of TB vaccination should be the generation of central memory T cells that are long-lived and maintain self-renewal [75, 76]. Models of alternative routes of BCG vaccination, which correlate to enhanced efficacy, demonstrate that the greatest levels of protection are positively correlated with the presence of central memory T cells [73, 77, 78]. These cells not only have the ability to rapidly expand and produce cytokines, but also replenish pools of cells that have undergone convalescence in response to chronic infection. Adoptive transfer studies support the important role that these less differentiated cells play in mediating protection against TB disease. In comparison to Th1 differentiated IFN-γ-producing T cells, less differentiated non-IFN-γ producing cells showed superior protection following Mtb challenge due to their persistence and superior proliferative capacity [79]. Additionally, cells that expressed the checkpoint inhibitor PD-1, which limits T cell effector function, displayed superior proliferation, cytokine production, and protection following cell transfer in comparison to IFN-γ and TNF-α secreting effector cells [80]. These results suggest that a successful vaccine against TB must generate T cells that maintain plasticity and the ability to replenish and respond to infection during chronic stages of disease.

1.2 Immunopathogenesis of Tuberculosis.

Innate Immunity.

The innate branch of the immune system plays multiple important roles in the response against Mtb infection. It serves as the first line of defense upon pathogen recognition, initiates the development of the antigen-specific adaptive response, and maintains bacteria in an organized structure to prevent the spread of infection. Mtb is transmitted by the inhalation of respiratory

droplets containing viable bacilli that travel from the upper respiratory tract into the lower airways where it establishes infection in the alveoli [81]. On the journey to the alveoli, bacteria traverse through mucus lined airways composed of tightly organized alveolar epithelial cells (AECs), which serve as the first line of defense against Mtb infection [82]. AECs provide physical barriers of protection by blocking bacterial entry into the body and producing a secretory substance called airway surface liquid (ASL). This thin layer of mucus contains various antimicrobial elements including enzymes, reactive oxygen and nitrogen species, and immunoglobulins, which provide immediate defense following pathogen entry [81, 82, 83]. In addition, AECs initiate cell-mediated effector responses following antigen recognition. They express various pattern recognition receptors (PRRs) on their surface that recognize Mtb molecules and initiate phagocytosis and the production of cytokines and chemokines [82, 84]. AECs role in pathogen clearance through phagocytosis is shown to be limited, however, their corresponding recruitment of professional immune cells to the site of infection is an important aspect of the early immune response to Mtb infection [82, 85].

Alveolar resident macrophages are considered the most important innate immune cell involved in Mtb infection [86]. They play a dual role in both protection and pathogenesis by providing cell-mediated bacterial killing while also serving as the predominant host cell for Mtb survival and replication [81, 87, 88]. The determination of whether macrophages successfully kill the bacteria upon initial recognition or whether Mtb virulence mechanisms allow the bacteria to persist, ultimately dictates progression to infection [89, 90]. Like AECs, macrophages contain a variety of PRRs on their surface. As a general response to bacterial infection, macrophages phagocytose and compartmentalize the bacteria into vacuoles called phagosomes that undergo a series of events leading to phagosome maturation, or the result of phagosome-lysosome fusion. This process ultimately yields acidification of the vacuole, a pre-requisite to produce digestive enzymes and reactive oxygen and nitrogen molecules that are used to degrade intracellular antigens [89, 91].

Bacterial survival strategies of Mtb have evolved to circumvent this process by inhibiting phagosome-lysosome fusion to maintain their residence within macrophages [92, 93]. Additionally, Mtb has developed multiple other virulence mechanisms in order to persist, replicate, and disseminate. These include escape from the phagosome into the cytosol, modulation of controlled cell death pathways, interruption of cytokine production and effector function, and acquisition of nutrients from the host [87, 94].

Granulocytic cells, or neutrophils, are also implicated to play important roles in innate immune defense against Mtb, yet their exact role is less clear. Neutrophils have a biphasic response to Mtb, where they appear in large numbers immediately following infection, disappear, and then influx again at around days 8-15 until the end of infection [95]. In one study, the depletion of neutrophils was associated with decreased iNOS expression during early stages of infection, which is required for nitric oxide production involved in macrophage-mediated bacterial killing [91, 95]. Evaluation of neutrophil numbers in the blood of humans has also been shown to correspond to the risk of becoming infected with Mtb, while those with higher neutrophil counts are shown to have a decreased risk of infection, suggesting their importance in controlling early infection [86]. Like macrophages, neutrophils are phagocytic cells that can ingest and kill bacteria internally, though their traditional role is to release toxic substances into their surroundings resulting on non-specific microbial and cellular destruction. Interestingly, although they have phagocytic capacity and aggregate in the lungs in high numbers during early infection, neutrophils are not found to be associated with bacilli, discounting their role in Mtb killing through phagocytosis or direct mechanisms [95]. Rather, these findings suggest that neutrophils elicit their antimicrobial effects through indirect processes, such as enhancing macrophage-induced Mtb death [96]. In support of this, when neutrophilic material is added to Mtb-infected macrophage cultures, there is an observed increase in macrophage antimycobacterial activity in comparison to cultures without the material [96]. Additionally, entrapment of bacteria within neutrophil NETs, or neutrophil extracellular

traps composed of DNA and antimicrobial proteins, is shown to increase bacterial phagocytosis and enhance killing by macrophages [97, 98]. Importantly, although neutrophils play an important role during the early course of infection by mediating bacterial killing, their aggregation within granulomas during later course of infection is also associated with necrosis, inflammation, and bacterial dissemination [86, 99, 100]. In further support of disease promotion by neutrophils, our lab has also shown that lysed neutrophils provide an extracellular matrix composed of macromolecules and extracellular DNA that facilitate the growth of complex Mtb communities [101]. It is therefore important to recognize both the immune-mediated benefits and dangers of neutrophilic involvement at specific timepoints during infection.

While initial attempts to ward off bacteria with the innate response can be effective, the generation of the adaptive immune response significantly enhances cell-mediated bacterial killing and is critical for preventing the development of active disease. At the interface between the innate and adaptive immune response, professional antigen presenting cells called dendritic cells are responsible for mediating the development of antigen-specific cells [102]. In the early stages of infection monocyte derived inflammatory DCs in the lung internalize bacteria and migrate to nearby draining lymph nodes in response to a CCL19/CCL21 chemokine gradient [103, 104]. Once in the lymph node, these cells facilitate antigen presentation and the maturation of antigen-specific lymphocytes that make up the adaptive immune response [105].

Adaptive Immunity.

The importance of T cell-mediated immunity to Mtb infection has been demonstrated in both animal models and in human diseases that possess aberrations to a conventional T cell response [106]. This central role for T cells in protection against active TB is highly recognized in HIV-infected persons, which have a dramatically increased risk of developing disease [107]. Importantly, the risk of disease is reduced following restoration of CD4 T cell counts following

ART [108]. In addition, animal models of TB show similar findings, where CD4 or CD8 T cell depletion leads to enhanced disease progression and death compared to immunocompetent hosts [60, 74].

A defining characteristic of the adaptive response against Mtb is the delayed accumulation of antigen-specific T cells within the lungs of infected individuals, which doesn't occur until days 14-19 following infection [109]. This delayed recruitment is thought to contribute to the early establishment of infection, allowing for continuous recruitment, apoptosis, and reinfection of macrophages, ultimately allowing the bacterial multiplication and propagation [102]. Preceding the development of antigen-specific effector lymphocytes and their migration into the lungs, T cells must be appropriately activated through MHC antigen presentation, co-stimulatory signals, and cytokines in the lymphoid tissues. Relative to the delayed activation and migration of T cells, DCs experience delayed recruitment into the lymph nodes, which directly corresponds to becoming infected with Mtb [109]. Furthermore, once in the lymph node, only selective subsets of DCs are shown to be effective at facilitating T cell activation. While monocyte-derived pro-inflammatory DCs are responsible for trafficking antigen to the lung, only classical lymph node residing DCs are capable of presenting antigen to and activating T cells. Studies show that the transfer of soluble antigen within the lymph nodes to cDCs occurs in order to facilitate T cell activation [110, 111].

Once activated, effector CD4 and CD8 T cells leave the lymph nodes and migrate to the early granuloma in response to cytokines produced by endothelial and epithelial cells as well as macrophages within the local microenvironment. Increased production of chemokines CCL19 and CCL21 are induced in the lung to attract antigen-specific T cells to the site of infection while enhanced CXCL13 enables their localization within lymphoid follicles where they come into maximal contact with Mtb infected macrophages and mediate killing of infected cells [112, 113]. Early studies identified IFN-γ as the central component of T cell-mediated protection through its induction of macrophage apoptotic cell death and intracellular induced bacterial killing [65, 91]. In

support of this, mice that lack IFN-γ display an inability to produce reactive nitrogen species, which are required for macrophage-mediated bacterial clearance, and in-turn, results in uncontrolled bacterial growth and a rapid progression to TB disease [65, 114].

The primary production of IFN-γ has been attributed to CD4 T cells of the Th1 lineage, which traditionally protect the host against intracellular pathogens by initiating cell death through macrophage induced bacterial killing. Following transfer of CD4 Th1, Th2, or Th17 lineage differentiated cells into Mtb infected mice, Th1 cells indeed displayed superior protection against TB disease compared to the other cellular subsets [115]. Interestingly, however, in both mouse and non-human primate models lacking CD4 T cells, IFN-γ levels are maintained following chronic Mtb infection [63, 74, 107]. Rather, CD8 T cells compensated for the loss of CD4-derived IFN-γ. In non-human primates, IFN-γ levels were even increased in CD4-depleted animals in response to Mtb in comparison to those with intact lymphocyte populations. Despite the sustained levels of IFN-γ, however, CD4-depletion was associated with increased disease progression and reduced survival in comparison to animals with CD4 T cells, inferring that IFN-γ levels alone is not predictive of protection [63, 74]. In further support of this, a cell transfer experiment with Th1 cells that lacked the transcriptional regulator Tbet, which controls IFN-γ production, showed that Tbet knockout cells provided the same level of protection as wild type Th1s [115]. Therefore, other mechanisms must exist for Th1-induced protection.

More recently, it has been suggested that the production of multiple cytokines through a coordinated response is more closely associated with bacterial clearance and protection against TB disease progression [116]. Evaluation of immune environments within individual granulomas from Mtb infected non-human primates shows an inverse correlation between bacterial burden and the presence of both Th1 and Th17 cytokines, including IFN-γ, IL-2, TNF-α, and IL-17 [117]. Additionally, T cell deficient mice displayed significant protection when administered either Th1

or Th17 differentiated CD4 T cells, indicating an important role for the generation of Th17 mediated immunity [118]. In response to Mtb infection, the predominant Th17 cytokine, IL-17, has been shown to be required for T cell localization within lymphoid follicles, which is necessary for maximal macrophage activation [112]. Furthermore, IL-17 has been demonstrated to be critical for neutrophil recruitment early during infection and mice that lack the IL-17 receptor succumb to increased bacterial burden and have decreased lengths of survival following infection [119].

In addition, TNF-α production is also implicated as an indispensable T cell-generated cytokine that mediates lymphocyte recruitment to the site of infection and is required for the formation and maintenance of the granuloma [120, 121]. Following chronic Mtb infection in non-human primates, TNF-α neutralization resulted in disorganization of the granuloma and enhanced disease progression [122]. Interestingly, TNF-α production during chronic disease has also been associated with increased expression of anti-inflammatory molecules and is hypothesized to help sustain a balance between pro- and anti-inflammatory mediator, which are required to maintain stability of the granuloma [122]. Evidence suggesting the benefit of this balance is demonstrated in sterilized granulomas, which possess a higher proportion of IL-10 producing T cells to IL-2, TNF-α, and IL-17 generating effector cells [117].

In addition to generating the cytokines necessary for promoting bacterial clearance and preventing tissue destruction, the temporal and kinetic qualities of the T cell response to Mtb infection are also critically important. Macrophage activation in the lung must be facilitated by T lymphocytes that have traversed from the draining lymph node in an activated state and extravasated across the endothelium into the interstitial space. Conclusions from multiple studies characterizing the T cell response to Mtb in the lung have been drawn on the assumption that the cells being evaluated reflect that of the local lung immune environment. To discriminate between lung and vascular resident lymphocytes, recent studies demonstrate that the injection of fluorescently labeled antibodies into the vasculature prior to euthanasia results in the identification

19

of these two unique populations. Using this technique, findings reveal that the majority of cells evaluated from single cell isolates following tissue digestion reside in the vasculature rather than lung tissue [123]. Interestingly, recent studies using intravascular (iv) staining show that antigen-primed T cells in the vasculature can be discriminated from those in the parenchyma through their expression of the terminal differentiation marker KLRG1 [124, 125, 126]. In comparison to tissue-homing antigen-specific T cells, KLRG1+ cells from the vasculature produce higher levels of IFN-γ but provide significantly reduced levels of protection in the lung, suggesting that T cell-mediated protection corresponds more with the level of T cell differentiation and lung homing capability than their capacity to produce IFN-γ [125, 127].

In further support of these findings, T cell effector populations are shown to delineate into either KLRG1+ or PD-1+ lineages following Mtb infection in mice [80]. In contrast to KLRG-1, PD-1 is a checkpoint inhibitor associated with reduced T cell effector functions and is often associated with T cell exhaustion— though it is more recently recognized as a critical regulator of immune function rather than an indicator of dysfunction. Consistent with previous findings, transfer of KLRG1+ cells into Mtb infected mice resulted in cytokine production, but the cells were short lived and unable to provide long lasting protection against Mtb infection [80]. Alternatively, PD-1+ T cells were highly proliferative and upon transfer and following antigen encounter converted into a KLRG1 cytokine-secreting phenotype capable of restoring functional immune populations with provided protection against Mtb infection [80, 128]. Data from human studies further support the importance of the level of T cell differentiation in response to Mtb infection, where accumulation of highly differentiated T cells in the blood are found to correspond with increased tissue destruction in the lung [129].

Furthermore, the influence of T cell differentiation on the capacity to elicit a protective immune response against Mtb has also been demonstrated following vaccination [130]. The waning of BCG-induced protection corresponds to the accumulation of terminally differentiated T cells in

20

the lung [131, 132]. Also, in comparison to T cells primed by a subunit vaccine, Mtb- and BCG-primed T cells expressed KLRG-1 and had decreased lung-homing capacity, which corresponded to decreased protection [133]. Moreover, persistent expression of the immunodominant Mtb protein ESAT-6 is found to coincide with KLRG1 expression during Mtb infection and with ineffective immune control [134]. Taken together, these studies provide robust evidence that in addition to cytokine production, the level of T cell differentiation in response to infection is a critical indicator of whether T cells will possess the survival and homing capacity required to adequately respond to Mtb infection.

The development of functional exhaustion has also been proposed to contribute to the inadequate T cell response against Mtb infection. Exhaustion is characterized by the up-regulation of check-point molecules, including PD-1, TIM-3, and CTLA-4, to name a few, which are associated with the reduced capacity of T cells to secrete effector molecules [135, 136]. Consistent with the exhaustion phenotype, T cells from mice chronically infected with Mtb display reduced levels of pro-inflammatory cytokines, including IL-2 and TNF-α, increase their production of the anti-inflammatory cytokine IL-10, and are demonstrated to express the exhaustion markers TIM3 and PD-1 [137, 138]. To mediate improved T cell function in other chronic inflammatory diseases— predominantly cancer—antibody-mediated blockade of checkpoint signaling has been exploited as a successful immunotherapeutic strategy. Surprisingly, in the context of Mtb infection, loss of PD-1 signaling is associated with exacerbated disease progression [139, 140, 141]. Evidence of this is demonstrated in PD-1 knockout mice, which display uncontrolled bacterial growth and advanced necrosis that is associated with infiltration of neutrophils and increased expression of pro-inflammatory cytokines [140]. Likewise, blockade of PD-1 signaling in a 3-dimmensional cell culture model of human tuberculosis resulted in increased Mtb growth and pro-inflammatory cytokine secretion [139]. In humans, treatment with anti PD-1/PDL1 therapy is associated with an increased

risk of developing active TB disease, suggesting the importance of immune regulation during Mtb infection [142].

Furthermore, there is a large body of evidence that suggests that while pro-inflammatory cytokines are necessary for controlling infection, they are equally as important in contributing to disease pathogenesis [86, 117]. For example, IFN-γ levels in bronchoalveolar lavage (BAL) fluid from humans have been shown to correspond to disease severity while increasing IFN-γ production in mice directly leads to exacerbated lung infection and early death [138]. Furthermore, although TNF-α is implicated to play an important role in maintaining the granuloma, its overproduction leads to increased bacterial replication [139]. Thus, despite their roles in protection, the levels of pro-inflammatory cytokines must be intricately balanced to avoid bacterial growth, tissue destruction, and ensuing disease.

Taken together, the T cell response to Mtb infection is highly complex and depends on a multitude of factors to provide appropriate immune protection. While CD8 T cells contribute to IFN-γ production and play important roles in limiting disease, the majority of protection is still considered to be associated with the generation of a successful CD4 antigen-specific response. The coordinated production of multiple cytokines is one important element of protection, but more recent findings suggest that the degree of T cell differentiation is critically important for enhancing migration to infection and in maintaining a pool of self-renewing cells that provide prolonged protection against chronic infection. Moreover, maintaining the balance between pro and anti-inflammatory mediators during different stages of infection is critical for maintaining bacterial control and limiting disease pathogenesis. There are obvious contradictory findings that convolute our understanding of the acquired response to TB. However, by focusing on components of the immune response that are not solely dependent on cytokine production, such as localization and timing of the response, a better understanding of T cell immunity is being attained.

The Granuloma.

As a consequence of persistent immune stimulation by Mtb infection, aggregates of cells form into organized structures known as granulomas. Granulomas are composed of multiple cell types including macrophages, neutrophils, DCs, B and T cells, NK cells, and fibroblasts and are thought to be formed as an immune defense mechanism to prevent bacterial dissemination [143]. Considering only a small proportion of Mtb infected individuals develop active progressive disease, one can argue that the granuloma is a relatively effective immune-mediated defense strategy. On the contrary, granulomas provide an ideal niche for Mtb replication and survival within macrophages and, therefore, their formation is also seen as an immune evasion strategy that favors Mtb persistence within the host.

Early following infection, Mtb induces a pro-inflammatory response that initiates the migration of macrophages across the lung epithelium into the interstitium [144]. This process is, in part, mediated by the production of metalloproteinase 9 (MMP9) by epithelial cells [143]. Once inside the lung tissue, persistent macrophage stimulation induces the production of pro-inflammatory intermediates, further propagating the recruitment of macrophages to the site of infection. Newly arriving macrophages phagocytose Mtb-containing apoptotic compartments, which subsequently becoming infected and aggregate, resulting in the development of the early granuloma. Following the generation of the adaptive immune response, the infected core of macrophages becomes surrounded by multiple cell types including mononuclear phagocytes, foamy macrophages, and lymphocytes. Progressive development of the lesion is characterized by the formation of a fibrous capsule surrounding the macrophage core, which ultimately prevents ensuing macrophage killing through lymphocyte-mediated mechanisms [143].

Subsequent with mature granuloma formation, local immune cells switch from a pro- to an anti-inflammatory state and display increased production of the regulatory cytokine IL-10. This altered phenotype is thought to stabilize the granuloma by limiting inflammation and tissue

destruction [88, 145]. In addition, despite low antigen availability, surveillance of the granuloma is ensued throughout infection by CD11c$^+$ DCs, demonstrated by their continuous migration to lung draining lymph nodes and the priming and activation of naïve CD4 T cells [86, 146]. This phenomenon can be observed through the waxing and waning of activated cells in the blood of infected individuals and corresponds to a cyclical pattern of inflammation [147]. In most cases, this immune-mediated structure remains stable and successfully prevents the progression to active disease. However, and for reasons not well understood, in a small percentage of infected individuals the granuloma collapses and necrosis of infected cells leads to bacterial escape and dissemination to other regions of the lung and other organs throughout the body [148].

1.3 T Cell Differentiation.

Preceding their development into naïve T cells, double negative (CD4$^-$/CD8$^-$) hematopoietic lymphoid precursors that originate in the bone marrow migrate to the thymus where they undergo a series of maturation events. A small portion of these cells (~5%) will develop into a population of γ:δ T cells, while the majority will take on an α:β phenotype, distinguished by differences in T cell receptor (TCR) chain composition [149]. Following their entry into the thymus, T cells are distributed between the thymic cortex and medulla, where they undergo TCR rearrangement and positive and negative selection. Within the cortex, the TCR is formed as a result of rearrangement of the alpha and beta chains and the concurrent up-regulation of both CD4 and CD8 molecules. Double-positive cells then move into the medulla where they undergo positive and negative selection. These processes eliminate cells based on their inability to recognize self MHC molecules and those that respond to self-antigens, respectively. Additionally, these cells lose either CD4 or CD8 surface marker expression and identify as single-positive lymphocytes [149]. This process occurs most efficiently in young children, as thymic output is observed to decline over time [150]. Interestingly, of the immature progenitors that enter the thymus

for maturation, only approximately 2% survive maturation and comprise the circulating T-cell repertoire, which is estimated to comprise at least 10^8 different T cell antigen specificities [151].

Following their maturation in the thymus, naïve antigen-inexperienced T lymphocytes circulate between the blood and secondary lymphoid organs in search of their cognate antigen. This migration pattern of continuous surveillance is enabled by their expression of lymphoid homing receptors CCR7 and CD62L [152]. These molecules interact with ligands lining blood vessels that directly lead to lymph node entry, known as high endothelial venules, by facilitating rolling and extravasation through the vessel walls [152]. Inside the lymphoid tissues, T cells aggregate into specialized T cell zones, which permits their interaction with antigen presenting cells to ensue activation and differentiation [153]. Successful T cell activation is accomplished by the participation of three processes including: 1. recognition of cognate antigen presented on MHC complexes, 2. co-stimulatory signaling, and 3. cytokine production [154]. Upon receiving these three signals, T lymphocytes differentiate into CD8 cytotoxic or CD4 T helper subsets that are distinguished by their transcriptional programs and cytokine producing capabilities [155]. Typically, lineage-differentiated CD4 cells are classified into Th1, Th2, Th17, T follicular helper (Tfh), or induced regulatory T cell (iTreg) subsets, though the identification of new subsets is continuously increasing in complexity [127, 156, 157]. Cytokine availability within the local activation environment ultimately dictates T helper cell lineage differentiation by inducing the expression of various transcription factors. Th1 cells, which respond to intracellular bacterial and viral infections by promoting cell-death of infected cells through IFN-γ production, up-regulate the transcription factor Tbet in response to IL-12 [158]. Th2 cells, which are required for the humoral immune response and the clearance of extracellular pathogens, are induced through IL-4 production and are distinguished by the transcriptional regulator GATA3 [159]. Th17 cells, which play an important role in mediating extracellular pathogen clearance, are induced by a combination of TGF-β with IL-6, IL-21, and IL-23 and require the transcription factor RORγt [160]. Tfh cells, which are important

for the generation of antibody production by B cells, become induced by IL-21 and are dependent on BCL6 for their transcriptional regulation [161]. And finally, iTregs, which regulate the pro-inflammatory effector response through their production of the anti-inflammatory cytokine IL-10, are induced by TGF-β and are characterized by the transcription factor FOXP3 [162]. Together, these individual cell types comprise a multi-faceted response against numerous pathogens but intriguingly, evidence is building to show that there is also a fair amount of plasticity among them following their initial lineage commitment [155, 163].

In addition to their lineage differentiation, CD4 T cells are classified into different clusters based on their effector functions, migratory capacity, maintenance of stemness and self-renewal and susceptibility to activation-induced cell death [164]. Based on these characteristics, cells are classified into stem cell memory (T_{scm}), central memory (T_{cm}), effector memory (T_{em}), effector (T_{ef}), or end stage terminally differentiated subsets (T_{emra}), where the former are associated with a less differentiated phenotype capable of self-renewal and persistence and the latter possess high effector functions but succumb to rapid cell death following activation [165, 166]. The least differentiated of these subsets, T_{scm}s, are a newly classified subset of memory cells that display a naïve-like phenotype, with the exception of activation markers CD95 and IL-2β [167, 168]. These cells have become a target for vaccination due to their stem-cell like characteristics including maintained self-renewal, robust proliferation following antigen re-challenge, a high level of plasticity, and long-lasting survival after primary infection [168, 169, 170]. There is evidence that following secondary challenge, T_{scm}s differentiate into both effector and memory T cell subsets, enabling the generation of cells that can both rapidly respond to infection and maintain a memory pool [167].

Following T_{scm}s along the differentiation gradient are the more well characterized central and effector memory T cells subsets [171]. Unlike T_{scm}, these cells effectively up-regulate expression of the activation marker CD44 following antigen encounter, which gives them the capacity to

migrate from the vasculature into peripheral tissues [172, 173]. These cells are found to persist following the resolution of infection and can proliferate and differentiate into responsive, cytokine-secreting effector cells following secondary challenge [171]. The long-term maintenance of antigen-specific memory T cells is facilitated by their interactions with cytokines IL-15 and IL-7, in an MHCII independent manner [174]. T_{cm} and T_{em} subsets are unique from one another based on their homing capacities and differential effector functions. Central memory T cells are the least differentiated of the two and are identified by their retained expression of the lymphoid homing molecules CCR7 and CD62L [171]. Like naïve T cells, T_{cm}s follow a migratory route through the blood and into secondary lymphoid organs where they can interact with DCs that carry antigen from peripheral sites of infection [154]. Following their primary activation and differentiation, these cells produces low levels of inflammatory cytokines required for effector functions, but high amounts of IL-2 needed for proliferation [175]. In response to secondary challenge, T_{cm}s display extensive capacity to proliferate and produce effector cytokines [176]. Conversely, effector memory T cells lose their expression of CCR7 and CD62L and inherit cytotoxic effector functions following primary antigen challenge, yet they are shown to persist within the blood many years after antigen clearance [154]. Following antigen-specific re-challenge in the peripheral organs, these cells rapidly proliferate and increase production of inflammatory cytokines required for antigen clearance. Unlike T_{cm}s however, these cells are committed effector T cell progenitors that succumb to cell death after a limited number of cell divisions. Therefore, T_{em}s are unable to replenish the memory pool, and over time, repeated antigen recognition contributes to a decline in the availability of this protective memory population [177].

In contrast to long-lived memory populations, the most highly differentiated cells are those that attain full-blown effector functions and subsequently die during the convalescence stage of the T cell response. These cells are identified as effector and terminally differentiated end stage effector subsets [166]. In response to antigen stimulation, effector cells up-regulate their expression

of activation markers including CD44, CD69, and CD25. These markers facilitate migration (CD44) and retention (CD69) in peripheral tissues as well as responsiveness to IL-2 induced proliferation (CD25) [177]. Effector cells are responsible for mediating initial antigen clearance at sites of infection by producing large amounts cytokines to mediate cell-induced microbial killing by macrophages and granulocytes (Th1/Th17) or antibody production by B cells (Th2) [177]. Following a limited number of cell divisions, effector cells become terminally differentiated and are characterized by altered transcriptional profiles and are identified by their surface expression of KLRG1. These cells maintain high levels of effector functions but lose proliferative and self-renewal potential and have a relatively shortened life spans [178]. In various disease models, including TB, terminally differentiated T cells have been shown to provide limited protection against Mtb due to their inability to migrate, survive long-term, and produce adequate cytokines following secondary challenge and/or chronic infection [125, 126, 141].

To determine the extent of T cell differentiation, the levels of expression between the antagonistic transcriptional regulators Blimp-1 and BCL6 can be measured. High Blimp-1 expression is associated with high secretory and low proliferative capacity, the inability to self-renew, and decreased survival [166, 179, 180]. Mice that lack Blimp-1 expression fail to activate and mount a cytotoxic response, demonstrating its importance in effector T cell development [181, 182]. Furthermore, Blimp-1 depletion is associated with increased cell longevity and decreased IFN-γ production in effector T cells as well as the inability to form short-lived KLRG1+ effector cells [178]. Interestingly, in contrast to the importance of Blimp-1 in promoting an effector T cell phenotype, studies suggest that the development of terminal differentiation is important for the maintenance of T cell homeostasis and regulation [183]. For example, Blimp-1-induced cell elimination has been described in a subset of lymphomas, where those that highly express the transcriptional regulator undergo pre-mature differentiation and cell death compared to those with no expression, which undergo persistent proliferation and contribute to aggressive disease progression[184]. Presumably,

this is a consequence of their increased survival in the absence of Blimp-1 expression [178]. BCL6 on the other hand, is directly associated with longevity and is highly expressed in memory T cells [179, 185, 186]. The predominant role of BCL6 in CD4 lymphocytes is to regulate the development of follicular T helper cells and promote antibody affinity maturation and activation of the humoral response within germinal centers [187]. The sustained interactions of CD4 T cells with B cells, however, simultaneously blocks the development of T helper cells by repressing the expression of effector associated transcription factors Blimp-1 and Tbet and promoting memory T cell development [128, 186, 187, 188]. Together, the graded levels of expression between Blimp-1 and BCL6 can be used to evaluate the extent of T cell differentiation, which may not be fully captured by surface marker expression.

The usefulness of identifying and characterizing the extent of T cell differentiation and survival following activation is critical for the development of effective vaccines and immune-based therapies. This has recently been highlighted in the effectiveness of adoptive cell transfer therapies for the treatment of cancer. Traditionally, the goal of many T cell-based immune therapies has been to generate a robust effector-like phenotype that produces potent cytokines and initiates tumor killing *in vitro*. However, an *in vivo* comparison between highly differentiated T cells that display superior anti-tumor activity *in vitro* with their less-differentiated counterparts, showed that there was an inverse relationship in *in vitro* and *in vivo* killing capacity.Therefore, while the less differentiated cells were unable to promote tumor killing *in vitro*, they provided superior protection *in vivo* due to their homing, proliferative, and survival capacity [165]. Similar results have been summarized in other studies showing that the adoptive transfer of early effector and even naïve cells induce increased tumor eradication in comparison to more-differentiated effector cells [189]. Furthermore, recent studies are finding that following vaccination, less differentiated cells have increased proliferative and cytokine responses following secondary challenge and persist in the body for many years and can provide long-lasting protection [175].

Different levels of T cell differentiation are achieved by modifying the strength and duration of the primary activating signals [177, 189, 190]. Generation of more terminally differentiated effector T cells is attained following strong TCR engagement and an increase in cytokine availability [191]. Multiple studies have demonstrated that by modulating either the concentration of anti-CD3, which binds the TCR co-receptor complex CD3 and induces activation signals, or the amount of activating cytokine, graded levels of transcription factor expression and functional "effectorness" are achieved [187, 192, 193, 194]. For example, the amount of IL-12 present in cell culture during T cell priming directly influenced the level of Tbet expression, which increasingly corresponded to the upregulation of KLRG1 and short-term survival following activation [193]. *In vivo*, T cells that are activated in the lymph nodes at later points during T cell priming and have reduced interactions with DCs display a surface phenotype indicative of reduced stimulation and show decreased levels of proliferation, consistent with a less differentiated but non-memory phenotype [195]. Moreover, high dose infection with cytomegalovirus coincides with more highly differentiated cells in comparison to low-dose infection, suggesting that increased antigen availability promotes increased differentiation [196]. Consistent with increased antigen availability, the continuous availability and interaction with the immunodominant Mtb antigen, ESAT-6, induces terminally differentiated cells while Ag85b, which is only acutely present, generates cells with a less-differentiated memory-like phenotype [134].

Lastly, an important consideration for the generation of different T cell subsets is the evolutionary path of development. As previously described, signal strength and duration are important for generating more- or less-differentiated T cell phenotypes. What is less well understood regarding T cell differentiation is whether cells undergo a progressive path of differentiation following antigen encounter or if they become committed to one cell type. Various developmental models have been proposed for the generation of effector and memory T cell subsets, including the linear, progressive, and divergent differentiation models. The linear model

is the most traditional view of differentiation and is based off the idea that following activation, T cells undergo rapid proliferation and develop into cytotoxic effector T cell subsets [197]. Following their response to infection, most of these cells undergo contraction, or cell death, while a small proportion revert to a less differentiated memory phenotype that persist and respond to secondary challenge [177]. Evidence of this model is supported by the observation that Th1 or Th2 conditioned cells with effector properties maintain a small population after antigen clearance that remain viable and provide an anamnestic response to re-challenge [197, 198]. Alternatively, oppositions to this model suggest that memory is generated independent of the need to differentiate into an effector T cell phenotype, citing that in comparison to memory T cells, effector T cells have reduced telomerase activity and telomere length, indicating their high replication history that is not apparent in memory subsets [199]. Rather, it is hypothesized that memory and effector cells go through progressive differentiation, in which they sequentially gain effector functions depending on the strength of the activating signal. This is observed in memory cells responding to infection that acquire a KLRG1+ effector phenotype following subsequent antigen challenge and the generation of central memory T cells from naïve cells [200]. Recent evidence supporting this hypothesis is the use of new technologies that allow single cell, epigenetic modifications and transcriptional profiles associated with cell differentiation to be tracked from naïve T cells into more differentiated phenotypes [201, 202]. The last model of differentiation, the divergent model, suggests that during proliferation, proteins that determine the generation of memory or effector T cells are unevenly distributed, yielding two phenotypically distinct daughter cells [203, 204]. Evidence of this phenomenon is observed in the unequal partitioning of Tbet and other proteins involved in cellular functions such as the metabolic coordinator, mTORC1 [203, 205].

In conclusion, the activation and differentiation of T lymphocytes is a complex process that results in the generation of many different subsets with specialized responses to disease. Regardless of the cell type however, T cell subsets appear to exist on a differentiation continuum

that corresponds with their ability to either persist through self-renewal or provide a robust, but deadly, effector response.

1.4 T Cell Metabolism.

Historically, immune cell metabolism was commonly regarded for its role in producing adenosine triphosphate (ATP) to fill basic cellular energy demands. More recently, however, the discovery that many aspects of cellular metabolism directly influence immune cell fate and function, termed immunometabolism, has garnered interest to understand it on a deeper level. T cell metabolism, has gained considerable attention as a therapeutic target to functionally enhance the T cell response against chronic illnesses including cancer, autoimmune disorders, and infectious diseases. The basic understanding of how T cells modulate their metabolism in accordance with their function and, in turn, how this is affected by individual diseases has been an area of recent and rapid investigation.

The two major pathways of energy metabolism are oxidative phosphorylation (OXPHOS), also referred to as mitochondrial metabolism due to its mitochondrial localization, and glycolysis. OXPHOS is the most efficient method of energy production, yielding ~32 ATP molecules per mole of glucose and serves as the predominate energy source for quiescent T cells [206]. Alternatively, glycolysis, which results from glucose fermentation into lactate, yields only 2 ATP per glucose and is engaged by activated T cells experiencing rapid expansion [207]. Generally, glycolysis predominates under oxygen replete conditions in which OXPHOS cannot function efficiently. T cell dependence on this pathway, however, is independent of oxygen availability (aerobic glycolysis) and commences even when oxygen is available and can support more efficient modes of energy production. Utilization of aerobic glycolysis is not unique to T cells but was first discovered by the scientist Otto Warburg in the 1920's, who noticed that cancer cells consumed glucose at a rapid rate under aerobic conditions relative to normal cells in surrounding tissues. This phenomenon was termed the Warburg Effect and was postulated to occur because of

dysfunctional mitochondria. More recent evidence show that the Warburg Effect is intentionally regulated by cells and is required for cell growth and proliferation through the generation of biosynthetic intermediates [208].

Glycolysis

Increased glycolytic programming in T cells has been well characterized following T cell activation. More specifically, TCR and CD28 co-ligation mediate the upregulation of glycolysis by activating the AKT/mTOR pathway. The important role of mTOR in the immunometabolic phenotype of activated T cells has been shown using the specific mTOR inhibitor rapamycin. T cells that are stimulated in the presence of rapamycin are characterized by dramatically reduced glycolytic activity and loss of effector differentiation and function compared to untreated cells [209, 210, 211]. Repression of this pathway is also achieved under natural conditions by the phosphorylation of adenosine monophosphate-activated protein kinase (AMPK), which senses energy levels through AMP:ATP ratios to either inhibit or promote mTOR activation [212]. mTOR activation induces the expression of transcription factors that regulate the production of glycolytic enzymes, T cell cytotoxic molecules, and epigenetic modifications that promote an effector T cell response, including c-Myc, HIF1α, and ERRα [213, 214, 215, 216, 217, 218, 219]. One of the earliest events observed following T cell receptor co-ligation is increased expression of the glucose transporter, Glut1, on cell surfaces, which coincides with dramatically increased glucose transport that is in excess of what is required to maintain cellular energy demands [217, 220]. In the absence of glucose, T cells fail to gain full effector functions, even in the presence of alternative substrates that fuel OXPHOS for energy generation [221]. Additionally, the inhibition of glycolytic metabolism with the inhibitor 2-deoxyglucose (2-DG) suppresses the development of effector functions and redirects cellular differentiation towards a non-inflammatory phenotype, demonstrating the essential role that glycolysis plays in the development of effector T cells [216, 222].

The substantial increase in glycolysis following T cell activation is primarily attributed to increased demand for biosynthetic precursors required for cell growth and proliferation. For example, the generation of glucose-6-phosphate (G6P) from glucose feeds into the pentose phosphate pathway (PPP), which is required for nucleotide synthesis and is responsible for maintaining cellular redox status through the generation of NADPH [207]. Additionally, 3-phosphoglycerate, which is generated during the seventh step of glycolysis, is shuttled into the serine biosynthesis pathway to generate the amino acid serine. Additionally, glycolytic generation of pyruvate not only contributes to mitochondrial ATP production through tricarboxylic acid cycle (TCA)-generated reducing intermediates but is also used to synthesize fatty acids through its conversion to citrate in the TCA cycle. Fatty acids can then by synthesized into triglycerides for storage or immediately utilized for membrane biogenesis in actively dividing cells [223]. Inhibition of cellular proliferation, but not survival, by 2-DG following T cell activation further demonstrates the critical contribution glycolysis plays in generating metabolic intermediates needed for the expansion of activated T cells.

Interestingly, despite the role that glycolysis plays in the generation of biosynthetic molecules, only a small proportion of glucose consumed during activation is attributed to the building of these intermediates. Rather, the majority of glucose taken up by cells is converted into lactate by lactate dehydrogenase (LDHA) and is ultimately secreted into the extracellular environment [212, 213]. Notably, lactate, which is traditionally regarded as a biproduct of glycolysis, has recently been found to serve as an energy source, gluconeogenic precursor, and signaling molecule through cellular uptake by lactate shuttles [224]. In T cells, the expression of these lactate transporters, monocarboxylate lactate transporters MCT1 and MCT4, are shown to be upregulated in response to activation, and inhibition of MCT1 during T cell activation resulted in the inhibition of cell division supporting a role for lactate in T cell function [225]. In contrast however, environments with exceedingly high concentrations of extracellular lactate, such as the tumor

microenvironment, have shown that lactate also inhibits T cell proliferation and cytokine production by blocking lactate export [226]. These studies highlight the need to better understand the influence that lactate has on T cell function within the context of various diseases.

Nonetheless, lactate production through glycolysis and LDHA activity is an important component of T cell function. Deletion of LDHA results in a significant reduction in glucose uptake which corresponds with the loss of effector functions, suggesting that glucose fermentation is also an important component of the glycolytic switch. One explanation for the engagement of LDHA is to prevent lactate buildup within the cell and maintain cellular redox and glycolytic flux by recycling NAD from NADH [207, 212, 227]. Because NAD is required for constant cycling through glycolysis, maintaining an NAD pool enables the continuous shunting of substrates into anabolic pathways to promote cell growth. Regulation of NAD:NADH ratios by LDHA can also be used as a cell signaling mechanism or to induce epigenetic modifications that influence cellular function [228]. Additionally, high utilization of glycolysis may be employed as a primary means to generate ATP in order to free up TCA cycle intermediates and mitochondrial function.

Independent from the role in biosynthesis, glycolysis also directly influences cytokine production. Deletion of LDHA results in T cells with diminished IFN-γ production that are unable to develop into potent effector T cells with anti-tumor activity [217, 229, 230]. Under quiescent conditions, the glycolytic enzyme glyceraldehyde 3-phosphate dehydrogenase (GAPDH) allosterically binds to mRNA encoding IFN-γ, thus preventing translation. Following up-regulation of glycolysis, however, GAPDH is reassigned to perform its metabolic functions, resulting in dissociation from mRNA and the subsequent translation of IFN-γ [231]. Due to the role that metabolic substrates have on epigenetic manipulation, there are likely many other similar processes that occur in response to glycolysis that impact the production of cytotoxic intermediates required for effector function that have not yet been identified [232].

Mitochondrial Metabolism.

Though not as well recognized, enhanced utilization of OXPHOS must also occur following T cell receptor engagement for the induction of cellular activation and proliferation [231]. The mitochondria are major producers of cellular ATP and engage in important cell signaling events, both of which are required to maintain cell survival and facilitate T cell activation. Glucose is a major mitochondrial substrate that must be broken down through a series of chemical reactions in order to drive ATP production by OXPHOS. First, glucose is converted to pyruvate by glycolysis in the cytoplasm and then pyruvate subsequently enters the mitochondria and is converted into acetyl-CoA by the enzyme pyruvate dehydrogenase. Acetyl-CoA then undergoes an aldol condensation reaction with oxaloacetate to form citrate and proceeds through a series of chemical reactions to generate reduction intermediates (NADH and $FADH_2$) that feed into the ETC [207]. Under quiescent conditions glucose can efficiently be used to fuel this process, however, under highly glycolytic conditions in which glucose is diverted to generate biosynthetic molecules, other fuel sources can also enter the TCA cycle to produce NADH and $FADH_2$.

The amino acid glutamine fuels mitochondrial respiration following conversion into α-ketoglutarate [207]. The metabolic intermediate α-ketoglutarate is produced through a process called glutaminolysis and enters the TCA cycle and progresses through the normal series of reactions that produce NADH and $FADH_2$. Following T cell stimulation, glutamine is an indispensable nutrient for cell proliferation and effector functions, which has been demonstrated by the inability of activated cells to proliferate or produce cytokines in the absence of glutamine [233, 234]. In response to TCR engagement, increased expression of amino acid transporters, such as SLC7A5 and SLC1A5, and intracellular glutamine levels as well as enhanced rates of glutaminolysis are detected in T cells [212]. Under highly glycolytic conditions, glutamine serves as an alternative source of fuel for OXPHOS-mediated energy production, which then allows the carbons derived from glucose to be used for the synthesis of other biosynthetic intermediates [235].

Additionally, intracellular amino acid levels have the capacity to regulate anabolic growth by mediating mTOR activation [210].

Fatty acids are also an energy rich fuel source that give rise to electron donors through the TCA cycle [236]. They can either be taken up from the extracellular environment by the fatty acid transporter CD36, or in some cases by passive diffusion, or endogenously created from the TCA cycle intermediate citrate. Before entry into the TCA cycle, fatty acids must be transported into the mitochondria then broken down into Acetyl-CoA through a process called β-oxidation. A carnitine shuttle system is used to transport long-chain fatty acids into the mitochondria by converting the fatty acid into acylcarnitine through a series of chemical reactions and transport by the mitochondrial membrane protein CPT1A and the inner membrane shuttles carnitine/acylcarnitine translocase (CACT) [237]. Once inside of the mitochondria, fatty acids are converted into acyl-CoA and broken down into acetyl-CoA through β-oxidation. Depending on the length of the fatty acid, β-oxidation yields different numbers of acetyl-CoA molecules by undergoing multiple cycles. Each cycle consists of a series of four reactions which require the removal of two-carbon units to produce acetyl-CoA [237]. This makes fatty acids an extremely efficient fuel source; for example, a single palmitate containing 16 carbons yields 8 acetylCoA and a final yield of approximately 106 ATP molecules.

Due to increased efficiency in generating ATP, fatty acids are predominantly oxidized by cells that survive for long periods of time under quiescent conditions. In contrast, in response to TCR engagement, T cells upregulate *de novo* synthesis of fatty acids for their incorporation into cell membranes and use as posttranslational protein modifiers [238]. In addition, synthesized fatty acids can be stored as triglycerides for future metabolic retrieval [238]. Studies in T cells show that inhibition of *de novo* fatty acid production does not compromise effector differentiation, but instead results in reduced proliferation and subsequent death of antigen-specific T cells [239, 240]. Studies in cancer, which represent a proliferation and survival dynamic like T cells, also show decreased

proliferation and survival after blocking fatty acid synthesis [238, 241]. These results indicate that in addition to providing macromolecules required for cell growth, fatty acid generation is also a critical component of maintaining cell survival.

Quiescent T cell subsets including naïve, regulatory, and memory T cells are metabolically characterized by predominate dependence on mitochondrial metabolism [242]. These cells rely both on glucose and fatty acids to maintain energy demands through OXPHOS, though relative reliance on one or the other is more accurately attributed to the distinct cell type. Naïve T cells, for example, harness most of the energy from glucose metabolism while memory and regulatory T cells are characterized metabolically by increased utilization of fatty acid oxidation. Because quiescent T cells do not have internal glycogen stores, these cells are highly dependent on glucose import to maintain metabolic and energy demands [213]. Survival promoting signals by growth factors such as IL-7 and IL-15 are shown to keep cells alive by maintaining metabolic function, while cells that lack growth factors display a decreased metabolic rate that is associated with loss of Glut1 expression and cell death [243] [216].

The reliance on mitochondrial metabolism by Treg and memory T cell subsets is so important for their phenotypic development that pharmacologic inhibition of glycolysis and thus, promotion of OXPHOS can be exploited to generate the respective phenotypes. Studies have demonstrated that the deletion of mTOR in mice results in the formation of regulatory T cells following TCR-activation instead of effector T cell subsets. In addition, inhibition of mTOR in mice that are predisposed to develop autoimmune diseases increases the Treg:Th17 T cell ratio, resulting in decreased inflammation and improved disease outcome [244, 245, 246]. Furthermore, memory T cell generation is also enhanced following mTOR inactivation. This has been demonstrated in infection and in vaccination models comparing vaccination alone or in combination with rapamycin or metformin, both of which are mTOR inhibitors [247]. In these studies,

mice receiving the combined treatment plus vaccination had increased development of antigen-specific memory T cells that corresponded to improved disease outcome.

Complementary to reliance on OXPHOS, more detailed characterization of Treg and memory T cell metabolism has revealed the critical importance of β-oxidation in directing subset development and maintenance of cell survival. Regulatory T cells continuously import extracellular fatty acids, which then undergo oxidation in the mitochondria. This is a result of expression of LKB1, a central regulator that promotes mitochondrial metabolism, and simultaneously, *de novo* fatty acid synthesis. Diverting glycolytic flux following activation therefore is critical for promoting regulatory over effector T cells by preventing biogenesis and cell growth. Like Tregs, memory T cells are also highly reliant on fatty acids for energy. The importance of fatty acid utilization for memory T cell development was first demonstrated in tumor necrosis factor receptor-associated factor 6 (TRAF6) deficient mice. TRAF6 deficiency is associated with defective AMPK activation, altered expression of genes required for fatty acid metabolism, and decreased memory T cell formation [248]. Restoration of β-oxidation with metformin however, reestablished memory T cell generation in TRAF6 deficient mice, demonstrating its critical importance for memory T cell development [248]. Interestingly, unlike Tregs, memory T cells derive most of their fatty acids from endogenous biosynthesis to provide immediate ATP for energy and a metabolic reserve that contributes to their longevity and secondary response [249]. Furthermore, the importance of fatty acid metabolism for memory T cell survival has been demonstrated by blocking fatty acid transport into the mitochondria with etomoxir, which ultimately impaired T cell survival [250].

In addition to β-oxidation, a defining characteristic of memory T cell mitochondrial dynamics is the generation of a mitochondrial spare respiratory capacity (SRC) [250]. SRC is the maximal amount of mitochondrial respiration that is available to a cell under times of stress. In comparison to other cell types, memory T cells possess a dramatically increased SRC that

provides them with a bioenergetic advantage to quickly produce energy in order to sustain viability and rapidly generate effector functions following re-challenge [251]. There are two primary ways that SRC can be achieved. First, dampening the extent of OXPHOS engagement following TCR-induced activation maintains respiratory reserve. This type of SRC is displayed in T cells that have been treated with OXPHOS inhibitors such as metformin, which dampens mitochondrial flux, and thereby preserves respiratory reserve. Alternatively, SRC can be enhanced by increasing mitochondrial mass through mitochondrial biogenesis. This phenomenon is observed in T cells in response to IL-15 signaling, which facilitates the generation of memory T cells with elongated mitochondria and increased overall mitochondrial mass [250, 251, 252]. These fused mitochondria not only provide more surface area to increase OXPHOS but are also thought to spatially localize complexes of the ETC for more efficient energy production [252]. This is in contrast with punctate mitochondria in effector T cells that promote glycolytic upregulation and maintain little to no SRC following cell activation [252]. Mitochondrial morphology and SRC are, therefore, unique features that can be used to define memory versus effector T cells.

Furthermore, differences in mitochondrial membrane potential ($\Delta\Psi$m) is also unique among memory and effector T cell populations [253]. Membrane potential is the charge or difference in hydrogen ions across the intermembrane space and the lumen of the mitochondria [254] and is generated by the pumping of protons across the inner mitochondrial membrane at complexes I, III, and IV, in coordination with electron transfer through the ETC complexes. The electrochemical gradient achieved by the pumping of protons provides a proton-motive force that is essential for ATP production by driving the F0F1 ATPase, or ATP synthase. Membrane potential is required to maintain viability of healthy cells, while those that experience mitochondrial damage undergo depolarization, a point of no return for subsequent apoptotic cell death [254]. Additionally, mitochondria undergo hyperpolarization following TCR engagement, which is necessary for full T cell activation [253, 254, 255]. Increased rates of respiration are accompanied by saturation of

respiratory chain complexes with reducing intermediates and the extrusion of hydrogen ions into the mitochondrial matrix. These excess ions ultimately reduce cytochromes in the ETC and lead to the generation of reactive oxygen intermediates that are required for cell signaling [255, 256]. Mitochondria that fail to generate an increase in ΔΨm following activation are targeted for destruction through mitophagy [256]. Although necessary for activation, ΔΨm is found to have a direct influence on ROS production and associated DNA damage that can ultimately lead to impaired self-renewal [253]. Moreover, ΔΨm has been found to be directly linked to mTORC1 activation through IL-2 induction and can be significantly reduced following inhibition with rapamycin [253]. In association with cellular phenotype identification corresponding to mTORC1 activation, low ΔΨm is characteristic of memory T cells with low mTORC1 and high self-renewal while high ΔΨm typifies effector T cells with increased mTORC1 and associated effector functions [253]. Furthermore, ΔΨm is found to serve as a biomarker and therapeutic target for the autoimmune diseases including type 1 diabetes and systemic lupus erythematosus (SLE) [254, 256, 257]. Autoreactive T cells from SLE patients display persistently hyperpolarized mitochondria and elevated mTOR activity [256, 258]. Normalization of T cell activation was successfully achieved with rapamycin, resulting in ΔΨm maintenance and decreased disease [259, 260]. Together, these results suggest the importance of the mitochondria in energy production, signaling, and T cell differentiation through ΔΨm regulation.

Finally, mitochondria are also extremely important mediators of T cell signaling, primarily through mitochondrial ROS (mtROS) production. Mitochondrial derived ROS makes up a large portion of overall cellular ROS and is produced predominantly at complexes I and III of the ETC [233, 261]. Immediately following T cell activation, mtROS spikes in association with a rapid influx of calcium. By increasing calcium concentrations, mitochondria become hyperpolarized resulting in ETC saturation and electron leakage, and ultimately mtROS formation. This phenomenon is

essential for appropriate T cell activation, whereby inhibition of mtROS, both *in vitro* and *in vivo*, resulted in attenuated IL-2 production and the loss of antigen-specific T cell expansion [233]. One of the ways that mtROS promotes T cell activation is through its oligomerization of mitochondrial antiviral signaling proteins (MAVS), which are key signaling proteins that regulate the expression of immune pro-inflammatory genes including NFAT, NF-κβ, and IRFs [206, 261, 262]. In addition, induction of mtROS through the inhibition of complex I is found to activate the NLRP3 inflammasome, leading to the activation of caspase I and subsequently, IL-1β production [263]. Though necessary for development of an effective T cell response, pharmacological inhibition of mtROS has been shown to reduce airway inflammation in mice infected with influenza A virus, demonstrating potential as a therapeutic target [264]. Together, these studies demonstrate the importance of mitochondrial function beyond its role in metabolism for the formation of a successful T cell response.
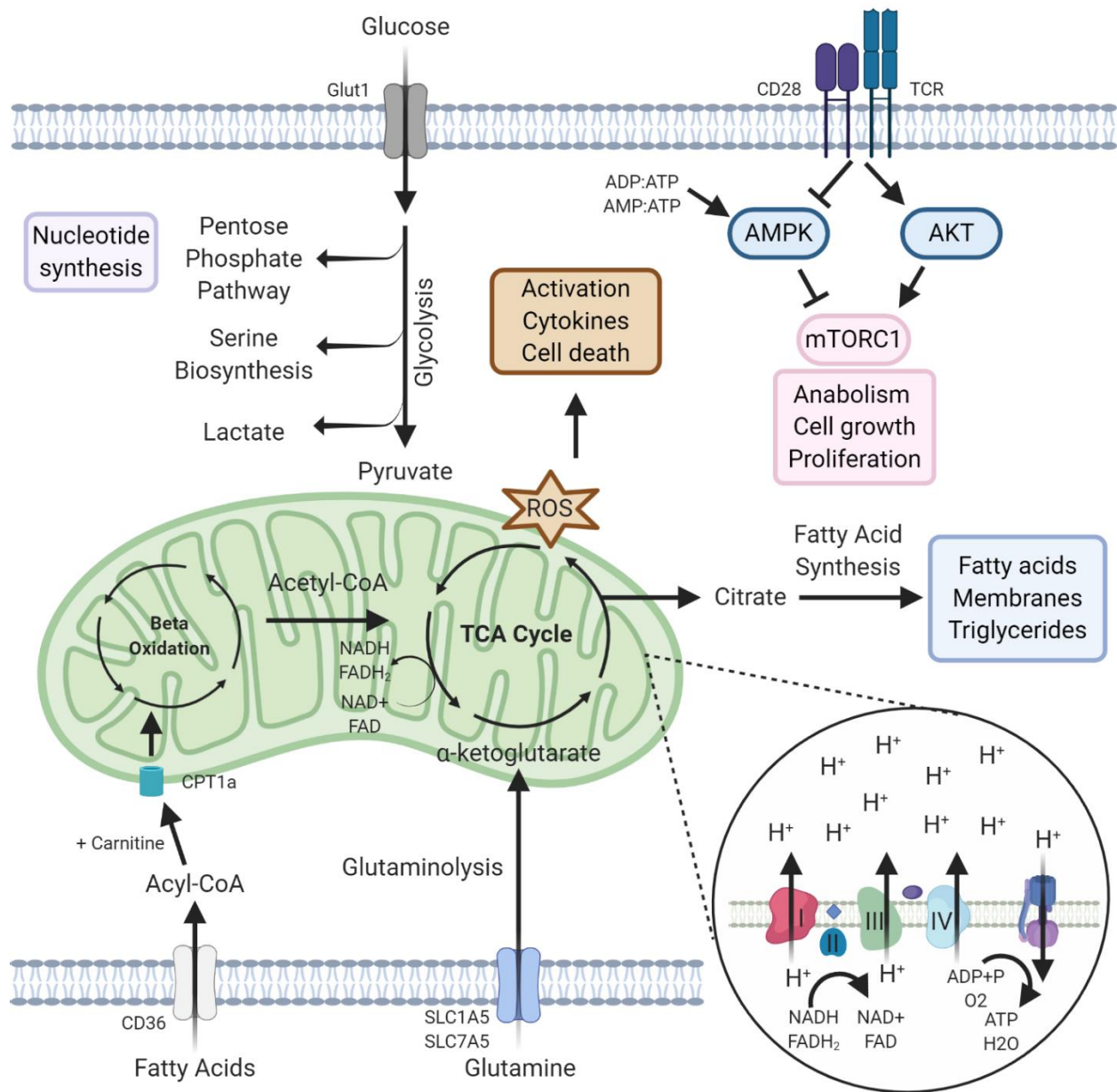
Figure 2. T cell metabolism. Under homeostatic conditions, T cells uptake glucose through the glucose transporter Glut1 and metabolize it through glycolysis and the TCA cycle to generate the reduction intermediates, NADH and $FADH_2$. These electron donors feed electrons to complexes I and II of the ETC and facilitate the pumping of hydrogen ions into the intermembrane space to generate a charge differential that drives ATP production by ATP synthase. Following TCR engagement and co-activation with CD28, the AKT/mTOR pathway is activated causing global metabolic changes that promote anabolism, cell growth, and proliferation. Increased Glut1 expression following TCR activation drives glycolytic flux to provide intermediates required for cell growth. Increased flux through the ETC also promotes ROS production, which is found to play important roles in T cell activation, cytokine production, and cell death. In addition to increased glucose internalization, glutamine uptake is increased through SLC1A5 and SLC7A5 transporters and undergoes glutaminolysis for entry into the TCA cycle. Fatty acid metabolism is utilized by long lived naïve and memory T cells through breakdown by β-oxidation or *de novo* synthesis using the TCA intermediate, citrate.

1.5 Metformin: Mechanisms of action and use as a host-directed therapy.

Metformin's mechanism of action.

Metformin is an anti-hyperglycemic drug that is most commonly prescribed for the treatment of type II diabetes. It is derived from the naturally occurring compound galagine, which was originally isolated from the French lilac, or *Galega officinalis,* and was used as an herbal medication in medieval Europe [265]. In the 1920's, galagine was found to induce glucose-lowering effects but treatment corresponded with high liver toxicity and it was therefore, unable to be used as an anti-glycemic therapeutic in its native form. Metformin, a synthetic derivative of galagine, is a member of the biguanide family along with phenformin that also possesses glucose lowering properties but is non-toxic. As a result, metformin has become the most widely prescribed drug for the treatment of type II diabetes, approved by the Food and Drug Adminstration (FDA) for clinical use in the United States in 1994 [266]. In addition to its anti-glycemic effects, metformin is more recently being evaluated for the treatment of various diseases including cancer, autoimmune, and infectious diseases, due to its less well-known effects on cellular proliferation, cell death, and immune modulation [267, 268, 269]. Exploiting these off-target effects has been complicated, however, due to an incomplete understanding of metformin's mechanisms of action, which appears to vary in response to individual diseases, timing of treatment, and dosage. Over the past 20 years, a vast amount of research has been performed to better understand these mechanisms, and though great advancements have been made, variability between studies and the multiple off-target effects has delayed the wide spread use of metformin as a host-directed therapy for other communicable and non-communicable diseases.

The main anti-glycemic affects by metformin are attributed to decreased hepatic gluconeogenesis and increased glucose uptake by muscle cells [270, 271]. Following oral delivery, metformin is predominantly absorbed through the gastrointestinal tract and delivered to the liver via the hepatic portal vein and then cleared from the body by renal excretion [272]. Metformin is

detected at its highest concentration in the liver— around 40-80μM compared to ~10μM that is observed in the plasma— making hepatocytes one of its primary targets [273]. Due to its cationic nature, metformin must be delivered into cells by organic cation transporters (OCT1, OCT2, and OCT3), which are expressed on many different tissues including the small intestine, liver, kidney, heart, skeletal muscle, placenta, lung, brain, immune cells, and even tumors [274, 275, 276]. Organic cation transporter 1 is highly expressed in the liver, and mice lacking its expression display a 30-fold decrease in metformin uptake. Moreover, studies show that OCT1 expression is required for anti-glycemic activity by metformin [274, 275]. Following entry into the cell, metformin accumulates in the mitochondria due to its attraction to the negative charge differential, where it is found to inhibit complex I of the ETC. Early studies evaluating the mechanism of action of metformin demonstrated that treated cells displayed decreased OXPHOS, depolarized mitochondria, and a drop in ATP/ADP ratios, indicating a loss of mitochondrial function, or mitochondrial insufficiency [277]. Likewise, insufficient energy production by mitochondria corresponded to heightened cellular lactate excretion due to an increase in aerobic glycolysis [278, 279]. Mitochondrial perturbations are most attributed to metformin's partial inhibition of complex I of the ETC. This has been demonstrated using isolated mitochondria or functionally isolated complex I, which show that in response to metformin treatment, cells are unable to consume oxygen and become energetically inefficient [279, 280]. The inability to facilitate ATP production by OXPHOS results in an overall decrease in ATP, corresponding to increased ADP: ATP and AMP: ATP ratios that alert energetic sensors to alter functionality. Selective binding of AMP or ADP to the γ subunit of AMPK induces phosphorylation and activation, which participates in various metabolic functions including the inhibition of fat synthesis and promotion of fat oxidation and thus reduced hepatic lipid stores and increased insulin sensitivity [265, 281]. Moreover, increased AMP:ATP ratios are found to inhibit gluconeogenesis by repressing the expression of genes and the function of enzymes required for gluconeogenic processing [265, 271, 282, 283]. These results and others imply that the inhibition of

complex I and AMPK activation are central to metformin's downstream effects. Other studies exist, however, that suggest alternative mechanisms of action and downstream consequences.

In one study evaluating the mechanistic effects of metformin on various cancer cell lines, whether metformin acted through an AMPK dependent mechanism was dependent on the cell line being assessed. While some cells displayed AMPK activation following metformin treatment, others failed to activate AMPK and rather displayed an increase in mitochondrial ROS production. The authors, therefore, suggested that ROS production may be an alternative mechanism that is employed by metformin [284]. Further evidence demonstrating the dispensability of AMPK for metformin to elicit its function effects show that mice lacking liver AMPK maintain similar blood glucose levels following metformin treatment in comparison to WT mice [271]. Based on these findings, the authors hypothesized that AMP accumulation and the allosteric inhibition of the key gluconeogenic enzymes, such as fructose 1,6-bisphosphatase, may be responsible for these effects [271]. In support of AMPs ability to induce metabolic modulations independent of AMPK, another study has demonstrated that AMP build-up following metformin treatment antagonizes glucagon actions, which also decreased glucose levels [285].

To make sense of differences in the literature suggesting differences in the requirement for AMPK for the action of metformin, recent studies have begun to evaluate the influence that drug concentrations have on mechanistic targeting— an important consideration since many studies are carried out using supra-physiological concentrations. One study has argued the validity of the results reported from AMPK deficient mice demonstrating that when treated with physiological concentrations, AMPK activation is in fact required to suppress glucose production [273, 286]. Other studies evaluating alternative mechanisms of action using low-dose concentrations suggest that metformin functions by altering cellular redox status; specifically, by regulating glycerol-3-phosphate dehydrogenase activity, a key component of a transport system used to shuttle reducing equivalents from the cytosol to the mitochondria [287, 288]. Results from these

studies and others, therefore, demonstrate the challenges faced in defining a clear picture of metformin's mechanisms of action.

As previously mentioned, a major complication in studying the mechanisms of action of metformin correspond to the dose used during experimentation. Extreme variations of drug concentration are used in *in vitro* versus *in vivo* settings as well as human versus animal dosing, which brings into question the biological relevance of many studies. Compared to the roughly 10μM metformin concentration found in the plasma of human patients, *in vitro* studies require at least 100x this concentration to see comparable molecular alterations. In one study evaluating the pharmacokinetics of metformin in mouse tumors, they found that to achieve similar levels of AMPK activation *in vitro* as *in vivo*, concentrations in excess of 300-fold were required compared to the circulating concentrations measured in mice [289]. Moreover, they demonstrated that only 10-15% of the metformin concentration applied in the media was found inside of *in vitro* cultured cells, and cells treated with 1mM metformin *in vitro* possessed similar intracellular concentrations to that observed in the plasma *in vivo* [289]. Additionally, metformin is known to accumulate in negatively charged organelles in the cell, hence its localization to the mitochondria, at 100- to 500- fold higher concentrations than what is observed in the plasma. Therefore, differences in cellular membrane potential between cells that are maintained either *in vitro* or *in vivo* may also account for the differential concentrations required to see molecular effects [290]. Cellular sensitivity to metformin is also found to vary greatly based on nutrient availability [290, 291]. One study, which assessed the impact of serine availability on the antineoplastic effects of phenformin— a biguanide molecule that is structurally similar to metformin—found that serine withdrawal dramatically improved antineoplastic function [291]. Therefore, the excessive nutrient availability in cell culture media is not a true representation of nutrient limitations that are encountered in biological microenvironments. In addition to *in vitro* dosing variations, high doses that are used to treat mice are also met with scrutiny. The human metformin dose is approximately 20mg/kg/day

47

while doses used in mouse studies exceed that by at least ten times, ranging from 250-500mg/kg [272]. Multiple studies have now demonstrated, however, that these much higher doses are required to achieve equivalent human serum concentrations and are therefore physiologically relevant (~10μM) [290].

Metformin as a host-directed therapy.

In addition to metformin's traditional use as an anti-glycemic drug, it possesses many off target effects that have been shown to be beneficial in the treatment of various diseases. The use of metformin as an adjunctive cancer therapeutic has widely been explored due to its anti-cancer properties, including inhibition of cellular proliferation and promotion of cell death pathways [292, 293, 294, 295]. Interestingly, in addition to its direct influence on cancer cells, metformin has been shown to contribute to cancer clearance by enhancing immune-mediated mechanisms. In multiple studies, metformin enhances tumor rejection in normal mice, yet fails to mediate protection in T cell immunodeficient mice, indicating the specific influence that it has on the T cell anti-tumor response [292, 293]. In support of these data, increased tumor T cell infiltration and altered cytokine production are observed in response to metformin treatment, which contributed to enhanced protection. Specifically, metformin is shown to decrease the production of pro-inflammatory cytokines and subsequently, protects T cells from becoming functionally exhausted [293]. The anti-inflammatory effects of metformin have not only been exploited in cancer, but also for the treatment of various autoimmune and chronic inflammatory diseases including SLE, rheumatoid arthritis, type 1 diabetes (T1D), and tuberculosis [269, 296, 297, 298]. In experimental models of arthritis and T1D metformin alters the Th17: Treg cell ratio, favoring the generation of an anti-inflammatory immune environment and abolished disease. Furthermore, metformin has been used to facilitate the generation of memory T cells by inducing β-oxidation, suggesting its use to potentiate vaccine responses [248, 293]. Considering these recent findings, metformin has become an attractive candidate for use as a host-directed therapy through its immunomodulatory effects.

As a chronic inflammatory disease, the therapeutic potential for the treatment of tuberculosis with metformin has gained considerable attention. Epidemiological studies have found T2DM patients receiving metformin treatment dramatically decreases their risk of developing active TB and improves their treatment outcomes, hence providing evidence that metformin elicits protection against TB [299, 300, 301, 302]. However, whether there is true value in treating TB patients with metformin and the mechanisms by which it may enhance host-mediated protection are currently not well understood. One hypothesis is that systemic hyperglycemia, as demonstrated in guinea pig models of Mtb infection, contributes to disease progression, whereby normalization of blood glucose by metformin results in improved disease outcome [29, 303]. Alternatively, metformin may directly alter immune cell function, similar to what is observed in other chronic inflammatory diseases.

Singhal et al. provided the first line of evidence indicating metformin's potential use for the treatment of TB in the absence of underlying T2DM. His group demonstrated that following Mtb challenge, mice that received metformin treatment displayed an increase in macrophage-induced bacterial killing, presumably through increased mitochondrial ROS and phagosome-lysosome fusion [302]. Additionally, lung lesion burden and inflammation were reduced in metformin treated mice, which was associated with an increase in both the number and proportion of Mtb-specific CD8 T cells in the lung [302]. A recent study has since validated these findings by showing an increased accumulation of CD8 T cell in the lungs of metformin treated compared to untreated Mtb infected mice [304]. Furthermore, this study suggests that metformin rejuvenates metabolic and cellular function of CD8 T cells in response to Mtb infection, which corresponds with decreased production of pro-inflammatory cytokines including IL-2 and TNF-α [304]. In another recent study, the investigators evaluated whether metformin confers the same anti-inflammatory and metabolic properties in human Mtb-exposed immune cells as in mice. Peripheral blood mononuclear cells (PBMC) were isolated from healthy humans and treated *ex vivo* with Mtb lysate in the presence

or absence of metformin [305]. This study found that like mouse studies, metformin treated Mtb stimulated PBMCs produced significantly decreased amounts of pro-inflammatory cytokines (TNF-α, IFN-γ, and IL-17) and enhanced cellular metabolism [305]. Based on these studies, there is a growing body of evidence that supports the positive influence that metformin has on TB outcome, the mechanism of which is largely unexplored.

REFERENCES

1.   Cambau, E. & Drancourt, M. Steps towards the discovery of Mycobacterium tuberculosis by Robert Koch, 1882. *Clin Microbiol Infect* **20**, 196-201 (2014).

2.   Houben, R.M. & Dodd, P.J. The Global Burden of Latent Tuberculosis Infection: A Re-estimation Using Mathematical Modelling. *PLoS Med* **13**, e1002152 (2016).

3.   WHO | Global tuberculosis report 2018. *WHO* (2019).

4.   WHO | Compendium of WHO guidelines and associated standards: ensuring optimum delivery of the cascade of care for patients with tuberculosis. *WHO* (2019).

5.   Churchyard, G. *et al.* What We Know About Tuberculosis Transmission: An Overview. *J Infect Dis* **216**, S629-s635 (2017).

6.   Hermans, S., Horsburgh, C.R., Jr. & Wood, R. A Century of Tuberculosis Epidemiology in the Northern and Southern Hemisphere: The Differential Impact of Control Interventions. *PLoS One* **10**, e0135179 (2015).

7.   Hargreaves, J.R. *et al.* The Social Determinants of Tuberculosis: From Evidence to Action. *Am J Public Health*, vol. 101, 2011, pp 654-662.

8.   Baker, M., Das, D., Venugopal, K. & Howden-Chapman, P. Tuberculosis associated with household crowding in a developed country. *J Epidemiol Community Health* **62**, 715-721 (2008).

9.   Lonnroth, K., Williams, B.G., Cegielski, P. & Dye, C. A consistent log-linear relationship between tuberculosis incidence and body mass index. *Int J Epidemiol* **39**, 149-155 (2010).

10.   Leung, C.C. *et al.* Smoking adversely affects treatment response, outcome and relapse in tuberculosis. *Eur Respir J* **45**, 738-745 (2015).

11.   WHO | Tuberculosis and HIV. *WHO* (2020).

12.   Bell, L.C.K. & Noursadeghi, M. Pathogenesis of HIV-1 and Mycobacterium tuberculosis co-infection. *Nat Rev Microbiol* **16**, 80-90 (2018).

13. Mogues, T., Goodrich, M.E., Ryan, L., LaCourse, R. & North, R.J. The relative importance of T cell subsets in immunity and immunopathology of airborne Mycobacterium tuberculosis infection in mice. *J Exp Med* **193**, 271-280 (2001).

14. Liu, E. *et al.* Tuberculosis incidence rate and risk factors among HIV-infected adults with access to antiretroviral therapy in Tanzania. *AIDS* **29**, 1391-1399 (2015).

15. Amelio, P. *et al.* HIV Infection Functionally Impairs Mycobacterium tuberculosis-Specific CD4 and CD8 T-Cell Responses. (2019).

16. Toossi, Z. *et al.* Increased replication of HIV-1 at sites of Mycobacterium tuberculosis infection: potential mechanisms of viral activation. *J Acquir Immune Defic Syndr* **28**, 1-8 (2001).

17. Zhang, Y., Nakata, K., Weiden, M. & Rom, W.N. Mycobacterium tuberculosis enhances human immunodeficiency virus-1 replication by transcriptional activation at the long terminal repeat. *J Clin Invest* **95**, 2324-2331 (1995).

18. Getahun, H., Gunneberg, C., Granich, R. & Nunn, P. HIV infection-associated tuberculosis: the epidemiology and the response. *Clin Infect Dis* **50 Suppl 3**, S201-207 (2010).

19. Campos, L.C., Rocha, M.V.V., Willers, D.M.C. & Silva, D.R. Characteristics of Patients with Smear-Negative Pulmonary Tuberculosis (TB) in a Region with High TB and HIV Prevalence. *PLoS One* **11** (2016).

20. Lee, P.H. *et al.* Glycemic Control and the Risk of Tuberculosis: A Cohort Study. *PLoS Med* **13**, e1002072 (2016).

21. Hayashi, S. & Chandramohan, D. Risk of active tuberculosis among people with diabetes mellitus: systematic review and meta-analysis. *Trop Med Int Health* **23**, 1058-1070 (2018).

22. Shen, T.C. *et al.* Increased risk of tuberculosis in patients with type 1 diabetes mellitus: results from a population-based cohort study in Taiwan. *Medicine (Baltimore)* **93**, e96 (2014).

23. Jeon, C.Y. & Murray, M.B. Diabetes mellitus increases the risk of active tuberculosis: a systematic review of 13 observational studies. *PLoS Med* **5**, e152 (2008).

24. Lee, M.R. *et al.* Diabetes Mellitus and Latent Tuberculosis Infection: A Systemic Review and Metaanalysis. *Clin Infect Dis*, vol. 64, 2017, pp 719-727.

25. Lee, P.H., Fu, H., Lee, M.R., Magee, M. & Lin, H.H. Tuberculosis and diabetes in low and moderate tuberculosis incidence countries. *Int J Tuberc Lung Dis* **22**, 7-16 (2018).

26. Dungan, K.M., Braithwaite, S.S. & Preiser, J.C. Stress hyperglycaemia. *Lancet* **373**, 1798-1807 (2009).

27. Leegaard, A. *et al.* Diabetes, glycemic control, and risk of tuberculosis: a population-based case-control study. *Diabetes Care* **34**, 2530-2535 (2011).

28. Baker, M.A. *et al.* The impact of diabetes on tuberculosis treatment outcomes: a systematic review. *BMC Med* **9**, 81 (2011).

29. Podell, B.K. *et al.* Non-diabetic hyperglycemia exacerbates disease severity in Mycobacterium tuberculosis infected guinea pigs. *PLoS One* **7**, e46824 (2012).

30. Tackling Drug-Resistant Infections Globally: Final Report and Recommendations; 2016.

31. Seaworth, B.J. & Griffith, D.E. Therapy of Multidrug-Resistant and Extensively Drug-Resistant Tuberculosis. *Microbiol Spectr* **5** (2017).

32. Furin, J., Cox, H. & Pai, M. Tuberculosis. *Lancet* **393**, 1642-1656 (2019).

33. Law, S., Piatek, A.S., Vincent, C., Oxlade, O. & Menzies, D. Emergence of drug resistance in patients with tuberculosis cared for by the Indian health-care system: a dynamic modelling study. *Lancet Public Health* **2**, e47-e55 (2017).

34. Gegia, M., Winters, N., Benedetti, A., van Soolingen, D. & Menzies, D. Treatment of isoniazid-resistant tuberculosis with first-line drugs: a systematic review and meta-analysis. *Lancet Infect Dis* **17**, 223-234 (2017).

35. Zelner, J.L. *et al.* Age-Specific Risks of Tuberculosis Infection From Household and Community Exposures and Opportunities for Interventions in a High-Burden Setting. *Am J Epidemiol*, vol. 180, 2014, pp 853-861.

36. Acuña-Villaorduña, C. *et al.* Host Determinants of Infectiousness in Smear-Positive Patients With Pulmonary Tuberculosis. *Open Forum Infect Dis* **6** (2019).

37. Davies, P.D. & Pai, M. The diagnosis and misdiagnosis of tuberculosis. *Int J Tuberc Lung Dis* **12**, 1226-1234 (2008).

38. WHO | Chest radiography in tuberculosis detection. *WHO* (2017).

39. Peter, J. *et al.* Urine for the diagnosis of tuberculosis: current approaches, clinical applicability, and new developments. *Curr Opin Pulm Med* **16**, 262-270 (2010).

40. Goletti, D., Lee, M.R., Wang, J.Y., Walter, N. & Ottenhoff, T.H.M. Update on tuberculosis biomarkers: From correlates of risk, to correlates of active disease and of cure from disease. *Respirology* **23**, 455-466 (2018).

41. Sigal, G.B. *et al.* A Novel Sensitive Immunoassay Targeting the 5-Methylthio-d-Xylofuranose-Lipoarabinomannan Epitope Meets the WHO's Performance Target for Tuberculosis Diagnosis. *J Clin Microbiol* **56** (2018).

42. Lee, J.Y. Diagnosis and treatment of extrapulmonary tuberculosis. *Tuberc Respir Dis (Seoul)* **78**, 47-55 (2015).

43. Chakravorty, S. *et al.* The New Xpert MTB/RIF Ultra: Improving Detection of Mycobacterium tuberculosis and Resistance to Rifampin in an Assay Suitable for Point-of-Care Testing. *mBio*, vol. 8, 2017.

44. Steingart, K.R. *et al.* Xpert® MTB/RIF assay for pulmonary tuberculosis and rifampicin resistance in adults. *Cochrane Database Syst Rev*, vol. 2014, 2014.

45. Pai, M. *et al.* Gamma interferon release assays for detection of Mycobacterium tuberculosis infection. *Clin Microbiol Rev* **27**, 3-20 (2014).

46. Farhat, M., Greenaway, C., Pai, M. & Menzies, D. False-positive tuberculin skin tests: what is the absolute effect of BCG and non-tuberculous mycobacteria? *Int J Tuberc Lung Dis* **10**, 1192-1204 (2006).

47. Behr, M.A., Edelstein, P.H. & Ramakrishnan, L. Revisiting the timetable of tuberculosis. *Bmj* **362**, k2738 (2018).

48. WHO | Latent TB Infection : Updated and consolidated guidelines for programmatic management. *WHO* (2019).

49. Haley, C.A. Treatment of Latent Tuberculosis Infection. *Microbiol Spectr* **5** (2017).

50. Seddon, J.A. *et al.* Hearing loss in patients on treatment for drug-resistant tuberculosis. *Eur Respir J* **40**, 1277-1286 (2012).

51. Akolo, C., Adetifa, I., Shepperd, S. & Volmink, J. Treatment of latent tuberculosis infection in HIV infected persons. *Cochrane Database Syst Rev*, Cd000171 (2010).

52.   Gengenbacher, M., Nieuwenhuizen, N.E. & Kaufmann, S. BCG - old workhorse, new skills. *Curr Opin Immunol* **47**, 8-16 (2017).

53.   Mahomed, H. *et al.* The impact of a change in bacille Calmette-Guerin vaccine policy on tuberculosis incidence in children in Cape Town, South Africa. *Pediatr Infect Dis J* **25**, 1167-1172 (2006).

54.   Colditz, G.A. *et al.* Efficacy of BCG vaccine in the prevention of tuberculosis. Meta-analysis of the published literature. *Jama* **271**, 698-702 (1994).

55.   Mangtani, P. *et al.* Protection by BCG vaccine against tuberculosis: a systematic review of randomized controlled trials. *Clin Infect Dis* **58**, 470-480 (2014).

56.   Pym, A.S. *et al.* Recombinant BCG exporting ESAT-6 confers enhanced protection against tuberculosis. *Nat Med* **9**, 533-539 (2003).

57.   Ritz, N. *et al.* The influence of bacille Calmette-Guerin vaccine strain on the immune response against tuberculosis: a randomized trial. *Am J Respir Crit Care Med* **185**, 213-222 (2012).

58.   Luca, S. & Mihaescu, T. History of BCG Vaccine. *Maedica (Buchar)* **8**, 53-58 (2013).

59.   Orme, I.M. The Achilles heel of BCG. *Tuberculosis (Edinb)* **90**, 329-332 (2010).

60.   Chen, C.Y. *et al.* A critical role for CD8 T cells in a nonhuman primate model of tuberculosis. *PLoS Pathog* **5**, e1000392 (2009).

61.   Chackerian, A.A., Perera, T.V. & Behar, S.M. Gamma interferon-producing CD4+ T lymphocytes in the lung correlate with resistance to infection with Mycobacterium tuberculosis. *Infect Immun* **69**, 2666-2674 (2001).

62.   Saunders, B.M., Frank, A.A., Orme, I.M. & Cooper, A.M. CD4 is required for the development of a protective granulomatous response to pulmonary tuberculosis. *Cell Immunol* **216**, 65-72 (2002).

63.   Lin, P.L. *et al.* CD4 T cell depletion exacerbates acute Mycobacterium tuberculosis while reactivation of latent infection is dependent on severity of tissue depletion in cynomolgus macaques. *AIDS Res Hum Retroviruses* **28**, 1693-1702 (2012).

64.   Sullivan, B.M. *et al.* Increased susceptibility of mice lacking T-bet to infection with Mycobacterium tuberculosis correlates with increased IL-10 and decreased IFN-gamma production. *J Immunol* **175**, 4593-4602 (2005).

65.   Flynn, J.L. *et al.* An essential role for interferon gamma in resistance to Mycobacterium tuberculosis infection. *J Exp Med* **178**, 2249-2254 (1993).

66.   Kaveh, D.A., Bachy, V.S., Hewinson, R.G. & Hogarth, P.J. Systemic BCG immunization induces persistent lung mucosal multifunctional CD4 T(EM) cells which expand following virulent mycobacterial challenge. *PLoS One* **6**, e21566 (2011).

67.   Ravn, P., Boesen, H., Pedersen, B.K. & Andersen, P. Human T cell responses induced by vaccination with Mycobacterium bovis bacillus Calmette-Guerin. *J Immunol* **158**, 1949-1955 (1997).

68.   Fletcher, H.A. *et al.* T-cell activation is an immune correlate of risk in BCG vaccinated infants. *Nat Commun* **7**, 11290 (2016).

69.   Verreck, F.A. *et al.* MVA.85A boosting of BCG and an attenuated, phoP deficient M. tuberculosis vaccine both show protective efficacy against tuberculosis in rhesus macaques. *PLoS One* **4**, e5264 (2009).

70.   Scriba, T.J. *et al.* Modified vaccinia Ankara-expressing Ag85A, a novel tuberculosis vaccine, is safe in adolescents and children, and induces polyfunctional CD4+ T cells. *Eur J Immunol* **40**, 279-290 (2010).

71.   Goonetilleke, N.P. *et al.* Enhanced immunogenicity and protective efficacy against Mycobacterium tuberculosis of bacille Calmette-Guerin vaccine using mucosal administration and boosting with a recombinant modified vaccinia virus Ankara. *J Immunol* **171**, 1602-1609 (2003).

72.   McShane, H. *et al.* Recombinant modified vaccinia virus Ankara expressing antigen 85A boosts BCG-primed and naturally acquired antimycobacterial immunity in humans. *Nat Med* **10**, 1240-1244 (2004).

73.   Sharpe, S. *et al.* Alternative BCG delivery strategies improve protection against Mycobacterium tuberculosis in non-human primates: Protection associated with mycobacterial antigen-specific CD4 effector memory T-cell populations. *Tuberculosis (Edinb)* **101**, 174-190 (2016).

74.   Caruso, A.M. *et al.* Mice deficient in CD4 T cells have only transiently diminished levels of IFN-gamma, yet succumb to tuberculosis. *J Immunol* **162**, 5407-5416 (1999).

75.   Andersen, P. & Smedegaard, B. CD4(+) T-cell subsets that mediate immunological memory to Mycobacterium tuberculosis infection in mice. *Infect Immun* **68**, 621-629 (2000).

76.   Kaushal, D. *et al.* Mucosal vaccination with attenuated Mycobacterium tuberculosis induces strong central memory responses and protects against tuberculosis. *Nat Commun* **6**, 8533 (2015).

77.   Mittrucker, H.W. *et al.* Poor correlation between BCG vaccination-induced T cell responses and protection against tuberculosis. *Proc Natl Acad Sci U S A* **104**, 12434-12439 (2007).

78.   Perdomo, C. *et al.* Mucosal BCG Vaccination Induces Protective Lung-Resident Memory T Cell Populations against Tuberculosis. (2016).

79.   Wu, C.Y. *et al.* Distinct lineages of T(H)1 cells have differential capacities for memory cell generation in vivo. *Nat Immunol* **3**, 852-858 (2002).

80.   Reiley, W.W. *et al.* Distinct functions of antigen-specific CD4 T cells during murine Mycobacterium tuberculosis infection. (2010).

81.   Lerner, T.R., Borel, S. & Gutierrez, M.G. The innate immune response in human tuberculosis. *Cell Microbiol* **17**, 1277-1285 (2015).

82.   Li, Y., Wang, Y. & Liu, X. The role of airway epithelial cells in response to mycobacteria infection. *Clin Dev Immunol* **2012**, 791392 (2012).

83.   Roy, S., Sharma, S., Sharma, M., Aggarwal, R. & Bose, M. Induction of nitric oxide release from the human alveolar epithelial cell line A549: an in vitro correlate of innate immune response to Mycobacterium tuberculosis. *Immunology* **112**, 471-480 (2004).

84.   Debbabi, H. *et al.* Primary type II alveolar epithelial cells present microbial antigens to antigen-specific CD4+ T cells. *Am J Physiol Lung Cell Mol Physiol* **289**, L274-279 (2005).

85.   Ryndak, M.B. & Laal, S. Mycobacterium tuberculosis Primary Infection and Dissemination: A Critical Role for Alveolar Epithelial Cells. *Front Cell Infect Microbiol* **9**, 299 (2019).

86.   Orme, I.M., Robinson, R.T. & Cooper, A.M. The balance between protective and pathogenic immune responses in the TB-infected lung. *Nat Immunol* **16**, 57-63 (2015).

87.   Awuh, J.A. & Flo, T.H. Molecular basis of mycobacterial survival in macrophages. *Cell Mol Life Sci* **74**, 1625-1648 (2017).

88. Huang, Z. *et al.* Mycobacterium tuberculosis-Induced Polarization of Human Macrophage Orchestrates the Formation and Development of Tuberculous Granulomas In Vitro. *PLoS One* **10**, e0129744 (2015).

89. Queval, C.J., Brosch, R. & Simeone, R. The Macrophage: A Disputed Fortress in the Battle against Mycobacterium tuberculosis. *Front Microbiol* **8**, 2284 (2017).

90. Refai, A., Gritli, S., Barbouche, M.R. & Essafi, M. Mycobacterium tuberculosis Virulent Factor ESAT-6 Drives Macrophage Differentiation Toward the Pro-inflammatory M1 Phenotype and Subsequently Switches It to the Anti-inflammatory M2 Phenotype. *Front Cell Infect Microbiol* **8**, 327 (2018).

91. Herbst, S., Schaible, U.E. & Schneider, B.E. Interferon gamma activated macrophages kill mycobacteria by nitric oxide induced apoptosis. *PLoS One* **6**, e19105 (2011).

92. Sturgill-Koszycki, S. *et al.* Lack of acidification in Mycobacterium phagosomes produced by exclusion of the vesicular proton-ATPase. *Science* **263**, 678-681 (1994).

93. Queval, C.J. *et al.* Mycobacterium tuberculosis Controls Phagosomal Acidification by Targeting CISH-Mediated Signaling. *Cell Rep* **20**, 3188-3198 (2017).

94. Houben, D. *et al.* ESX-1-mediated translocation to the cytosol controls virulence of mycobacteria. *Cell Microbiol* **14**, 1287-1298 (2012).

95. Pedrosa, J. *et al.* Neutrophils play a protective nonphagocytic role in systemic Mycobacterium tuberculosis infection of mice. *Infect Immun* **68**, 577-583 (2000).

96. Silva, M.T., Silva, M.N. & Appelberg, R. Neutrophil-macrophage cooperation in the host defence against mycobacterial infections. *Microb Pathog* **6**, 369-380 (1989).

97. Braian, C., Hogea, V. & Stendahl, O. Mycobacterium tuberculosis- induced neutrophil extracellular traps activate human macrophages. *J Innate Immun* **5**, 591-602 (2013).

98. Ramos-Kichik, V. *et al.* Neutrophil extracellular traps are induced by Mycobacterium tuberculosis. *Tuberculosis (Edinb)* **89**, 29-37 (2009).

99. Dallenga, T. *et al.* M. tuberculosis-Induced Necrosis of Infected Neutrophils Promotes Bacterial Growth Following Phagocytosis by Macrophages. *Cell Host Microbe* **22**, 519-530.e513 (2017).

100. Panteleev, A.V. *et al.* Severe Tuberculosis in Humans Correlates Best with Neutrophil Abundance and Lymphocyte Deficiency and Does Not Correlate with Antigen-Specific CD4 T-Cell Response. *Front Immunol* **8**, 963 (2017).

101.	Ackart, D.F. *et al.* Expression of Antimicrobial Drug Tolerance by Attached Communities of Mycobacterium tuberculosis. *Pathog Dis* **70**, 359-369 (2014).

102.	Wolf, A.J. *et al.* Initiation of the adaptive immune response to Mycobacterium tuberculosis depends on antigen production in the local lymph node, not the lungs. *J Exp Med*, vol. 205, 2008, pp 105-115.

103.	Wolf, A.J. *et al.* Mycobacterium tuberculosis infects dendritic cells with high frequency and impairs their function in vivo. *J Immunol* **179**, 2509-2519 (2007).

104.	Reiley, W.W. *et al.* ESAT-6-specific CD4 T cell responses to aerosol Mycobacterium tuberculosis infection are initiated in the mediastinal lymph nodes. *Proc Natl Acad Sci U S A* **105**, 10961-10966 (2008).

105.	Marino, S. *et al.* Dendritic cell trafficking and antigen presentation in the human immune response to Mycobacterium tuberculosis. *J Immunol* **173**, 494-506 (2004).

106.	Al-Muhsen, S. & Casanova, J.L. The genetic heterogeneity of mendelian susceptibility to mycobacterial diseases. *J Allergy Clin Immunol* **122**, 1043-1051; quiz 1052-1043 (2008).

107.	Scanga, C.A. *et al.* Depletion of CD4(+) T cells causes reactivation of murine persistent tuberculosis despite continued expression of interferon gamma and nitric oxide synthase 2. *J Exp Med* **192**, 347-358 (2000).

108.	Lawn, S.D., Myer, L., Edwards, D., Bekker, L.G. & Wood, R. Short-term and long-term risk of tuberculosis associated with CD4 cell recovery during antiretroviral therapy in South Africa. *Aids* **23**, 1717-1725 (2009).

109.	Chackerian, A.A., Alt, J.M., Perera, T.V., Dascher, C.C. & Behar, S.M. Dissemination of Mycobacterium tuberculosis is influenced by host factors and precedes the initiation of T-cell immunity. *Infect Immun* **70**, 4501-4509 (2002).

110.	Samstein, M. *et al.* Essential yet limited role for CCR2(+) inflammatory monocytes during Mycobacterium tuberculosis-specific T cell priming. *Elife* **2**, e01086 (2013).

111.	Srivastava, S. & Ernst, J.D. Cell-to-cell transfer of M. tuberculosis antigens optimizes CD4 T cell priming. *Cell Host Microbe* **15**, 741-752 (2014).

112.	Gopal, R. *et al.* Unexpected role for IL-17 in protective immunity against hypervirulent Mycobacterium tuberculosis HN878 infection. *PLoS Pathog* **10**, e1004099 (2014).

113. Khader, S.A. *et al.* In a murine tuberculosis model, the absence of homeostatic chemokines delays granuloma formation and protective immunity. *J Immunol* **183**, 8004-8014 (2009).

114. Disseminated tuberculosis in interferon gamma gene-disrupted mice. *J Exp Med*, vol. 178, 1993, pp 2243-2247.

115. Gallegos, A.M. *et al.* A gamma interferon independent mechanism of CD4 T cell mediated control of M. tuberculosis infection in vivo. *PLoS Pathog* **7**, e1002052 (2011).

116. Cruz, A. *et al.* BCG vaccination-induced long-lasting control of Mycobacterium tuberculosis correlates with the accumulation of a novel population of CD4(+)IL-17(+)TNF(+)IL-2(+) T cells. *Vaccine* **33**, 85-91 (2015).

117. Gideon, H.P. *et al.* Variability in tuberculosis granuloma T cell responses exists, but a balance of pro- and anti-inflammatory cytokines is associated with sterilization. *PLoS Pathog* **11**, e1004603 (2015).

118. Wozniak, T.M., Saunders, B.M., Ryan, A.A. & Britton, W.J. Mycobacterium bovis BCG-specific Th17 cells confer partial protection against Mycobacterium tuberculosis infection in the absence of gamma interferon. *Infect Immun* **78**, 4187-4194 (2010).

119. Freches, D. *et al.* Mice genetically inactivated in interleukin-17A receptor are defective in long-term control of Mycobacterium tuberculosis infection. *Immunology* **140**, 220-231 (2013).

120. Algood, H.M., Lin, P.L. & Flynn, J.L. Tumor necrosis factor and chemokine interactions in the formation and maintenance of granulomas in tuberculosis. *Clin Infect Dis* **41 Suppl 3**, S189-193 (2005).

121. Roach, D.R. *et al.* TNF regulates chemokine induction essential for cell recruitment, granuloma formation, and clearance of mycobacterial infection. *J Immunol* **168**, 4620-4627 (2002).

122. Chakravarty, S.D. *et al.* Tumor necrosis factor blockade in chronic murine tuberculosis enhances granulomatous inflammation and disorganizes granulomas in the lungs. *Infect Immun* **76**, 916-926 (2008).

123. Anderson, K.G. *et al.* Intravascular staining for discrimination of vascular and tissue leukocytes. *Nat Protoc* **9**, 209-222 (2014).

124. Sakai, S. *et al.* Control of Mycobacterium tuberculosis infection by a subset of lung parenchyma homing CD4 T cells. *J Immunol* **192**, 2965-2969 (2014).

125. Sakai, S. *et al.* Cutting edge: control of Mycobacterium tuberculosis infection by a subset of lung parenchyma-homing CD4 T cells. *J Immunol* **192**, 2965-2969 (2014).

126. Sallin, M.A. *et al.* Th1 Differentiation Drives the Accumulation of Intravascular, Non-protective CD4 T Cells during Tuberculosis. *Cell Rep* **18**, 3091-3104 (2017).

127. Lyadova, I. & Nikitina, I. Cell Differentiation Degree as a Factor Determining the Role for Different T-Helper Populations in Tuberculosis Protection. *Front Immunol* **10**, 972 (2019).

128. Moguche, A.O. *et al.* ICOS and Bcl6-dependent pathways maintain a CD4 T cell population with memory-like properties during tuberculosis. *J Exp Med* **212**, 715-728 (2015).

129. Nikitina, I.Y. *et al.* Mtb-specific CD27low CD4 T cells as markers of lung tissue destruction during pulmonary tuberculosis in humans. *PLoS One* **7**, e43733 (2012).

130. Lindenstrom, T., Knudsen, N.P., Agger, E.M. & Andersen, P. Control of chronic mycobacterium tuberculosis infection by CD4 KLRG1- IL-2-secreting central memory cells. *J Immunol* **190**, 6311-6319 (2013).

131. Carpenter, S.M., Yang, J.D., Lee, J., Barreira-Silva, P. & Behar, S.M. Vaccine-elicited memory CD4+ T cell expansion is impaired in the lungs during tuberculosis. *PLoS Pathog* **13**, e1006704 (2017).

132. Nandakumar, S., Kannanganat, S., Posey, J.E., Amara, R.R. & Sable, S.B. Attrition of T-cell functions and simultaneous upregulation of inhibitory markers correspond with the waning of BCG-induced protection against tuberculosis in mice. *PLoS One* **9**, e113951 (2014).

133. Lindenstrom, T. *et al.* T Cells Primed by Live Mycobacteria Versus a Tuberculosis Subunit Vaccine Exhibit Distinct Functional Properties. *EBioMedicine* **27**, 27-39 (2018).

134. Moguche, A.O. *et al.* Antigen Availability Shapes T Cell Differentiation and Function during Tuberculosis. *Cell Host Microbe* **21**, 695-706.e695 (2017).

135. Wong, E.A. *et al.* Low Levels of T Cell Exhaustion in Tuberculous Lung Granulomas. *Infect Immun* **86** (2018).

136. Wherry, E.J. & Kurachi, M. Molecular and cellular insights into T cell exhaustion. *Nat Rev Immunol* **15**, 486-499 (2015).

137. Jayaraman, P. *et al.* TIM3 Mediates T Cell Exhaustion during Mycobacterium tuberculosis Infection. *PLoS Pathog* **12**, e1005490 (2016).

138. Sakai, S. *et al.* CD4 T Cell-Derived IFN-gamma Plays a Minimal Role in Control of Pulmonary Mycobacterium tuberculosis Infection and Must Be Actively Repressed by PD-1 to Prevent Lethal Disease. *PLoS Pathog* **12**, e1005667 (2016).

139. Tezera, L.B. *et al.* Anti-PD-1 immunotherapy leads to tuberculosis reactivation via dysregulation of TNF-alpha. *Elife* **9** (2020).

140. Lázár-Molnár, E. *et al.* Programmed death-1 (PD-1)–deficient mice are extraordinarily sensitive to tuberculosis. (2010).

141. Barber, D.L., Mayer-Barber, K.D., Feng, C.G., Sharpe, A.H. & Sher, A. CD4 T cells promote rather than control tuberculosis in the absence of PD-1-mediated inhibition. *J Immunol* **186**, 1598-1607 (2011).

142. Anastasopoulou, A., Ziogas, D.C., Samarkos, M., Kirkwood, J.M. & Gogas, H. Reactivation of tuberculosis in cancer patients following administration of immune checkpoint inhibitors: current evidence and clinical practice recommendations. *J Immunother Cancer* **7**, 239 (2019).

143. Ramakrishnan, L. Revisiting the role of the granuloma in tuberculosis. *Nat Rev Immunol* **12**, 352-366 (2012).

144. Russell, D.G., Cardona, P.J., Kim, M.J., Allain, S. & Altare, F. Foamy macrophages and the progression of the human TB granuloma. *Nat Immunol* **10**, 943-948 (2009).

145. Pessanha, A.P., Martins, R.A., Mattos-Guaraldi, A.L., Vianna, A. & Moreira, L.O. Arginase-1 expression in granulomas of tuberculosis patients. *FEMS Immunol Med Microbiol* **66**, 265-268 (2012).

146. Schreiber, H.A. *et al.* Inflammatory dendritic cells migrate in and out of transplanted chronic mycobacterial granulomas in mice. *J Clin Invest* **121**, 3902-3913 (2011).

147. Scriba, T.J. *et al.* Sequential inflammatory processes define human progression from M. tuberculosis infection to tuberculosis disease. *PLoS Pathog* **13**, e1006687 (2017).

148. Stek, C. *et al.* The Immune Mechanisms of Lung Parenchymal Damage in Tuberculosis and the Role of Host-Directed Therapy. *Front Microbiol* **9**, 2603 (2018).

149. Charles A Janeway, J., Travers, P., Walport, M. & Shlomchik, M.J. Generation of lymphocytes in bone marrow and thymus. *Immunobiology: The Immune System in Health and Disease.*, 5 edn. Garland Science: New York, 2001.

150. den Braber, I. *et al.* Maintenance of peripheral naive T cells is sustained by thymus output in mice but not humans. *Immunity* **36**, 288-297 (2012).

151. Bains, I., Antia, R., Callard, R. & Yates, A.J. Quantifying the development of the peripheral naive CD4+ T-cell pool in humans. *Blood* **113**, 5480-5487 (2009).

152. Campbell, J.J. & Butcher, E.C. Chemokines in tissue-specific and microenvironment-specific lymphocyte homing. *Curr Opin Immunol* **12**, 336-341 (2000).

153. Jenkins, M.K. *et al.* In vivo activation of antigen-specific CD4 T cells. *Annu Rev Immunol* **19**, 23-45 (2001).

154. Opata, M.M. & Stephens, R. Early Decision: Effector and Effector Memory T Cell Differentiation in Chronic Infection. *Curr Immunol Rev* **9**, 190-206 (2013).

155. Zhou, L., Chong, M.M. & Littman, D.R. Plasticity of CD4+ T cell lineage differentiation. *Immunity* **30**, 646-655 (2009).

156. Kaplan, M.H. Th9 cells: differentiation and disease. *Immunol Rev* **252**, 104-115 (2013).

157. Eyerich, S. *et al.* Th22 cells represent a distinct human T cell subset involved in epidermal immunity and remodeling. *J Clin Invest* **119**, 3573-3585 (2009).

158. Szabo, S.J. *et al.* A novel transcription factor, T-bet, directs Th1 lineage commitment. *Cell* **100**, 655-669 (2000).

159. Zheng, W. & Flavell, R.A. The transcription factor GATA-3 is necessary and sufficient for Th2 cytokine gene expression in CD4 T cells. *Cell* **89**, 587-596 (1997).

160. Ivanov, II *et al.* The orphan nuclear receptor RORgammat directs the differentiation program of proinflammatory IL-17+ T helper cells. *Cell* **126**, 1121-1133 (2006).

161. Nurieva, R.I. *et al.* Bcl6 mediates the development of T follicular helper cells. *Science* **325**, 1001-1005 (2009).

162. Kanamori, M., Nakatsukasa, H., Okada, M., Lu, Q. & Yoshimura, A. Induced Regulatory T Cells: Their Development, Stability, and Applications. *Trends Immunol* **37**, 803-811 (2016).

163. Harrison, O.J. *et al.* Commensal-specific T cell plasticity promotes rapid tissue adaptation to injury. (2019).

164. Lanzavecchia, A. & Sallusto, F. Progressive differentiation and selection of the fittest in the immune response. *Nat Rev Immunol* **2**, 982-987 (2002).

165. Gattinoni, L., Powell, D.J., Jr., Rosenberg, S.A. & Restifo, N.P. Adoptive immunotherapy for cancer: building on success. *Nat Rev Immunol* **6**, 383-393 (2006).

166. Kishton, R.J., Sukumar, M. & Restifo, N.P. Metabolic Regulation of T Cell Longevity and Function in Tumor Immunotherapy. *Cell Metab* **26**, 94-109 (2017).

167. Gattinoni, L. *et al.* A human memory T cell subset with stem cell-like properties. *Nat Med* **17**, 1290-1297 (2011).

168. Lugli, E. *et al.* Superior T memory stem cell persistence supports long-lived T cell memory. *J Clin Invest* **123**, 594-599 (2013).

169. Mpande, C.A.M. *et al.* Functional, Antigen-Specific Stem Cell Memory (TSCM) CD4(+) T Cells Are Induced by Human Mycobacterium tuberculosis Infection. *Front Immunol* **9**, 324 (2018).

170. Fuertes Marraco, S.A. *et al.* Long-lasting stem cell-like memory CD8+ T cells with a naive-like profile upon yellow fever vaccination. *Sci Transl Med* **7**, 282ra248 (2015).

171. Sallusto, F., Lenig, D., Forster, R., Lipp, M. & Lanzavecchia, A. Two subsets of memory T lymphocytes with distinct homing potentials and effector functions. *Nature* **401**, 708-712 (1999).

172. Ponta, H., Sherman, L. & Herrlich, P.A. CD44: from adhesion molecules to signalling regulators. *Nat Rev Mol Cell Biol* **4**, 33-45 (2003).

173. Baaten, B. *et al.* Regulation of Antigen-Experienced T Cells: Lessons from the Quintessential Memory Marker CD44. *Frontiers in Immunology* **3** (2012).

174. Purton, J.F. *et al.* Antiviral CD4+ memory T cells are IL-15 dependent. *J Exp Med* **204**, 951-961 (2007).

175. Raud, B., McGuire, P.J., Jones, R.G., Sparwasser, T. & Berod, L. Fatty acid metabolism in CD8(+) T cell memory: Challenging current concepts. *Immunol Rev* **283**, 213-231 (2018).

176.   Klebanoff, C.A. *et al.* Central memory self/tumor-reactive CD8+ T cells confer superior antitumor immunity compared with effector memory T cells. *Proc Natl Acad Sci U S A* **102**, 9571-9576 (2005).

177.   Farber, D.L., Yudanin, N.A. & Restifo, N.P. Human memory T cells: generation, compartmentalization and homeostasis. *Nat Rev Immunol* **14**, 24-35 (2014).

178.   Rutishauser, R.L. *et al.* Transcriptional repressor Blimp-1 promotes CD8(+) T cell terminal differentiation and represses the acquisition of central memory T cell properties. *Immunity* **31**, 296-308 (2009).

179.   Crotty, S., Johnston, R.J. & Schoenberger, S.P. Effectors and memories: Bcl-6 and Blimp-1 in T and B lymphocyte differentiation. *Nat Immunol* **11**, 114-120 (2010).

180.   Vodnala, S.K. *et al.* T cell stemness and dysfunction in tumors are triggered by a common mechanism. *Science* **363** (2019).

181.   Kallies, A., Xin, A., Belz, G.T. & Nutt, S.L. Blimp-1 transcription factor is required for the differentiation of effector CD8(+) T cells and memory responses. *Immunity* **31**, 283-295 (2009).

182.   Fu, S.H., Yeh, L.T., Chu, C.C., Yen, B.L. & Sytwu, H.K. New insights into Blimp-1 in T lymphocytes: a divergent regulator of cell destiny and effector function. *J Biomed Sci* **24**, 49 (2017).

183.   Bankoti, R. *et al.* Differential regulation of Effector and Regulatory T cell function by Blimp1. *Sci Rep*, vol. 7, 2017.

184.   Bach, M.P. *et al.* Premature terminal differentiation protects from deregulated lymphocyte activation by ITK-Syk. *J Immunol* **192**, 1024-1033 (2014).

185.   Ichii, H. *et al.* Bcl6 is essential for the generation of long-term memory CD4+ T cells. *Int Immunol* **19**, 427-433 (2007).

186.   Pepper, M., Pagan, A.J., Igyarto, B.Z., Taylor, J.J. & Jenkins, M.K. Opposing signals from the Bcl6 transcription factor and the interleukin-2 receptor generate T helper 1 central and effector memory cells. *Immunity* **35**, 583-595 (2011).

187.   Gasper, D.J., Tejera, M.M. & Suresh, M. CD4 T-Cell Memory Generation and Maintenance. *Crit Rev Immunol* **34**, 121-146 (2014).

188.   Fearon, D.T., Manders, P. & Wagner, S.D. Arrested differentiation, the self-renewing memory lymphocyte, and vaccination. *Science* **293**, 248-250 (2001).

189. Gattinoni, L. *et al.* Acquisition of full effector function in vitro paradoxically impairs the in vivo antitumor efficacy of adoptively transferred CD8+ T cells. *J Clin Invest*, vol. 115, 2005, pp 1616-1626.

190. Kim, C., Wilson, T., Fischer, K.F. & Williams, M.A. Sustained interactions between T cell receptors and antigens promote the differentiation of CD4(+) memory T cells. *Immunity* **39**, 508-520 (2013).

191. Sarkar, S. *et al.* Strength of stimulus and clonal competition impact the rate of memory CD8 T cell differentiation. *J Immunol* **179**, 6704-6714 (2007).

192. Marshall, H.D. *et al.* Differential expression of Ly6C and T-bet distinguish effector and memory Th1 CD4(+) cell properties during viral infection. *Immunity* **35**, 633-646 (2011).

193. Joshi, N.S. *et al.* Inflammation directs memory precursor and short-lived effector CD8(+) T cell fates via the graded expression of T-bet transcription factor. *Immunity* **27**, 281-295 (2007).

194. Jaeger-Ruckstuhl, C.A. *et al.* TNIK signaling imprints CD8(+) T cell memory formation early after priming. *Nat Commun* **11**, 1632 (2020).

195. D'Souza, W.N. & Hedrick, S.M. Cutting edge: latecomer CD8 T cells are imprinted with a unique differentiation program. *J Immunol* **177**, 777-781 (2006).

196. Pardieck, I.N., Beyrend, G., Redeker, A. & Arens, R. Cytomegalovirus infection and progressive differentiation of effector-memory T cells. *F1000Res* **7** (2018).

197. Lohning, M. *et al.* Long-lived virus-reactive memory T cells generated from purified cytokine-secreting T helper type 1 and type 2 effectors. *J Exp Med* **205**, 53-61 (2008).

198. Harrington, L.E., Janowski, K.M., Oliver, J.R., Zajac, A.J. & Weaver, C.T. Memory CD4 T cells emerge from effector T-cell progenitors. *Nature* **452**, 356-360 (2008).

199. Romero, P. *et al.* Four functionally distinct populations of human effector-memory CD8+ T lymphocytes. *J Immunol* **178**, 4112-4119 (2007).

200. Plumlee, C.R., Sheridan, B.S., Cicek, B.B. & Lefrancois, L. Environmental cues dictate the fate of individual CD8+ T cells responding to infection. *Immunity* **39**, 347-356 (2013).

201. Cano-Gamez, E. *et al.* Single-cell transcriptomics identifies an effectorness gradient shaping the response of CD4+ T cells to cytokines. *Nat Commun*, vol. 11, 2020.

202. Crompton, J.G. *et al.* Lineage relationship of CD8(+) T cell subsets is revealed by progressive changes in the epigenetic landscape. *Cell Mol Immunol* **13**, 502-513 (2016).

203. Pollizzi, K.N. *et al.* Asymmetric inheritance of mTORC1 kinase activity during division dictates CD8(+) T cell differentiation. *Nat Immunol* **17**, 704-711 (2016).

204. Chang, J.T. *et al.* Asymmetric T lymphocyte division in the initiation of adaptive immune responses. *Science* **315**, 1687-1691 (2007).

205. Chang, J.T. *et al.* Asymmetric proteasome segregation as a mechanism for unequal partitioning of the transcription factor T-bet during T lymphocyte division. *Immunity* **34**, 492-504 (2011).

206. Mills, E.L., Kelly, B. & O'Neill, L.A.J. Mitochondria are the powerhouses of immunity. *Nature Immunology* **18**, 488 (2017).

207. O'Neill, L.A., Kishton, R.J. & Rathmell, J. A guide to immunometabolism for immunologists. *Nat Rev Immunol* **16**, 553-565 (2016).

208. Liberti, M.V. & Locasale, J.W. The Warburg Effect: How Does it Benefit Cancer Cells? *Trends Biochem Sci* **41**, 211-218 (2016).

209. Rao, R.R., Li, Q., Odunsi, K. & Shrikant, P.A. The mTOR kinase determines effector versus memory CD8+ T cell fate by regulating the expression of transcription factors T-bet and Eomesodermin. *Immunity* **32**, 67-78 (2010).

210. Delgoffe, G.M. *et al.* The mTOR kinase differentially regulates effector and regulatory T cell lineage commitment. *Immunity* **30**, 832-844 (2009).

211. Brown, N.F., Stefanovic-Racic, M., Sipula, I.J. & Perdomo, G. The mammalian target of rapamycin regulates lipid metabolism in primary cultures of rat hepatocytes. *Metabolism* **56**, 1500-1507 (2007).

212. Salmond, R.J. mTOR Regulation of Glycolytic Metabolism in T Cells. *Front Cell Dev Biol* **6**, 122 (2018).

213. Frauwirth, K.A. *et al.* The CD28 signaling pathway regulates glucose metabolism. *Immunity* **16**, 769-777 (2002).

214. Liu, Y., Zhang, D.T. & Liu, X.G. mTOR signaling in T cell immunity and autoimmunity. *Int Rev Immunol* **34**, 50-66 (2015).

215. Wang, R. *et al.* The transcription factor Myc controls metabolic reprogramming upon T lymphocyte activation. *Immunity* **35**, 871-882 (2011).

216. Fox, C.J., Hammerman, P.S. & Thompson, C.B. Fuel feeds function: energy metabolism and the T-cell response. *Nat Rev Immunol* **5**, 844-852 (2005).

217. Cham, C.M. & Gajewski, T.F. Glucose availability regulates IFN-gamma production and p70S6 kinase activation in CD8+ effector T cells. *J Immunol* **174**, 4670-4677 (2005).

218. Hedeskov, C.J. Early effects of phytohaemagglutinin on glucose metabolism of normal human lymphocytes. *Biochem J* **110**, 373-380 (1968).

219. Michalek, R.D. *et al.* Estrogen-related receptor-alpha is a metabolic regulator of effector T-cell activation and differentiation. *Proc Natl Acad Sci U S A* **108**, 18348-18353 (2011).

220. Greiner, E.F., Guppy, M. & Brand, K. Glucose is essential for proliferation and the glycolytic enzyme induction that provokes a transition to glycolytic energy production. *J Biol Chem* **269**, 31484-31490 (1994).

221. Tripmacher, R. *et al.* Human CD4(+) T cells maintain specific functions even under conditions of extremely restricted ATP production. *Eur J Immunol* **38**, 1631-1642 (2008).

222. Shi, L.Z. *et al.* HIF1α–dependent glycolytic pathway orchestrates a metabolic checkpoint for the differentiation of TH17 and Treg cells. *J Exp Med*, vol. 208, 2011, pp 1367-1376.

223. Pearce, E.L., Poffenberger, M.C., Chang, C.-H. & Jones, R.G. Fueling Immunity: Insights into Metabolism and Lymphocyte Function. (2013).

224. Brooks, G.A. The Science and Translation of Lactate Shuttle Theory. *Cell metabolism* **27**, 757-785 (2018).

225. Murray, C. *et al.* Monocarboxylate transporter MCT1 is a target for immunosuppression. *Nature chemical biology* **1**, 371-376 (2005).

226. Fischer, K. *et al.* Inhibitory effect of tumor cell–derived lactic acid on human T cells. (2007).

227. DeBerardinis, R.J., Lum, J.J., Hatzivassiliou, G. & Thompson, C.B. The biology of cancer: metabolic reprogramming fuels cell growth and proliferation. *Cell Metab* **7**, 11-20 (2008).

228. Gubser, P.M. *et al.* Rapid effector function of memory CD8+ T cells requires an immediate-early glycolytic switch. *Nat Immunol* **14**, 1064-1072 (2013).

229. Peng, M. *et al.* Aerobic glycolysis promotes T helper 1 cell differentiation through an epigenetic mechanism. *Science* **354**, 481-484 (2016).

230. Hermans, D. *et al.* Lactate dehydrogenase inhibition synergizes with IL-21 to promote CD8(+) T cell stemness and antitumor immunity. *Proc Natl Acad Sci U S A* **117**, 6047-6055 (2020).

231. Chang, C.H. *et al.* Posttranscriptional Control of T Cell Effector Function by Aerobic Glycolysis. *Cell* **153**, 1239-1251 (2013).

232. Reid, M.A., Dai, Z. & Locasale, J.W. The impact of cellular metabolism on chromatin dynamics and epigenetics. *Nat Cell Biol* **19**, 1298-1306 (2017).

233. Sena, L.A. *et al.* Mitochondria are required for antigen-specific T cell activation through reactive oxygen species signaling. *Immunity* **38**, 225-236 (2013).

234. Carr, E.L. *et al.* Glutamine uptake and metabolism are coordinately regulated by ERK/MAPK during T lymphocyte activation. *J Immunol* **185**, 1037-1044 (2010).

235. DeBerardinis, R.J. *et al.* Beyond aerobic glycolysis: transformed cells can engage in glutamine metabolism that exceeds the requirement for protein and nucleotide synthesis. *Proc Natl Acad Sci U S A* **104**, 19345-19350 (2007).

236. Pearce, E.L., Poffenberger, M.C., Chang, C.H. & Jones, R.G. Fueling immunity: insights into metabolism and lymphocyte function. *Science* **342**, 1242454 (2013).

237. Ma, Y. *et al.* Fatty acid oxidation: An emerging facet of metabolic transformation in cancer. *Cancer Lett* **435**, 92-100 (2018).

238. Feng, W.W. & Kurokawa, M. Lipid metabolic reprogramming as an emerging mechanism of resistance to kinase inhibitors in breast cancer. *Cancer Drug Resist* **3** (2020).

239. Lee, J. *et al.* Regulator of fatty acid metabolism, acetyl coenzyme a carboxylase 1, controls T cell immunity. *J Immunol* **192**, 3190-3199 (2014).

240. Berod, L. *et al.* De novo fatty acid synthesis controls the fate between regulatory T and T helper 17 cells. *Nat Med* **20**, 1327-1333 (2014).

241. Hatzivassiliou, G. *et al.* ATP citrate lyase inhibition can suppress tumor cell growth. *Cancer Cell* **8**, 311-321 (2005).

242.   Callender, L.A. *et al.* Mitochondrial mass governs the extent of human T cell senescence. *Aging Cell*, vol. 19, 2020.

243.   Rathmell, J.C., Vander Heiden, M.G., Harris, M.H., Frauwirth, K.A. & Thompson, C.B. In the absence of extrinsic signals, nutrient utilization by lymphocytes is insufficient to maintain either cell size or viability. *Mol Cell* **6**, 683-692 (2000).

244.   Son, H.J. *et al.* Metformin attenuates experimental autoimmune arthritis through reciprocal regulation of Th17/Treg balance and osteoclastogenesis. *Mediators Inflamm* **2014**, 973986 (2014).

245.   Kim, E.K. *et al.* Metformin ameliorates experimental-obesity-associated autoimmune arthritis by inducing FGF21 expression and brown adipocyte differentiation. *Exp Mol Med* **50**, e432 (2018).

246.   Kang, K.Y. *et al.* Metformin downregulates Th17 cells differentiation and attenuates murine autoimmune arthritis. *Int Immunopharmacol* **16**, 85-92 (2013).

247.   Araki, K. *et al.* mTOR regulates memory CD8 T-cell differentiation. *Nature* **460**, 108 (2009).

248.   Pearce, E.L. *et al.* Enhancing CD8 T Cell Memory by Modulating Fatty Acid Metabolism. *Nature* **460**, 103-107 (2009).

249.   O'Sullivan, D. *et al.* Memory CD8(+) T Cells Use Cell-Intrinsic Lipolysis to Support the Metabolic Programming Necessary for Development. *Immunity* **41**, 75-88 (2014).

250.   van der Windt, G.J. *et al.* Mitochondrial Respiratory Capacity Is A Critical Regulator Of CD8+ T Cell Memory Development. *Immunity* **36**, 68-78 (2012).

251.   van der Windt, G.J. *et al.* CD8 memory T cells have a bioenergetic advantage that underlies their rapid recall ability. *Proc Natl Acad Sci U S A* **110**, 14336-14341 (2013).

252.   Buck, M.D. *et al.* Mitochondrial Dynamics Controls T Cell Fate through Metabolic Programming. *Cell* **166**, 63-76 (2016).

253.   Sukumar, M. *et al.* Mitochondrial Membrane Potential Identifies Cells with Enhanced Stemness for Cellular Therapy. *Cell Metab* **23**, 63-76 (2016).

254.   Perl, A., Gergely, P., Nagy, G., Koncz, A. & Banki, K. Mitochondrial hyperpolarization: a checkpoint of T-cell life, death and autoimmunity. *Trends Immunol* **25**, 360-367 (2004).

255. Nagy, G., Koncz, A. & Perl, A. T Cell Activation-Induced Mitochondrial Hyperpolarization Is Mediated by Ca2+- and Redox-Dependent Production of Nitric Oxide1. *J Immunol* **171**, 5188-5197 (2003).

256. Gergely, P., Jr. *et al.* Mitochondrial hyperpolarization and ATP depletion in patients with systemic lupus erythematosus. *Arthritis Rheum* **46**, 175-190 (2002).

257. Sukumar, M. *et al.* Inhibiting glycolytic metabolism enhances CD8+ T cell memory and antitumor function. (2013).

258. Fernandez, D.R. *et al.* Activation of mammalian target of rapamycin controls the loss of TCRzeta in lupus T cells through HRES-1/Rab4-regulated lysosomal degradation. *J Immunol* **182**, 2063-2073 (2009).

259. Fernandez, D., Bonilla, E., Mirza, N., Niland, B. & Perl, A. Rapamycin Reduces Disease Activity and Normalizes T Cell Activation–Induced Calcium Fluxing in Patients With Systemic Lupus Erythematosus. *Arthritis Rheum* **54**, 2983-2988 (2006).

260. Harrison, D.E. *et al.* Rapamycin fed late in life extends lifespan in genetically heterogeneous mice. *Nature* **460**, 392-395 (2009).

261. Weinberg, S.E., Sena, L.A. & Chandel, N.S. Mitochondria in the regulation of innate and adaptive immunity. *Immunity* **42**, 406-417 (2015).

262. Buskiewicz, I.A. *et al.* Reactive oxygen species induce virus-independent MAVS oligomerization in systemic lupus erythematosus. *Sci Signal* **9**, ra115 (2016).

263. Gross, C.J. *et al.* K(+) Efflux-Independent NLRP3 Inflammasome Activation by Small Molecules Targeting Mitochondria. *Immunity* **45**, 761-773 (2016).

264. To, E.E. *et al.* Mitochondrial Reactive Oxygen Species Contribute to Pathological Inflammation During Influenza A Virus Infection in Mice. *Antioxidants & redox signaling* **32**, 929-942 (2020).

265. Rena, G., Hardie, D.G. & Pearson, E.R. The mechanisms of action of metformin. *Diabetologia* **60**, 1577-1585 (2017).

266. Sanchez-Rangel, E. & Inzucchi, S.E. Metformin: clinical use in type 2 diabetes. *Diabetologia* **60**, 1586-1593 (2017).

267. Rodriguez, J., Hiel, S. & Delzenne, N.M. Metformin: old friend, new ways of action-implication of the gut microbiome? *Curr Opin Clin Nutr Metab Care* **21**, 294-301 (2018).

268. Zi, F. *et al.* Metformin and cancer: An existing drug for cancer prevention and therapy. *Oncol Lett*, vol. 15, 2018, pp 683-690.

269. Yew, W.W., Chang, K.C., Chan, D.P. & Zhang, Y. Metformin as a host-directed therapeutic in tuberculosis: Is there a promise? *Tuberculosis (Edinb)* **115**, 76-80 (2019).

270. Natali, A. & Ferrannini, E. Effects of Metformin and Thiazolidinediones on Suppression of Hepatic Glucose Production and Stimulation of Glucose Uptake in Type 2 Diabetes: A Systematic Review. *Diabetologia* **49** (2006).

271. Foretz, M. *et al.* Metformin inhibits hepatic gluconeogenesis in mice independently of the LKB1/AMPK pathway via a decrease in hepatic energy state. *J Clin Invest* **120**, 2355-2369 (2010).

272. Foretz, M., Guigas, B., Bertrand, L., Pollak, M. & Viollet, B. Metformin: from mechanisms of action to therapies. *Cell Metab* **20**, 953-966 (2014).

273. Cao, J. *et al.* Low Concentrations of Metformin Suppress Glucose Production in Hepatocytes Through AMP-activated Protein Kinase (AMPK). *The Journal of biological chemistry* **289**, 20435-20446 (2014).

274. Wang, D.S. *et al.* Involvement of Organic Cation Transporter 1 in Hepatic and Intestinal Distribution of Metformin. *The Journal of pharmacology and experimental therapeutics* **302**, 510-515 (2002).

275. Shu, Y. *et al.* Effect of Genetic Variation in the Organic Cation Transporter 1 (OCT1) on Metformin Action. *The Journal of clinical investigation* **117**, 1422-1431 (2007).

276. Koepsell, H., Lips, K. & Volk, C. Polyspecific Organic Cation Transporters: Structure, Function, Physiological Roles, and Biopharmaceutical Implications. *Pharmaceutical research* **24**, 1227-1251 (2007).

277. Jalling, O. & Olsen, C. The Effects of Metformin Compared to the Effects of Phenformin on the Lactate Production and the Metabolism of Isolated Parenchymal Rat Liver Cell. *Acta pharmacologica et toxicologica* **54**, 327-332 (1984).

278. Piel, S., Ehinger, J.K., Elmér, E. & Hansson, M.J. Metformin Induces Lactate Production in Peripheral Blood Mononuclear Cells and Platelets Through Specific Mitochondrial Complex I Inhibition. *Acta physiologica (Oxford, England)* **213**, 171-180 (2015).

279. Andrzejewski, S., Gravel, S.P., Pollak, M. & St-Pierre, J. Metformin directly acts on mitochondria to alter cellular bioenergetics. *Cancer Metab* **2**, 12 (2014).

280. Bridges, H., Jones, A.Y., Pollak, M. & Hirst, J. Effects of metformin and other biguanides on oxidative phosphorylation in mitochondria. *Biochem J*, vol. 462, 2014, pp 475-487.

281. Geerling, J.J. *et al.* Metformin Lowers Plasma Triglycerides by Promoting VLDL-triglyceride Clearance by Brown Adipose Tissue in Mice. *Diabetes* **63**, 880-891 (2014).

282. Takashima, M. *et al.* Role of KLF15 in Regulation of Hepatic Gluconeogenesis and Metformin Action. *Diabetes* **59**, 1608-1615 (2010).

283. Dowling, R.J., Zakikhani, M., Fantus, I.G., Pollak, M. & Sonenberg, N. Metformin Inhibits Mammalian Target of Rapamycin-Dependent Translation Initiation in Breast Cancer Cells. *Cancer research* **67**, 10804-10812 (2007).

284. Mogavero, A. *et al.* Metformin transiently inhibits colorectal cancer cell proliferation as a result of either AMPK activation or increased ROS production. *Scientific Reports* **7**, 15992 (2017).

285. Miller, R.A. *et al.* Biguanides Suppress Hepatic Glucagon Signalling by Decreasing Production of Cyclic AMP. *Nature* **494**, 256-260 (2013).

286. Wang, Y. *et al.* Metformin Improves Mitochondrial Respiratory Activity through Activation of AMPK. *Cell Rep* **29**, 1511-1523 e1515 (2019).

287. Madiraju, A.K. *et al.* Metformin Inhibits Gluconeogenesis via a Redox-Dependent Mechanism in Vivo. *Nature medicine* **24**, 1384-1394 (2018).

288. Madiraju, A.K. *et al.* Metformin Suppresses Gluconeogenesis by Inhibiting Mitochondrial Glycerophosphate Dehydrogenase. *Nature* **510**, 542-546 (2014).

289. Dowling, R.J. *et al.* Metformin Pharmacokinetics in Mouse Tumors: Implications for Human Therapy. *Cell Metab* **23**, 567-568 (2016).

290. Chandel, N.S. *et al.* Are Metformin Doses Used in Murine Cancer Models Clinically Relevant? *Cell Metab* **23**, 569-570 (2016).

291. Gravel, S.P. *et al.* Serine Deprivation Enhances Antineoplastic Activity of Biguanides. *Cancer research* **74**, 7521-7533 (2014).

292. Pereira, F.V. *et al.* Metformin exerts antitumor activity via induction of multiple death pathways in tumor cells and activation of a protective immune response. *Oncotarget* **9**, 25808-25825 (2018).

293. Eikawa, S. *et al.* Immune-mediated antitumor effect by type 2 diabetes drug, metformin. *Proc Natl Acad Sci U S A*, vol. 112, 2015, pp 1809-1814.

294. Salani, B. *et al.* Metformin, Cancer and Glucose Metabolism. *Endocrine-related cancer* **21**, R461-R471 (2014).

295. Matsushita, M. & Kawaguchi, M. Immunomodulatory Effects of Drugs for Effective Cancer Immunotherapy. *J Oncol* **2018**, 8653489 (2018).

296. Yin, Y. *et al.* Normalization of CD4+ T Cell Metabolism Reverses Lupus. *Sci Transl Med* **7**, 274ra218 (2015).

297. Lee, C.F. *et al.* Preventing Allograft Rejection by Targeting Immune Metabolism. *Cell Rep* **13**, 760-770 (2015).

298. Ursini, F. *et al.* Metformin and Autoimmunity: A "New Deal" of an Old Drug. *Front Immunol* **9**, 1236 (2018).

299. Lee, M.C. *et al.* Metformin Use Is Associated With a Low Risk of Tuberculosis Among Newly Diagnosed Diabetes Mellitus Patients With Normal Renal Function: A Nationwide Cohort Study With Validated Diagnostic Criteria. *PloS one* **13**, e0205807 (2018).

300. Degner, N.R., Wang, J.Y., Golub, J.E. & Karakousis, P.C. Metformin Use Reverses the Increased Mortality Associated With Diabetes Mellitus During Tuberculosis Treatment. *Clin Infect Dis* **66**, 198-205 (2018).

301. Marupuru, S. *et al.* Protective effect of metformin against tuberculosis infections in diabetic patients: an observational study of south Indian tertiary healthcare facility. *The Brazilian Journal of Infectious Diseases* **21**, 312-316 (2017).

302. Singhal, A. *et al.* Metformin as adjunct antituberculosis therapy. *Sci Transl Med* **6**, 263ra159 (2014).

303. Podell, B.K. *et al.* Increased Severity of Tuberculosis in Guinea Pigs with Type 2 Diabetes: A Model of Diabetes-Tuberculosis Comorbidity. *Am J Pathol* **184**, 1104-1118 (2014).

304. Russell, S.L. *et al.* Compromised Metabolic Reprogramming Is an Early Indicator of CD8(+) T Cell Dysfunction during Chronic Mycobacterium tuberculosis Infection. *Cell Rep* **29**, 3564-3579.e3565 (2019).

305. Lachmandas, E. *et al.* Metformin alters human host responses to Mycobacterium tuberculosis in healthy subjects. *J Infect Dis* (2019).

CHAPTER 2 - METFORMIN ENHANCES PROTECTION IN GUINEA PIGS CHRONICALLY INFECTED WITH MYCOBACTERIUM TUBERCULOSIS[1]

Summary

Tuberculosis (TB) is a chronic inflammatory disease that is often associated with alterations in systemic and cellular metabolism that resolves following successful antimicrobial drug treatment. We hypothesized that altered systemic glucose metabolism as a consequence of *Mycobacterium tuberculosis* (Mtb) infection, contributes to TB pathogenesis, and when normalized with anti-glycemic drugs would improve clinical outcomes. To test this hypothesis, guinea pigs were treated daily with the anti-diabetic drug metformin starting 4 weeks prior or concurrent with aerosol exposure to the H37Rv strain of Mtb. In the chronic stages of infection, Mtb infected metformin-treated animals had restored systemic insulin sensitivity but remained glucose intolerant as determined by oral glucose tolerance testing. Despite persistent glucose intolerance, metformin-treated guinea pigs had a 2.8- fold reduction in lung lesion burden and a 0.7 log decrease in CFUs. An alternative hypothesis that metformin treatment improved clinical disease by having a direct effect on immune cell energy metabolism was tested using extracellular flux analysis and flow cytometry. The proinflammatory immune response to Mtb infection in untreated guinea pigs was associated with a marked increase in energy metabolism (glycolysis and mitochondrial respiration) of peripheral blood mononuclear cells (PBMCs), which was normalized in metformin-treated guinea pigs. Moreover, both CD4+ and CD8+ T lymphocytes from Mtb infected, metformin treated animals maintained a more normal mitochondrial membrane potential while those isolated from untreated animals had persistent mitochondrial hyperpolarization. These data suggest that metformin promotes natural host resistance to Mtb

infection by maintaining immune cell metabolic homeostasis and function during the chronic stages of active TB disease.

Introduction

The persistent proinflammatory immune response associated with active *Mycobacterium tuberculosis* (Mtb) infection in some TB patients contributes to alterations in systemic glucose and lipid metabolism [1-3]. The role elevated blood glucose levels has on TB disease severity and progression has been best characterized in diabetic patients, which have a 1.5 to 3-fold increased risk for developing active TB disease and are twice as likely to die or develop reactivation of a latent Mtb infection [4-8]. However, the impact non-diabetic hyperglycemia has on TB pathogenesis is less well understood. To determine the impact non-diabetic hyperglycemia has on the pathogenesis of TB we treated guinea pigs with the anti-diabetic drug metformin prior to or concurrent with aerosol exposure to Mtb. Metformin is among the safest and most widely prescribed drugs used to control blood glucose levels in patients with type 2 diabetes mellitus (T2DM). Metformin helps lower and maintain more normal blood glucose levels in diabetic patients by improving systemic insulin sensitivity and lowering glucose production by the liver [9,10]. In the context of TB, several studies have suggested that Mtb infected individuals with T2DM taking metformin, have slower TB disease progression and improved clinical outcomes and survival compared to individuals not treated with metformin or with poor diabetes control [11-13].

In addition to its anti-glycemic affects, metformin has also been widely studied as an immunomodulatory drug for the treatment of various other communicable and non-communicable diseases [14], with observed clinical improvement in patients with cancer, a variety chronic bacterial and viral infections as well as autoimmune diseases such as systemic lupus erythematosus (SLE) [15-20]. Although the exact mechanisms of action have not been determined, metformin has been shown to have a direct effect on immune cell metabolism, which is linked to T lymphocyte differentiation, function, and survival [21-26]. This suggests that in addition to normalizing systemic

glucose metabolic derangements caused by chronic inflammation, metformin may also modulate the function of immune cells that are important in the protection and pathogenesis of TB. We show here that metformin treatment of Mtb infected guinea pigs improved clinical disease in part by partially restoring systemic glucose metabolism as well as having a direct effect on cellular metabolism of immune cells that are important in the protection against TB.

Materials and Methods

Animals and sample collection

4-week, female, outbred Dunkin–Hartley guinea pigs, n=14 per group, were purchased from Charles River Laboratories and housed in a biosafety level 3 laboratory at the Colorado State University Laboratory Animal Resources facility accredited by the American Association for Accreditation of Laboratory Animal Care (AAALAC). All animal experiments were performed in accordance with the National Research Council's Guide for the Care and Use of Laboratory Animals and were approved by the Animal Care and Usage Committee at Colorado State University.

Animals were chipped (BioMedic Data Systems, Inc.) for animal identification and continuous recording of body temperature. For serial blood collection, guinea pigs were anesthetized via isoflurane inhalation and blood collected by percutaneous venipuncture of the cranial vena cava. At the time of euthanasia, guinea pigs were administered 50 mg/kg of ketamine and 5 mg/kg of Xylazine via intramuscular injection for anesthetic induction. Under terminal anesthesia, blood was collected, and guinea pigs were euthanized by IP overdose of pentobarbital. Tissues were collected for histopathology by fixing in 4% paraformaldehyde or stored at -80℃ for homogenization and quantification of Mtb.

Metformin treatment

Guinea pigs received oral administration of either 20mg/kg of metformin (Spectrum Chemical MFG Corp, New Brunswick, NJ), purchased through the CSU Veterinary Teaching Hospital Pharmacy, in a carrier suspension of 50% ORA-sweet® (Perrigo) 50% water or mock treatment, carrier suspension of 50% ORA-sweet®(Perrigo) 50% water, daily beginning 28 days prior to or concurrent with Mtb infection. Dosage was chosen based on the human equivalent serum concentration of ~10µM, confirmed by pharmacokinetic analysis (Figure S6). Treatment was continued once daily throughout the duration of the study.

Mtb aerosol exposure

Culture stocks of *Mtb* strain H37Rv (TMC #102, Trudeau Institute) were agitated in glass test tubes, collected at an OD600nm between 0.8-1.0, and frozen at -80°C in Proskauer-Beck liquid medium containing 0.05% Tween-80. Titer was determined and bacteria were diluted in water to 1×10^6 CFU/ml. Approximately 20 bacilli were delivered to each animal using a Madison chamber aerosol generation device [3].

Oral glucose and insulin tolerance testing

Glucose and insulin tolerance were measured as previously described [3]. In brief, following an 8-12 hour fasting period glucose tolerance was measured by oral challenge with a 2 g/kg bolus of D-glucose (0.5 g/ml). Serum glucose concentrations were measured using the Freestyle Lite glucometer (Abbot) from a skin-prick site adjacent to the most peripheral vein on the pinna at 0, 30, 60, 90, and 120 minutes following administration. Similarly, insulin sensitivity was measured following the SC injection of 0.5 units/kg of regular-acting human recombinant insulin (Humulin-R, Eli Lilly). Glucose concentrations were measured at 0, 25, 50, 75, and 100 minutes following insulin injection.

Metabolic phenotyping

Peripheral blood mononuclear cells were isolated from whole blood by density gradient centrifugation with lympholyte mammal (1.086 gm/cm^3) according to manufacturer instructions (Cedarlane). Single-cell suspensions from BAL were prepared by centrifugation at 500xg followed by RBC lysis with Gey's solution. 2x10^5 or 4x10^5 PBMCs and 1x10^5 BAL cells suspended in seahorse XF assay media (Agilent Technologies, Inc), were seeded onto CellTak (Corning Inc.) coated 8 or 24 well cell culture microplates, respectively. Cell adherence to microplates was achieved prior to assaying by centrifuging plates at 500xg for 5 minutes with no brake followed by a 30-minute incubation at 37℃ in the absence of CO_2. OCR and ECAR were measured using a Seahorse XFp or Seahorse XFe24 bioanalyzer (Agilent Technologies, Inc). OCR and ECAR were measured basally and following the injection of 1μM oligomycin, 2μM fluorocarbonyl cyanide phenylhydrazone (FCCP), 0.5μM rotenone + antimycin A, and 50mM 2-deoxyglucose.

Flow cytometry

Peripheral blood mononuclear cells and BAL single-cell suspensions were prepared for antibody surface staining by seeding 1x10^6 cells in FACs buffer, PBS+1% BSA+0.1% sodium azide, into 96 well round-bottom plates. Fc blocking was performed in FACs buffer + guinea pig IgG + rabbit IgG on a rocker at 4℃ for 30 minutes prior to antibody staining. Fluorochrome-conjugated antibodies including CD4, CD8 (Bio-Rad Laboratories Inc.), and MHCII (hybridoma line producing mAb IVA12 [27]) were prepared in FACs blocking buffer and added to cells for 20 minutes at 4℃ on a rocker. Live/dead exclusion was assessed by staining with either Live/Dead aqua or 7-AAD. Data was collected with an LSR II (BD Biosciences) flow cytometer maintained within BSL-3 facilities and the data was analyzed using FlowJo software (FlowJo, LLC).

Mitochondrial staining

Mitochondrial membrane potential was evaluated by incubating PBMCs with 25nM $DiOC_6(3)$ (ThermoFisher Scientific) for 30 minutes at 37℃ + 5% CO_2. Mitochondrial mass was assessed by staining by staining PBMCs with 100nM mitotracker deep red (ThermoFisher Scientific) for 30 minutes at 37℃ + 5% CO_2. To quantify mitochondrial superoxide production, MitoSOX red (ThermoFisher Scientific) was suspended at a final concentration of 2.5µM in HBSS and incubated with PBMCs for 10 minutes at 37℃ with CO_2. To obtain a positively stained MitoSOX control, PBMCs were incubated with 93nM tert-butyl hydroperoxide for 30 minutes at 37℃ + CO_2 prior to MitoSOX staining. All samples were analyzed using an LSR II (BDBiosciences) flow cytometer maintained within BSL-3 facilities and the data was analyzed using FlowJo software (FlowJo, LLC).

GSH/GSSG ratio

GSH/GSSG ratios were analyzed in isolated PBMCs during acute, subacute, and chronic stages of Mtb infection by luciferin detection using the GSH/GSSG-Glo™ Assay kit (Promega). $2.5x10^5$ live PBMCs were assayed in a 96 well white-walled plate, according to manufacturer instructions, and luminescence was read on a BioTek Synergy2 instrument.

qRT-PCR

The right caudal lung lobe was collected post-mortem from metformin and mock treated animals and minced in RNAlater (Qiagen), incubated at 4℃ for 24 hours, then frozen at -80℃ for extraction at a later date. Approximately 50mg of minced tissue was homogenized with a bead beater in RLT buffer then digested with proteinase K for 30 minutes at 55℃. Nucleic acid was extracted with an RNeasy mini kit (Qiagen). The nucleic acid was eluted, and DNA was digested in solution with DNase I (Qiagen) for 30 minutes at RT then re-purified on the RNeasy mini columns. The resulting RNA was quantified by nanodrop and integrity determined by agarose gel

electrophoresis. 1ug of RNA was reverse transcribed to cDNA and quantitative RT-PCR was performed with the SYBR Green detection kit (Bio-Rad) and signal detected in the Bio-Rad CFX-96 real-time thermal cycler. Each reaction was performed in duplicate for each animal with 0.2mmol/L of each primer and 50ng of cDNA template. The gene expression was normalized using two reference genes- hypoxanthine-guanine phosphoribosyltransferase (HPRT) and TATA-box binding protein (TBP), which were validated for consistent expression with these experimental conditions. The primer design and sequences for guinea pig TNFα, IL-6, IL-12p40, IL-1β MCP-1, TGFβ, IL-10, IFNγ, IL-17A, and FOXP3 are thoroughly described in our previous work [8].

Bacterial burden/CFU

Lung, spleen, and liver were weighed and diluted 1:10 in PBS prior to homogenization. Serial dilutions of tissue homogenates were performed in PBS and plated on BD Difco™ 7H11 agar (VWR). Following 3-6 weeks of incubation at 37℃, colony-forming units were counted, and CFUs per gram of tissue was calculated.

Histology

Tissue sections fixed with 4% paraformaldehyde were paraffin embedded, sectioned at 5µm, and stained with hematoxylin and eosin. Total and lesion area of lung, spleen, and liver were quantified using Stereo Investigator area fraction fractionator software (MBF Bioscience) and the Nikon Eclipse 80i microscope. The area of inflammation relative to the area of normal tissue parenchyma was estimated from representative lung, liver, and spleen tissue sections evaluated at 200X magnification. A total of 20 to 25 fields were randomly selected by the computer, and a counting frame (2,000 µm^2) containing probe points with a grid spacing of 200 µm was used to define the areas of interest (lesions and lungs). Lesion burden was calculated as ratio of tissue area to lesion area and expressed as a percentage of lesion to tissue [3].

Data analysis

Lesion burden and metabolic phenotyping data set was normalized to the initial time point of mock treated. Tukey's IQR method was used to identify outliers in data sets. Based on data sets, Two-way ANOVA or T-test were used to determine differences between groups. When necessary, data was log transformed to achieve normality and homoscedasticity of residuals or data. If normality or homoscedasticity could not be achieved, data was analyzed using non-parametric methods. Post-hoc comparisons methods were Tukey, Sidak's, or Mann-Whitney multiple comparisons test, respectively. Data was analyzed with Graph Pad Prism v.8.

Results

Metformin restores insulin sensitivity but not glucose intolerance during Mtb infection.

Previously, human and animal studies have demonstrated that glucose intolerance, consistent with systemic insulin resistance, develops in response to chronic Mtb infection [1, 3, 28]. We hypothesized that insulin resistance is responsible for altered systemic glucose metabolism that is characteristic of chronic infection. We tested whether treatment with metformin initiated prior to Mtb infection restored systemic glucose metabolism. Guinea pigs infected with Mtb developed non-diabetic hyperglycemia (Figure 2.1B) and systemic insulin resistance as determined by glucose and insulin tolerance testing, respectively (Figure 2.1A and Figure 2.2A). In contrast, guinea pigs treated with metformin maintained systemic insulin sensitivity comparable to uninfected animals (Figure 2.1A and Figure 2.2A). Consistent with previous findings in humans, oral glucose tolerance testing showed Mtb infected guinea pigs developed systemic glucose intolerance that was not reversed by metformin treatment.
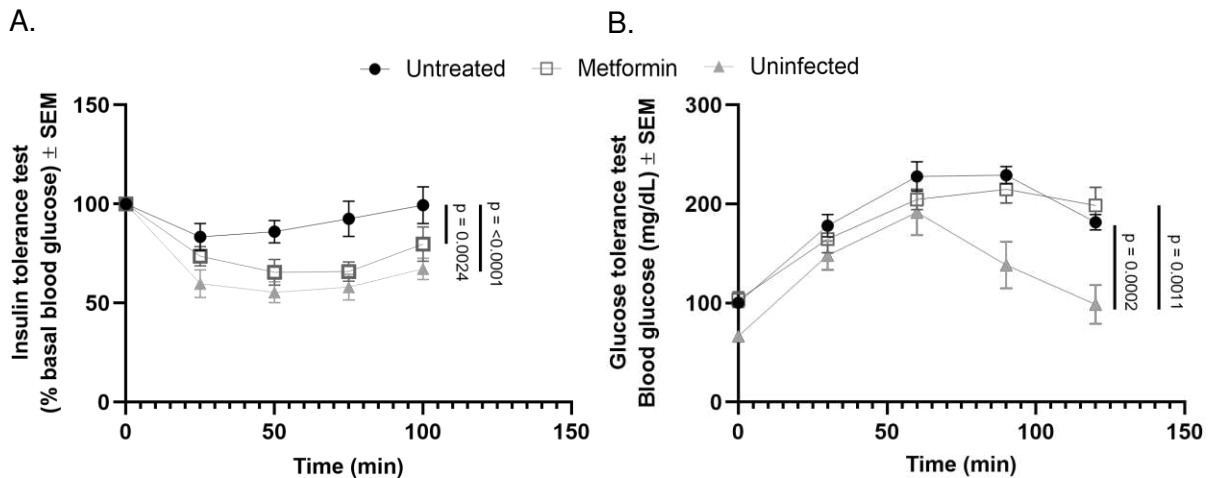
Figure 2.1. Metformin restores insulin sensitivity but not glucose tolerance 30 days following Mtb infection. Duncan Hartley guinea pigs received oral administration of 25mg/kg metformin or mock treatment once daily beginning 28 days prior to low-dose aerosol infection with Mtb H37Rv. Thirty days following infection guinea pigs were subjected to an insulin tolerance test by injecting 0.5 units/kg human recombinant insulin SC (A) or an oral glucose tolerance test by challenging fasted animals with a 2g/kg bolus of D-glucose (B). Blood glucose concentrations were measured at 0, 25, 50, 75, and 100 minutes post insulin injection and 0, 30, 60, 90, and 120 minutes post oral glucose challenge. A 2-factor mix model was used to determine significances with Tukey's correction for multiple comparisons. N=9 *** $p \leq 0.001$ ** $p \leq 0.01$
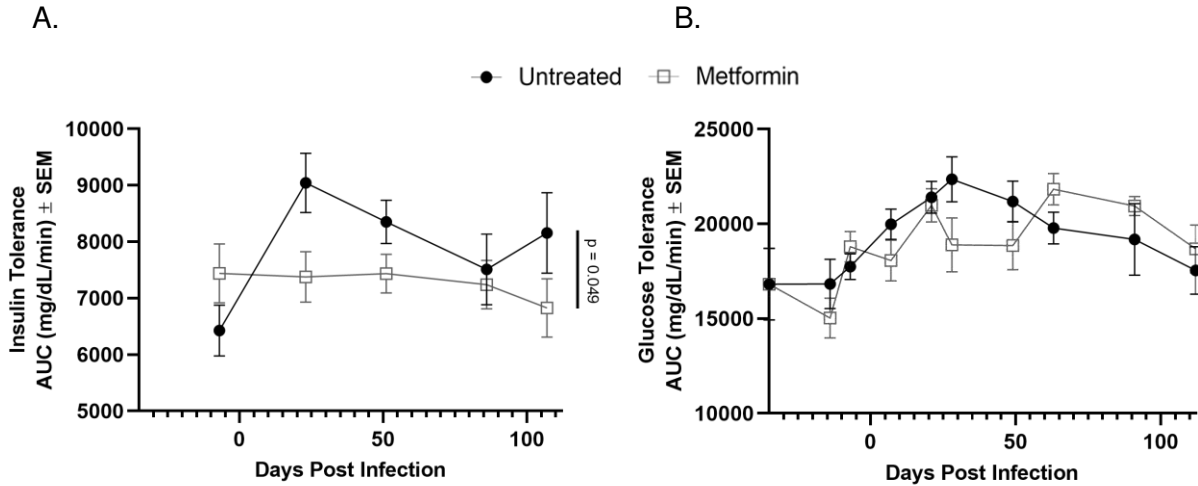
Figure 2.2. Oral glucose and insulin tolerance tests over the course of Mtb infection. On days -7, 23, 51, 86, and 107 following Mtb infection, guinea pigs were subjected to an insulin tolerance test by injecting 0.5 units/kg human recombinant insulin SC (A). Blood glucose concentrations were measured at 0, 25, 50, 75, and 100 minutes post insulin injection. On days -35, -14, -7, 7, 21, 28, 49, 63, 91, and 112 following infection guinea pigs were subjected to an oral glucose tolerance test by challenging fasted animals with a 2g/kg bolus of D-glucose (B). Similarly, blood glucose was measured at 0, 30, 60, 90, and 120 minutes post oral glucose challenge. The area under the curve (AUC) was calculated for each treatment group at each individual timepoint (A-B). Graphs represent the corresponding averages of the AUC of either untreated or metformin treated guinea pigs at each timepoint. Significance of treatment effect was found using a 2-factor ANOVA. There was no significant difference in glucose tolerance between mock- and metformin-treated Mtb infected pigs over the course of infection (B). N=9

Metformin enhances host resistance to Mtb.

To evaluate whether the effects of metformin on systemic metabolism influenced the outcome of TB disease severity, we quantified Mtb colony forming units (CFUs) and lesion burden at acute (21-30 days), subacute (45-60 days), and chronic (75-90 days) stages of infection. At acute and subacute timepoints, there were no differences in lesion burden nor CFUs in the lungs, spleens, or livers of infected animals (Figure 2.3 A-E). During chronic stages of infection however, we observed a 2.8-fold decrease in lung lesion burden and 0.7 log reduction in CFUs in metformin-treated compared to untreated guinea pigs (Figure 2.3A and B).
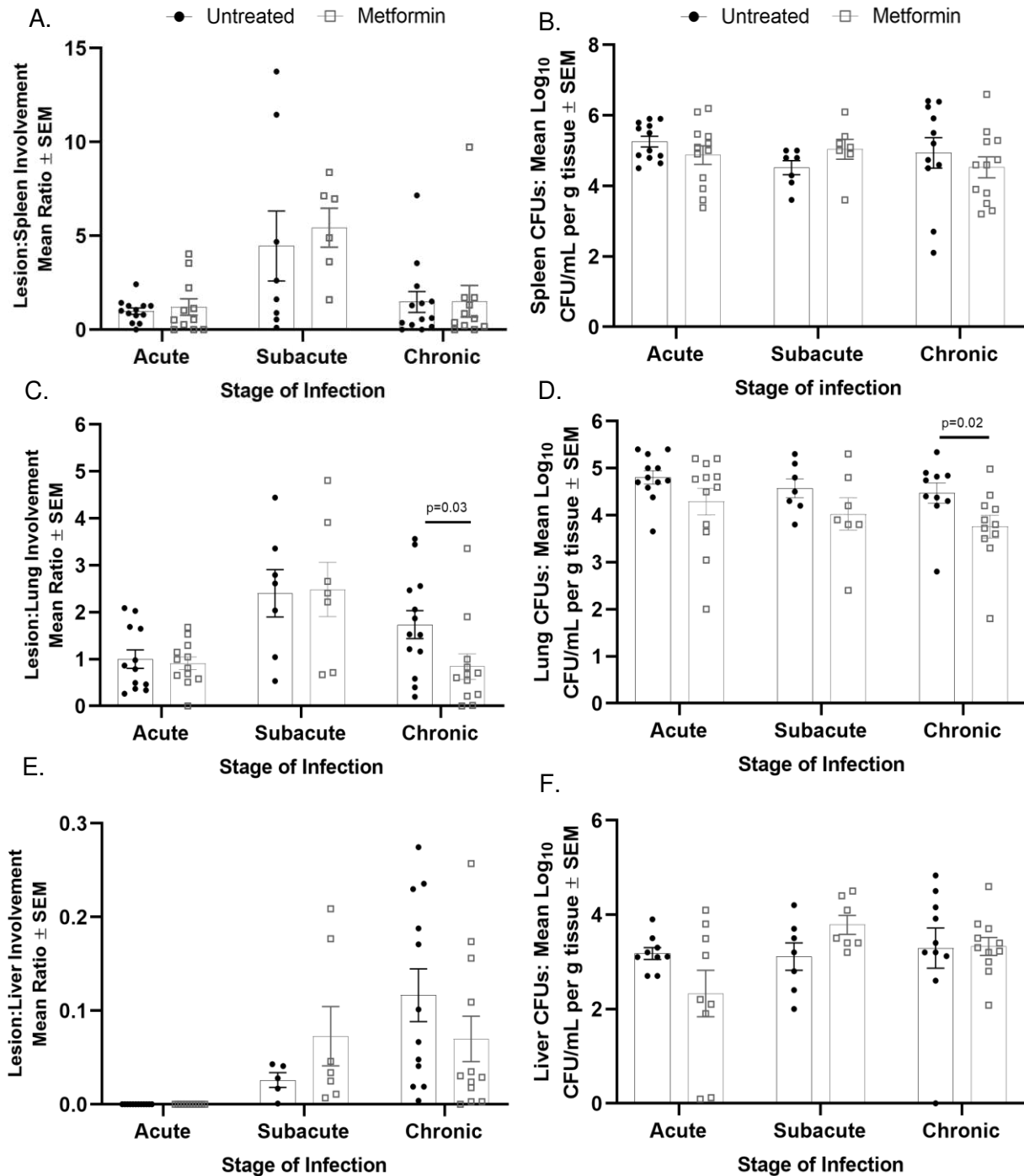
Figure 2.3. Metformin enhances host resistance to Mtb. During acute, subacute, and chronic stages of infection lungs, spleens, and livers were harvested from euthanized, Mtb infected untreated- and metformin-treated guinea pigs to evaluate lesion burden (A, C, & E) and bacterial burden (CFUs) (B, D, & F). Stereo Investigator software was used to calculate the percent of lesion to uninvolved tissue in guinea pig lungs and spleens (A, C, & E). Percent lesion involvement was normalized to acute untreated. Colony forming units were generated by plating homogenized (C) lung, (D) spleen, or (E) liver tissue on 7H11 agar plates and were quantified per gram of tissue. N=7-12 animals per group per timepoint. Two outliers were found using Tukey IQR method (B). All outliers were greater then 2.0 times the IQR. Mann-Whitney test was used to determine significances between treatments within stage of infection * p ≤ 0.05.

Lung tissue histology showed distinct differences in granuloma morphology in comparison to those from untreated animals. Granulomas from metformin-treated animals had a higher proportion of lymphocytes at acute and subacute time points that progressed to well organized and delineated granulomas with less severe perilesional inflammation in the chronic stages of disease (Figure 2.4A-E).
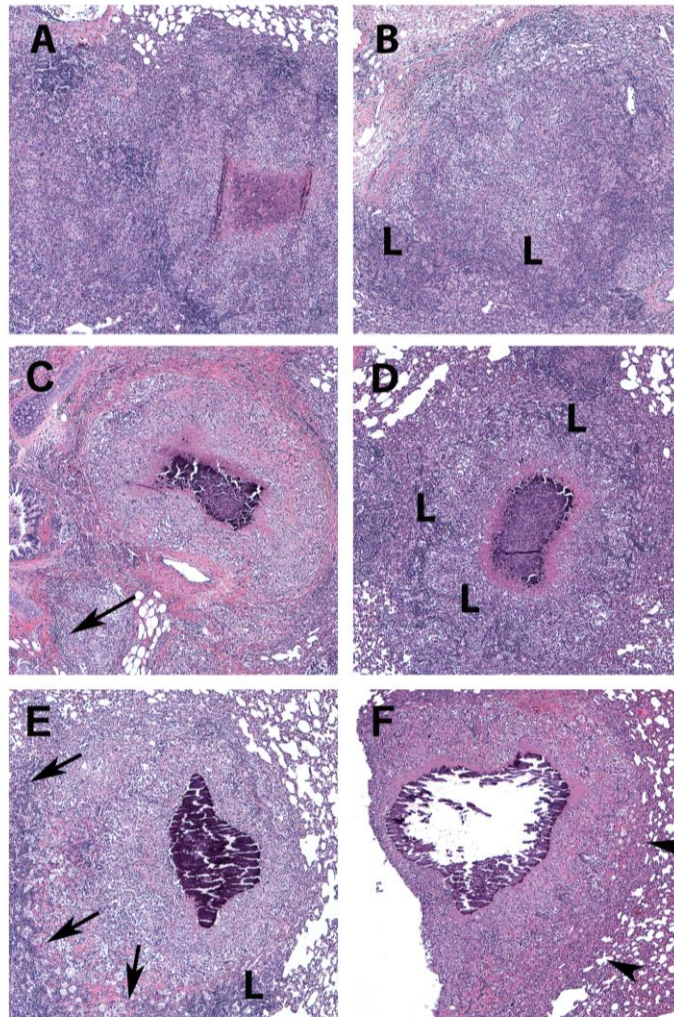
Figure 2.4. Metformin treatment of Mtb infected guinea pigs resolve lung lesions in the chronic stages of infection. Guinea pigs were treated orally with mock treatment (OraSweet) (A, C, E) or metformin (B, D, F) and euthanized during the acute (A, B), subacute (C, D) or chronic (E, F) stages of infection with the H37Rv strain of Mtb. The progression of disease from the acute to chronic stages of infection in mock treated animals showed progressive perilesional inflammation (arrows) that corresponded to a higher lung lesion burden. In contrast, in metformin treated guinea pigs, inflammatory cells in the acute and subacute stages of infection are predominately lymphocytes (L) with less perileional spread (arrowheads). In the chronic stages of infection in metformin treated animals the decreased overall lung lesion burden was accompanied by well-encapsulated granulomas that were sharply demarcated from the more normal lung parenchyma (arrowheads). H and E stain, 100X magnification.

Clinical signs of disease were only modestly improved in metformin-treated animals with a less, but nonsignificant, increase in body temperature in metformin-treated compared to untreated animals (Figure 2.5A-B). There were no significant differences in body weights between treated and untreated animals over the course of infection (Figure 2.5 C), and survival at 250 days was not significantly different between the treatment groups (Figure 2.5D)
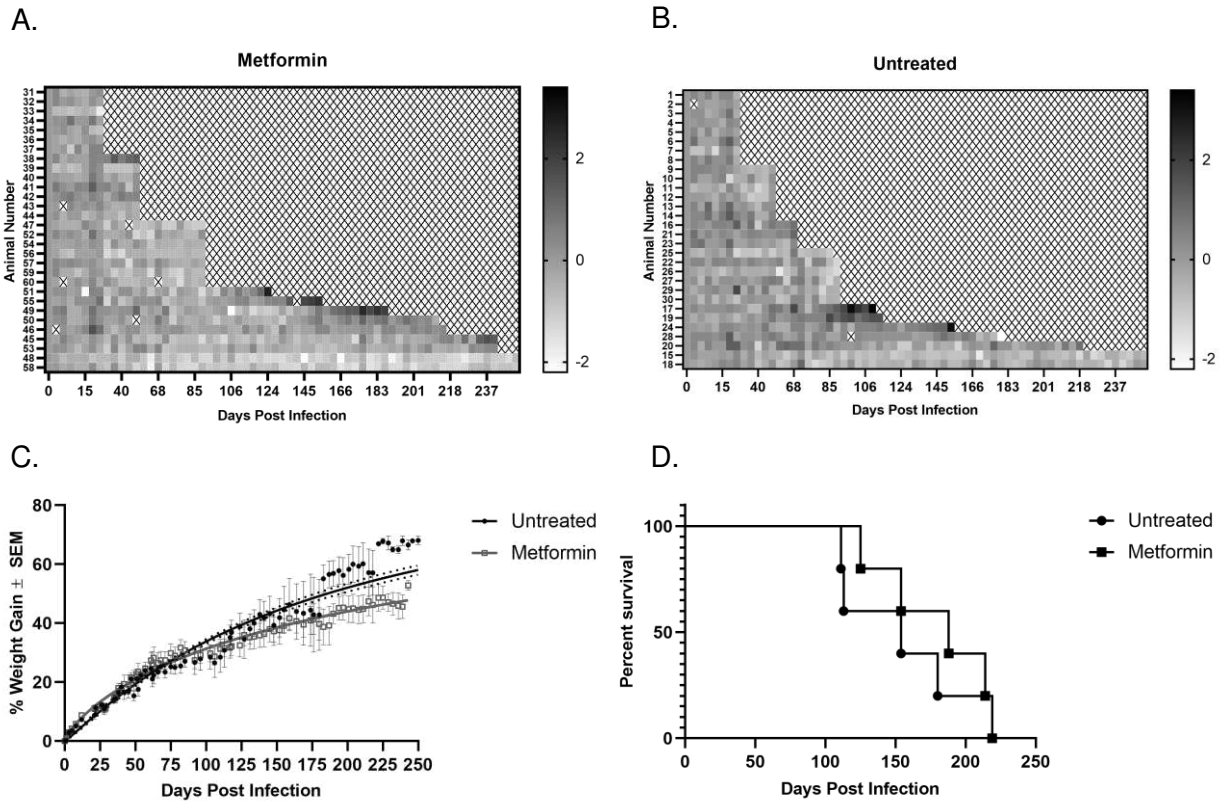

Figure 2.5. Clinical parameters of TB disease. Clinical signs of disease were assessed in metformin-treated (A) and untreated (B) Mtb infected guinea pigs by tracking and body temperature, body weight (C), and animal survival (D) up to 250 days following Mtb infection.

T cell metabolism is regulated by metformin.

Given metformin's effect in decreasing disease burden without fully restoring systemic glucose metabolism, we hypothesized that improved protection might be due to restoration of cellular rather than systemic metabolic alterations. To assess whether metformin modulated immune cell metabolism following Mtb infection, we evaluated metabolic profiles and the relative abundance of CD4$^+$, CD8$^+$, and MHCII$^+$ cells of PBMCs from Mtb infected, treated and untreated guinea pigs. At all stages of infection, PBMCs were comprised of approximately 60% T cells with no significant changes in the proportions of phenotypes, regardless of treatment (Figure 2.6A-C). Metabolic profiles were assessed in PBMCs *ex vivo* using extracellular flux analysis, which measures the rate of oxidative phosphorylation (OXPHOS), expressed as oxygen consumption rate (OCR), and the rate of glycolysis, measured by the change in extracellular pH, expressed as extracellular acidification rate (ECAR).

Following acute Mtb infection, dramatic increases in the utilization of OXPHOS and glycolysis were observed in both metformin-treated and untreated animals (Figure 2.7A and C). During subacute infection, PBMC metabolic rates decreased to levels comparable to uninfected animals in both metformin treated and untreated groups (Figure 2.7A and C). Following the onset of chronic infection however, PBMCs from untreated animals increased OXPHOS and glycolysis by roughly 3 and 2- fold, respectively. In contrast, PBMCs from metformin-treated guinea pigs maintained OXPHOS and glycolysis levels similar to that of uninfected guinea pigs during chronic infection (Figure 2.7A-D).
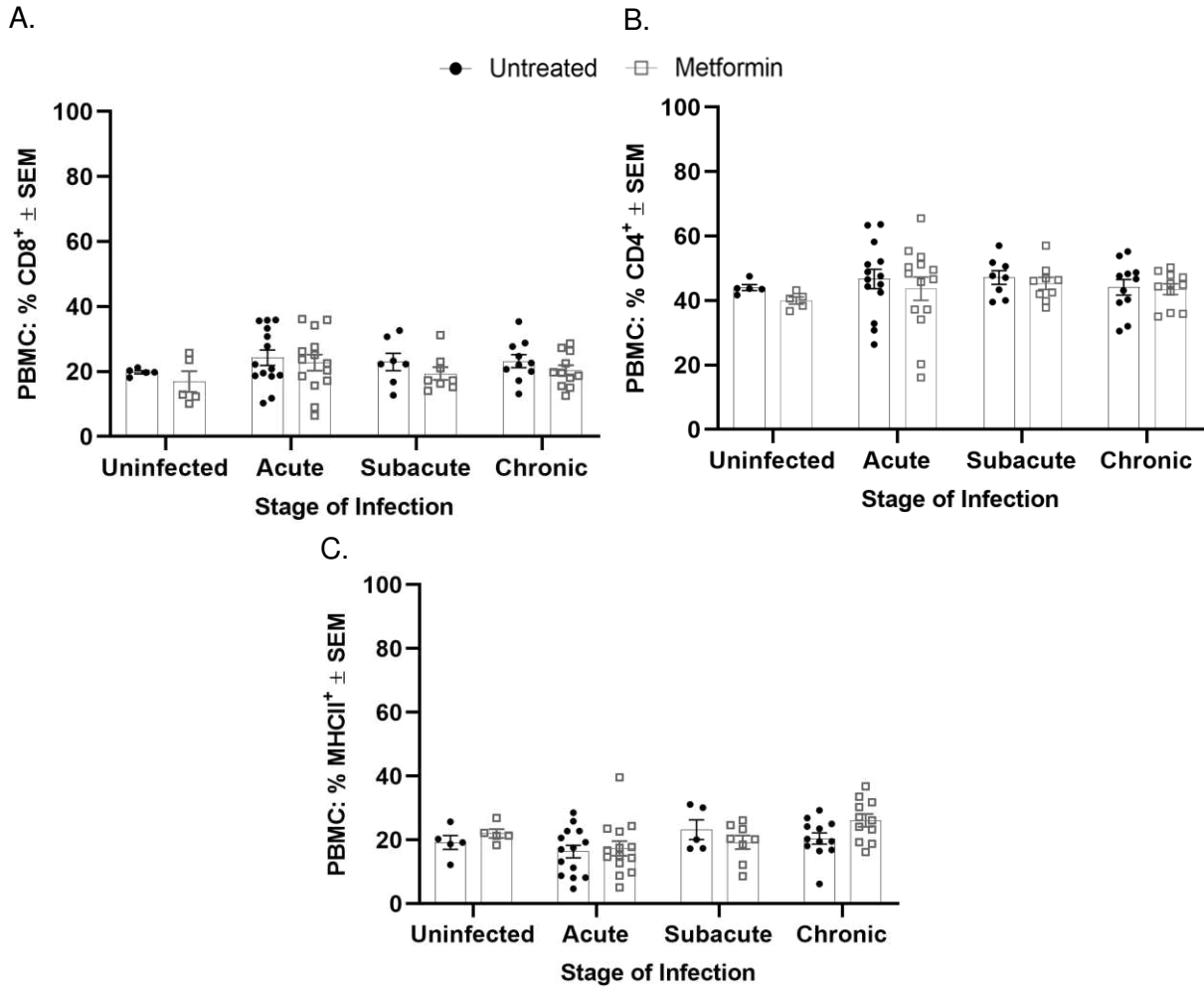
Figure 2.6. CD4+ and CD8+ T cell and MHCII+ cell analysis and metabolic profiles. Flow cytometry analysis was used to quantify the percentages of CD4$^+$ (A), CD8$^+$ (B), and MHCII$^+$ (C) cells from untreated and metformin-treated guinea pigs prior to and following low dose aerosol infection with Mtb at acute, subacute, and chronic stages of infection.
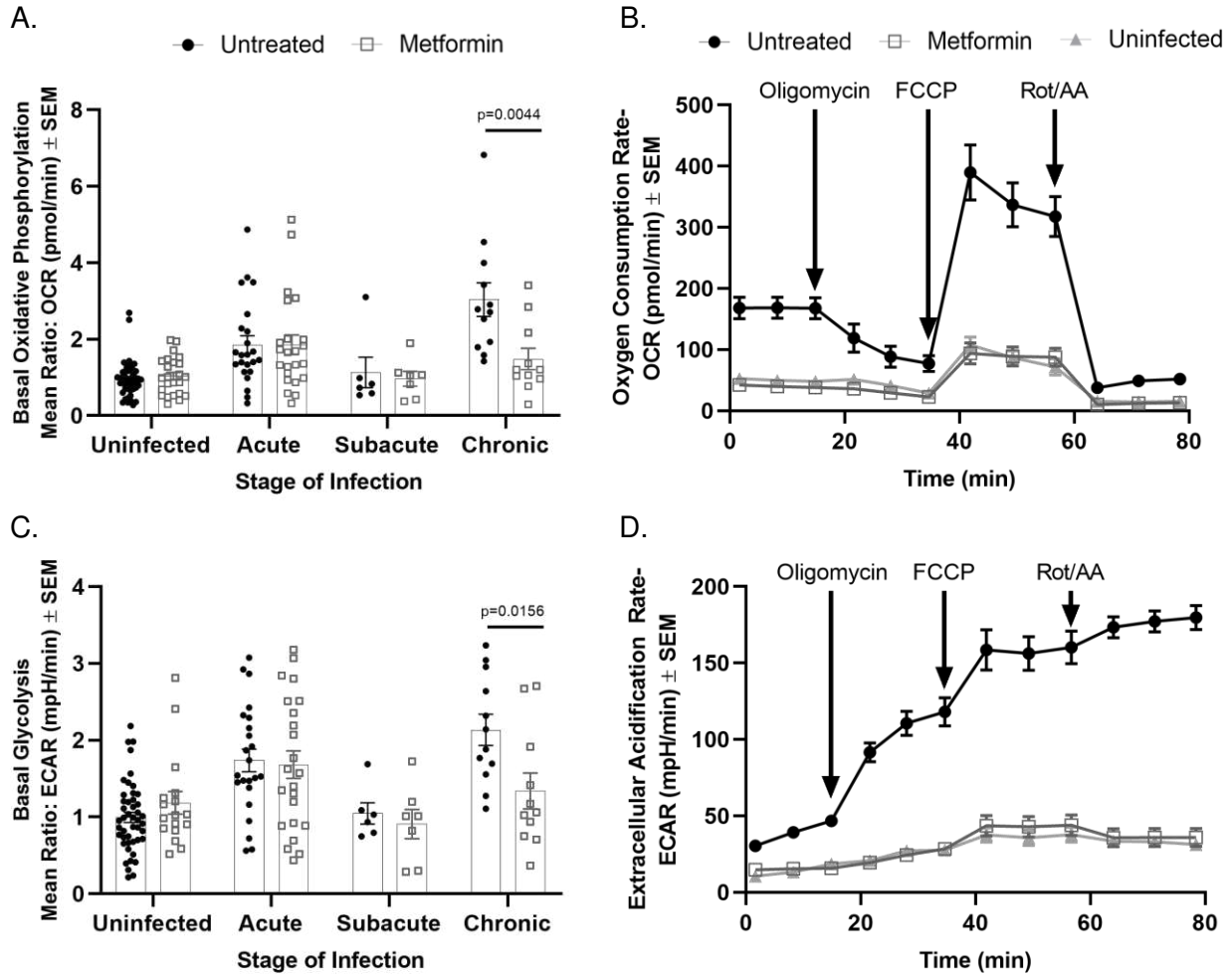
Figure 2.7. T cell metabolism is regulated by metformin. Live PBMCs were isolated from untreated or metformin-treated guinea pigs prior to or during acute, subacute, or chronic Mtb infection. Basal oxidative phosphorylation (OCR) and (C) basal glycolysis (ECAR) were measured in live PBMCs by extracellular flux analysis (A). Data was normalized to the mean of the uninfected untreated group between two independent experiments. Mean values from a mitochondrial stress test performed 75 days post infection (B & D). Curves represent raw OCR (B) and ECAR (D) values generated in response to the addition of oligomycin, FCCP, or rotenone and antimycin A. Mann-Whitney test was used to determine significance between treatments within stage of infection. N=24, * $p \leq 0.05$ ** $p \leq 0.01$.

Metformin modulates T cell mitochondrial membrane potential and superoxide production.

Previous studies have shown that metformin reduces pathology associated with chronic inflammation in a mouse arthritis model by reprogramming metabolism, and thus function, of T lymphocytes [29, 30]. In particular, mitochondrial membrane potential (ΔΨm) and mitochondrial superoxide (mtSO) are found to be heightened in persistently activated T cells in models of

chronic inflammation, ultimately leading to cell death and oxidative damage [31, 32]. To determine whether the differences in PBMC metabolic phenotypes are linked to alterations in T cell metabolism, we measured mitochondrial membrane potential and mitochondrial superoxide production in $CD4^+$ and $CD8^+$ T cells from PBMCs of Mtb-infected guinea pigs. During acute and chronic stages of infection, we observed significantly lower mitochondrial membrane potential in $CD4^+$ and $CD8^+$ T cells from metformin-treated guinea pigs compared to untreated animals (Figure 2.8A-B). We ensured that the differences in membrane potential were not due to variations in mitochondrial size or numbers by measuring mitochondrial mass; and despite differences in membrane potential, mitochondrial mass remained consistent between both groups at all stages of infection (Figure 2.8C-D). We noted that mitochondrial superoxide was increased nearly 2-fold higher in $CD4^+$ T cells from metformin-treated compared to untreated animals during chronic infection (Figure 2.9A). Because superoxide is produced in response to oxidative stress, we measured the ratio of glutathione (GSH) to glutathione disulfide (GSSG) to determine whether an increase in superoxide resulted in cellular stress. Although superoxide was increased in $CD4^+$ T cells from metformin treated animals during chronic infection, cellular redox status was not different between groups (Figure 2.9C).
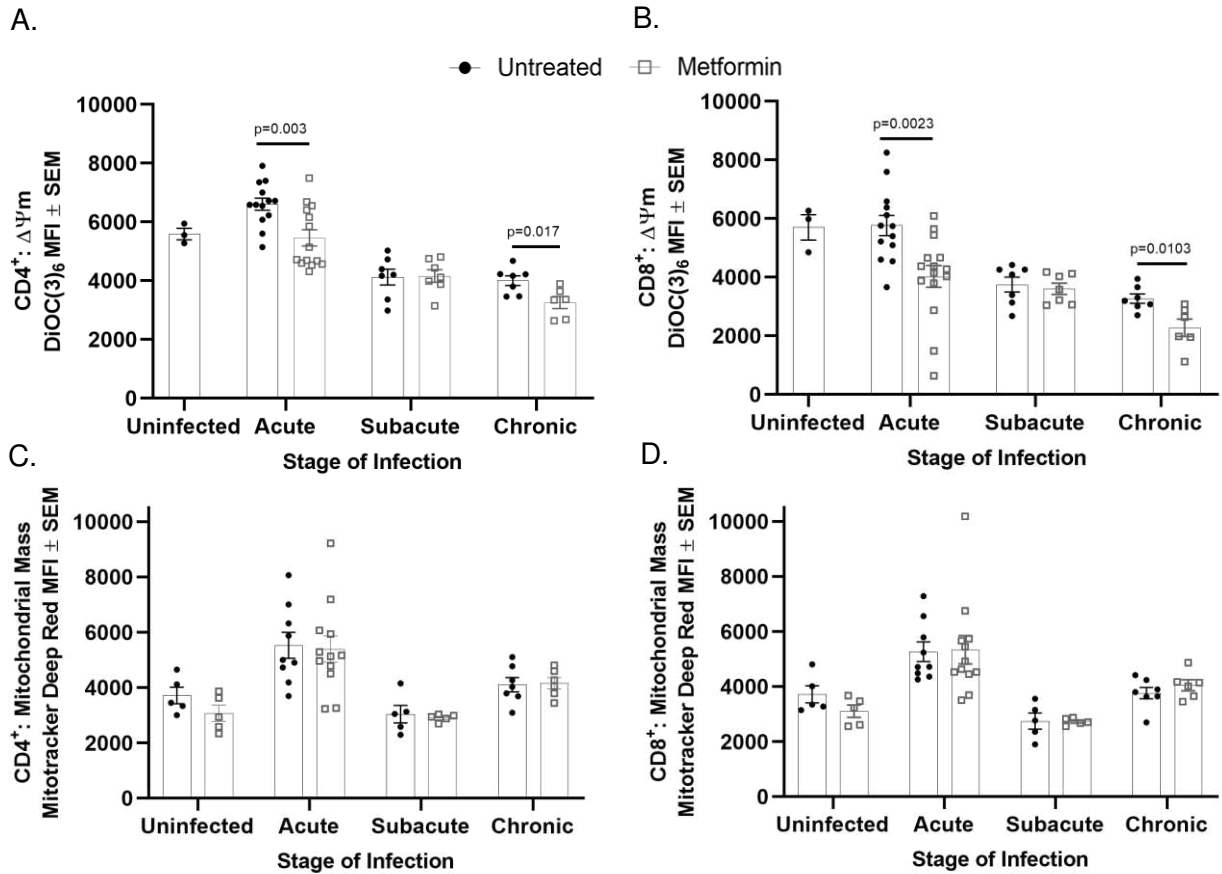
Figure 2.8. Metformin modulates T cell mitochondrial membrane potential. Peripheral mononuclear cells isolated from Mtb infected untreated and metformin-treated guinea pigs were stained with anti-CD4, anti-CD8, anti-MHC II, the ΔΨm dye $DiOC(6)_3$ (25nm), and the mitochondrial specific dye Mitotracker deep red (100nM) at different stages pre- or post-infection. Differential ΔΨm was determined between (A) CD4+ and (B) CD8+ by measuring the median fluorescent intensity of $DiOC(6)_3$ by flow cytometry. Mitochondrial mass was measured in (C) CD4+ and (D) CD8+ by mitotracker deep red staining and MFI measurement. (A) One outlier was identified using Tukey IQR method which was greater than 2.0 times the IQR. (A-B) Unpaired t-tests with Welch's correction was used to determine significance between groups within stage of infection. N=3-12 animals per group per timepoint. * p ≤
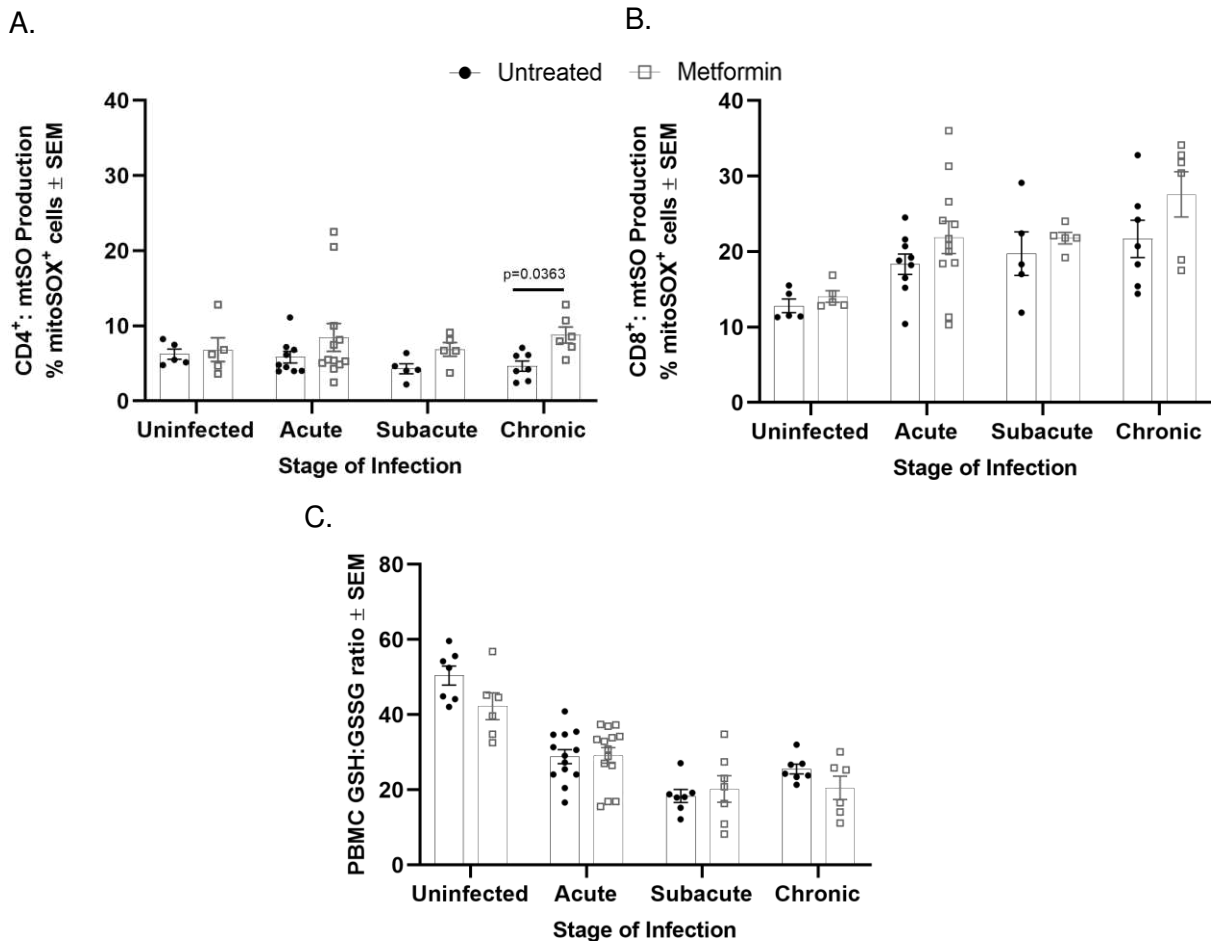
Figure 2.9. Metformin modulates CD4+ T cell mitochondrial superoxide production. (A-B) Peripheral mononuclear cells isolated from Mtb infected untreated and metformin-treated guinea pigs were stained with anti-CD4, anti-CD8, and the mitochondrial superoxide inicator dye mitoSOX at different stages pre- or post-infection. Data represents the % of total mitosox+ (A) CD4+ or (B) CD8+ cells. (C) GSH to GSSG ratios were measured in PBMCs by lucierein detection. N=6-13 per group per timepoint.

Metformin decreases inflammatory cytokine production in the lung during Mtb infection.

To further understand the differences observed between disease burden and granuloma morphology in response to metformin treatment, we sought to evaluate cytokine and transcription factor gene expression in granulomas from untreated and metformin-treated animals during chronic Mtb infection. In comparison to metformin-treated animals, untreated guinea pigs

displayed significantly more production of the pro-inflammatory cytokines TNFα, IL-12p40, and IL-1β, and enhanced production of IFN-γ and IL-6, though not statistically significant (Figure 2.10). Furthermore, metformin-treated animals displayed significantly higher expression of the regulatory T cell transcription factor FOXP3, however there were no significant differences in the abundance of anti-inflammatory IL-10 or TGF-β. Additionally, we observed a significant increase in monocyte chemoattractant protein (MCP-1) in granulomas from metformin compared to untreated animals.

A.
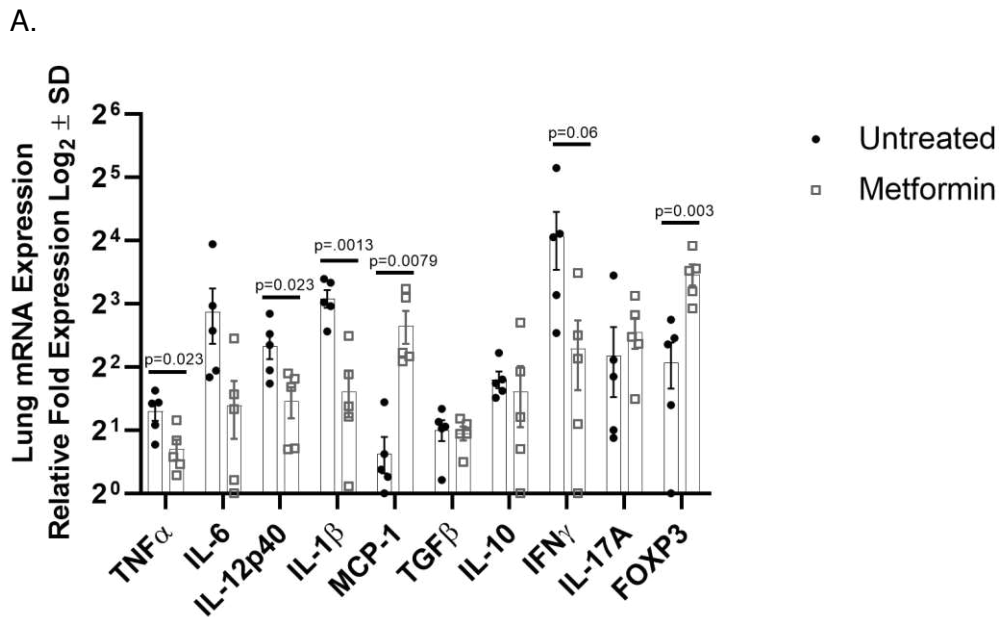
Figure 2.10. Metformin decreases inflammatory cytokine production in the lung during Mtb infection. Rneasy columns were used to extract RNA from homogenized lung tissue from chronically Mtb infected guinea pigs (day 75), which were either untreated or received metformin-treatment. 1ug RNA was converted to cDNA and primers against TNFα, IL-6, IL-12p40, IL-1β MCP-1, TGFβ, IL-10, IFNγ, IL-17A, and FOXP3 were used to quantify gene expression by qRT-PCR. Unpaired Student's t-test with Welch's correction or Mann-Whitney test was used to determine significances with Bonferroni correction for multiple comparisons. N=5 * p ≤ 0.05 ** p ≤ 0.01

Discussion

In these studies, we tested the hypothesis that reversing non-diabetic hyperglycemia in response to Mtb infection with metformin, would improve clinical outcomes in Mtb infected guinea pigs. When metformin treatment was initiated 28 days prior to Mtb infection, treated guinea pigs had significantly reduced lung lesion and bacterial burdens in the chronic stages of infection compared to untreated animals. This improvement corresponded with improved systemic insulin sensitivity, similar to the expected treatment response in diabetic patients. However, significant improvements in fasting blood glucose levels or glucose tolerance following Mtb infection were not achieved following metformin treatment. These data suggest that although metformin improved TB disease outcome, maintenance of systemic glucose tolerance alone was not responsible for these effects and suggests an alternative mechanism of action.

Multiple reports have shown metformin's potential use as an immune-modulatory drug in the treatment of various chronic inflammatory diseases [14,17,19,33]. These effects are, in part, due to its partial inhibition of complex I of the electron transport chain, which leads to downstream signaling events that regulate cell metabolism, growth, and function in T cells and other cell types [34-36]. Here, we show that following chronic Mtb infection, metabolic flux through mitochondrial respiration and glycolysis are dramatically upregulated in T cells isolated *ex vivo* from untreated Mtb infected guinea pigs. This response was not unexpected given the systemic inflammation and resulting acute and chronic immune cell activation associated with active TB disease [37,38]. Interestingly however, our results are in contrast with recent studies performed by Russell et al, in which they report a decrease in CD8^{+} T cell mitochondrial respiration following Mtb infection in mice [24]. It is therefore, important to note that among differences in animal models and evaluation of PBMCs versus isolated CD8^{+} T cells, we found that different stages of disease corresponded to fluctuating metabolic phenotypes, which may help to explain variability within the literature. Furthermore, we show that during chronic infection, PBMC metabolism is restored to normal in

metformin but not untreated animals. This was not due to variations in the percentages of circulating immune cells, but rather resulted from inherent cellular metabolic changes in response to metformin treatment. These findings are consistent with those observed in mouse models of systemic lupus erythematosus, in which metformin combined with 2-deoxyglycose normalized PBMC metabolism and resulted in decreased immune activation and the subsequent resolution of clinical disease [19]. We therefore, reasoned that changes in peripheral blood T cell metabolism reflect the waxing and waning of inflammation in response to persistent antigen stimulation, which was normalized by metformin treatment [39-41]. These data are consistent with similar studies and suggest that the beneficial effects of metformin treatment were not due to the restoration of normal systemic glucose metabolism, but rather a direct immunomodulatory effect on immune cells responding to Mtb infection [24,42].

In addition to similar work done in TB, non-TB studies also show that metformin treatment dampens inflammation and limits tissue destruction in a variety of communicable and non-communicable diseases by limiting the differentiation and pro-inflammatory potential of T lymphocytes [28,29]. Although we were limited in our ability to directly assess T cell function and differentiation of other T cell subsets due to the lack of available guinea pig reagents, we evaluated direct parameters of CD4$^+$ and CD8$^+$ T cell energy metabolism that correspond to their function, including mitochondrial membrane potential and mitochondrial superoxide production. Mitochondrial membrane potential, a measure of the gradient of hydrogen ions in the mitochondrial inner membrane space, is the primary driver of ATP production by the cellular electron transport chain. Inhibition of complex I has been shown to decrease mitochondrial membrane potential and lead to the downregulation of anabolic metabolism that is associated with effector T cell growth and function [31,43,44]. In addition, a recent study found that T cells with a high mitochondrial membrane potential correspond to highly differentiated effector cells with increased metabolism, while those with low membrane potential are less differentiated cells that

possess the ability to self-renew and retain immunological plasticity [31]. In our studies, peripheral CD4^{+} and CD8^{+} T cells isolated from guinea pigs treated with metformin had significantly reduced membrane potential compared to untreated animals during acute and chronic stages of Mtb infection. These data suggest that metformin, by maintaining a lower mitochondrial membrane potential, has the potential to influence the differentiation and function of T cells responding to Mtb infection, which is currently being investigated in our laboratory.

Mitochondrial superoxide production is also critical for the functional response of T cells and is found to play dual roles in both the promotion of effector functions and/or oxidative damage that can ultimately lead to cell death [30,31,45]. A direct link between membrane potential and superoxide has been described in systemic lupus erythematosus (SLE), where high membrane potential and inadequate ATP production correspond to obstructed electron flow, resulting in electron leakage and ROS production [30]. Due to the increased respiratory rates observed in response to Mtb infection, we hypothesized that mitochondrial superoxide would also be increased in T cells from untreated Mtb infected guinea pigs, while animals that received metformin would display reduced superoxide. Surprisingly, metformin significantly enhanced mitochondrial superoxide production by CD4^{+} T cells during chronic infection. This result was unexpected given that both mitochondrial respiration and membrane potential were reduced in T cells from metformin treated animals. One possible explanation is that increased mitochondrial superoxide is associated with maintenance of T cell functionality during chronic infection rather than oxidative damage and dysfunction [46,47].

To assert whether increased superoxide production was indicative of increased oxidative stress we measured the relative abundance of GSH: GSSG. Despite the increase in superoxide by CD4^{+} T cells from metformin treated animals, GSH: GSSG ratios remained consistent between both groups. These data provide further evidence that metformin's influence on CD4^{+} superoxide production may function to maintain important cell signaling events in CD4^{+} T cells [48].

The differential expression of cytokine genes in metformin treated and untreated guinea pigs by mRNA analysis also supports the hypothesis that metformin elicits its effects by altering immune cell function during Mtb infection and is consistent with findings by others [24]. We found that animals treated with metformin had dramatically decreased expression of pro-inflammatory cytokines. Moreover, although we observed increased expression of FOXP3, there was no difference in the production of regulatory cytokines, suggesting that the anti-inflammatory response was due to decreased pro-inflammatory cytokine production by effector cells. Taken together, these data provide strong evidence that metformin exerts its immunomodulatory effects directly on T cells during Mtb infection, resulting in a decreased pro-inflammatory response which explains the decreased lung inflammation and evidence of lesion resolution seen primarily in treated animals.

Importantly however, although metformin significantly reduced disease manifestation during chronic stages of infection in our studies, these findings did not correspond to increased guinea pig survival. In contrast to decreased lung lesion burden, there were no significant differences in the extrapulmonary lesion or bacterial burden in metformin treated animals, which likely explains the lack of improved survival. In addition, these studies did not assess the use of metformin as a therapy for pre-existing infection or as adjunctive therapy in combination with antimicrobial drug treatment of TB [49]. These are critical questions that will be evaluated in our future work and must be taken into consideration before metformin is evaluated as a practical host-directed therapy in humans.

Together, these studies show that alterations to host metabolism play an important role in the progression and severity of TB disease. Although we were unable to directly link the impact of non-diabetic hyperglycemia to TB disease pathogenesis using metformin, we discovered novel immune metabolic correlates of protection. Moreover, our results are consistent with previous

reports showing metformin's protective efficacy against Mtb infection in mice [14,18,24]. Our results

and others, therefore, warrants further evaluation of metformin and other drugs that target immune

cell metabolism in the ongoing discovery and development of novel TB therapeutics [50].

REFERENCES

1. Boillat-Blanco, N. *et al.* Transient Hyperglycemia in Patients With Tuberculosis in Tanzania: Implications for Diabetes Screening Algorithms. *J Infect Dis* **213**, 1163-1172 (2016).

2. Magee, M.J. *et al.* Stress Hyperglycemia in Patients with Tuberculosis Disease: Epidemiology and Clinical Implications. *Curr Diab Rep* **18**, 71 (2018).

3. Podell, B.K. *et al.* Non-diabetic hyperglycemia exacerbates disease severity in Mycobacterium tuberculosis infected guinea pigs. *PLoS One* **7**, e46824 (2012).

4. Jeon, C.Y. & Murray, M.B. Diabetes mellitus increases the risk of active tuberculosis: a systematic review of 13 observational studies. *PLoS Med* **5**, e152 (2008).

5. Hayashi, S. & Chandramohan, D. Risk of active tuberculosis among people with diabetes mellitus: systematic review and meta-analysis. *Trop Med Int Health* **23**, 1058-1070 (2018).

6. Lee, P.H., Fu, H., Lee, M.R., Magee, M. & Lin, H.H. Tuberculosis and diabetes in low and moderate tuberculosis incidence countries. *Int J Tuberc Lung Dis* **22**, 7-16 (2018).

7. Baker, M.A. *et al.* The impact of diabetes on tuberculosis treatment outcomes: a systematic review. *BMC Med* **9**, 81 (2011).

8. Podell, B.K. *et al.* Increased Severity of Tuberculosis in Guinea Pigs with Type 2 Diabetes: A Model of Diabetes-Tuberculosis Comorbidity. *Am J Pathol* **184**, 1104-1118 (2014).

9. Hundal, R.S. *et al.* Mechanism by Which Metformin Reduces Glucose Production in Type 2 Diabetes. *Diabetes* **49**, 2063-2069 (2000).

10. Foretz, M. *et al.* Metformin inhibits hepatic gluconeogenesis in mice independently of the LKB1/AMPK pathway via a decrease in hepatic energy state. *J Clin Invest* **120**, 2355-2369 (2010).

11. Marupuru, S. *et al.* Protective effect of metformin against tuberculosis infections in diabetic patients: an observational study of south Indian tertiary healthcare facility. *The Brazilian Journal of Infectious Diseases* **21**, 312-316 (2017).

12. Pan, S.W. *et al.* The Risk of TB in Patients With Type 2 Diabetes Initiating Metformin vs Sulfonylurea Treatment. *Chest* **153**, 1347-1357 (2018).

13. Degner, N.R., Wang, J.Y., Golub, J.E. & Karakousis, P.C. Metformin Use Reverses the Increased Mortality Associated With Diabetes Mellitus During Tuberculosis Treatment. *Clin Infect Dis* **66**, 198-205 (2018).

14. Malik, F. *et al.* Is metformin poised for a second career as an antimicrobial? *Diabetes Metab Res Rev* **34**, e2975 (2018).

15. Foretz, M., Guigas, B., Bertrand, L., Pollak, M. & Viollet, B. Metformin: from mechanisms of action to therapies. *Cell Metab* **20**, 953-966 (2014).

16. Lachmandas, E. *et al.* Metformin alters human host responses to Mycobacterium tuberculosis in healthy subjects. *J Infect Dis* (2019).

17. Kim, E.K. *et al.* Metformin ameliorates experimental-obesity-associated autoimmune arthritis by inducing FGF21 expression and brown adipocyte differentiation. *Exp Mol Med* **50**, e432 (2018).

18. Singhal, A. *et al.* Metformin as adjunct antituberculosis therapy. *Sci Transl Med* **6**, 263ra159 (2014).

19. Yin, Y. *et al.* Normalization of CD4+ T Cell Metabolism Reverses Lupus. *Sci Transl Med* **7**, 274ra218 (2015).

20. Zi, F. *et al.* Metformin and cancer: An existing drug for cancer prevention and therapy. *Oncol Lett* **15**, 683-690 (2018).

21. Pearce, E.L. *et al.* Enhancing CD8 T Cell Memory by Modulating Fatty Acid Metabolism. *Nature* **460**, 103-107 (2009).

22. Andrzejewski, S., Gravel, S.P., Pollak, M. & St-Pierre, J. Metformin directly acts on mitochondria to alter cellular bioenergetics. *Cancer Metab* **2**, 12 (2014).

23. Pearce, E.L., Poffenberger, M.C., Chang, C.H. & Jones, R.G. Fueling immunity: insights into metabolism and lymphocyte function. *Science* **342**, 1242454 (2013).

24. Russell, S.L. *et al.* Compromised Metabolic Reprogramming Is an Early Indicator of CD8(+) T Cell Dysfunction during Chronic Mycobacterium tuberculosis Infection. *Cell Rep* **29**, 3564-3579.e3565 (2019).

25. Buck, M.D., Sowell, R.T., Kaech, S.M. & Pearce, E.L. Metabolic Instruction of Immunity. *Cell* **169**, 570-586 (2017).

26.   Eikawa, S. *et al.* Immune-mediated antitumor effect by type 2 diabetes drug, metformin. (2015).

27.   Hiromatsu, K. *et al.* Characterization of guinea-pig group 1 CD1 proteins. *Immunology* **106**, 159-172 (2002).

28.   Philips, L., Visser, J., Nel, D. & Blaauw, R. The Association Between Tuberculosis and the Development of Insulin Resistance in Adults With Pulmonary Tuberculosis in the Western Sub-District of the Cape Metropole Region, South Africa: A Combined Cross-Sectional, Cohort Study. *BMC infectious diseases* **17** (2017).

29.   Kang, K.Y. *et al.* Metformin downregulates Th17 cells differentiation and attenuates murine autoimmune arthritis. *Int Immunopharmacol* **16**, 85-92 (2013).

30.   Son, H.J. *et al.* Metformin attenuates experimental autoimmune arthritis through reciprocal regulation of Th17/Treg balance and osteoclastogenesis. *Mediators Inflamm* **2014**, 973986 (2014).

31.   Perl, A., Hanczko, R. & Doherty, E. Assessment of mitochondrial dysfunction in lymphocytes of patients with systemic lupus erythematosus. *Methods Mol Biol* **900**, 61-89 (2012).

32.   Sukumar, M. *et al.* Mitochondrial Membrane Potential Identifies Cells with Enhanced Stemness for Cellular Therapy. *Cell Metab* **23**, 63-76 (2016).

33.   Lee, S.Y. *et al.* Metformin Ameliorates Inflammatory Bowel Disease by Suppression of the STAT3 Signaling Pathway and Regulation of the between Th17/Treg Balance. *PLoS One* **10**, e0135858 (2015).

34.   Bridges, H., Jones, A.Y., Pollak, M. & Hirst, J. Effects of metformin and other biguanides on oxidative phosphorylation in mitochondria. *Biochem J* **462**, 475-487 (2014).

35.   Delgoffe, G.M. *et al.* The kinase mTOR regulates the differentiation of helper T cells through the selective activation of signaling by mTORC1 and mTORC2. *Nat Immunol* **12**, 295-303 (2011).

36.   Araki, K. *et al.* mTOR regulates memory CD8 T-cell differentiation. *Nature* **460**, 108 (2009).

37.   Sasindran, S.J. & Torrelles, J.B. Mycobacterium Tuberculosis Infection and Inflammation: what is Beneficial for the Host and for the Bacterium? *Front Microbiol* **2** (2011).

38.   Yu, Y. *et al.* Different patterns of cytokines and chemokines combined with IFN-gamma production reflect Mycobacterium tuberculosis infection and disease. *PLoS One* **7**, e44944 (2012).

39.   Scriba, T.J. *et al.* Sequential inflammatory processes define human progression from M. tuberculosis infection to tuberculosis disease. *PLoS Pathog* **13**, e1006687 (2017).

40.   O'Garra, A. *et al.* The immune response in tuberculosis. *Annu Rev Immunol* **31**, 475-527 (2013).

41.   Ordway, D. *et al.* The cellular immune response to Mycobacterium tuberculosis infection in the guinea pig. *J Immunol* **179**, 2532-2541 (2007).

42.   Tsai, S. *et al.* Insulin Receptor-Mediated Stimulation Boosts T Cell Immunity during Inflammation and Infection. *Cell Metab* **28**, 922-934.e924 (2018).

43.   Fernandez, D., Bonilla, E., Mirza, N., Niland, B. & Perl, A. Rapamycin Reduces Disease Activity and Normalizes T Cell Activation–Induced Calcium Fluxing in Patients With Systemic Lupus Erythematosus. *Arthritis Rheum* **54**, 2983-2988 (2006).

44.   Ledderose, C. *et al.* Mitochondria are gate-keepers of T cell function by producing the ATP that drives purinergic signaling. *J Biol Chem* **289**, 25936-25945 (2014).

45.   Perl, A., Gergely, P., Nagy, G., Koncz, A. & Banki, K. Mitochondrial hyperpolarization: a checkpoint of T-cell life, death and autoimmunity. *Trends Immunol* **25**, 360-367 (2004).

46.   Gill, T. & Levine, A.D. Mitochondria-derived hydrogen peroxide selectively enhances T cell receptor-initiated signal transduction. *J Biol Chem* **288**, 26246-26255 (2013).

47.   Sena, L.A. *et al.* Mitochondria are required for antigen-specific T cell activation through reactive oxygen species signaling. *Immunity* **38**, 225-236 (2013).

48.   Franchina, D.G., Dostert, C. & Brenner, D. Reactive Oxygen Species: Involvement in T Cell Signaling and Metabolism. *Trends Immunol* **39**, 489-502 (2018).

49.   Dutta, N.K., Pinn, M.L. & Karakousis, P.C. Metformin Adjunctive Therapy Does Not Improve the Sterilizing Activity of the First-Line Antitubercular Regimen in Mice. *Antimicrob Agents Chemother* **61** (2017).

50.   Leung, C.C. Repurposing metformin to prevent and treat tuberculosis. *Respirology* **23**, 974-975 (2018).

CHAPTER 3 – METFORMIN PREVENTS TERMINAL DIFFERENTIATION OF AND PROVIDES BIOENERGETIC ADVANTAGE TO CD4$^+$ EFFECTOR T CELLS

Summary

Despite major efforts to elucidate what constitutes a protective immune response against *Mycobacterium tuberculosis* (Mtb) infection, knowledge gaps exist that hinder our ability to prevent or treat Tuberculosis (TB) disease. Our data show that metformin has *in vitro* and *in vivo* immunomodulatory activity and enhances protection against Mtb in guinea pigs. The mechanisms by which metformin alters T cell function following activation and whether these cells are responsible for the protection observed against Mtb is currently unknown. *We hypothesize that metformin promotes the development of more-protective, memory like T cells that are capable of self-renewal, multipotency, and persistence by targeting mitochondrial function.* To test this, we used an *in vitro* model system that generates different levels of T cell differentiation through anti-CD3/anti-CD28 activation. In response to metformin treatment, we find that *in vitro* differentiated CD4$^+$ T cells display decreased levels of differentiation as determined by functional and phenotypic profiling. Increased expression of the lymphocyte homing and tissue retention markers CD44 and CD69 were observed while the T cell activation marker, CD25, was significantly decreased in metformin treated compared to untreated T cells. Altered surface marker expression corresponded with significant reduction of the terminal differentiation marker KLRG1 and an increase in the ratio of expression between the antagonistic transcription factors Blimp-1 and BCL6, which control terminal differentiation and memory T cell properties, respectively. Metabolic profiling of non-terminally differentiated metformin treated T cells revealed a novel metabolic phenotype displaying characteristics of both effector and memory T cell phenotypes, including increased glycolytic reliance, reduced mitochondrial metabolism, maintenance of spare respiratory capacity, and reduced mitochondrial membrane potential. Altered differentiation potential and metabolism by metformin treatment ultimately resulted in enhanced cellular survival

and recall capacity following secondary antigen challenge. These results demonstrate that during differentiation, metformin provides T cells with metabolic and functional advantages corresponding to enhanced protection against chronic Mtb infection. With this study, we provide insights into favorable CD4+ T cell phenotypic and metabolic properties that aide our understanding of immune protection against Mtb and provide markers in which future vaccines can be designed and evaluated.

Introduction

The first vaccine approved for the prevention of tuberculosis disease (TB), bacille Calmette-Guérin (BCG), was discovered over 100 years ago following the attenuation of a virulent strain of bovine tuberculosis [1]. Today, BCG remains the only available TB vaccine, and although a significant contribution to science and medicine, it fails to provide full protection against the most common form of disease, adult pulmonary TB [2, 3]. As a result, TB is the current single cause of death by an infectious disease worldwide [4]. One barrier that has significantly hindered the development of new and more effective vaccines is our incomplete understanding of the immune response against the bacteria that causes TB, *Mycobacterium tuberculosis*— and particularly, what constitutes immune protection.

Based on evidence from animal models and human patients with underlying T cell immunodeficiencies, the CD4 T cell response is well appreciated for its protective role against Mtb infection [5, 6, 7]. Specifically, the T helper type 1 (Th1) response, which is characterized by the production of IFN-γ and macrophage mediated killing of intracellular pathogens [8]. As a result, recent vaccination strategies have focused on generating robust IFN-γ responses; however, the translational value of IFN-γ as a biomarker of protection has proven inadequate. This is exemplified by various BCG vaccination strategies, which induce differential amounts of IFN-γ, yet provide comparable levels of protection [9, 10]. In addition, studies have demonstrated that while CD4 knock-out mice are at greater risk of TB disease progression and death, IFN-γ levels are not

compromised, but are compensated for by increased production by CD8 T cells [10, 11]. These studies suggest that IFN-γ alone is not responsible for CD4 T cell mediated protection, highlighting the critical need to discover novel immune correlates of CD4 T cell mediated protection for the development of effective vaccines.

In our laboratory, we have shown that the anti-diabetic drug metformin can be repurposed to enhance host resistance against Mtb infection. Metformin is commonly prescribed for the treatment of type II diabetes due to its glucose lowering effects and demonstrates a high safety profile in human patients, rendering its approval by the Food and Drug Administration (FDA) [12]. In addition to its anti-glycemic affects, metformin also has various other off-target effects that correspond with improved clinical outcomes of both communicable and non-communicable diseases [12, 13, 14, 15, 16, 17]. Studies performed in guinea pigs by our laboratory, and mice by others, show that when initiated prior to Mtb infection, metformin leads to significantly reduced disease severity. The exact mechanism by which this occurs, however, is not well understood.

One way that metformin is known to influence the host response to disease is through immunomodulation [18, 19]. T cell function has been shown to be a direct target of metformin in multiple chronic inflammatory illnesses, corresponding to decreased production of pro-inflammatory mediators that results in reduced tissue damage and inflammation [14, 15, 18, 20]. Moreover, increased generation of memory T cells following metformin treatment has been demonstrated in an *in vivo* vaccination model, which is attributable to increased fatty acid metabolism [19]. These studies suggest that T cell functionality and differentiation in response to metformin treatment are also a rational and important are for investigation during Mtb infection. Furthermore, data from our studies in Mtb infected guinea pig studies show direct changes to T cell metabolism in response to metformin treatment, which are likely to correspond to altered cell functions and phenotypes.

Immunometabolism, or the study of immune cell metabolism has emerged as a novel means to investigate temporal changes in immune cell phenotypes due to the intricate relationship between metabolism and cellular fate and function [21, 22]. This strategy of cellular identification is particularly attractive due to the unnecessary reliance on known surface marker expression, opening the opportunity to discover novel cell types without pre-determined phenotypic bias. In response to chronic Mtb infection, T cells from peripheral blood mononuclear cells dramatically upregulate their utilization of both oxidative phosphorylation (OXPHOS) and glycolysis and undergo mitochondrial hyperpolarization, which are classic characteristics of highly differentiated pro-inflammatory T cells [23]. In contrast, PBMC T cells from metformin treated Mtb infected animals had normalized rates of glycolysis and OXPHOS and maintained mitochondrial membrane potential, similar to uninfected animals. Notably, cells with this metabolic phenotype are characterized as less differentiated phenotypes (i.e. memory T cells) that possess the ability to persist and self-renew following antigen encounter [23]. Importantly, while highly differentiated T cells produce cytokines that imply their protection against Mtb, recent studies show that less differentiated cell phenotypes confer increased protection against Mtb challenge [24, 25, 26, 27]. In addition, non-terminally differentiated T cell phenotypes show superior plasticity, proliferative capacity, migration and long-term survival in response to recurring antigen stimulation [24].

Based on our studies and the literature, we therefore, hypothesized that metformin, through metabolic regulation, enhances the generation of a memory T cell phenotype that has the capacity to persist and confer protection throughout chronic infection. Our studies address the impact that metformin has on T cell differentiation by evaluating functional and metabolic T cell phenotypes in response to *in vitro* activation. We demonstrate that, metformin, rather than increasing memory T cell formation, prevents pre-mature terminal differentiation of effector T cells, which have an increased capacity to respond to secondary Mtb antigen challenge, demonstrated by enhanced proliferation and survival. Furthermore, we discovered a novel metabolic phenotype of non-

terminally differentiated effector T cells that has not been previously described, that may be used to distinguish cell types in response to both infection and disease.

Materials and Methods

Animals and sample collection

Spleens were collected from eight- to twelve-week old, mixed gender, C57BL/6-Tg(H2-Kb-Tcra,-Tcrb)P25Ktk/J (P25 TCR-Tg) mice (generously provided by Kevin Urdahl, Seattle Children's Research Institute, Seattle, WA). Prior to tissue collection, animals were euthanized by carbon dioxide (CO_2) overdose. Spleens were aseptically removed and splenocytes were isolated by pushing tissue through a 70μM cell strainer with the plunger of a 3ml syringe. Isolated splenocytes were resuspended at a concentration of $2x10^6$ cells/ml in T cell media (TCM) (RPMI-1640 with L-glutamine + 1x non-essential amino acids + 10mM HEPEs + 0.5μM 2-mercaptoethanol) containing either 0μM, 600μM, or 1200μM metformin. Cell suspensions were then plated at a final concentration of $2x10^6$ cells/ml in a volume of 1ml into a 48-well tissue culture treated plate. T cell activation was achieved using either plate bound anti-CD3 (2μg/ml; clone 17A2; Biolegend, San Diego, CA) with anti-CD28 (1μg/ml; clone 37.51; Biolegend, San Diego, CA) (T_{EL}) or soluble anti-CD3 (5μg/ml; clone 17A2) with anti-CD28 (1μg/ml; clone 37.51) (T_{ML}). For plate-bound activation, 200μl of 2μg/ml anti-CD3 antibody in 1x PBS was added to each well of a 48-well tissue culture treated plate and incubated at 4°C overnight. Each well was gently rinsed with 1x PBS two times prior to adding cells to wells. Cell cultures were incubated in a humidified incubator held at 37°C + 5% CO_2 for 120 hours prior to analysis.

All animals were housed at the Colorado State University Laboratory Animal Resources facility in a BSL-1 laboratory. Experiments were performed in accordance with the National Research Council's Guide for the Care and Use of Laboratory Animals and were approved by the Animal Care and Usage Committee at Colorado State University.

Metabolic extracellular flux analysis

Activated CD3$^+$ T cells were negatively selected for 120 hours following activation using a MojoSort Cell Isolation Kit (Biologend Inc., San Diego, CA). Dead cells were simultaneously removed from cell suspension using biotinylated annexin and streptavidin labeled MojoSort beads. A total of 2x10^5 live CD3$^+$ T cells were suspended in seahorse XF assay media and were seeded onto a 24 well microplate (Agilent Technologies Inc., Santa Clara, CA) coated with CellTak (22.4μg/ml) (Corning Inc., Corning, NY.). Cell adherence to microplates was achieved by centrifugation (500xg, without brake) and confirmed by microscope evaluation, followed by a 30-minute incubation at 37°C in the absence of CO_2. Oxygen consumption rates (OCR) and extracellular acidification rates (ECAR) were measured using a Seahorse XFe24 bioanalyzer (Agilent Technologies, Inc., Santa Clara, CA). Injection of 1μM oligomycin, 2.5μM fluorocarbonyl cyanide phenylhydrazone (FCCP), 0.5μM rotenone + antimycin A, and 50mM 2-deoxyglucose was performed for quantification of basal OCR and ECAR, mitochondrial ATP production (basal – oligomycin), maximum respiration (FCCP – antimycin A/rotenone), spare respiratory capacity (FCCP – basal), glycolytic capacity (oligomycin - 2-DG), proton leak (oligomycin – antimycin a/rotenone), and non-mitochondrial oxygen consumption (antimycin a/rotenone).

Flow cytometry

At 0- and 120-hours following T cell activation, single-cell suspensions were prepared for antibody surface staining and/or intracellular staining. First, cells were harvested from 48-well plates and transferred into 5 ml polystyrene tubes, spun down at 500xg, and washed in 1x PBS prior to staining. Next, cells were resuspended in 200μl of the viability dye Zombie NIR (1:3500) (Biolegend Inc., San Diego, CA) prepared in 1x PBS, incubated in the dark for 15 minutes at room temperature, and then washed in 200μl FACs Buffer (1x PBS + 1% BSA). Fluorochrome-

conjugated surface antibodies including CD4 -BV510, -FITC, or -PECy7 (clone RM4-5), CD8 -BV421, or -BV570 (clone 53-6.7), CD44-FITC (clone IM7), CD25-Alexa Fluor 700 (clone PC61), CD69-PECy7 (clone H1.2F3), CD62L-Pacific Blue (clone MEL-14), CCR7-PE/Dazzle 594 (clone 4B12), and KLRG-1-BV605 (clone 2F1/KLRG1) were prepared in FACs buffer containing 1μg CD16/32 (clone 93) and added to cells for 20 minutes at 4℃ in the dark. Samples that were not prepared for intracellular staining were then washed with 200μl FACs buffer and resuspended in a final volume of 300μl for flow cytometry analysis.

Samples that were stained for intracellular markers were spun down and washed with 200μl of 1x permeabilization buffer three times following extracellular staining. Intracellular antibodies were then suspended in 200μl of 1x permeabilization buffer + 1μg CD16/32 (clone 93) per sample, added to cell pellets, and incubated at 4℃ for 20 minutes in the dark. Samples were then washed in 1x permeabilization buffer, suspended in 200μl fixation buffer, and incubated in the dark for 20 minutes at room temperature. Following fixation, samples were washed two times in FACs buffer and resuspended in a final volume of 300μl FACs buffer for flow cytometry analysis (Biolegend Inc., San Diego, CA). Fluorochrome-conjugated intracellular antibodies assessed include: Blimp-1-Alexa Fluor 647 (clone 5E7, BD Bioscience, San Jose, CA), Bcl-6-PE (clone IG191E/A8), FOXP3-Alexa Fluor 488 (clone MF-14), T-bet-APC (clone 4B10), RORgt-BV786 (clone Q31-378, BD Bioscience, San Jose, CA), and GATA3-Alexa Fluor 647 (clone 16E10A23). All antibodies were purchased from Biolegend Inc., San Diego, CA unless otherwise stated.

All samples were run on a Cytek™ Aurora Spectral Flow Cytometer (Cytek Biosciences, Fremont, CA). Data was interpreted using the median fluorescent intensity of each indicated dye following gating on live, CD4$^+$/CD8$^+$, single cells using FlowJo software (FlowJo, LLC, Ashland, OR).

Metabolic staining

The mitochondrial sensitive dye tetramethylrhodamine (TMRM) (ThermoFisher Scientific, Waltham, MA) was used to measure mitochondria membrane potential of naïve and activated T cells at 0- and 120-hours following *in vitro* activation. Briefly, 200μl of 25nm TMRM prepared in Hank's Balanced Salt Solution was added to cell suspensions following live/dead and extracellular antibody staining. Cells were then incubated in the dark for 30 minutes at 37℃ + 5% CO_2, washed in FACs buffer, and resuspended in 300μl FACs for flow cytometry analysis.

Glucose uptake was measured in live T cells at 0- and 120-hours following *in vitro* activation using the glucose analogue D-Glucose, 2-deoxy-2-((7-nitro-2,1,3-benzoxadiazol-4-yl)amino) (2-NBDG) (ThermoFisher Scientific, Waltham, MA). Following splenocyte isolation/cellular activation, cells were harvested from 48-well plates, transferred into 5 ml polystyrene tubes, and washed with 1x PBS prior to staining. Cell pellets were then resuspended in 200μl of 50μM 2-NBDG prepared in glucose-free RPMI-1640 + 10% FBS at 37℃ + 5% CO_2 for 2 hours in the dark. Samples were subsequently stained for viability and CD4/CD8 surface markers, as previously described, suspended in 300μl FACs buffer, and analyzed by flow cytometry.

Fatty acid uptake was assessed at 0- and 120-hours following *in vitro* T cell activation using the palmitate analogy BODIPY FL C16 (ThermoFisher Scientfic, Waltham, MA). As previously described, cells were harvested from 48-well plates into 5ml polystyrene tubes and washed with 1x PBS. Cell pellets were then resuspended in 200μl of 0.5μM BODIPY FL C16 in RPMI-1640 + 1% fatty acid free BSA and incubated in for two hours at 37C + 5% CO_2 in the dark. Samples were subsequently washed with 1x PBS and then stained for viability and CD4/CD8 cell surface markers, as previously described.

All samples were run on a Cytek™ Aurora Spectral Flow Cytometer (Cytek Biosciences, Fremont, CA). Data was interpreted using the median fluorescent intensity of each indicated dye following gating on live, CD4+/CD8+, single cells using FlowJo software (FlowJo, LLC, Ashland, OR).

LEGENDplex cytokine analysis

Cell culture supernatants were collected from T_{EL} and T_{ML} cells 120 hours following primary activation. Additionally, supernatants were collected from antigen re-challenged cells 96 hours following secondary stimulation ± Ag85b peptide. Concentrations of the cytokines IFN-γ, IL-6, IL-2, IL-5, IL-4, IL-21, IL-22, IL-17A, IL-10, and TGF-β1 were quantified using a custom designed LEGENDplex™ bead array (Biolegend Inc., San Diego, CA). Briefly, 25µl of supernatant was combined with an equal volume of assay buffer and 25µl of LEGENDplex™ beads in a V-bottom plate. Samples were then incubated at room temperature on a plate shaker for two hours protected from light. Following incubation, samples were washed two times with wash buffer and 25µl of detection antibodies were added to each well. Samples were incubated for one hour at room temperature on a plate shaker. Next, 25µl of SA-PE was added directly to each well and incubated at room temperature on a plate shaker for 30 minutes. Samples were then washed two times in wash buffer and resuspended in a final volume of 150µl of wash buffer for analysis. A standard curve was prepared in parallel using the provided standard. All samples were prepared in duplicate and were ran using a FacsAria flow cytometer (BD Biosciences). Data was analyzed using LEGENDplex™ software (Biolegend Inc., San Diego, CA).

NAD: NADH and ADP: ATP ratios

At 120 hours following activation, CD3+ T cells were negatively isolated from T_{EL} activated cells that were either left untreated (0µM) or treated with 600µM or 1200µM metformin using a

MojoSort magnetic bead cell separation kit (Biolegend Inc., San Diego, CA). Prior to cell separation, activated cells were harvested from 48-well plates and counted using a hemocytometer and trypan blue dead cell exclusion dye. A total of 1×10^7 live cells were then added to 5 ml polypropylene tubes, washed in 1x MojoSort buffer, and resuspended to a total volume of 100µl in 1x MojoSort buffer. A 10µl volume of antibody cocktail was added to each tube and samples were incubated for 20 minutes at room temperature on ice. A total of 10ul of MojoSort beads was then added to cell samples and incubated for 20-minutes on ice. Beads were then removed from cell samples by placing tubes on a magnetic tube rack for 5 minutes. $CD3^+$ cells were collected from the remaining supernatant into a fresh tube, washed in 1x PBS, and counted. A total of 1×10^4 live $CD3^+$ cells per sample was transferred into a white walled white bottom plate and assessed for NAD and NADH using an NAD: NADH luminescence detection kit (Promega, Madison, WI). Additionally, ratios of ADP: ATP were measured by transferring 1×10^5 live cells into a white walled white bottomed plate for ADP and ATP quantification by luminescence detection (BioAssay Systems, Hayward, CA). For both assays, a Beckman Coulter LD400 plate reader was used to measure luminescence. Values were calculated by generating standard curves of each respective substrate.

Fatty acid utilization

Cellular fatty acid utilization capacity was measured using a Biolog Mitochondrial Function Assay (Biolog, Hayward, CA). Live $CD3^+$ T_{EL} cells that were treated with either 0µM, 600µM, or 1200µM metfomin were negatively isolated 120 hours following *in vitro* activation using a magnetic bead cell isolation kit (Biolegend Inc., San Diego, CA). Cells were suspended in Biolog MAS buffer + redox dye + saponin at a final concentration of 5×10^6 cells/ml. A total of 1.5×10^5 lysed cells were then seeded into the wells of a Biolog 96 well plate pre-coated with acetyl-l-carnitine, octanoyl-l-carnitine, or palmitoyl-d, l-carnitine. Absorbance (OD_{590}) measurements were recorded every 15 minutes using a SpectraMax M2e plate reader held at 37℃ for a total of four hours. All analyses

were conducted in Rstudio 1.3.959. Interaction second-degree polynomial models were constructed with an interaction on the Time variable alone, and with separate intercepts for each grouped substate by run, using the lm test function for p-values. The rates of change presented are the coefficients for the linear effect; Time was centered on 2 (that is, 2 was subtracted from each Time value) so that the coefficients reflected the instantaneous rate of change at Time = 2. Confidence intervals were constructed using the standard errors for the differences as estimated by the models. Degrees of freedom were calculated with Satterthwaite's method for denominator degrees of freedom to account for the unbalanced data [28]. P-values for the differences in rate of change were adjusted within each substate with a Bonferroni method [29]. Adjustments were made separately for each group represented in a plot.

Ag85b recall

Splenocytes from p25 mice were stimulated under T_{EL} or T_{ML} conditions for 120 hours (described above). After 120 hours, cells were harvested and stained with 0.5µM CellTrace violet (ThermoFisher, Waltham, MA) in 1x PBS for 20 minutes at room temperature in the dark. Following staining, cells were counted, re-suspended in fresh TCM at a density of $1x10^6$ live cells/ml, and re-plated into 48-well cell culture treated plate. Cells were rested at 37°C + 5% CO_2 for 24 hours prior to re-stimulation. Re-stimulation was performed with either 1µg/ml Ag85b$_{aa240-254}$ (GenScript Biotech, Piscataway, NJ) or dimethyl sulfoxide (DMSO) mock treatment. Cells were incubated an additional 96 hours at 37°C + 5% CO_2 to achieve secondary stimulation and then harvested and stained with Zombie NIR, anti-CD4, and anti-CD8 for flow cytometry analysis. Live, CD4$^+$/CD8$^+$, single cells were evaluated for CellTrace violet dye dilution to quantify proliferation. The parent population (P0) was set to include all cells in unstimulated samples, and therefore, eliminate residual proliferation from primary stimulation. P1 was set to include all cells that proliferated beyond P0. Samples were ran using a Cytek™ Aurora Spectral Flow Cytometer

(Cytek Biosciences, Fremont, CA) and analysis was performed using FlowJo software (FlowJo LLC., Ashland, OR).

Data analysis

Tukey's IQR method was used to identify outliers in data sets. Based on data sets, One-way ANOVAs or T-tests were used to determine differences between groups. When necessary, data was normalized to account for technical variations between experimental data sets. If normality or homoscedasticity could not be achieved, data was analyzed using non-parametric methods. Post-hoc comparison methods were Tukey, Sidak's, or Mann-Whitney multiple comparisons test. Data was analyzed with Graph Pad Prism v.8 (GraphPad Software, San Diego, CA).

Results

Varying anti-CD3 signal strength generates effector-like and memory-like T cell subsets, in vitro.

To evaluate whether metformin has a direct influence on T cell differentiation, and the mechanism by which this occurs, we utilized an *in vitro* model of effector-like and memory-like T cell development. Splenocytes from P25 TCR-Tg mice, which specifically recognize the MHC class II restricted Mtb antigen, Ag85b$_{aa\ 240-254}$, were isolated and stimulated with varying strengths of activating antibodies, including plate bound anti-CD3 plus anti-CD28 or soluble anti-CD3 plus CD28. Flow cytometry tSNE analysis of the memory/effector T cell differentiating surface makers CD62L, CCR7, and CD44 demonstrate spatial clustering into two distinct populations unique to different activation conditions (Figure 3.1A). Consistent with typical effector (CD62L$^-$CCR7$^-$CD44$^+$) and memory (CD62L$^+$CCR7$^+$CD44$^+$) T cell phenotypes, plate bound stimulation generated cells that expressed CD62L$^-$CCR7$^-$CD44$^+$ (effector-like) while soluble conditions generated CD62L$^+$CCR7$^+$CD44$^+$ (memory-like) cells (Figure 3.1A-B). To confirm complete cellular activation of both phenotypes, the transient activation marker CD69 was quantified by flow

cytometry 48 hours following stimulation. We show that >90% of all CD4$^+$ T cells positively expressed CD69, regardless of the activating condition (Figure 1C). Memory- and effector-like phenotypes were also confirmed by performing a re-call response with Ag85b peptide and measuring cellular proliferation with the dye CellTrace Violet. At 96 hours following re-challenge we show that approximately twice as many (51.1%) soluble anti-CD3 stimulated cells underwent recall proliferation compared to cells activated under plate bound conditions (25.7%; p=0.0007) (Figure 1C & D). Based on these distinguishing characteristics, the remainder of our studies utilize plate bound anti-CD3 activated T cells as an effector like phenotype and soluble anti-CD3 activated cells as a memory like phenotype, referred to as T_{EL} and T_{ML} subsets, respectively.
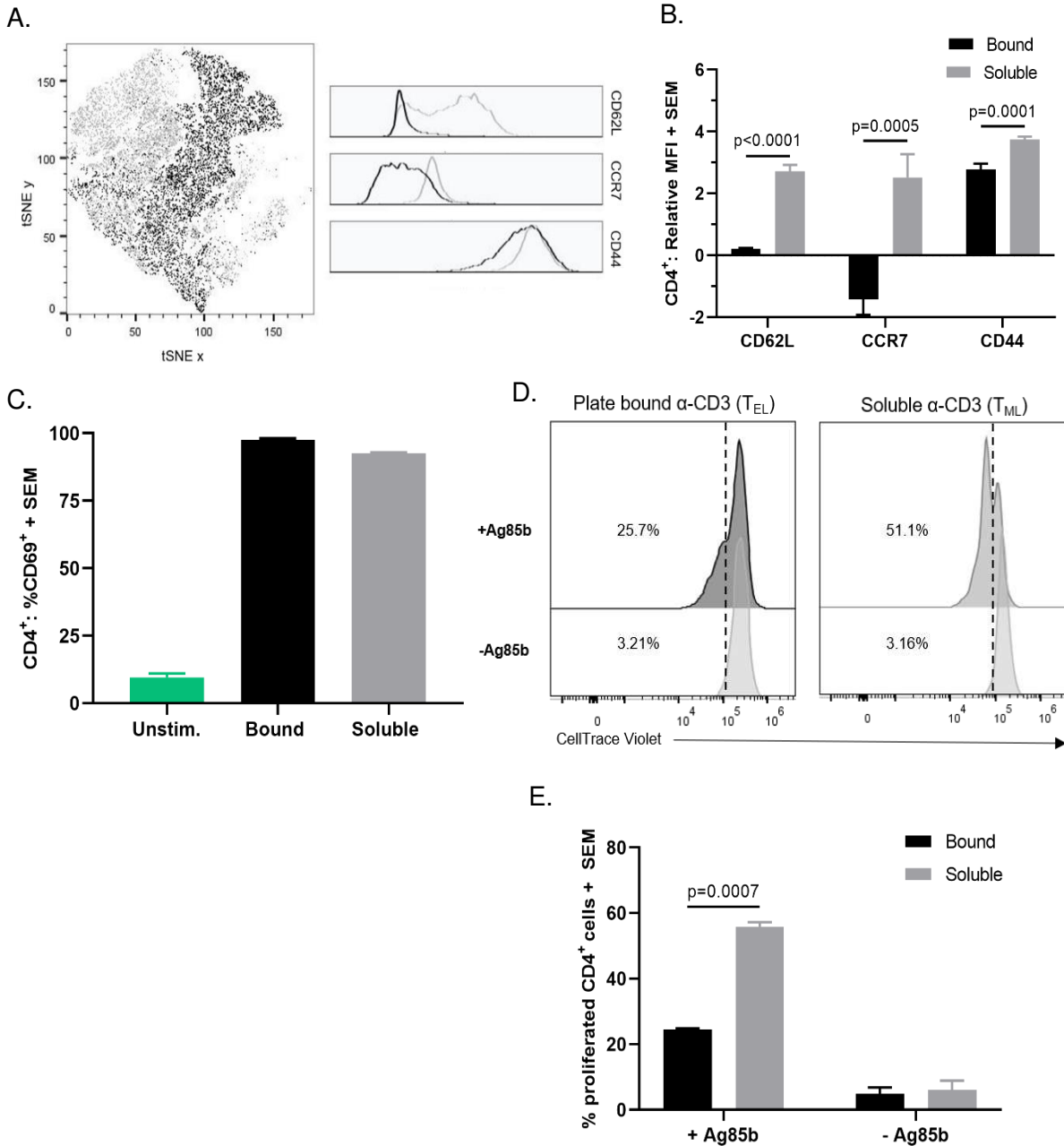
Figure 3.1. Phenotypic and functional features of *in vitro* differentiated CD4⁺ T cells. Splenocytes were isolated from 8-12-week-old P25 mice and stimulated with either 2ug/ml plate bound α-CD3 plus 1ug/ml soluble α-CD28 or 5ug/ml soluble α-CD3 plus 1ug/ml soluble α-CD28. (A-C) Surface marker expression of CD44, CD62L, CCR7, and CD69 were measured by flow cytometry. (A) A tSNE plot of soluble (gray) versus bound (black) stimulated CD4+ T cells based on CD44, CD62L, and CCR7 expression and their corresponding histograms. (B) Differential comparison of surface marker expression normalized to the mean MFI values of naïve CD4+ T cells. (C) % CD69 expressing T cells 48 hours following stimulation. (D-E) 120 hours following primary activation, soluble or bound anti-CD3 differentiated T cells were stained with the proliferation dye CellTrace violet and re-challenged with Ag85b peptide (1μg/ml). (D) Flow cytometry histograms representing CD4⁺ T cell proliferation. (E) Comparison of percent proliferation between bound and soluble differentiated CD4+ T cells. Data represents three independent experiments

Metformin reduces CD4⁺ T cell mitochondrial membrane potential following activation, like a memory T cell phenotype.

In vivo experiments suggest that the level of mitochondrial polarization, or mitochondrial membrane potential ($\Delta\Psi$m), can be used to identify memory versus effector CD8⁺ T cell phenotypes. Within these studies, low $\Delta\Psi$m corresponds to memory while high $\Delta\Psi$m corresponds to effector T cell phenotypes [30]. To determine whether this observation is consistent with *in vitro* generated T_{EL} and T_{ML} cells and could be used as a predictive marker of cellular phenotype, we measured $\Delta\Psi$m using the membrane potential sensitive dye tetramethylrhodamine (TMRM) and flow cytometry. Relative to naïve T cells, CD4⁺ T_{EL}s possessed a 20-fold and T_{ML} a 10-fold increase in TMRM median fluorescence intensity (MFI), indicative of mitochondrial polarization (Figure 1A). Correspondingly, T_{EL} cells generated a two-fold greater $\Delta\Psi$m compared to T_{ML}s following differentiation, confirming the validity of $\Delta\Psi$m as a marker of T_{EL} or T_{ML} phenotypes (Figure 3.2A & B).
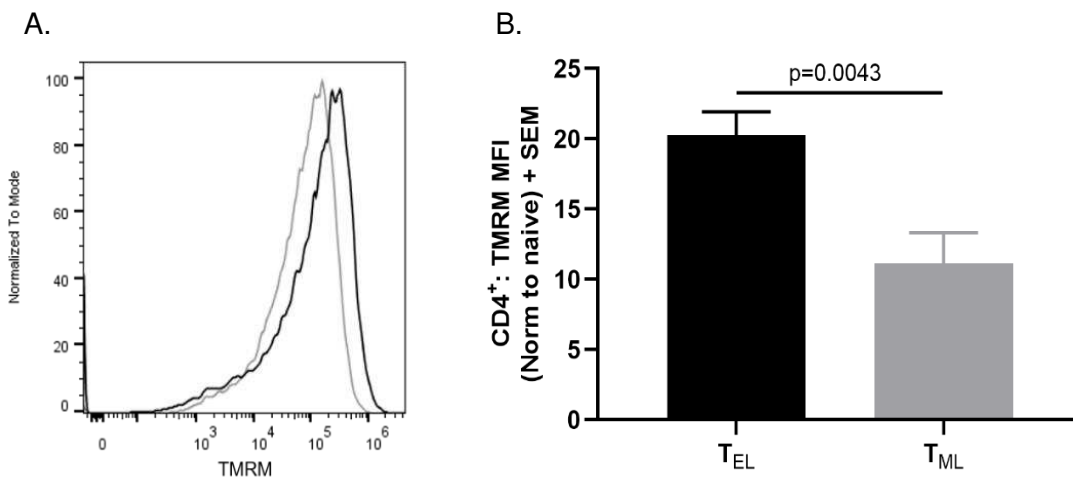
Figure 3.2. T_{EL} and T_{ML} mitochondrial membrane potential. T effector "like" (T_{EL}) or T memory (T_{ML}) T cells were differentiated *in vitro* for 120hrs and then stained with the viability dye Zombie NIR, anti-CD4, and $\Delta\Psi$m dye TMRM (25µM). (A-B) TMRM median fluorescence intensity (MFI) was measured by flow cytometry and used to compare $\Delta\Psi$m of CD4⁺ T_{EL} (black) and T_{ML} (gray) T cells. (B) Data was normalized to $\Delta\Psi$m of naïve T cells between three independent experiments (N=10-12). Significance was determined using an unpaired t-test.

Previously, our lab showed that metformin treatment was associated with decreased $\Delta\Psi m$ in CD4$^+$ T cells isolated from PBMCs of Mtb infected guinea pigs compared to animals that did not receive metformin. We, therefore, hypothesized that metformin reduces T cell $\Delta\Psi m$ in response to antigen recognition and ensuing differentiation. To evaluate this, we differentiated T_{ELS} in the presence of either 0, 600μM, or 1200μM metformin and measured $\Delta\Psi m$ by TMRM staining and flow cytometry. 1200μM metformin treatment was associated with a 2-fold reduction and 600μM with a 1.5-fold reduction in TMRM MFI compared to untreated cells, showing metformin's direct influence on $\Delta\Psi m$ (Figure 3.3A-B).
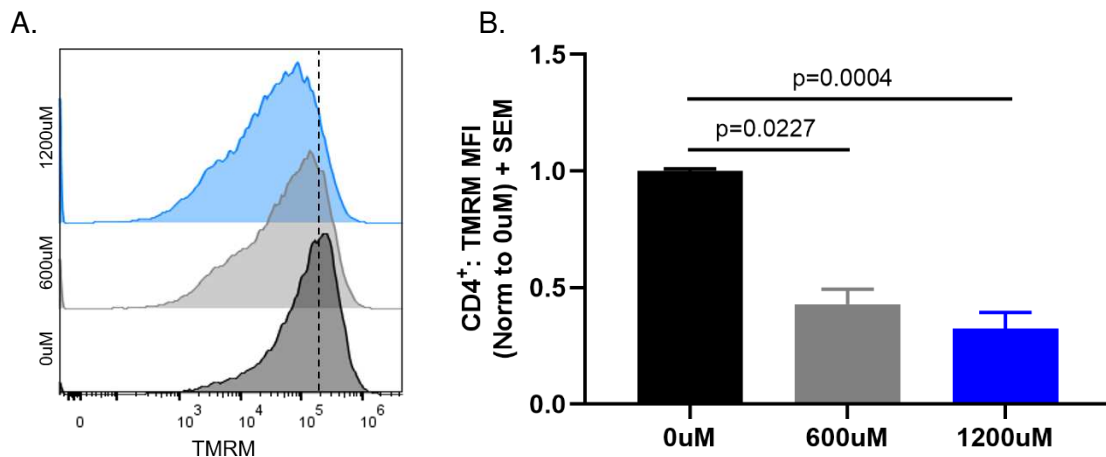
Figure 3.3. $\Delta\Psi m$ of T_{ELS} ± metformin. T_{ELS} cultured in the presence of 0μM, 600μM, or 1200μM metformin were stained with TMRM 120 hours following. TMRM MFI was evaluated by flow cytometry in CD4$^+$ gated T cells. A. TMRM histograms. B TMRM MFI quantification normalized to 0μM. Data represents four independent experiments (N=8). Significance determined using a non-parametric one-way ANOVA using a Kruskal-Wallis test.

Metformin modulates surface marker expression and cytokine production following T cell activation

Surface marker expression

Based on the relationship between T cell phenotype and $\Delta\Psi m$, we hypothesized that the decrease in $\Delta\Psi m$ associated with metformin treatment would correspond to increased generation of memory like T cells (CD44$^+$CD62L$^+$). There was no increase in the proportion of neither CD4$^+$

nor CD8$^+$ cells that resembled a T$_{ML}$ phenotype in the presence of metformin at any concentration (Figure 3.4). The relative expression of surface markers associated with T cell activation and differentiation— including CD25, CCR7, CD44, and CD62L— were measured by flow cytometry. In comparison to metformin un-exposed CD4$^+$ T$_{EL}$s, 600µM and 1200µM metformin reduced expression of CD25 by 10% or 22% (p=0.0014) and increased the expression of CD44 by 52% or 140% (p=0.0016) and CD69 by 38% or 76% (p=0.0077), respectively (Figure 3.4).
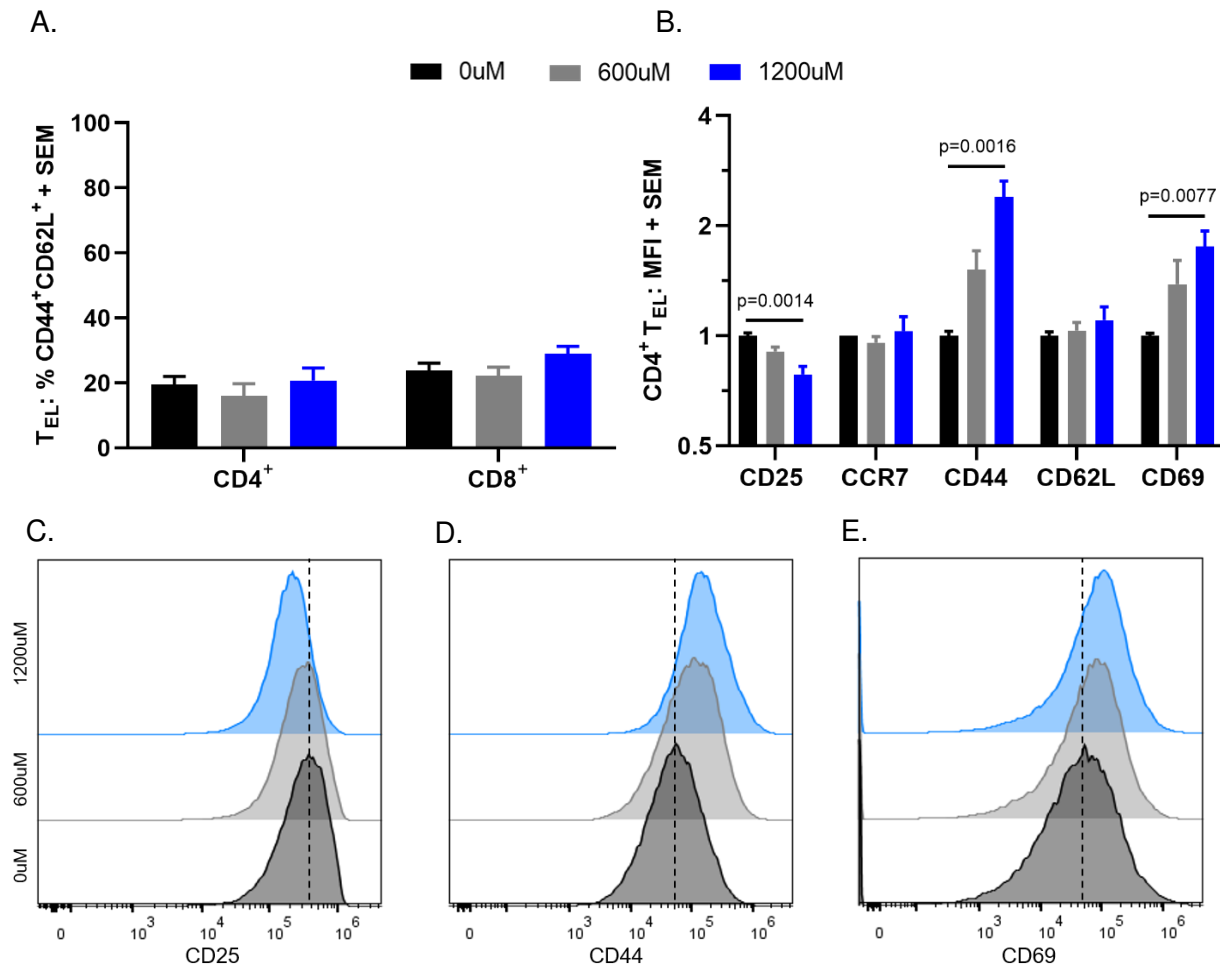
Figure 3.4. CD4$^+$ T$_{EL}$ surface marker expression, ± metformin. Surface markers were evaluated on CD4$^+$ T$_{EL}$s ± metformin (0µM: black; 600µM gray; 1200µM blue) at 120 hours post-activation using flow cytometry analysis. (A) Percent of CD4$^+$ or CD8$^+$ T cells that express the memory phenotype markers, CD44 and CD62L. (B) MFIs of the activation markers CD25, CCR7, CD44, CD62L, and CD69 on CD4$^+$ T$_{EL}$ cells. (C, D, &E) Representative flow cytometry histograms of (C) CD25, (D) CD44, and (E) CD69. (A-B) Data represents four independent experiments (N=6-8). (B) MFIs were normalized to the mean of the 0µM group for each experiment. Significance was determined using either an ordinary one-way ANOVA using Dunnet's multiple comparison.

To examine whether altered surface marker expression was associated with differences in T cell cytokine production, supernatant was collected from T_{EL}s cultured in the presence of 0 or 1200µM metformin 120 hours following activation. Concentrations of the T cell cytokines IFN-γ, IL-6, IL-2, IL-5, IL-4, IL-21, IL-22, IL-17A, IL-10, and TGF-β1 were quantified using a custom-designed LEGENDplex™ bead array and flow cytometry analysis. In comparison to untreated (0µM) samples, metformin significantly decreased concentrations of IL-6 by 1.67- (p=0.0011), IL-5 by 3.44 (p=0.0004), IL-4 by 6.87- (p=0.0002), IL-21 by 3.125- (p<0.0001), IL-22 by 7.51 (p=0.0002), and IL-10 by 11.5-fold (p=0.0016) (Figure 2E). IL-2 was increased 2.54-fold (p<0.0001) in metformin exposed compared to unexposed cells (Figure 2E).

A.
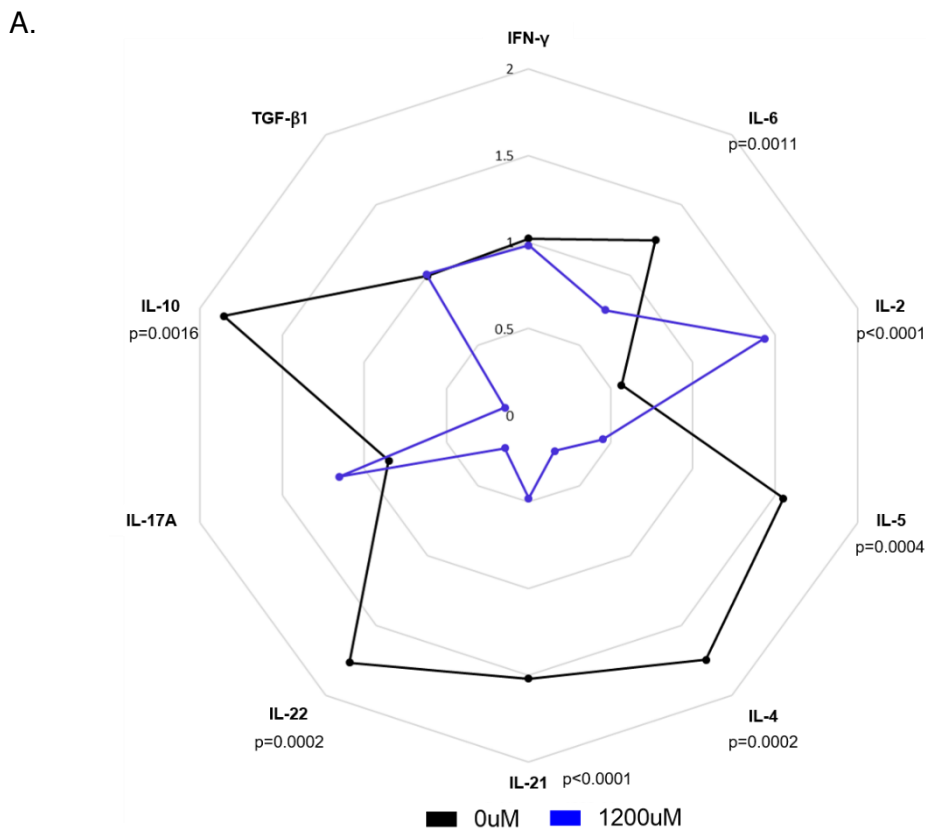
Figure 3.5. T_{EL} cytokine production ± metformin. (A) Supernatants were collected from T_{EL} cell suspensions, ± metformin (0µM: black; 1200µM blue), 120 hours post-activation and assessed for cytokine production (pg/ml) using a LEGENDplex™ bead array. Data represents four independent experiments (N=8). Concentrations were normalized to total cell numbers and values represent the concentration of each cytokine relative to the overall mean average. Significance was determined using paired or unpaired t-tests.

CD25 serves as both a marker of T cell activation and regulatory T cell (Treg) identification. To ensure that the high expression of CD25 on *in vitro* differentiated T cells did not correspond to the generation of Tregs we evaluated the Treg transcription factor FOXP3. FOXP3 expression was not detected in neither T_{ML} nor T_{EL} differentiated populations. Moreover, exposure to 1200μM metformin did not alter FOXP3 expression.
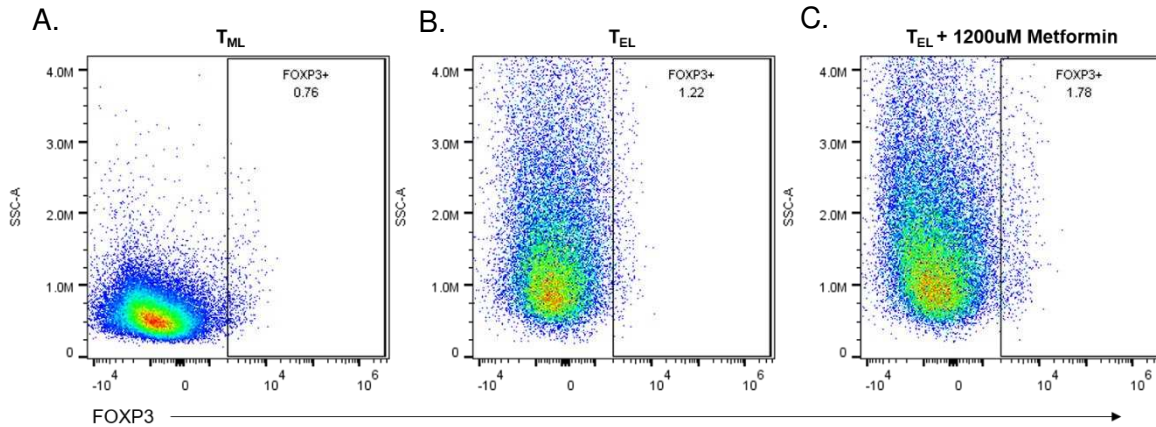

Figure 3.6. CD4+ FOXP3 expression ± metformin. FOXP3 expression was measured by flow cytometry in (A) T_{ML}, (B) T_{EL}, and (C) 1200uM metformin exposed T_{EL}s 120 hours following *in vitro* activation. (A-C) Flow cytometry dot plots representing FOXP3 staining.

In response to altered cytokine expression, lineage differentiating transcriptions factors Tbet (T helper 1), RORγt (T helper 17), GATA3 (T helper 2) were evaluated in 0μM and 1200μM metformin exposed CD4+ T_{EL} cells. Approximately 78% of cells expressed Tbet, 46% expressed GATA3, and 28% expressed RORγt (Figure 3.7A, C, & E). While no significant differences in the percent of cells expressing each transcription, factor were observed in association with metformin treatment, the MFI of GATA3 was reduced by 50% (p=0.0772) and RORγt expression was increased by 13% (p=0.0218) in cells exposed to 1200μM metformin compared to those that were unexposed (0μM) (Figure 3.7A-F).
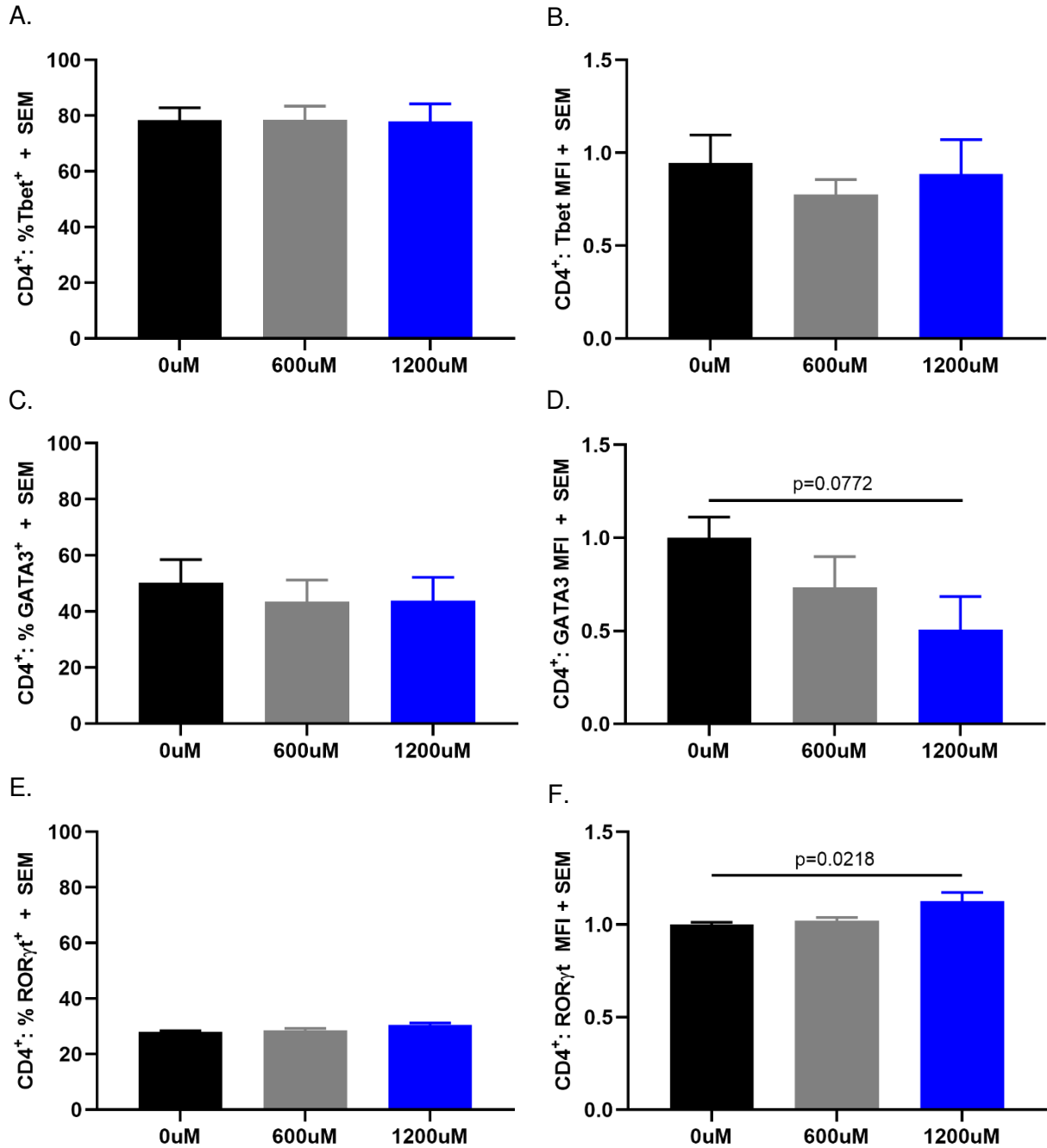
Figure 3.7. CD4$^+$ T$_{EL}$ Tbet, GATA3, and RORγt expression. Expression of the transcription factors (A-B) Tbet, (C-D) GATA3, and (E-F) RORγt were measured in CD4$^+$ T$_{EL}$ cells, ± metformin (0μM: black; 600μM gray; 1200μM blue), by flow cytometry. (A, C, & E) Percent of total CD4$^+$ T$_{EL}$s expressing (A) Tbet, (C) GATA3, or (E) RORγt. (B, D, & F) Total MFI of (B) Tbet, (D) GATA3, or (F) RORγt. Data represents three independent experiments (N=4-8). MFIs from each experiment were normalized to the mean of the 0μM group. (D) Significance was determined using an ordinary one-way ANOVA.

Metformin prevents terminal differentiation of T_{EL} cells

Although metformin did not increase the proportion of memory T cells, the dramatic changes in surface marker expression supports the hypothesis that metformin modulates T cell differentiation. The level at which this is occurs along the T cell differentiation axis, however, is yet to be defined. We hypothesized that rather than increasing the memory T cell pool, as defined by CD44 and CD62L expression and strict phenotypic compartmentalization, metformin interferes with the generation of highly differentiated pro-inflammatory T cells. To test this, we measured the expression of the terminal differentiation marker KLRG1 and the ratio of expression between the transcription factors Blimp-1 and BCL6, which act as antagonistic genetic switches underlying T cell death or self-renewal and persistence [31].

KLRG1

Following *in vitro* differentiation, approximately 21% of CD4$^+$ T_{EL} and 2% of T_{ML} cells positively expressed the terminal differentiation marker KLRG1 (<0.0001) (Figure 3.8A). In the presence of 600μM or 1200μM metformin, the percentage of CD4$^+$ T_{EL} KLRG1 positive cells decreased from 21% to 14.35% and 5.2%, respectively (p=0.0319, p<0.0001) (Figure 3.8A-D).
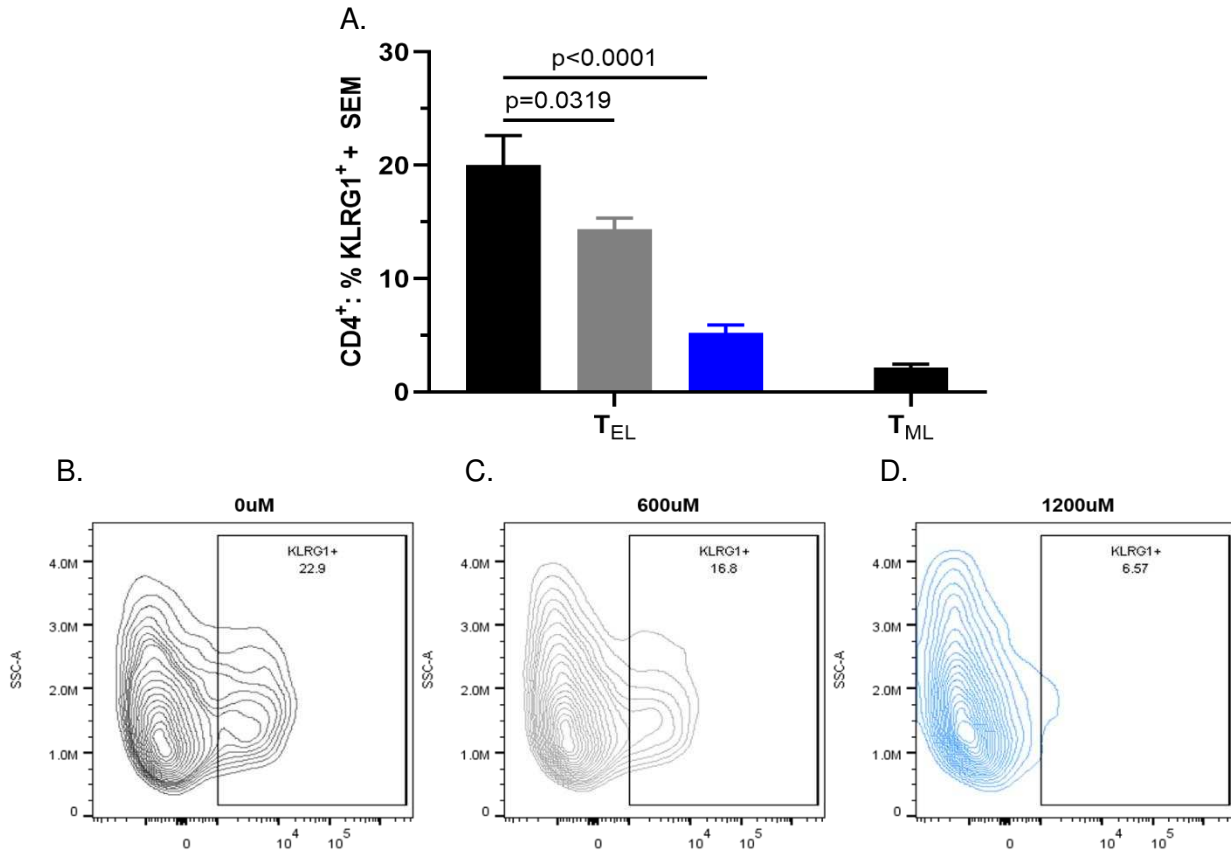
Figure 3.8. Differential KLRG1 expression on *in vitro* differentiated CD4⁺ T cells, ± metformin. KLRG-1 expression was measured on *in vitro* differentiated (A-D) T_{EL} and (C) T_{ML} cells by flow cytometry. Differential expression of KLRG1 on CD4⁺ T_{EL} cells that were differentiated in the presence of (B) 0µM, (C) 600µM, or (D) 1200µM metformin. Data represents four independent experiments (N= 6-8). Significance was determined using a non-parametric ANOVA with Dunn's multiple comparisons activation.

Blimp-1/BCL6

The ratio of Blimp-1 to BCL6 was measured in T_{EL} and T_{ML} cells by flow cytometry 120 hours following *in vitro* activation. Relative to CD4⁺ T_{EL} cells, T_{ML}s displayed an approximate 4-fold decrease in their ratio of expression of Blimp-1 to BCL6 (p=.0064) (Figure 3.9A). In CD4⁺ T_{EL}s differentiated in the presence of 1200µM metformin, this ratio was decreased by 7.58-fold in comparison to cells that were not exposed to metformin (p=0.0002) (Figure 3.9A), which is attributable to both a decrease in Blimp-1 expression and an increase in BCL6 (Figure 3.9B & C). Together, these data demonstrate that metformin dramatically reduces terminal differentiation

characteristics of CD4$^+$ T$_{EL}$ cells, resulting in a phenotype that more closely resembles their less-differentiated T$_{ML}$ counterparts (Figure3.9 D).
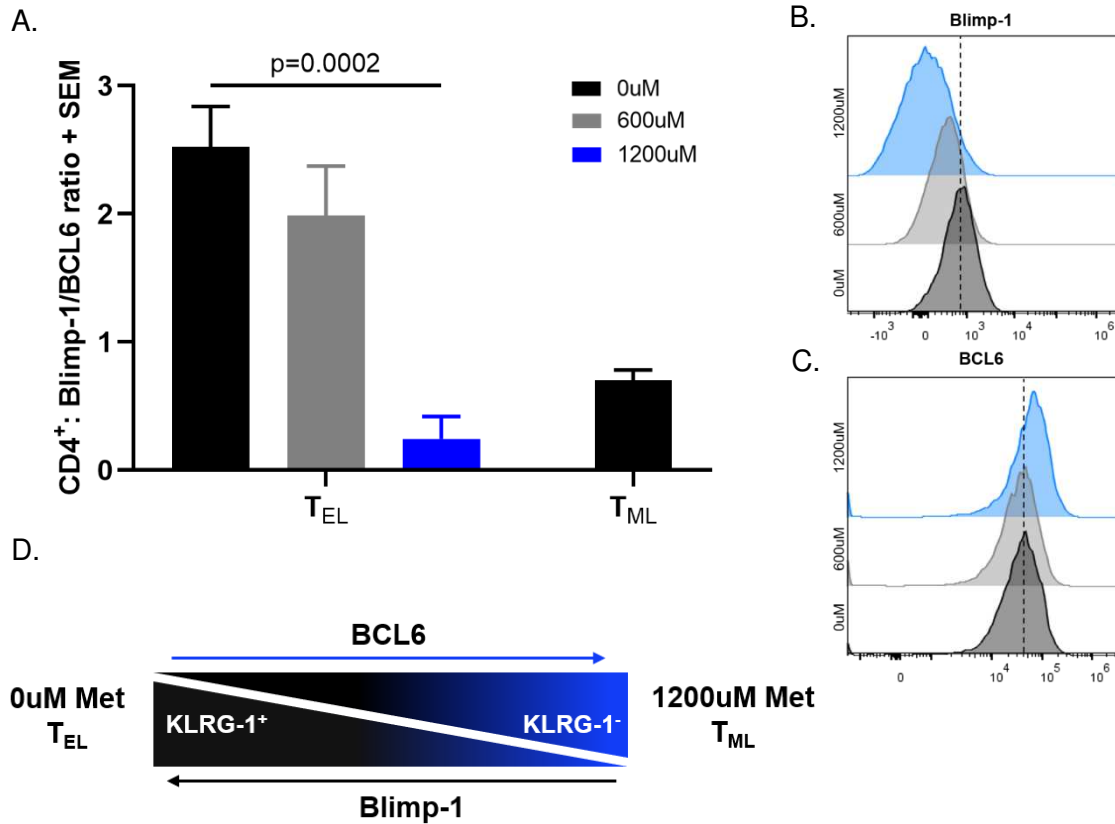

Figure 3.9. Differential expression of Blimp-1 and BCL6 in CD4$^+$ T cells, ± metformin. (A-C) Blimp-1 and BCL6 expression were measured by flow cytometry in CD4$^+$ T$_{ML}$s and T$_{EL}$s, ± metformin (0µM: black; 600µM gray; 1200µM blue). (A) The ratio of Blimp-1 to BCL6 expression was calculated by normalizing the MFI of each transcription factor to their respective mean MFI and dividing Blimp-1 by BCL6. Data represents four individual experiments (N= 7-8). (B) Representative histograms of Blimp-1 (B) and BCL6 (C) expression in CD4$^+$ T$_{EL}$s. (D) Graphic representation of the axis of expression between KLRG-1, BCL6, and Blimp-1 in response to metformin and levels of T cell differentiation. (A) Significance was determined using an ordinary one-way ANOVA with Dunnet's multiple comparison.

Metformin increases T$_{EL}$ glycolytic flux to maintain ATP production.

T cells are characterized by unique metabolic phenotypes that directly influence their phenotypic and functional properties. Highly differentiated effector T cells display high rates of glucose uptake and metabolic flux and increase their reliance on glycolytic metabolism for the generation of biosynthetic intermediates that are required for cell growth. Conversely, less

differentiated quiescent T cells, including memory and naïve subsets, maintain low levels of basal metabolism and predominantly rely on oxidative metabolism (OXPHOS) for the continuous production of ATP required for long-term cell survival. In our studies we evaluated 1. whether *in vitro* differentiated T_{EL} and T_{ML} cells align with these traditional metabolic phenotypes and 2. how metformin influences T cell metabolism following early differentiation.

Extracellular flux analysis

Metabolic function of negatively isolated CD3$^+$ T_{EL} and T_{ML} cells was characterized by extracellular flux analysis, which indirectly measures glycolysis by extracellular acidification rate (ECAR) and OXPHOS by oxygen consumption rate (OCR). T_{EL}s that were exposed to either 600µM or 1200µM metformin during differentiation displayed ECAR that was increased by 1.3- or 1.46-fold compared to untreated cells, respectively ($p=0.0048$; $p=0.0014$) (Figure 3.10A). Alternatively, 600µM metformin decreased OCR by 1.8-fold and 1200µM by 4.3-fold ($p=0.0286$; $p=0.0004$) (Figure 3.10B). Together, increased OCR and decreased ECAR in response to metformin corresponded to a dose-dependent decrease in the overall OCR to ECAR ratio, demonstrating increased reliance on glycolysis ($p<0.0001$) (Figure 3.10C & D). Additionally, T_{EL} OCR was found to be 2.6- and ECAR 8.55-fold greater than that measured in T_{ML}s ($p<0.0001$; $p<0.0001$) (Figure 3.10A-C). OCR to ECAR ratios show that, relative to their overall metabolic utilization, T_{ML}s were 3.42 times more reliant on OXPHOS than T_{EL}s (Figure 3.10D).

NAD: NADH ratios

One of the main ways that metformin targets cellular metabolism is through partial inhibition of complex I of the ETC, the primary site for oxidation of NADH into NAD$^+$ [32, 33]. To confirm that reductions in mitochondrial metabolism were due to inhibition of complex I, we measured the ratios of NAD: NADH in metformin treated and untreated T_{EL}s. In response to

127

600uM and 1200uM metformin, 3.07- and 4.09-fold decreases were observed in the ratios of NAD

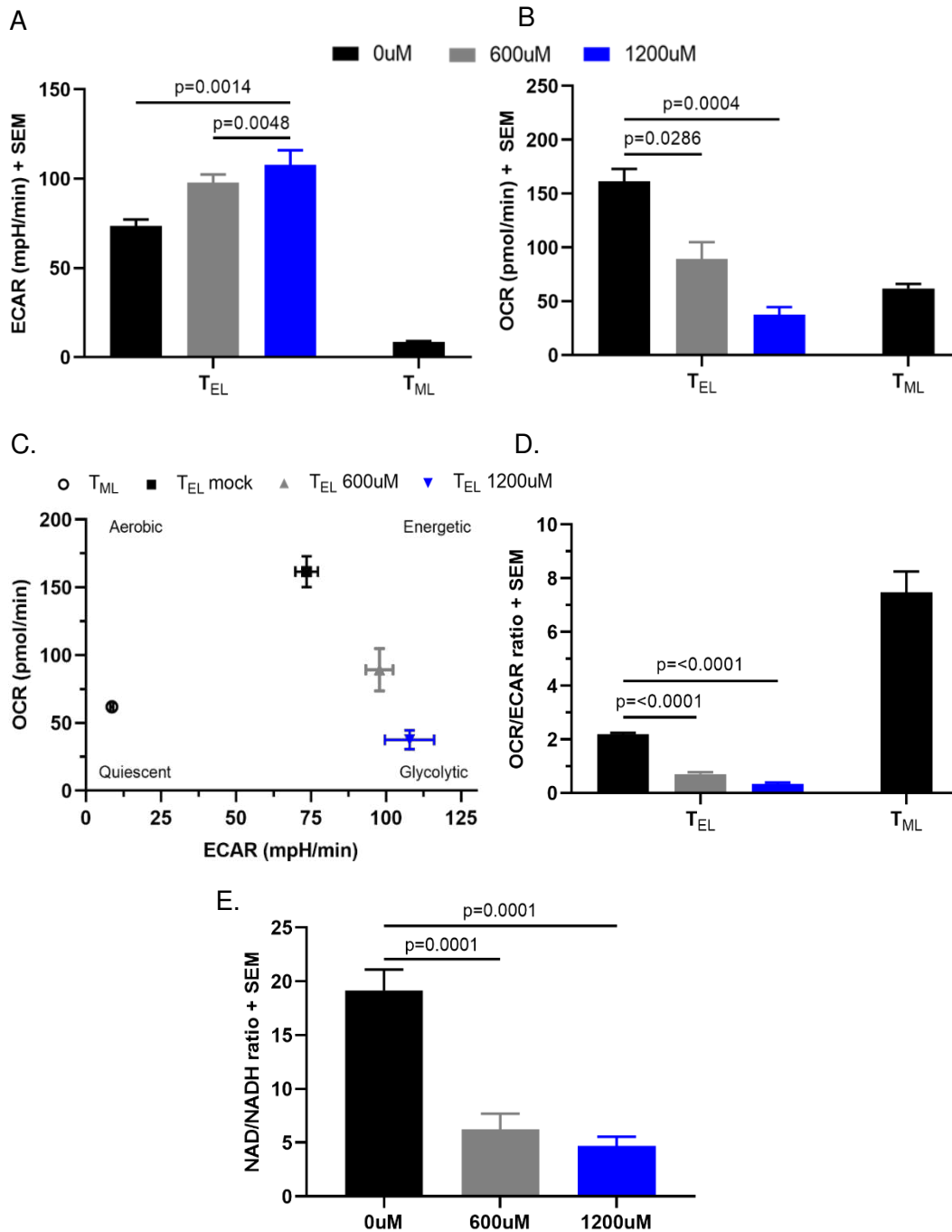to NADH compared to untreated cells, respectively (p=0.0001).

Figure 3.10. Energy metabolism of T_{ML} and T_{EL} cells ± metformin. CD3^{+} T cells were negatively purified from *in vitro* differentiated T_{ML} or T_{ELS}, ± metformin (0µM: black; 600µM gray; 1200µM blue). (A-D) Extracellular flux analysis was used to measure basal levels of (A) glycolysis (ECAR) and (B) OXPHOS (OCR). (C) Energy map of OCR and ECAR utilization. (D) OCR/ECAR ratio. (E) CD3^{+} T_{EL} NAD: NADH ratios. Data represent three independent experiments (N=6-13). Significance was determined using an ordinary one-way ANOVA or a Kruskal-Wallis test.

ATP production

Mitochondrial stress tests were performed to investigate mitochondrial functions through the addition of complex-specific inhibitors (oligomycin, rotenone, antimycin A) and a proton uncoupler (FCCP). Oligomycin, an ATP synthase inhibitor, was injected following basal readings to measure mitochondrial-derived ATP production. Compared to unexposed cells, T_{ELS} differentiated in the presence 600μM or 1200μM metformin displayed a 2.67- and 6.6-fold reduction in mitochondrial ATP production (p<0.0001) (Figure 3.11A). To determine whether this led to an overall change in ADP ATP redox balance, we further quantified cellular ADP and ATP concentrations by luciferase detection. Despite reduced mitochondrial-derived ATP, there was no difference in ADP/ATP ratios between metformin-exposed and unexposed cells, at any concentration (Figure 3.11B).
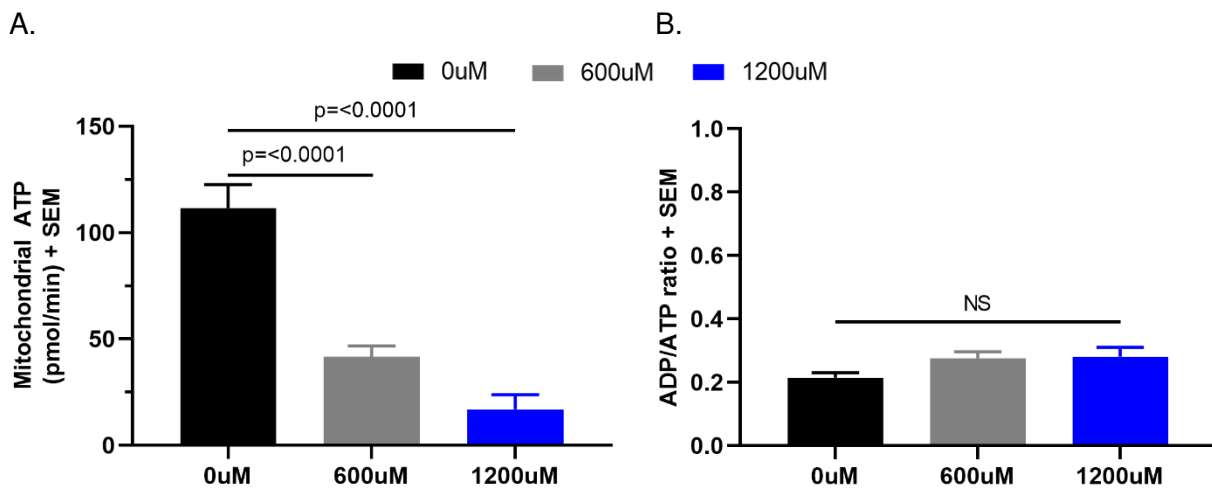

Figure 3.11. T_{EL} ATP production ± metformin. ATP production of negatively isolated CD3+ T_{ELS}, ± metformin (0μM: black; 600μM gray; 1200μM blue), measured by (A) extracellular flux analysis or (B) ADP/ATP ratios measured using a luminescent detection kit. Data represents three independent experiments (A. N=6-13; B. N=6). Significance was determined using ordinary one-way ANOVAs.

Glucose uptake

Relative glucose uptake between metformin exposed and unexposed T_{ELS} was measured to determine whether there was a contaminant increase in glucose demand associated with the

increased glycolytic flux. At 120 hours following *in vitro* activation, T_{EL}s were incubated with the fluorescent glucose analogue 2-NBDG and fluorescent intensity was measured by flow cytometry. Uptake of 2-NBDG was increased by ~32% in 1200μM metformin-exposed CD4$^+$ T_{EL}s compared to unexposed cells (p=0.0045) (Figure 3.12A & B). 1200μM metformin exposed CD8$^+$ T_{EL}s displayed a 16% increase in 2-NBDG uptake compared to unexposed cells, or the equivalent of 2-fold less (~16%) 2-NBDG uptake in comparison to CD4$^+$ cells (Figure 3.12A).
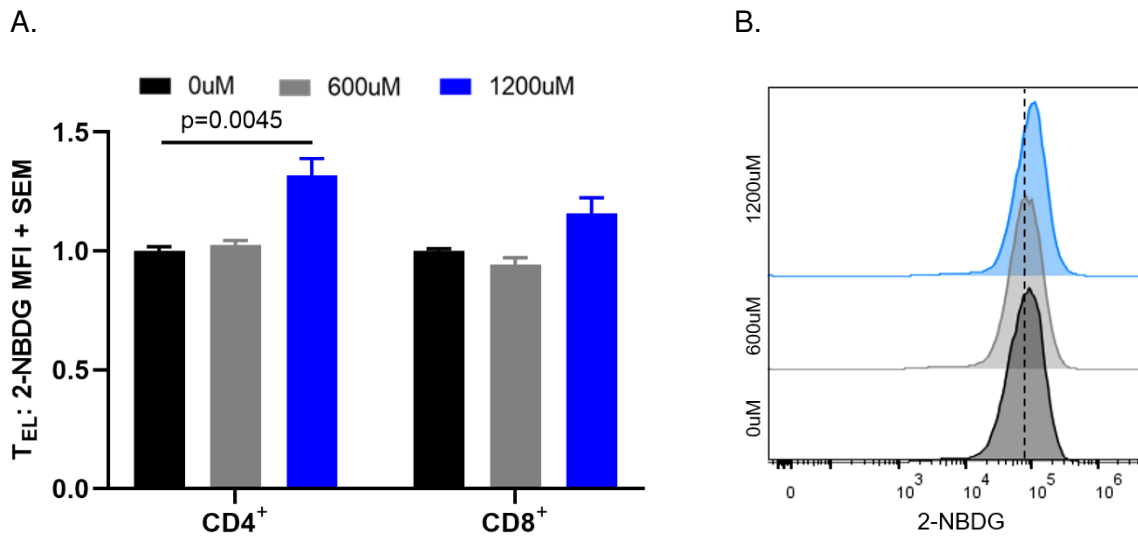

Figure 3.12. T_{EL} glucose uptake, ± metformin. Glucose uptake was measured in CD4$^+$ and CD8$^+$ T_{EL}s, ± metformin (0μM: black; 600μM gray; 1200μM blue), by flow cytometric measurement of 2-NBDG fluorescence. (A) Differential comparisons among treatment groups were made by normalizing 2-NBDG MFIs to the mean of 0μM group. (B) Representative 2-NBDG flow cytometry histograms. Data represents three independent experiments (N=6). Significance was determined using a Kruskal-Wallis test.

T_{EL} mitochondrial function is decreased by metformin.

Extracellular flux analysis

Other parameters of mitochondrial function, including proton leak and spare respiratory capacity, were measured by extracellular flux analysis. Proton leak is the amount of oxygen that is consumed independent of ATP synthase and is often attributable to an oversaturation of the electron transport chain (ETC) and corresponds to the formation of free radicals and mitochondrial

damage. In comparison to highly metabolic T_{ELS}, T_{ML} cells displayed 3.28-fold less proton leak 120 hours following *in vitro* differentiation (p<0.0001) (Figure 3.13A). Moreover, T_{ELS} displayed a dose-dependent decrease in proton leak corresponding to metformin treatment, including a 1.36-fold reduction following 600μM and a 2.41-fold reduction in response to 1200μM metformin (Figure 3.13A). Spare respiratory capacity (SRC), or the difference between a cell's basal and maximum respiration, represents a metabolic reserve that can be harnessed during times of stress and is a defining characteristic of memory T cells. While T_{EL} cells had no SRC remaining following their *in vitro* differentiation, T_{MLS} maintained an SRC equivalent to 143 times that of T_{ELS} (p<0.0001) (Figure 3.13B). A dose-dependent increase in SRC was observed in metformin treated T_{ELS} corresponding to a 23- and 62-fold increase in the presence of 600uM and 1200uM metformin, respectively (p=0.0065) (Figure 3.13B).
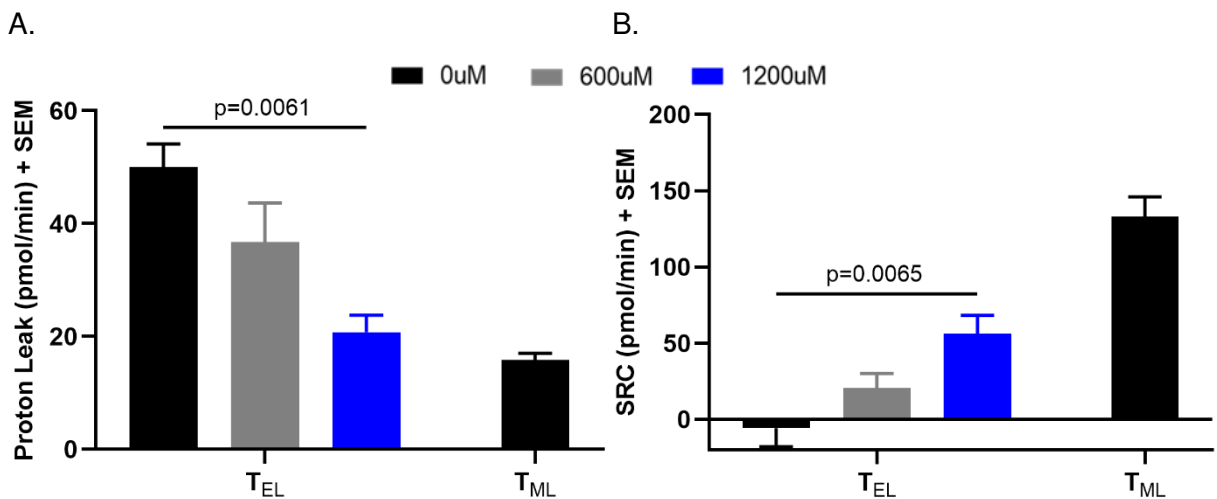

Figure 3.13. Mitochondrial function of T_{ML} and T_{EL} cells ± metformin. Extracellular flux analysis was used to measure (A) proton leak and (B) mitochondrial spare respiratory capacity (SRC) in negatively isolated CD3+ *in vitro* differentiated T_{ML} and T_{EL} cells, ± metformin (0μM: black; 600μM gray; 1200μM blue). Data represents three independent experiments (N=6-13). Significance was determined using Kruskal-Wallis tests.

Fatty acid metabolism

Given the increased SRC observed in metformin exposed T_{ELS}, we questioned whether metformin also promotes the uptake and storage of fatty acids, which are required for SRC

maintenance. To examine the extent to which metformin influenced fatty acid uptake, $T_{EL}s$ were incubated with the fluorescent palmitate analogue BODIPY FL C16. Both CD4+ and CD8+ $T_{EL}s$ exposed to 1200μM metformin displayed an approximate 35% increase (CD4: p=0.0034; CD8: p=0.0239) in BODIPY FL C16 uptake in comparison to unexposed cells, though only CD4+ cells significantly increased uptake in response to 600uM metformin (p=0.0137) (Figure 3.14A & B).
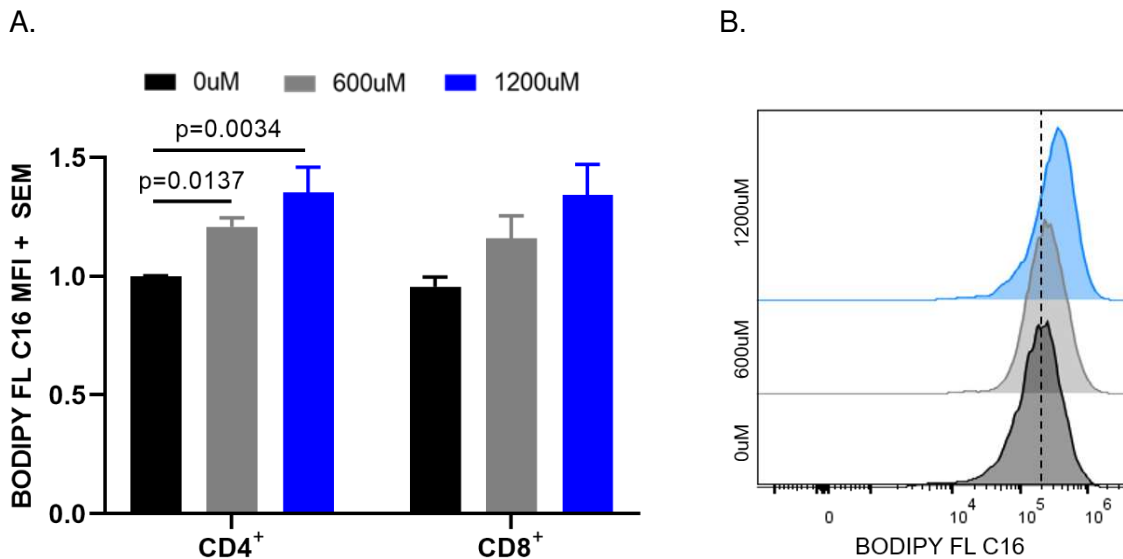
A.   B.

Figure 3.14. T_{EL} fatty acid uptake ± metformin. Fatty acid (palmitate) uptake was measured in CD4+ and CD8+ $T_{EL}s$, ± metformin (0μM: black; 600μM gray; 1200μM blue), by flow cytometric measurement of BODIPY™ FL C16 fluorescence. (A) Differential comparisons among treatment groups were made by normalizing BODIPY™ FL C16 MFIs to the mean of 0uM group. (B) Representative BODIPY™ FL C16 flow cytometry histograms from CD4+ $T_{EL}s$. Data represents three independent experiments (N=6). Significance was determined using a Kruskal-Wallis test.

To determine whether metformin increases fatty acid utilization by T_{EL} cells, we used a Biolog mitoplate assay to measure cellular capacity to undergo β-oxidation. The principle of this assay relies on the generation of reduction intermediates generated in response to substrate availability and utilization. These intermediates subsequently enter the ETC and undergo a reduction reaction with a tetrazolium redox dye creating a colorimetric reaction that provides quantifiable utilization of the available substrate. Capacity to utilize short chain, medium chain,

and long chain fatty acids was achieved by supplementing lysed cells with of acetyl-l-carnitine (short chain fatty acids), octanoyl-l-carnitine (medium and long chain fatty acids), and palmitoyl-d, l-carnitine (medium chain fatty acids). Additionally, L-malic acid was supplemented to each well to ensure continuous cycling of the tricarboxylic acid cycle. Using this assay, we show that supply of short chain fatty acids (acetyl-l-carnitine) alone do not facilitate ETC function in negatively isolated $CD3^+$ T_{EL} cells (Figure 3.15A). Medium and long chain fatty acids (octanoyl-l-carnitine and acetyl-l-carnitine), however, result in detectable metabolic activity in untreated $T_{EL}s$ (Figure 3.15A-B). In response to 600µm or 1200µM metformin treatment we show a dramatic decrease in both octanoyl-l-carnitine and palmitoyl-d, l-carnitine utilization capacity compared to untreated cells. These results correspond to an overall significant decrease in fatty acid utilization capacity following metformin treatment at either concentration (Figure 3.15B).
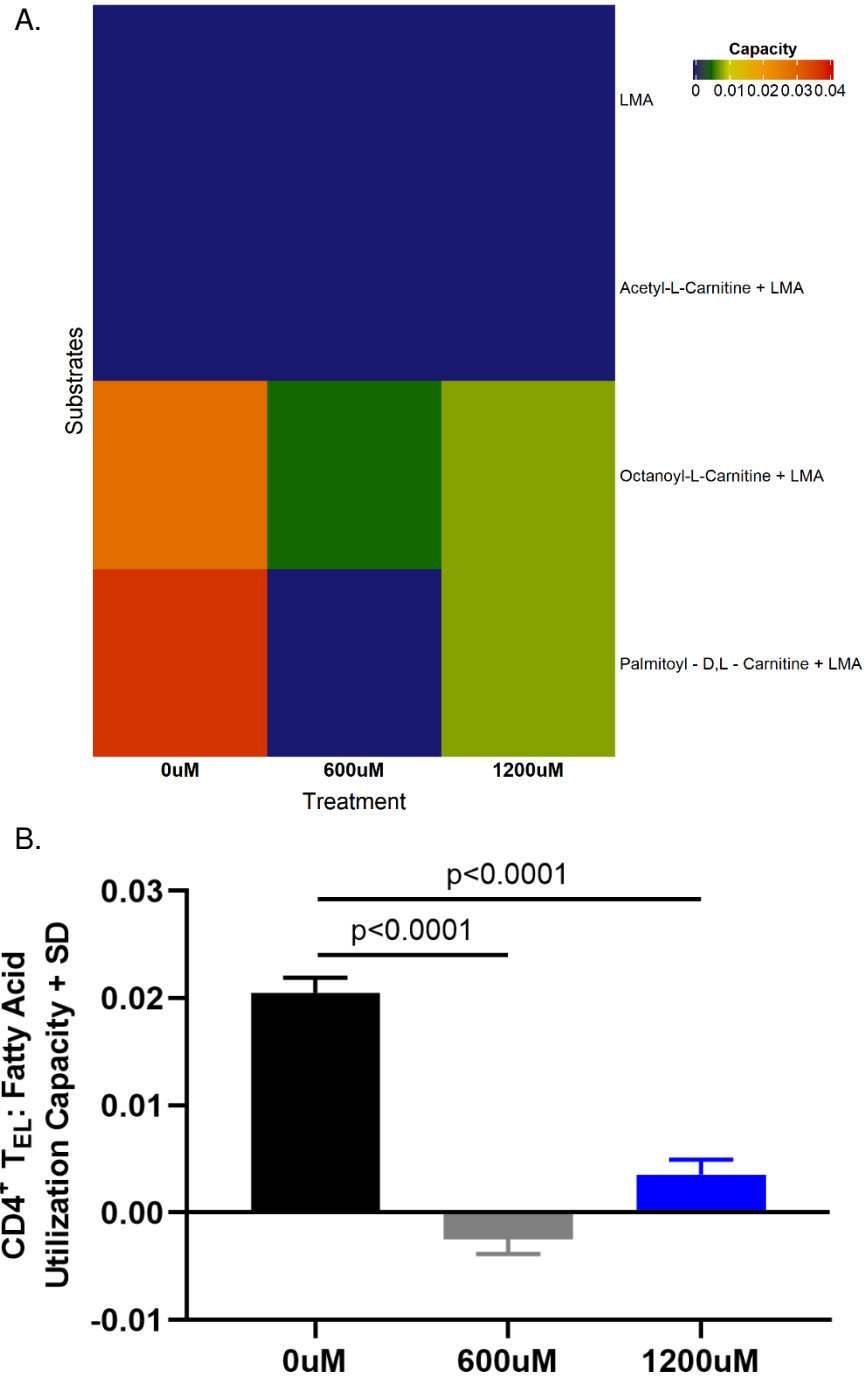
A.

B.

Figure 3.15. T$_{EL}$ fatty acid utilization capacity, ± metformin. Negatively isolated CD3$^+$ T$_{ELS}$ treated with either 0μM, 600μM, or 1200μM were subject to a Biolog Mitochondrial Functional assay 120 hours following activation. Data represents cellular utilization capacity of L-malic acid (LMA), acetyl-l-carnitine + LMA, octanoyl-l-carnitine + LMA, and palmitoyl-d, l-carnitine + LMA. The rate of substrate utilization was measured over 4 hours and differential comparison was achieved by fitting a quadratic curve to the data then calculating the slopes at 2 hours. LMA was subtracted from all groups to represent fatty acid utilization only. (A) Heatmap representation of differential substrate utilization between metformin treated and untreated cells. (B) Combined utilization capacity for all fatty acids. Data represents three individual experiments, significance determined using a contrast of a mixed model.

CD4+ T cell survival and proliferative capacity are enhanced by metformin following antigen re-challenge

Because metformin treatment promoted the generation of a T_{EL} phenotype that possessed T_{ML} characteristics, we hypothesized that these cells would also respond more effectively to secondary antigen challenge, as measured by increased proliferation and cell survival. At 96 hours following secondary challenge, we show that approximately 24% of CD4+ T_{EL} cells that were differentiated in the absence of metformin and 38% in the presence of 1200μM metformin proliferated beyond their parent population. This corresponds to an overall increase in cell division by cells exposed to metformin by 14% (p=<0.0001) (Figure 3.16B-C). To determine whether metformin exposure also enhances T_{ML} proliferation, we performed the same experiments using T_{ML} differentiated cells. While approximately 53% of metformin unexposed CD4+ T_{ML} proliferated following secondary Ag85b peptide challenge, 79% of 1200uM exposed CD4+ T_{ML}s proliferated beyond the parent population (Figure 13.16D-E). These data correspond to a 26% increase in cell division among metformin compared to unexposed CD4+ T_{ML} cells (p=0.0034) (Figure 13.14D-E).
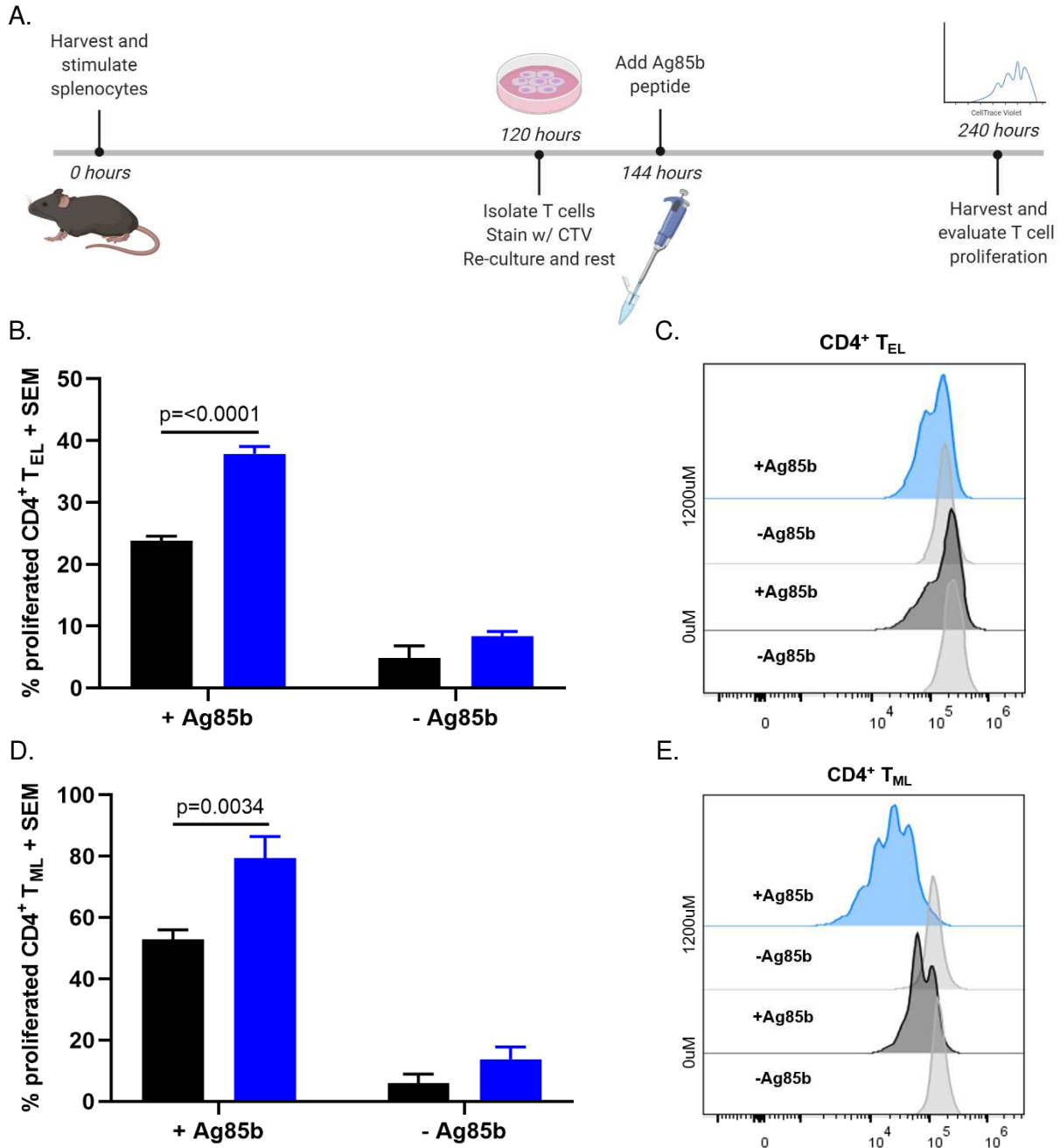
Figure 13.16. CD4+ TEL and TML, ± metformin, proliferation in response to Ag85b re-challenge. (A) Splenocytes were harvested from P25 mice and differentiated under T_{EL} or T_{ML} conditions, ± metformin (0μM: black; 1200μM blue) for 120 hours, stained with CellTrace violet (CTV), rested for 24 hours, then re-stimulated with ± Ag85b peptide (1μg/ml). Percent proliferation was assessed by CTV dilution and quantified flow cytometry in (B-C) T_{EL} and (D-E) T_{ML} cells. (C & D) Representative histograms of CTV staining 96 hours following (C) T_{EL} or (E) T_{ML} re-challenge. (B & D) Data represents three independent experiments (N=5-8). Significance was determined using unpaired t-tests.

To determine whether increased proliferation of metformin exposed cells corresponded to heightened production of the proliferation-inducing cytokine IL-2, supernatants of antigen re-challenged T_{EL} cells were collected and IL-2 was quantified using a LEGENDplex™ bead array. A modest, yet significant increase in IL-2 was found in the supernatants of 1200uM metformin exposed compared to unexposed T_{EL} cells (p=0.0188) (Figure 13.17A). Furthermore, differences in CD4+ T_{EL} viability were assessed and demonstrate that cells which were exposed to metformin during primary activation display three times greater survival compared to cells that did not receive metformin treatment (Figure 13.17B). Moreover, enhanced survival of metformin exposed CD4+ T cells occurred regardless of whether cells were re-challenged with antigen or not (Figure 13.17B).
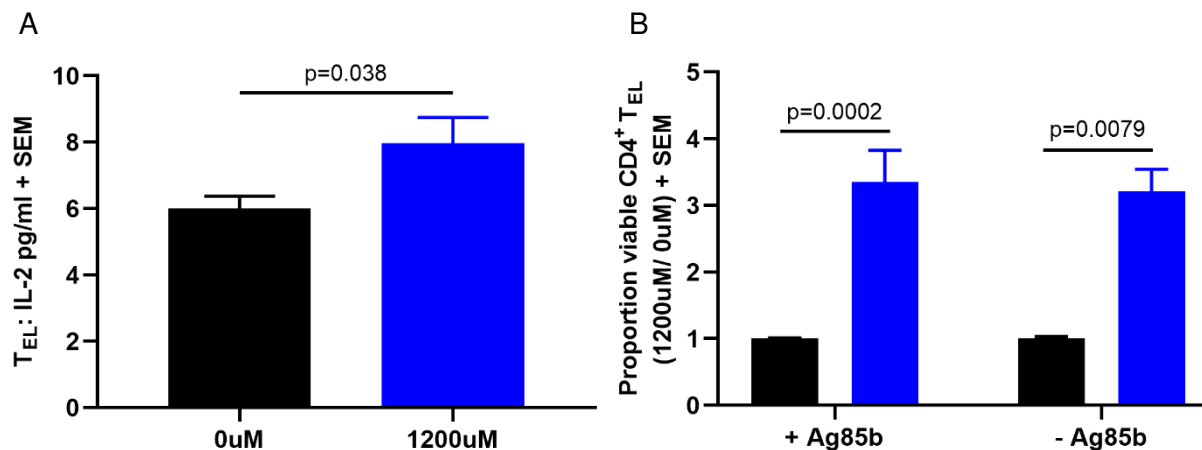

Figure 13.17. T_{EL} Ag85b recall IL-2 production and survival, ± metformin. *In vitro* differentiated T_{EL} cells, ± metformin (0μM: black; 1200μM blue), were re-challenged with Ag85b peptide as previously described. (A) Supernatants were collected 96 hours following re-challenge and IL-2 was quantified using a LEGENDplex™ bead array. Data represents four independent experiments (N=8). (B) Percent live CD4+ T cells were determined by flow cytometry 96 hours following re-challenge. Data represent the ratio between the percentage of live CD4+ cells from 1200μM metformin treatment compared to 0μM treatment between three independent experiments. (A-B) Significance was determined using unpaired t-tests.

Discussion

The goal of this study was to evaluate the impact of metformin on T cell differentiation and characterize the metabolic phenotypes associated with these cells. This study is in response to previous work performed by our laboratory, demonstrating metformin's protective efficacy against TB disease in guinea pigs. In these studies, we showed that when initiated prior to or concurrent with Mtb infection, metformin dramatically reduced TB disease severity, as measured by decreased lung Mtb colony forming units and percent lesion burden. In association with enhanced disease protection, PBMC T cell metabolic phenotypes from metformin treated animals were similar to those from uninfected controls, while T cells from Mtb infected untreated guinea pigs displayed increased metabolic flux through glycolysis and OXPHOS as well as mitochondrial hyperpolarization. Given that immune cell metabolism is so tightly linked to cell function, these results led us to hypothesize that the protective effects by metformin are due to direct modulation of T cell metabolism, which results in the enhanced generation of memory-like T cells that are capable of self-renewal, multipotency, and persistence in response to Mtb infection. Our hypothesis is supported by several studies that show metformin's beneficial effects against chronic inflammatory illnesses through regulation of pro-inflammatory potential by T cells as well as increased memory T cell formation in response to metformin [12, 19]. In our current study, we define the generation of a non-terminally differentiated CD4+ effector T cell population in response to metformin treatment, which possesses a unique metabolic phenotype that supports enhanced cell survival and increased capacity to respond to secondary antigen challenge, *in vitro*.

In these studies, we used a model of *in vitro* T cell differentiation to directly evaluate the influence of metformin on T cell phenotypic marker expression, function, and corresponding metabolism. By varying the strength of the T cell receptor activating signal by using either soluble or plate bound anti-CD3, two distinct T cell populations were generated [34, 35]. Surface marker expression and functional characterization revealed that cells activated with soluble antibody

expressed the typical memory T cell surface markers CD62L$^+$CCR7$^+$CD44$^+$ and had a greater capacity to proliferate upon secondary antigen challenge in comparison to bound stimulated cells, which displayed a typical effector like phenotype, CD62L$^-$CCR7$^-$CD44$^+$, and inability to robustly proliferate and survive. The controlled and predictable differentiation of these subsets were utilized to model T cell metabolism within effector-like (T$_{EL}$) and memory-like (T$_{ML}$) T cell populations and thus compare the differential gradients of T cell differentiation in response to metformin treatment.

A recently defined metabolic feature of memory versus effector T cells is the differential polarization of the mitochondria. A recent study by Sukumar et al., demonstrated that mitochondrial membrane potential, the gradient of hydrogen ions between the inner mitochondrial membrane space and the lumen of the mitochondria, which is responsible for driving ATP production through ATP synthase, could effectively be used to distinguish memory T cells (low membrane potential) from highly differentiated effector T cell subsets (high membrane potential) [30]. Like the *in vivo* differentiated T cells described in Sukumar's study, our *in vitro* differentiated T$_{EL}$ and T$_{ML}$ phenotypes also displayed differential membrane potential following the same dogma. Following chronic Mtb infection in guinea pigs, mitochondrial hyperpolarization was a defining feature that distinguished T cells from untreated versus metformin treated animals, which maintained non-hyperpolarized mitochondrial membranes following infection. Considering metformin's partial inhibition of complex I of the electron transport chain, abolished membrane potential was both expected and observed in a dose-dependent manner in T$_{EL}$ cells treated with metformin *in vitro*. Whether the decrease in membrane potential by metformin corresponded with increased memory generation, however, was unknown.

Previous work by Pearce et al. have shown that through modulating fatty acid metabolism, metformin enhances the production of antigen specific CD8$^+$ memory T cells in response to vaccination [19]. We, therefore, hypothesized that metformin would also enhance memory generation of CD4$^+$ T cells *in vitro,* corresponding with reduced mitochondrial membrane potential.

The traditional memory surface markers, CD62L and CD44, were evaluated to assess the proportion of memory T cells generated following activation. Surprisingly, metformin did not change the proportion of memory T cells generated, for neither CD4+ nor CD8+ T cell populations. One explanation for the inconsistencies between these studies may be due to the short time course in which T cells were differentiated in our *in vitro* model system. Nonetheless, more in depth analysis of surface markers associated with T cell activation and differentiation revealed dramatic differences between metformin exposed and unexposed T cells. Specifically, dose dependent decreases in CD25 and increases in CD44 and CD69 were observed following metformin exposure. These findings indicate that although an increase of memory T cell populations did not result from metformin, altered cellular differentiation does, in fact, occur. Due to the roles that CD44 and CD69 play in cellular migration and tissue retention, we hypothesize that metformin may promote more efficient T cell trafficking to sites of infection, a known barrier in an effective T cell response against Mtb infection [36, 37, 38]. Furthermore, reduced CD25, or the α chain of the IL-2 receptor, which serves as a marker of T cell activation and mediates signals for T cell activation in coordination with the β/γ chains, may correspond to a weaker primary activation response and reduced differentiation that is associated with enhanced self-renewal, survival, and plasticity.

Quantification of cytokine secretion also demonstrated the dramatic influence that metformin had on T_{EL} function. Polyfunctionality of T_{EL} cells were observed following *in vitro* activation as demonstrated by production of Th1, Th2, and Th17 cytokines and expression of the lineage associated transcription factors Tbet, GATA3, and RORγt. In response to metformin treatment, T_{EL} cells displayed significantly decreased production of IL-6, IL-5, IL-4, IL-10, IL-21, and IL-22 as well as decreased IL-7 and IL-1β, but differences were not statistically different. Alternatively, IL-2 production was significantly increased in the supernatants from metformin treated T_{EL}s. These results are consistent with our previous *in vivo* findings and the literature

140

suggesting that metformin reduces T cell pro-inflammatory potential [14, 39]. Interestingly, however, metformin did not reduce the levels of IFN-γ or IL-17A, two of the primary pro-inflammatory cytokines involved in the T cell response against Mtb [8, 40, 41, 42]. The failure to decrease these cytokines was unexpected, but suggest that early following activation, T cells possess the capacity to mediate effective bacterial killing.

In addition to pro-inflammatory cytokine characterization, we show that the regulatory cytokine TGF-β and Treg transcription factor FOXP3 were unchanged by metformin treatment, suggesting that decreased cytokine production is not due to the generation of regulatory T cells, but rather by direct influence on effector T cell function. It is important to note that supernatants were collected from heterogenous cell mixtures containing other populations capable of producing many of the measured cytokines, and therefore, may contribute to the observed differences. However, of the cells present in these samples, CD4+ T cells comprised the vast majority.

Altered surface marker expression and cytokine production next led us to hypothesize that metformin, rather than promoting memory T cell generation, modulates the extent of T cell differentiation along a broad, rather than narrowly defined, spectrum. Although the exact mechanism by which T cells differentiate into effector versus memory subsets is highly debated, evidence exists to suggest that T cells undergo progressive differentiation from less differentiated (i.e. naïve and memory T cells) to more highly differentiated subsets (i.e. effector and terminally differentiated T cells) [43, 44, 45]. Less differentiated T cells are defined by the capacity to self-renew, survive for long periods of time, and maintain plasticity [24, 30, 46]. In response to initial activation these cells produce low levels of cytokines and undergo limited numbers of cell division, but upon secondary antigen challenge display robust proliferative and cytokine responses. In contrast, highly differentiated T cells undergo robust proliferative expansion and produce large amounts of cytokines following primary antigen challenge, this however, is associated with pre-mature terminal differentiation resulting in rapid cell death [23]. Recently developed single cell technologies

provide evidence that T cells undergo these functional and development changes throughout their lifespans, supporting the progressive differentiation model [43]. To determine whether metformin impacts the extent of T cell differentiation in association with this model, the terminal differentiation marker KLRG1 as well as the ratio of expression between the antagonistic transcription factors Blimp-1, highly expressed in terminally differentiated T cells, and BCL-6, highly associated with memory T cells, were measured by flow cytometry [31]. Using our *in vitro* model, we found that approximately 20% of CD4$^+$ T$_{EL}$ cells expressed KLRG1 while T$_{ML}$ cells completely lacked KLRG1 expression. These results were expected and further supported by the increased ratios of Blimp-1 to BCL6 expression in T$_{EL}$ compared T$_{ML}$ cells, demonstrating the validity of these markers for characterizing progressive levels of T cell differentiation. In response to metformin treatment we found that like T$_{ML}$ cells, metformin decreases the expression of both KLRG1 and the ratio of expression between Blimp-1 and BCL-6 in a dose-dependent response. These results are novel in that we describe a new mechanism by which metformin causes T cell immunomodulation by preventing CD4$^+$ T cell terminal differentiation. Moreover, less differentiated T cells have been demonstrated to provide superior protection against Mtb infection, providing further evidence that it is through T cell targeting that metformin treatment improves TB disease outcome [24, 27, 36, 47].

To better understand the metabolic implications of metformin treatment on T cell metabolism and how this is linked to the generation of non-terminally differentiated CD4$^+$ T$_{EL}$s, we characterized *in vitro* generated T cell metabolic profiles, with or without metformin. Previous studies have extensively characterized the metabolism of memory and effector T cells and it has become well appreciated that memory T cells predominantly rely on fatty acids to fuel oxidative metabolism for efficient energy production required for cellular maintenance and longevity [21]. Alternatively, effector T cells predominantly rely on glycolysis, rather than OXPHOS, for rapid ATP production and the generation of biosynthetic intermediates that are needed for cell growth and proliferation [21]. Likewise, we show that *in vitro* differentiated T$_{ML}$ are highly dependent on OXPHOS in comparison to T$_{EL}$, which engage in higher rates of glycolysis. Interestingly, once

treated with metformin, T_{EL}s engage in a unique metabolic phenotype that neither fully identifies with effector or memory T cells. Glycolytic rates are significantly increased while rates of OXPHOS are significantly reduced, corresponding to an overall glycolytic phenotype. These results were surprising given that decreased T cell differentiation is generally associated with greater reliance on OXPHOS.

The inverse relationship between glycolysis and OXPHOS made us question whether glycolytic increases were enough to maintain cellular energy demands. As expected, mitochondrial ATP production was found to be significantly reduced in metformin treated cells when measured by extracellular flux analysis. The ratio of ADP to ATP, which indicates cellular stress and energy insufficiencies when increased, remained constant, however, and suggest that glycolysis maintained cellular energy demands. This is complemented by increased extracellular glucose uptake, as measured by 2-NBDG staining, in T_{EL}s that were treated with metformin, representing the heightened demand for glucose to maintain high rates of glycolysis for ATP production. Decreased mitochondrial dependency for energy production by metformin treated cells may be linked to the shuttling of biosynthetic intermediates required for macromolecular synthesis that equip T cells to more efficiently respond to secondary, or persistent, antigen stimulation through increased proliferation and cytokine production, a feature of less differentiated T cells. One reasonable explanation is that while glycolysis maintains energy demands, the TCA cycle intermediate citrate may be utilized for *de novo* fatty acid synthesis and storage, a process that is known to contribute to cellular proliferation and survival [48, 49]. However, further studies must be performed to validate this hypothesis.

To determine whether dramatically decreased mitochondrial activity of non-terminally differentiated metformin treated T_{EL} cells influenced other mitochondrial parameters associated with T cell function, we evaluated mitochondrial spare respiratory capacity (SRC) and proton leak. Spare respiratory capacity is a hallmark feature of memory T cells that is associated with T cell longevity and enhanced recall response to antigen re-challenge [50, 51]. Consistent with the

literature, we show that in comparison to *in vitro* differentiated T_{EL}s, T_{ML} cells displayed significantly greater SRC. Interestingly, when treated with metformin, T_{EL} were also able to maintain an SRC that was significantly greater than untreated cells. This was due to decreased use of OXPHOS following activation, thereby maintaining a respiratory reserve and function. In addition, these data correspond to decreased mitochondrial proton leak following metformin treatment, an indirect indicator of mitochondrial health and function. Proton leak measures uncoupled oxygen consumption and is often associated with high oxidative flux and the loss of electrons by the electron transport chain, yielding the production of reactive oxygen species [52]. While in some cases mitochondrial derived reactive oxygen species (ROS) are necessary for cell signaling and cytokine production, they can also lead to mitochondrial damage and subsequent cell death [52, 53]. However, whether ROS production was increased or decreased in T_{EL} cells treated with or without metformin was not evaluated, therefore, proton leak can only be used to interpret mitochondrial activity. As such, we conclude that by decreasing mitochondrial oxidation, metformin preserves mitochondrial function of activated T cells by increasing SRC and decreasing proton leak. In comparison to highly differentiated T cells that engage in rapid rates of glycolysis and OXPHOS and die shortly following activation, it is logical to predict that this unique metabolic state endows long term T cell survival and responsiveness in the face of chronic infection.

We next assessed fatty acid metabolism of CD4$^+$ T_{EL} cells to see whether decreased mitochondrial function was associated with the inability of non-terminally differentiated T cells to metabolize other fuel sources. Fatty acid metabolism is an essential component of memory T cell metabolism that has been directly linked to their formation and maintenance of SRC [19, 48]. In response to metformin treatment, we show that fatty acid uptake is significantly increased by CD4$^+$ T_{EL} cells, as measured by staining of the palmitate analogue BODIPY FL C16. The capacity of metformin treated T_{EL} cells to utilize fatty acids, however, was significantly decreased. We, therefore, hypothesize that rather than metabolizing fatty acids, metformin treated cells likely store them in lipid droplets for later retrieval and utilization. This is unique from memory T cells, which

endogenously create and metabolize fatty acids in a futile metabolic cycle, but is supported by the importance of fatty acids in maintaining survival of less differentiated cell phenotypes [48].

To assert whether the phenotypic and metabolic characteristics of metformin derived non-terminally differentiated CD4$^+$ T$_{EL}$ cells are equipped with superior re-call functionality, we measured proliferative potential, quantified IL-2 production, and evaluated the survival of antigen re-challenged cells. Following re-stimulation, we show that 14% more T$_{EL}$ cells proliferated beyond the parent population from metformin treated compared to untreated cells, which corresponded to significantly greater IL-2 production, and significantly increased CD4$^+$ T cell viability. Importantly, CD4$^+$ T$_{EL}$ survival was significantly increased regardless of whether cells were re-challenged with peptide or not, demonstrating the survival advantage of non-terminally differentiated T cells over highly differentiated subsets. In addition, we show that when treated with metformin, T$_{ML}$ cells also increase their proliferative capacity by 26% compared to untreated cells. Therefore, metformin may also have a desirable influence on memory T cell differentiation and function. These results are in support of our hypothesis and demonstrate that non-terminally differentiated metformin treated cells have an increased survival capacity and a superior recall response compared to untreated effector T cells.

Finally, while the *in vitro* model system used in this study was essential for obtaining these results, it is important to note the differences in metformin concentration used in this study compared to those used in human and animal models. In general, *in vivo* metformin serum concentrations of human patients and those achieved in guinea pigs correspond to approximately 10µM compared to the 1200uM dose used in these studies [12]. Given differential cellular uptake and accumulation of metformin in *in vitro* versus *in vivo* settings, however, studies have demonstrated the requirement of high *in vitro* concentrations to achieve the same molecular effects that are observed *in vivo* [54, 55, 56]. Therefore, while these concentrations appear high, they

are in line with concentrations used throughout the literature, which is backed by mechanistic evidence.

Also, it is important to point out that we have taken into consideration the fact that metformin may also influence other immune populations responding to Mtb infection, including macrophages, the predominant cell type that is responsible for direct Mtb killing. Data from our previous studies reveal that the timing of treatment initiation in conjunction with Mtb infection dramatically influenced disease outcome, providing temporal insights into what branch of the immune response is most likely affected by metformin. While early treatment, beginning either prior to or concurrent with infection, yielded decreased disease burden, metformin initiated during chronic infection resulted in increased disease severity (unpublished data). These results infer that early modifications to the adaptive immune response are critical for beneficial treatment outcome and had macrophages been the direct target of metformin, we would have expected similar protection regardless of treatment timing due to macrophages continuous presence throughout infection. Therefore, these studies, which focus solely on T cells, likely address the immune mediated protection by metformin, *in vivo*.

In conclusion, we show that while metformin does not enhance memory T cell generation in vitro, it prevents the terminal differentiation of effector T cells. Non-terminally differentiated T cells display overall decreased cytokine production, while maintaining their ability to produce IFN-γ and IL-17A. These cells have a unique metabolic phenotype that is defined by high reliance on glycolytic metabolism for ATP production and maintenance of mitochondrial function and spare respiratory capacity that corresponds with enhanced survival and increased proliferation and IL-2 production following secondary antigen challenge. With these results we have defined a novel cell phenotype with a metabolic advantage for survival and antigen recall. Current work is being

performed by our lab to address whether metformin treated non-terminally differentiated T cells do, in fact, elicit increased protection against Mtb infection and whether these cells can be used to define new correlates of protection for vaccine and therapeutic development.

REFERENCES

1.   Cambau, E. & Drancourt, M. Steps towards the discovery of Mycobacterium tuberculosis by Robert Koch, 1882. *Clin Microbiol Infect* **20**, 196-201 (2014).

2.   Colditz, G.A. *et al.* Efficacy of BCG vaccine in the prevention of tuberculosis. Meta-analysis of the published literature. *Jama* **271**, 698-702 (1994).

3.   Mangtani, P. *et al.* Protection by BCG vaccine against tuberculosis: a systematic review of randomized controlled trials. *Clin Infect Dis* **58**, 470-480 (2014).

4.   WHO | Global tuberculosis report 2018. *WHO* (2019).

5.   Scanga, C.A. *et al.* Depletion of CD4(+) T cells causes reactivation of murine persistent tuberculosis despite continued expression of interferon gamma and nitric oxide synthase 2. *J Exp Med* **192**, 347-358 (2000).

6.   Lin, P.L. *et al.* CD4 T cell depletion exacerbates acute Mycobacterium tuberculosis while reactivation of latent infection is dependent on severity of tissue depletion in cynomolgus macaques. *AIDS Res Hum Retroviruses* **28**, 1693-1702 (2012).

7.   Saunders, B.M., Frank, A.A., Orme, I.M. & Cooper, A.M. CD4 is required for the development of a protective granulomatous response to pulmonary tuberculosis. *Cell Immunol* **216**, 65-72 (2002).

8.   Flynn, J.L. *et al.* An essential role for interferon gamma in resistance to Mycobacterium tuberculosis infection. *J Exp Med* **178**, 2249-2254 (1993).

9.   Mittrucker, H.W. *et al.* Poor correlation between BCG vaccination-induced T cell responses and protection against tuberculosis. *Proc Natl Acad Sci U S A* **104**, 12434-12439 (2007).

10.   Sakai, S. *et al.* CD4 T Cell-Derived IFN-gamma Plays a Minimal Role in Control of Pulmonary Mycobacterium tuberculosis Infection and Must Be Actively Repressed by PD-1 to Prevent Lethal Disease. *PLoS Pathog* **12**, e1005667 (2016).

11.   Caruso, A.M. *et al.* Mice deficient in CD4 T cells have only transiently diminished levels of IFN-gamma, yet succumb to tuberculosis. *J Immunol* **162**, 5407-5416 (1999).

12.   Foretz, M., Guigas, B., Bertrand, L., Pollak, M. & Viollet, B. Metformin: from mechanisms of action to therapies. *Cell Metab* **20**, 953-966 (2014).

13. Kajiwara, C. *et al.* Metformin Mediates Protection against Legionella Pneumonia through Activation of AMPK and Mitochondrial Reactive Oxygen Species. *J Immunol* **200**, 623-631 (2018).

14. Yin, Y. *et al.* Normalization of CD4+ T Cell Metabolism Reverses Lupus. *Sci Transl Med* **7**, 274ra218 (2015).

15. Son, H.J. *et al.* Metformin attenuates experimental autoimmune arthritis through reciprocal regulation of Th17/Treg balance and osteoclastogenesis. *Mediators Inflamm* **2014**, 973986 (2014).

16. Pereira, F.V. *et al.* Metformin exerts antitumor activity via induction of multiple death pathways in tumor cells and activation of a protective immune response. *Oncotarget* **9**, 25808-25825 (2018).

17. Zi, F. *et al.* Metformin and cancer: An existing drug for cancer prevention and therapy. *Oncol Lett* **15**, 683-690 (2018).

18. Eikawa, S. *et al.* Immune-mediated antitumor effect by type 2 diabetes drug, metformin. *Proc Natl Acad Sci USA* **112**, 1809-1814 (2015).

19. Pearce, E.L. *et al.* Enhancing CD8 T Cell Memory by Modulating Fatty Acid Metabolism. *Nature* **460**, 103-107 (2009).

20. Ursini, F. *et al.* Metformin and Autoimmunity: A "New Deal" of an Old Drug. *Front Immunol* **9**, 1236 (2018).

21. O'Neill, L.A., Kishton, R.J. & Rathmell, J. A guide to immunometabolism for immunologists. *Nat Rev Immunol* **16**, 553-565 (2016).

22. Buck, M.D., Sowell, R.T., Kaech, S.M. & Pearce, E.L. Metabolic Instruction of Immunity. *Cell* **169**, 570-586 (2017).

23. Kishton, R.J., Sukumar, M. & Restifo, N.P. Metabolic Regulation of T Cell Longevity and Function in Tumor Immunotherapy. *Cell Metab* **26**, 94-109 (2017).

24. Reiley, W.W. *et al.* Distinct functions of antigen-specific CD4 T cells during murine Mycobacterium tuberculosis infection. *Proc Natl Acad Sci U S A* **107**, 19408-19413 (2010).

25. Nikitina, I.Y. *et al.* Mtb-specific CD27low CD4 T cells as markers of lung tissue destruction during pulmonary tuberculosis in humans. *PLoS One* **7**, e43733 (2012).

26.   Lyadova, I. & Nikitina, I. Cell Differentiation Degree as a Factor Determining the Role for Different T-Helper Populations in Tuberculosis Protection. *Front Immunol* **10**, 972 (2019).

27.   Barber, D.L., Mayer-Barber, K.D., Feng, C.G., Sharpe, A.H. & Sher, A. CD4 T cells promote rather than control tuberculosis in the absence of PD-1-mediated inhibition. *J Immunol* **186**, 1598-1607 (2011).

28.   Satterthwaite, F.E. An approximate distribution of estimates of variance components. *Biometrics* **2**, 110-114 (1946).

29.   Dunn, O.J. Multiple Comparisons Among Means. *Journal of the American Statistical Association* **56**, 52-64 (1961).

30.   Sukumar, M. *et al.* Mitochondrial Membrane Potential Identifies Cells with Enhanced Stemness for Cellular Therapy. *Cell Metab* **23**, 63-76 (2016).

31.   Crotty, S., Johnston, R.J. & Schoenberger, S.P. Effectors and memories: Bcl-6 and Blimp-1 in T and B lymphocyte differentiation. *Nat Immunol* **11**, 114-120 (2010).

32.   Andrzejewski, S., Gravel, S.P., Pollak, M. & St-Pierre, J. Metformin directly acts on mitochondria to alter cellular bioenergetics. *Cancer Metab* **2**, 12 (2014).

33.   Bridges, H., Jones, A.Y., Pollak, M. & Hirst, J. Effects of metformin and other biguanides on oxidative phosphorylation in mitochondria. *Biochem J* **462**, 475-487 (2014).

34.   Sarkar, S. *et al.* Strength of stimulus and clonal competition impact the rate of memory CD8 T cell differentiation. *J Immunol* **179**, 6704-6714 (2007).

35.   Kim, C., Wilson, T., Fischer, K.F. & Williams, M.A. Sustained interactions between T cell receptors and antigens promote the differentiation of CD4(+) memory T cells. *Immunity* **39**, 508-520 (2013).

36.   Sakai, S. *et al.* Cutting edge: control of Mycobacterium tuberculosis infection by a subset of lung parenchyma-homing CD4 T cells. *J Immunol* **192**, 2965-2969 (2014).

37.   Sakai, S. *et al.* Control of Mycobacterium tuberculosis infection by a subset of lung parenchyma homing CD4 T cells. *J Immunol* **192**, 2965-2969 (2014).

38.   Sallin, M.A. *et al.* Th1 Differentiation Drives the Accumulation of Intravascular, Non-protective CD4 T Cells during Tuberculosis. *Cell Rep* **18**, 3091-3104 (2017).

39. Kang, K.Y. *et al.* Metformin downregulates Th17 cells differentiation and attenuates murine autoimmune arthritis. *Int Immunopharmacol* **16**, 85-92 (2013).

40. Gopal, R. *et al.* Unexpected role for IL-17 in protective immunity against hypervirulent Mycobacterium tuberculosis HN878 infection. *PLoS Pathog* **10**, e1004099 (2014).

41. Gideon, H.P. *et al.* Variability in tuberculosis granuloma T cell responses exists, but a balance of pro- and anti-inflammatory cytokines is associated with sterilization. *PLoS Pathog* **11**, e1004603 (2015).

42. Freches, D. *et al.* Mice genetically inactivated in interleukin-17A receptor are defective in long-term control of Mycobacterium tuberculosis infection. *Immunology* **140**, 220-231 (2013).

43. Crompton, J.G. *et al.* Lineage relationship of CD8(+) T cell subsets is revealed by progressive changes in the epigenetic landscape. *Cell Mol Immunol* **13**, 502-513 (2016).

44. Cano-Gamez, E. *et al.* Single-cell transcriptomics identifies an effectorness gradient shaping the response of CD4+ T cells to cytokines. *Nat Commun* **11**, 1801 (2020).

45. Plumlee, C.R., Sheridan, B.S., Cicek, B.B. & Lefrancois, L. Environmental cues dictate the fate of individual CD8+ T cells responding to infection. *Immunity* **39**, 347-356 (2013).

46. Vodnala, S.K. *et al.* T cell stemness and dysfunction in tumors are triggered by a common mechanism. *Science* **363** (2019).

47. Wu, C.Y. *et al.* Distinct lineages of T(H)1 cells have differential capacities for memory cell generation in vivo. *Nat Immunol* **3**, 852-858 (2002).

48. O'Sullivan, D. *et al.* Memory CD8(+) T Cells Use Cell-Intrinsic Lipolysis to Support the Metabolic Programming Necessary for Development. *Immunity* **41**, 75-88 (2014).

49. Pearce, E.L., Poffenberger, M.C., Chang, C.H. & Jones, R.G. Fueling immunity: insights into metabolism and lymphocyte function. *Science* **342**, 1242454 (2013).

50. van der Windt, G.J. *et al.* CD8 memory T cells have a bioenergetic advantage that underlies their rapid recall ability. *Proc Natl Acad Sci U S A* **110**, 14336-14341 (2013).

51. van der Windt, G.J. *et al.* Mitochondrial respiratory capacity is a critical regulator of CD8+ T cell memory development. *Immunity* **36**, 68-78 (2012).

52.   Nanayakkara, G.K., Wang, H. & Yang, X. Proton leak regulates mitochondrial reactive oxygen species generation in endothelial cell activation and inflammation - A novel concept. *Arch Biochem Biophys* **662**, 68-74 (2019).

53.   Sena, L.A. *et al.* Mitochondria are required for antigen-specific T cell activation through reactive oxygen species signaling. *Immunity* **38**, 225-236 (2013).

54.   Dowling, R.J. *et al.* Metformin Pharmacokinetics in Mouse Tumors: Implications for Human Therapy. *Cell metabolism* **23**, 567-568 (2016).

55.   Chandel, N.S. *et al.* Are Metformin Doses Used in Murine Cancer Models Clinically Relevant? *Cell Metab* **23**, 569-570 (2016).

56.   Gravel, S.P. *et al.* Serine Deprivation Enhances Antineoplastic Activity of Biguanides. *Cancer research* **74**, 7521-7533 (2014).

CHAPTER 4 – *IN VIVO* RESPONSE OF METFORMIN TREATED NON-TERMINALLY DIFFERENTIATED CD4+ T CELLS TO MTB INFECTION

Summary

In chapter 2, we demonstrated that the anti-diabetic drug metformin confers increased protection against *Mycobacterium tuberculosis* (Mtb) infection in guinea pigs. Characterization of T cell phenotype and metabolic profiles suggest that the beneficial effects of metformin are, in part, due to altered T cell function and phenotype. We show that in response to metformin treatment *in vitro,* anti-CD3/CD28 activated CD4+ T cells undergo reduced levels of differentiation compared to untreated cells, which is demonstrated by phenotypic, functional, and metabolic changes. Importantly, metformin treatment was associated with increased CD4+ T cell survival and enhanced recall response to secondary antigen challenge. The next logical step in our studies, and the goal of this chapter, was to then evaluate whether these less differentiated T cells directly correspond to increased protection against Mtb infection *in vivo*. Following adoptive transfer of untreated or metformin treated *in vitro* differentiated Mtb Ag85b specific CD4+ T cells, recipient mice were infected with the virulent H37Rv strain of Mtb. Disease burden was assessed at 15- and 30-days post infection and lung homing capacity and surface marker expression of adoptively transferred T cells were characterized. No significant differences in neither Mtb colony forming units nor lesion burden were discovered between groups, suggesting that T cell phenotypes associated with metformin treatment are not protective against early Mtb infection and acute TB disease. Furthermore, no significant differences in lung homing capacity nor surface marker expression were observed between metformin treated and untreated adoptively transferred cells. Despite these negative results, important observations have been made regarding the study design that may have impacted the overall outcome of this work. We propose that the timing of cell transfer in relation to infection likely has important implications on the outcome of the response, and that non-terminally differentiated T cells may be more beneficial

during chronic rather than acute stages of infection. Future studies will be performed to determine the kinetic relationship between cell differentiation and protection against Mtb.

Introduction

In Chapter 2, we showed that treatment of *Mycobacterium tuberculosis* (Mtb) infected guinea pigs with metformin resulted in significantly reduced lung disease burden during chronic stages of infection. This was associated with metabolic alterations of T cells from peripheral blood mononuclear cells (PBMCs), suggesting functional and phenotypic changes of Mtb antigen specific T cells. In chapter 3, we evaluated the mechanisms by which metformin influences T cell differentiation following primary activation and found that treatment resulted in a non-terminally differentiated CD4$^+$ T effector cell phenotype compared to terminally differentiated T cells that were generated in the absence of metformin.

Unlike previous work done by Pearce *et al.* we did not observe increased formation of memory T cell populations in response to metformin treatment, as defined by positive expression of the memory T cell identifying markers CD44 and CD62L [1]. However, these cells displayed marked changes in surface marker expression, including an increase in the migration and adhesion markers CD44 and CD69, and a decrease in the T cell activation marker, CD25. Moreover, the terminal differentiation marker KLRG-1 was significantly decreased by metformin along with the ratio of expression between the transcription factors Blimp-1 and BCL-6, which define graded levels of differentiation based on their axis of expression [2, 3].

In association with altered surface marker expression, these cells revealed a unique metabolic phenotype that displayed reliance on glycolytic metabolism whilst decreasing mitochondrial function. Interestingly, although these cells did not phenotypically or metabolically resemble memory T cells, they did possess memory-like properties. First, metformin treated effector T cells possessed a significantly increased spare respiratory capacity compared to

untreated cells, a hallmark characteristic of memory T cells that is attributed to their capacity to quickly respond to antigen re-stimulation [4, 5]. Following secondary stimulation with the Mtb antigen Ag85b, we found that cells differentiated in the presence of metformin had an increased capacity to proliferate and produced higher levels of IL-2. Importantly, the percent of CD4^{+} T cells recovered from metformin treated compared to untreated samples was significantly higher, demonstrating their enhanced survival following primary differentiation. While our *in vitro* results are consistent with findings from our *in vivo* studies, the direct connection of whether these cells are responsible for enhanced host protection elicited by metformin treatment against Mtb are unknown and encompass the goal of this work.

We hypothesized that non-terminally differentiated CD4^{+} effector T cells generated *in vitro* in the presence of metformin would confer increased protection against Mtb infection in mice. This hypothesis is supported by evidence showing that terminally differentiated T cells are unable to provide adequate protection against Mtb infection. Specifically, the expression of the terminal differentiation marker KLRG-1 has been associated with the inability of T cells to effectively migrate from the endothelial lined vasculature into the tissue parenchyma and these cells lack a protective immune response against Mtb [6, 7, 8]. Furthermore, CD4^{+} T cells exhibiting decreased levels of differentiation have been found to provide superior protection against Mtb infection and other chronic inflammatory diseases in comparison to highly differentiated T cells in mice [9, 10]. These observations are further supported by data from human studies showing that increased accumulation of highly differentiated T cells in the blood correspond to increased tissue destruction in the lung [11].

To address this question, we performed an adoptive cell transfer experiment with *in vitro* differentiated CD4^{+} untreated effector-like (T_{EL}), metformin treated effector-like (T_{EL} + Met), untreated memory-like (T_{ML}), metformin treated memory-like (T_{ML} + Met), and naïve T cells (T_N). Disease severity as well as adoptively transferred T cell homing and surface marker expression

were assessed 30 days following Mtb aerosol challenge. No significant increase in protection against TB disease was observed between animals that received either metformin treated or untreated cells. Review of these results in conjunction with study design raise the question as to whether these data reflect the true protective potential of these subsets or if using another experimental design will alter protection outcomes. Nonetheless, these results provide valuable information that will guide the development of new experiments and potentially reveal the importance of T cell differentiation in association with the kinetics of Mtb infection, which is critical for the development of an effective vaccines against TB disease.

Materials and Methods

Animals and sample collection

Eight- week old male C57BL/6 mice were purchased from Jackson Laboratories and housed at the Colorado State University Laboratory Animal Resources facility in either a biosafety level 1 or 3 setting. At 30 days following Mtb aerosol infection, mice were euthanized by CO_2 overdose and blood was collected by heart stick using a 27-gauge EDTA-primed needle and 1ml syringe. The right cranial and middle lobes were collected following euthanasia and single cell suspensions were prepared by digestion with 0.5mg/ml Liberase TM (ThermoFisher Scientific Inc., Waltham, MA) + 0.25mg/ml DNase (2000units/mg) (Sigma-Aldrich, St. Louis, MO) in incomplete RPMI-1640. Suspensions were incubated in a rocking incubator held at 37°C for 30 minutes and tissues were pushed through a 70μM cell strainer followed by red blood cell lysis with 1x RBC lysis buffer until pellets were clear of RBC contamination (Biolegend Inc. San Diego, CA). The right caudal lung lobe, ½ of the spleen, and liver were collected for histopathology and fixed in 4% paraformaldehyde for 48 hours prior to processing. The left lung lobe and remaining spleen were suspended in 500ul 1x PBS and kept on ice until processed for Mtb colony forming unit quantification (same day).

Experiments were performed in accordance with the National Research Council's Guide for the Care and Use of Laboratory Animals and were approved by the Animal Care and Usage Committee at Colorado State University.

Mtb aerosol exposure

Culture stocks of Mtb strain H37Rv (TMC #102, Trudeau Institute) collected at mid-log phase of growth in Proskauer-Beck liquid medium containing 0.05% Tween-80 were diluted in water to 2×10^6 CFU/ml. Approximately 100 bacilli were delivered into the lungs of each mouse using a Glas-Col aerosol generation device. One day following aerosol infection, three mice were euthanized and the entire lungs were aseptically removed and plated to confirm Mtb delivery.

In vitro T cell differentiation

Spleens were aseptically removed from eight- to twelve-week, mixed gender, C57BL/6-Tg (H2-Kb-Tcra,-Tcrb)P25Ktk/J CD45.1 congenic (P25) mice (generously provided by Kevin Urdahl, Seattle Children's Research Institute, Seattle, WA). Splenocytes were isolated by pushing tissue through a 70µM cell strainer with the plunger of a 3ml syringe and suspended in T cell media (TCM) (RPMI-1640 with L-glutamine + 1x non-essential amino acids + 10mM HEPEs + 0.5µM 2-mercaptoethanol). Live cells were counted using a hemocytometer and the dead cell exclusion dye trypan blue and suspended at a concentration of $2x10^6$ cells/ml in TCM. 1, 1-dimethylbiguanide hydrochloride (metformin) was added to cell suspensions at a final concentration of 1200µM for treated samples. 1ml of cell suspensions ($2x10^6$ cells) were plated into 48-well tissue culture treated plates and activated with either pre plate-bound anti-CD3 (2µg/ml; clone 17A2) with soluble anti-CD28 (1µg/ml; clone 37.51) (T_{EL}) or soluble anti-CD3 (5µg/ml; clone 17A2) with soluble anti-CD28 (1µg/ml; clone 37.51) (T_{ML}). Cells were

incubated in a humidified incubator held at 37°C + 5% CO_2 for 120 hours. Cells were harvested

for cell transfer and stained with the viability dye Zombie NIR (1:3,500) (Biolegend Inc., San Diego,

CA), the fluorochrome-conjugated surface antibodies CD4-BV510 (clone RM4-5), CD8-BV570

(clone 53-6.7), CD44-FITC (clone IM7), CD25-Alexa Fluor 700 (clone PC61), CD69-PECy7

(clone H1.2F3), CD62L-Pacific Blue (clone MEL-14), CCR7-PE/Dazzle 594 (clone 4B12), and

tetramethylrhodamine (TMRM; 25nM). All antibodies were purchased from Biolegend Inc, San

Diego, CA. Samples were ran using a Cytek™ Aurora Spectral flow cytometer (Cytek Biosciences,

Fremont, CA) and data was analyzed using FlowJo software (BD Biosciences, San Jose, CA).

Adoptive Cell Transfer

Live $CD3^+$ T cells were purified using a $CD3^+$ negative selection MojoSort kit (Biolegend

Inc., San Diego, CA) and biotinylated annexin combined with streptavidin labeled MojoSort beads

(Biolegend Inc., San Diego, CA). T cell purity was assessed by flow cytometry staining with the

viability dye Zombie NIR, CD3-FITC (clone 17A2), CD4-PECy7 (clone RM4-5), and CD8-APC

(clone 53-6.7). For cell transfer, cells were resuspended to a final concentration of $5x10^6$ live $CD3^+$

cells/ml in sterile 1x PBS. $1x10^6$ cells in a 200ul volume were injected into the tail veins of eight-

week old C57BL/6 male mice using an insulin syringe with a 29-gauge needle.

Flow Cytometry

Lung

Lung single cell suspensions were prepared in 1x PBS and seeded into 96 well round-

bottom plates for staining. Live/Dead staining was performed with Zombie NIR (1:3500) in 1x PBS

for 15 minutes at room temperature. Antibody suspensions were prepared in 1x PBS + 1% BSA

+ 5µg/ml anti-mouse CD16/32 (clone 93) blocking antibody and included CD4-Alexa Fluor 532

(clone RM4-5; ThermoFisher Scientific, Waltham, MA), CD8-BV570 (clone 53.6-7), CD44-FITC

(clone IM7), CD25-Alexa Fluor 700 (clone PC61), CD62L-BV785 (clone MEL-14), PD-1-BV421

(clone 29F.1A12), CD45.1- PerCP/Cy5.5 (clone A20), KLRG-1- BV605 (clone 2F1/KLRG1), CD127- PE Dazzle 594 (clone A7R34), and CXCR3- PE/Cy7 (clone CXCR3-173). Samples were incubated for 20 minutes at 4°C, washed with 1x PBS, and fixed with 4% paraformaldehyde for 20 minutes. Cells were resuspended in 300µl total volume with 1x PBS + 1% BSA and ran on a Cytek™ Aurora Spectral flow cytometer (Cytek Biosciences, Fremont, CA). Sample collection volumes were recorded with SpectraFlo software (Cytek Biosciences, Fremont, CA) and used to calculate total cells/ lung. Data was analyzed using FlowJo software (BD Biosciences, San Jose, CA). All antibodies were purchased from Biolegend Inc, San Diego, CA, unless otherwise stated.

Blood/ i.v.

Prior to euthanasia, 1µg CD4- APC Fire 750 (clone GK1.5; Biolegend Inc, San Diego, CA) was suspended in 100ul 1x sterile PBS and administered to mice via tail vein injection. Mice were euthanized by CO_2 overdose ten minutes following antibody administration and blood was collected by heart stick using an EDTA-primed 27-gauge 5/8" needle and a 1ml syringe. Red blood cells were lysed with 1X RBC lysis buffer (Biolegend Inc, San Diego, CA) until cell pellets were clear of RBC contamination. >95% CD4$^+$ i.v. staining was confirmed by flow cytometry. Briefly, cell suspensions were stained, *ex vivo*, with CD4-AF532 (clone RM4-5) and evaluated by flow cytometry for dual staining of both i.v. and *ex vivo* CD4 antibodies using FlowJo analysis software (BD Biosciences, San Jose, CA).

Mtb CFU Enumeration

For day 0 counts, the entire lungs of three mice were aseptically collected following CO_2 euthanasia and homogenized in 1x PBS using a Bullet Blender Tissue Homogenizer set at speed 8 for 4 minutes (Next Advance, Troy, NY). Lung homogenates were suspended at a final volume of 6mls in 1x PBS and plated onto three BD Difco™ 7H11 agar (Fisher Scientific, Pittsburgh, PA) bug plates per animal. At necropsy, left lung lobes and 1/2 of each spleen were added to 1x PBS

in bullet blender tubes, homogenized—as previously described—, and plated by serial dilution onto BD Difco™ 7H11 agar quad plates. After 3-6 weeks of incubation at 37℃, colony-forming units were counted, and CFU/ml was calculated per tissue. Data are expressed as $\log_{10}$.

Histology

Tissues were fixed in 4% paraformaldehyde, paraffin embedded, sectioned at 5μm, and stained with hematoxylin and eosin. Total and lesion area of lung and spleen were quantified using Stereo Investigator area fraction fractionator software (MBF Bioscience, Williston, VT) and the Nikon Eclipse 80i microscope. Lesion burden was calculated as ratio of tissue area to lesion area and expressed as a percentage of lesion to tissue.

Data analysis

Tukey's IQR method was used to identify outliers in data sets. Based on data sets, One-way ANOVA or T-tests were used to determine differences between groups. When necessary, data was log transformed to achieve normality and homoscedasticity of residuals or data. If normality or homoscedasticity could not be achieved, data was analyzed using non-parametric methods. Post-hoc comparisons methods were Tukey, Sidak's, or Mann-Whitney multiple comparisons test, respectively. Data was analyzed with GraphPad Prism v.8 (GraphPad Software, San Diego, CA).

Results

Study Design

In chapter 3, we described the impact that metformin has on T cell differentiation, which corresponds to the increased capacity of treated cells to respond to secondary antigen challenge, *in vitro*. To determine whether these cells also display an enhanced response against Mtb *in vivo*, and whether this corresponds to increased protection against TB disease, we performed an

adoptive transfer study using *in vitro* differentiated cells. Splenocytes from Mtb Ag85b TCR transgenic mice (C57BL/6-Tg(H2-Kb-Tcra,-Tcrb)P25Ktk/J), also known as P25 mice, were isolated and activated under effector-like (T_{EL}) or memory-like (T_{ML}) generating conditions in the presence of either 1200µM metformin or left untreated, 0µM. Pre-differentiated T cells were phenotyped and transferred into wild type C57Bl/6 mice, followed by H37Rv Mtb aerosol challenge 24 hours following transfer. On days 15 and 30 of infection, necropsies were performed to assess cellular tissue localization, surface marker expression, and animal disease severity— assessed by quantification of bacterial and lesion burden in the lung and spleen. An intravascular (i.v.) staining technique was used to evaluate the localization of adoptively transferred cells to either the blood or the lung parenchyma [12] (Figure 4.1A-B).
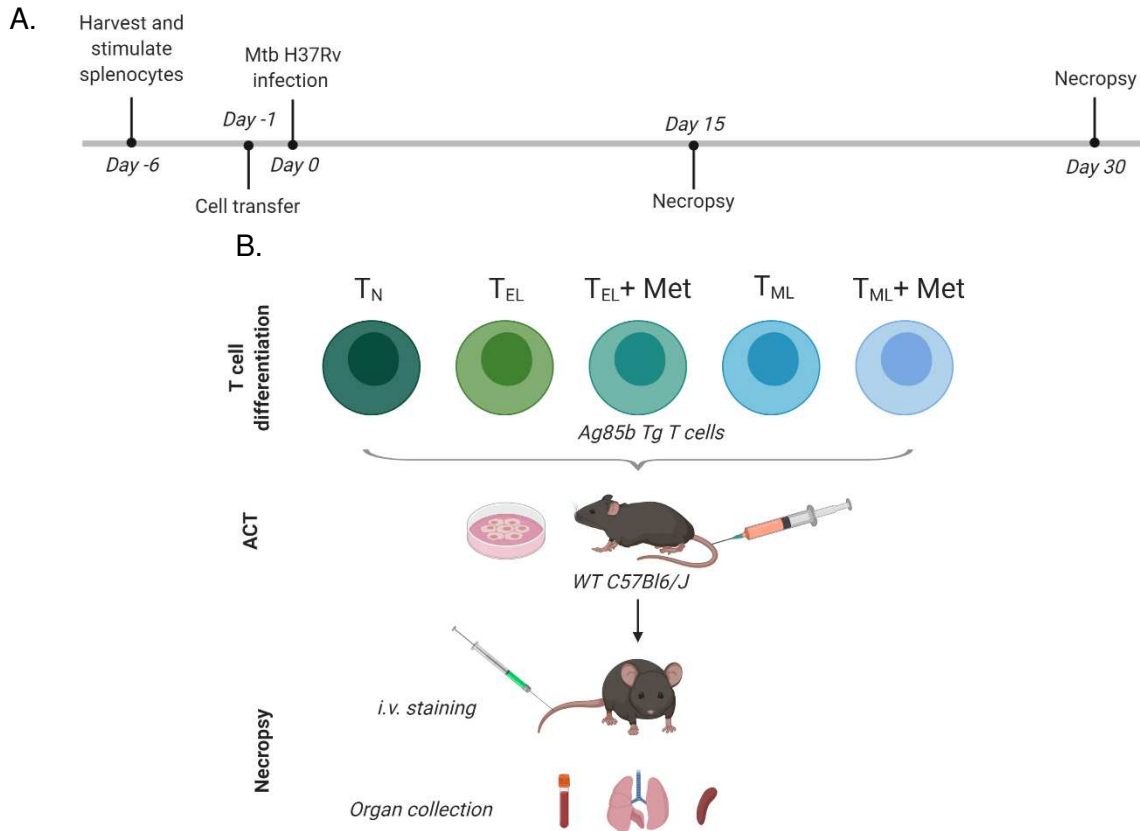
Figure 4.1. Adoptive cell transfer study design. (A) Study timeline. (B) Overview of study design.

T_{EL} and T_{ML} phenotypes (Day -1)

To ensure that T cell phenotypes were generated consistent with our findings from chapter 3, we evaluated surface marker expression by flow cytometry prior to cell transfer. At 120 hours following *in vitro* activation TEL expressed an effector phenotype ($CD62L^-CCR7^-CD44^-$) while T_{ML} differentiated cells expressed memory T cell markers ($CD62L^+CCR7^+CD44^+$). Exposure of T_{EL} cells to 1200μM metformin during differentiation decreased CD25 expression and mitochondrial membrane potential and increased CD44 and CD69 expression, much like data from chapter 3. Moreover, we characterized surface marker expression of metformin treated and untreated $CD4^+$ T_{ML} cells and show that in comparison to untreated (0μM) cells, metformin dramatically decreased

CD25 and CD69 expression and increased the expression of CCR7. Due to the low number of samples used in this study; significance was not achieved.
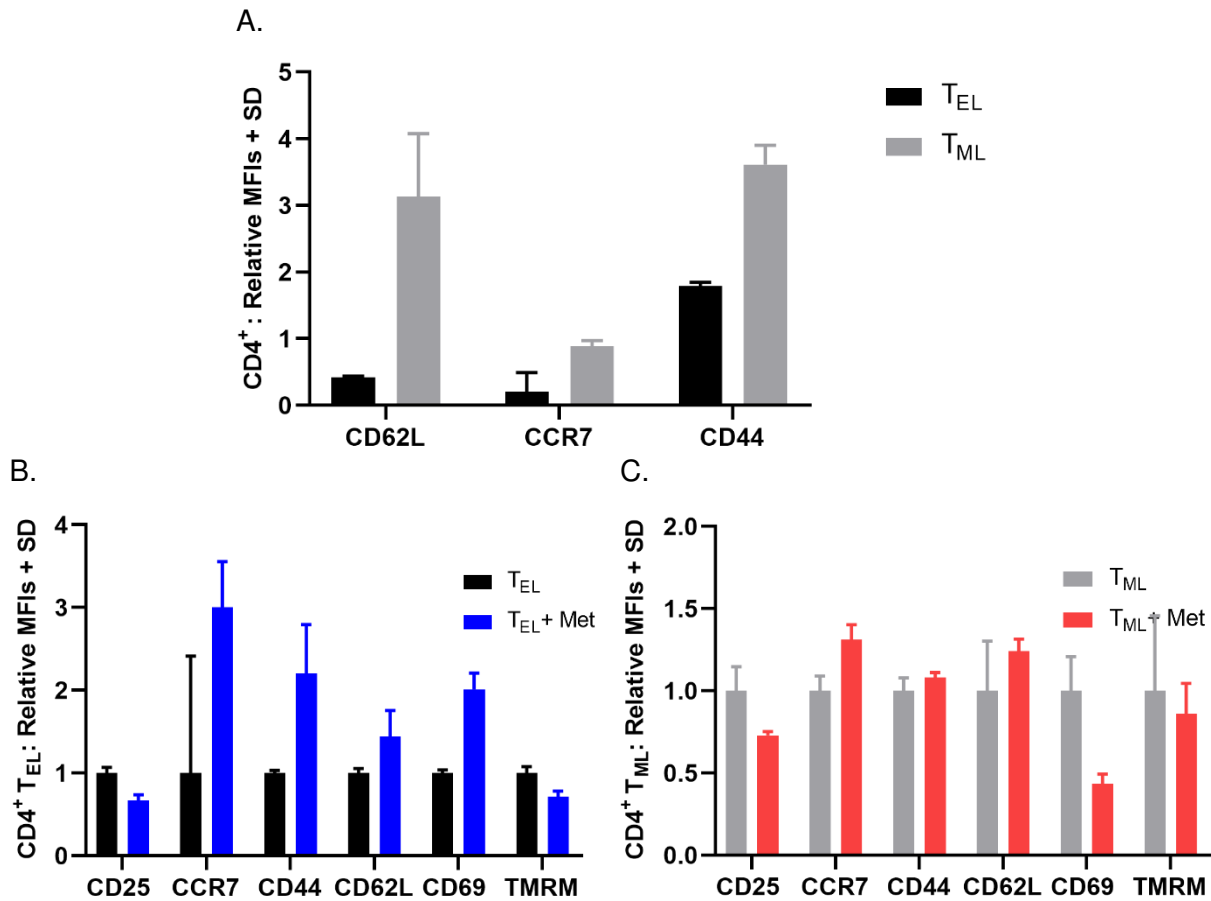

Figure 4.2. Differential surface marker expression and membrane potential T_{EL} and T_{ML} cells, ± metformin. T_{EL} or T_{ML} cells were differentiated in the presence of either 1200µM or 0µM metformin for cell transfer experiment. At 120 hours following differentiation surface marker expression and ΔΨm were measured by flow cytometry. (A) Differential expression of CD62L, CCR7, and CD44 between T_{EL} and T_{ML} cells. MFIs are normalized to the mean MFI values of naïve CD4$^+$ T cells (N=2). (B-C) Differential expression of CD25, CCR7, CD44, CD62L, CD69, and TMRM markers between (B) 0µM metformin and 1200µM metformin T_{EL} cells and (C) 0µM metformin and 1200µM metformin T_{ML} cells. MFIs are normalized to the mean MFI values of (B) 0µM T_{ELS} or (C) 0µM T_{MLS} (N=2).

T cell isolation efficacy

Prior to adoptive transfer, live CD3$^+$ T cells were isolated using magnetic bead separation. Following separation, viability, CD3 purity, and the percent of CD4$^+$ versus CD8$^+$ T cells were measured by flow cytometry. Percent viable cells ranged from 84.6% (T_{EL}) to 99% (T_N) and T cell purity (CD3$^+$) >97% was achieved for all conditions (Figure 4.3A). All samples predominantly

contained CD4$^+$ T cell populations, which ranged from 69.6%-80.5% of all viable CD3$^+$ cells, while CD8$^+$ cells only comprised 5.12%-10.9% of the population (Figure 4.3 B-C).
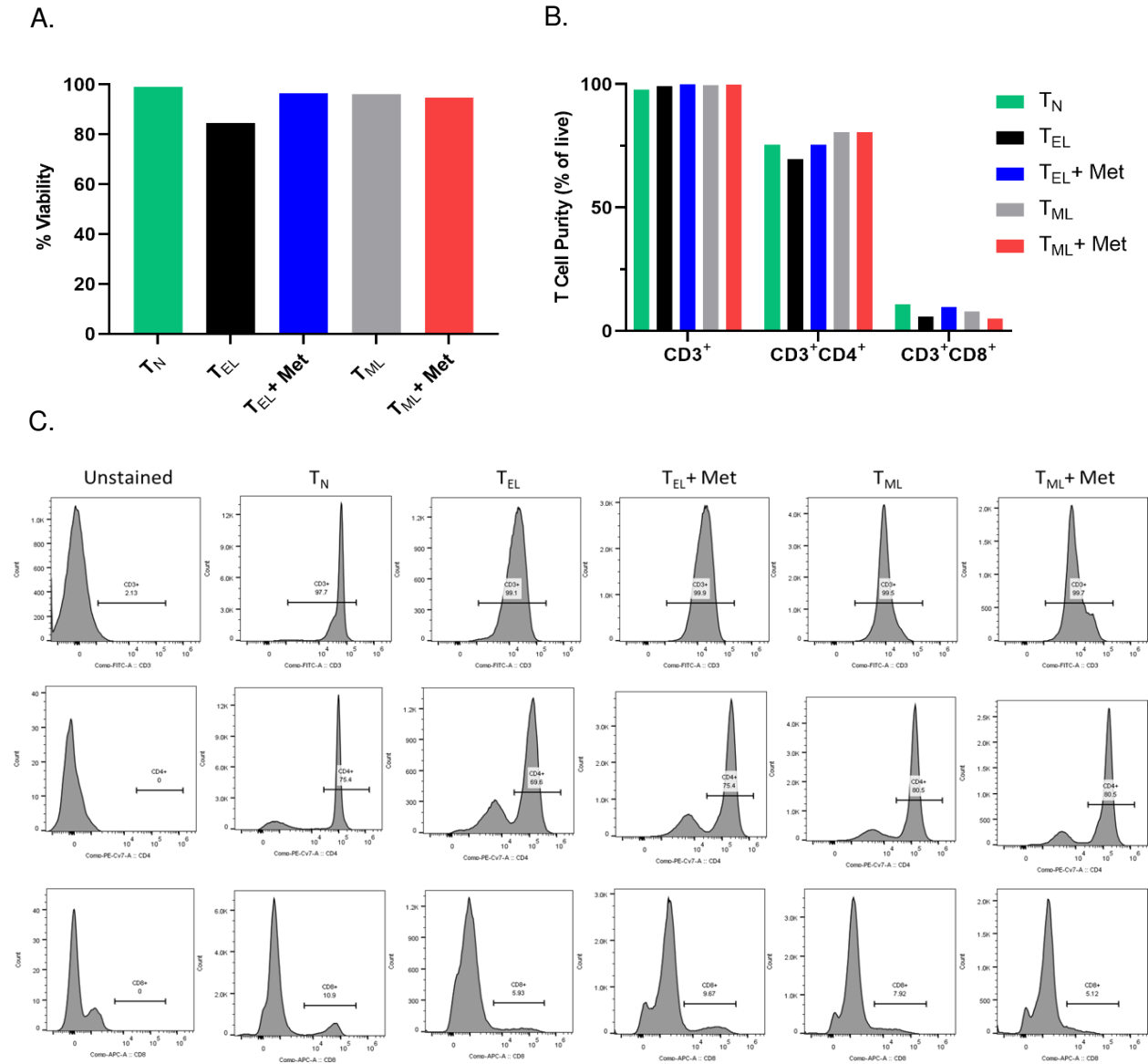

Figure 4.3. T cell viability and purity. Magnetic bead cell selection for live CD3$^+$ T cells was performed 120 hours following in vitro differentiation. Isolated cells were stained with the viability dye zombie NIR and anti-CD3, anti-CD4, and anti-CD8 antibodies to assess purity. (A) Total percent viable cells. (B-C) % of live cells positively expressing CD3, CD3/CD4, or CD3/CD8. (C) Flow cytometry histograms of CD3, CD4, and CD8 staining of isolated T cells.

CFUs and Histology

Bacterial burden was quantified by Mtb colony forming unit enumeration and lesion burden by histology to assess whether adoptively transferred T cells influenced the outcome of TB disease progression. On day 15 following infection, 3.13 (±0.078 SD; T_{ML}+ Met) to 3.59 (±0.191 SD; T_{EL}+ Met) logs of viable Mtb were recovered from the lungs of Mtb infected mice while no CFUs were recoverable from the spleens (Figure 4.4A-B). No significant differences in CFU counts were observed between treatment groups. Mean CFU counts from the lung increased roughly 1.6-fold by 30 days post-infection, with mean values ranging between 4.94 (±0.599 SD; T_{EL}+ Met) and 5.92 (±0.167 SD; T_{ML}) logs, yet no significant differences were found between treatment groups (Figure 4.4A). In addition, CFUs were recovered from the spleens at day 30 post-infection with mean log values ranging from 3.78 (±0.832 SD; TN) to 5.22 (±0.444 SD; TML) (Figure 4.4B). No significant differences were observed between groups. Lung and spleen lesion burden was quantified as the percent area of lesion to normal tissue at 30 days following Mtb infection. Percent lung lesion ranged from 2.943 (±2.313 SD; T_{EL}) to 8.271 (±6.243 SD; T_{ML}) with no significant differences between groups, though mice that received T_{EL}s displayed a 1.8-fold reduction in lesion burden compared to naïve T cell controls (Figure 4.4C). Total percent spleen lesion burden ranged from 0.112 (± 0.120 SD; T_N) to 0.494 (± 0.400 SD; T_{ML}) and no significant differences were observed between groups (Figure 4.4D).
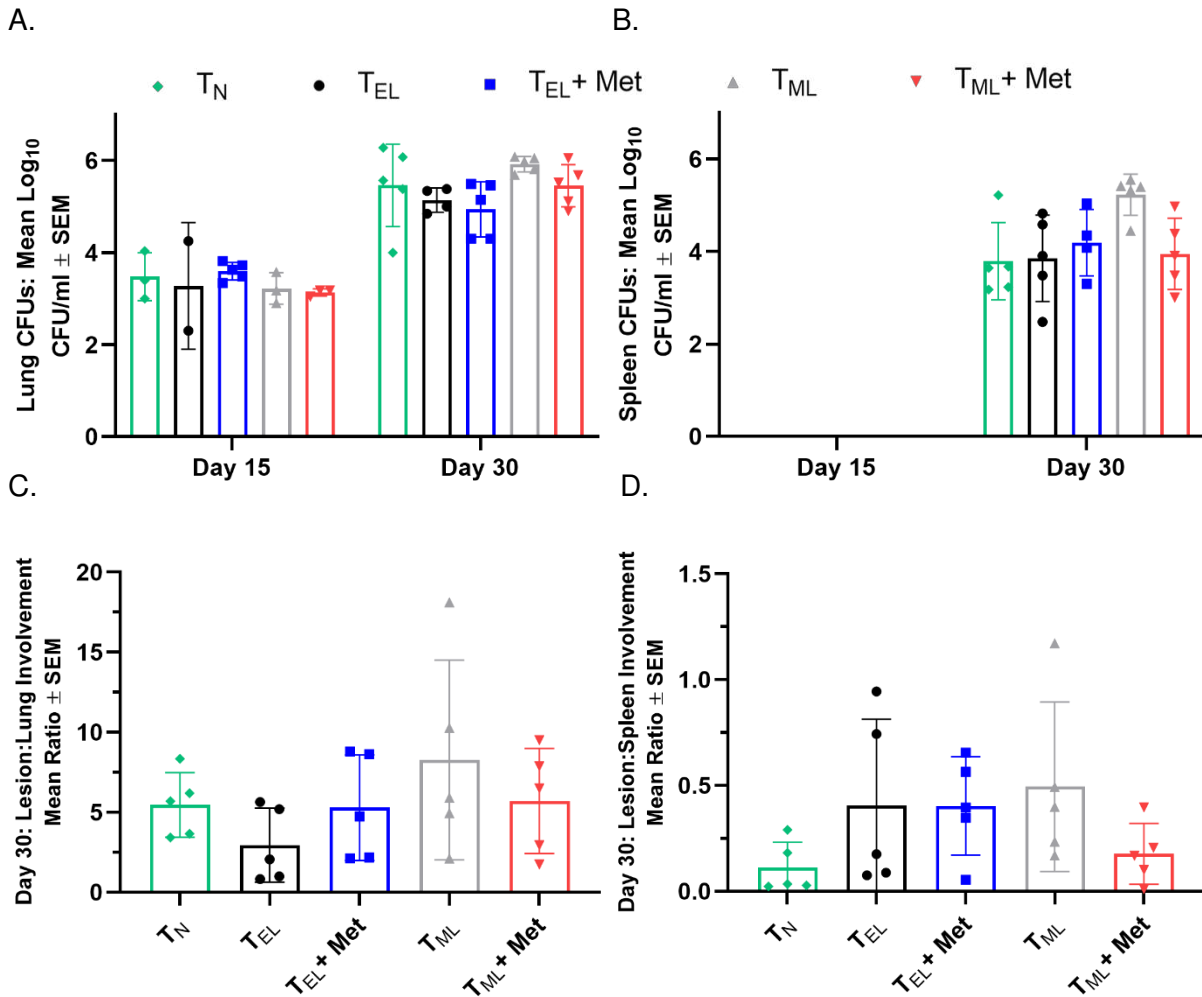
Figure 4.4. Bacterial and lesion burden at days 15 and 30 post Mtb challenge of ACT mice. Lung and spleen tissues were collected from ACT Mtb challenged mice on days 15 and 30 post-infection. (A-B) Mtb CFU quantification recovered from (A) lungs and (B) spleens. Data represents mean $\log_{10}$ values (N=2-5). (C-D) The ratio of lesion to normal tissue was quantified by histological analysis in the (C) lungs and (D) spleens of Mtb infected animals. Data represent mean values (N=5).

Lung homing capacity of adoptively transferred T cells

The migration of adoptively transferred T cells from the vasculature into the lungs of Mtb infected mice was evaluated using an intravenous staining technique. On days 15 and 30 post-infection, circulating CD4$^+$ T cells were labeled with CD4-APC Fire 750 by tail vein antibody injection prior to euthanasia. Intravascular staining efficacy was verified by subsequent blood collection and *ex vivo* co-staining with CD4-Alexa Flour 532. Positive expression of both i.v. and

ex vivo CD4 antibodies on >95% of all CD4 T cells was used to discriminate effective from ineffective i.v. staining (Figure 4.5A-B).
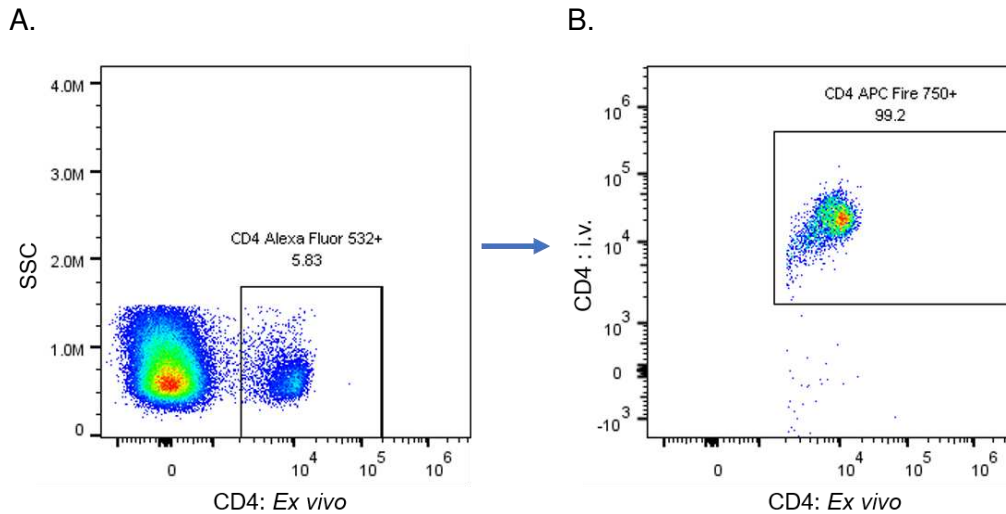
A.

B.

Figure 4.5. Intravascular staining efficacy. Blood was collected at necropsy to evaluate i.v. staining efficacy of CD4$^+$ T cells. (A) Total *ex vivo* stained CD4$^+$ T cells. (B) Percent CD4$^+$ T cells positively labeled by both *ex vivo* and i.v. staining.

Lung parenchyma versus blood homing of adoptively transferred CD4$^+$ T cells was evaluated in Mtb infected mice on days 15 and 30 following infection. Following i.v. staining and euthanasia, single cell suspensions from the lung were prepared and stained *ex vivo* with CD4-Alexa fluor 532 antibody and anti-CD45.1, the congenic marker used to differentiate between host derived (CD45.2$^+$) and adoptively transferred (CD45.1$^+$) CD4$^+$ T cells. Flow cytometry analysis was used to identify marker expression, whereby CD45.1 gated cells that positively expressed both i.v. administered CD4-APC Fire 750 and *ex vivo* CD4-Alexa fluor 532 were considered blood-homing, or i.v.$^+$, while those that only expressed *ex vivo* CD4-Alexa fluor 532, i.v.$^-$, were identified as lung parenchymal homing T cells. At both timepoints, small numbers of CD45.1$^+$CD4$^+$ T cells were positively identified in both the lungs and blood of Mtb infected mice. On day 15, the mean total numbers of lung homing cells ranged from 10.8±2.43 SD (T$_N$) to 929.88±90.56 SD (T$_{EL}$) and the number of blood residing cells ranged from 18.09±12.89 SD (T$_N$) to 106.57±78.27 SD (T$_{N+}$

Met) (Figure 4.6A). Significantly greater numbers of both T_{EL} and $T_{EL}+$ Met cells were found to home in the lungs of infected mice compared to T_N cells at this timepoint (p=0.190 and p=0.388; Figure 4.6A). On day 30, 123.92±109.441 SD ($T_{EL}+$ Met) to 2,315±768.69 SD (T_N) mean total cells were recovered from the lungs and 11.58±11.05 SD ($T_{EL}+$ Met) to 446.67±515.07 SD (T_N) from the blood of infected mice (Figure 4.6B). Contrary to day 15, significantly greater T_N compared to T_{EL} cells were recovered from the lungs of mice at this timepoint, which also corresponded to a greater recovery of blood homing T_N compared to T_{EL} cells (Figure 6B). Regardless of cell numbers, the ratio of lung (i.v.$^-$) to blood (i.v.$^+$) cells was calculated to assess the overall homing preference of each cell type. With the exception of T_N and $T_{EL}+$ Met, all cells displayed preference for lung homing on day 15 and by day 30, all cell types preferentially homed to the lung compared to the blood. Moreover, differential homing preference was observed between groups, where increased levels of differentiation positively impacted early lung homing capacity (Figure 4.6C).
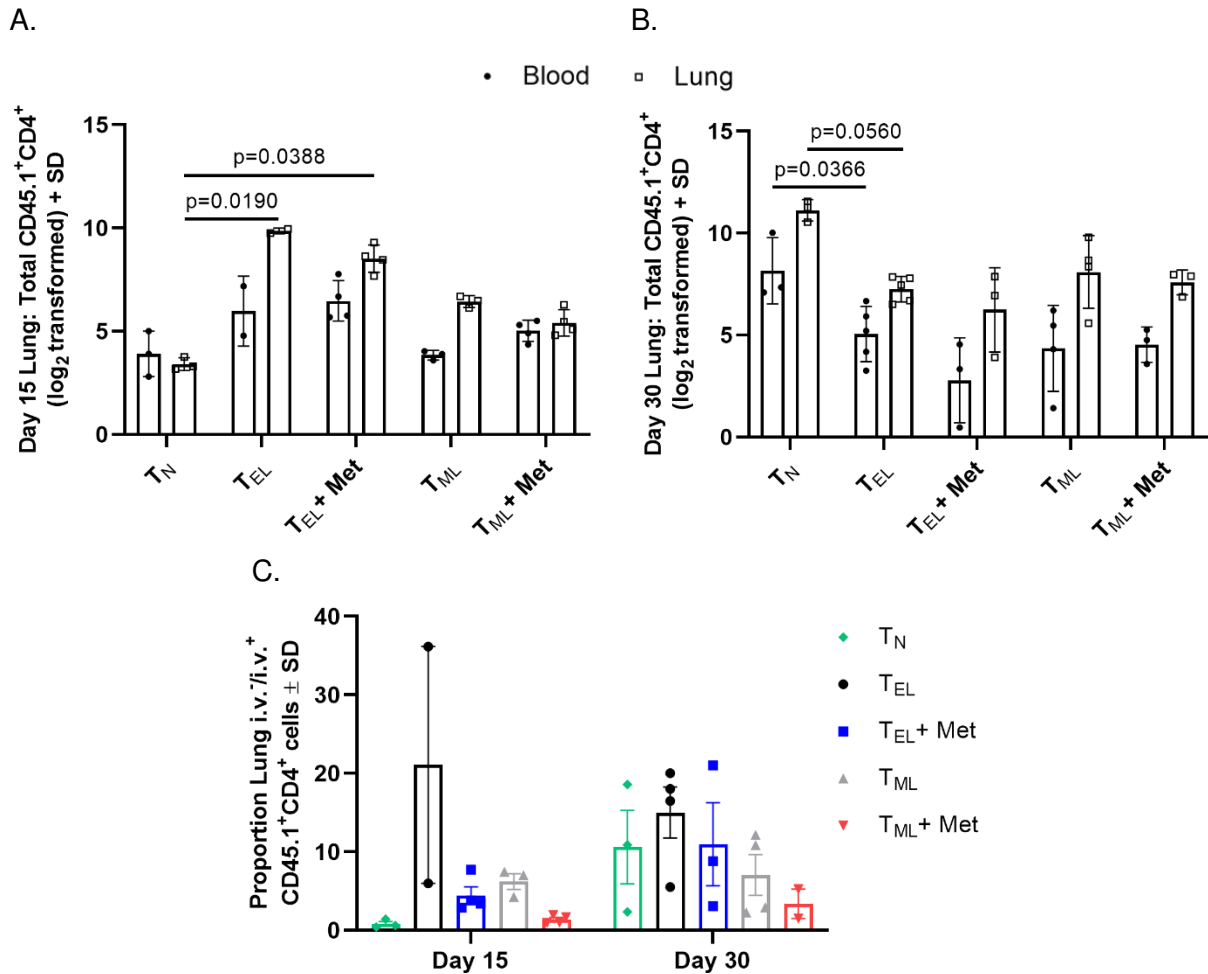
Figure 4.6. Differential homing of adoptively transferred T cells in response to Mtb infection. The total numbers of lung (i.v.$^-$) and blood (i.v.$^+$) homing adoptively transferred T cells was quantified using an i.v. staining technique. Data represents the total CD45$^+$CD4$^+$ T cells recovered from the right cranial and middle lung lobes at (A) 15 and (B) 30 days following Mtb infection. (C) Proportion of lung parenchyma- (i.v.$^-$) to vasculature-residing (i.v.$^+$) CD45.1$^+$CD4$^+$ T cells at 15- and 30-days post-infection. Data represents mean values (N=2-5).

In vivo adoptive transfer T cell marker characterization

To determine whether the Mtb-specific response by adoptively transferred T cells corresponds to the adoption of unique phenotypes *in vivo*, we evaluated the expression of markers commonly associated with known functional properties, including CD44, CD62L, CD25, KLRG-1, CD127, CXCR3, and PD-1 on CD45.1$^+$CD4$^+$ T cells. By manual gating analysis, we evaluated the % positive cells and MFI values of positive expressing markers and found that

among all markers, CD127 was the only one that displayed differential expression among groups. Approximately 30% more T_{EL}s and 28% more T_{EL}s+ metformin expressed CD127 in comparison to less differentiated subsets, T_N and T_{ML}, 30 days following Mtb infection (p=0.0133, p=0.0169; Figure 4.7A). Interestingly, T_{ML}+ metformin did not follow the same trend as T_N and T_{ML} cells, but rather showed a 10% increase in the percent of CD127 expressing CD45.1$^+$CD4$^+$ T cells in comparison to T_Ns and T_{ML}s (Figure 4.7A). Furthermore, by evaluating MFIs, we show that CD127 levels follow the same trends as percent measurements, indicating that not only is there an increase in the proportion of cells that express CD127, but also an increase on the level of CD127 expression on a per cell basis (Figure 4.7B).
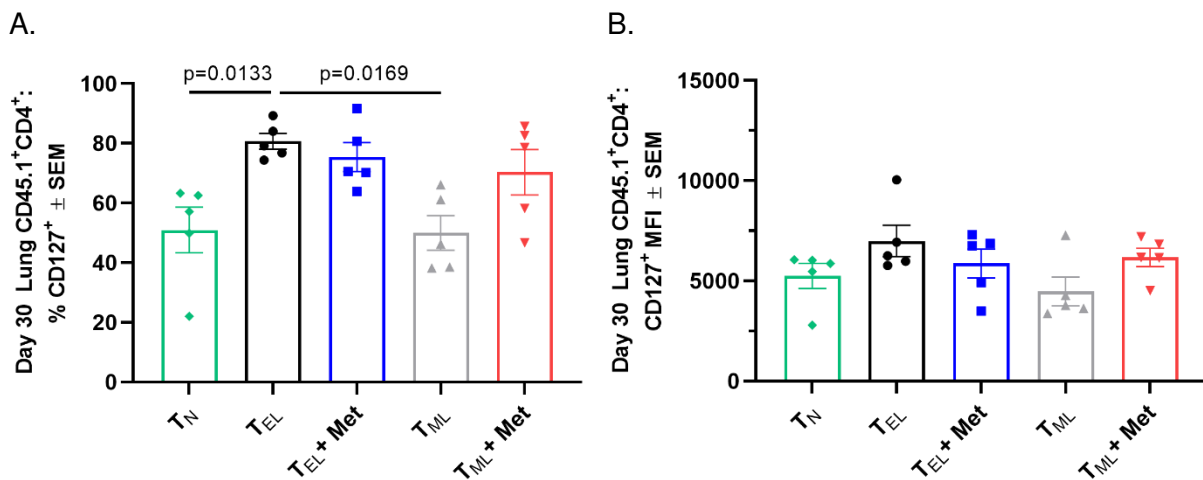

Figure 4.7. Differential CD127 expression on CD4$^+$ adoptively transferred T cells. 30 days following Mtb infection T cell surface marker expression of CD127 was analyzed by flow cytometry. (A) The percent CD45.1$^+$CD4$^+$ CD127 expressing cells was quantified among groups by manual gating analysis. (B) MFIs were quantified using median fluorescence of CD127 on CD127$^+$ cells. (A) Significance was determined using an ordinary one-way ANOVA (N=5).

FlowSOM analysis was explored as an unbiased gating technique to discover novel T cell populations among adoptively transferred T cells. Adequate samples sizes were obtained by combining, or concatenating, live CD45.1$^+$CD4$^+$ single cells from individual animals into one sample and running a consistent analysis on each respective group. Seven unique populations

were generated by FlowSOM by assigning cells into groups based on similar surface marker expression. The percent of cells within each population was calculated and visualization by heatmap representation demonstrates differential abundance of FlowSOM populations between groups (Figure 4.8A-B).
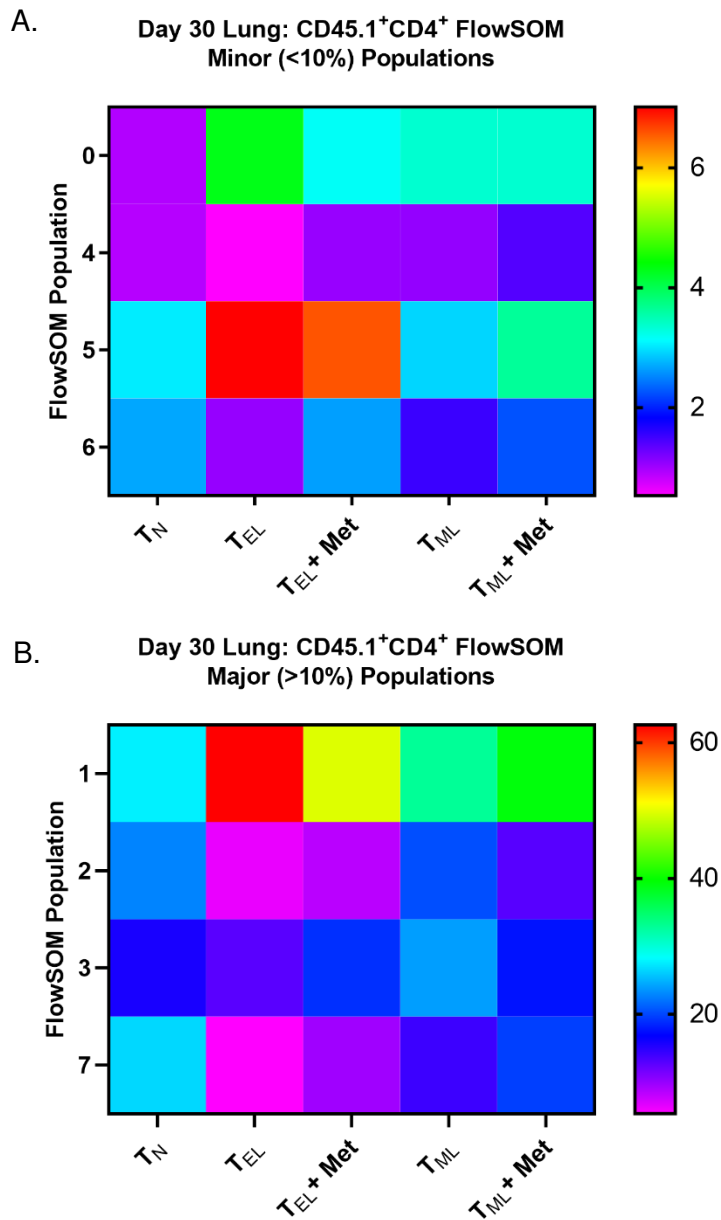

Figure 4.8. Differential abundance of FlowSOM-derived adoptively transferred T cell populations. Live CD45.1+CD4+ T cells from the lungs of Mtb infected mice 30 days following Mtb infection were analyzed by FlowSOM analysis. Seven populations were generated based on the expression of CD44, CD62L, CD25, KLRG-1, CD127, CXCR3, and PD-1. Heatmaps represent the differential abundance of (A) minor (<10%) and (B) major T cell populations (>10%).

Surface marker expression of FlowSOM identified T cell populations were defined by manual gating analysis (Table 4.1). Manual gating was also used to confirm the relative abundance of each population in comparison to FlowSOM generated values (Figure 4.9A-H). Slight variations in the percentage of cells attributable to each population exist, however, trends in population distribution among groups using either FlowSOM or manual gating remain the same. Collectively, population 1 comprised the largest percentages of cells from each treatment group, with equal to or greater than 50% of those from T_{EL} and $T_{EL}+$ metformin groups (Figure 4.8B and 4.9B). In comparison, only 27.6% of T_N cells belonged to population 1, while most of these cells were more evenly spread amongst populations 1, 2, 3, and 7 (Figure 4.8B and 4.9B). The most notable differences among adoptively transferred cell populations were observed in populations 5 and 1, both of which represent effector T cell phenotypes (Figure 4.8A-B and 4.9B & F).

Table 4.1. Surface marker identification of FlowSOM derived T cell populations.

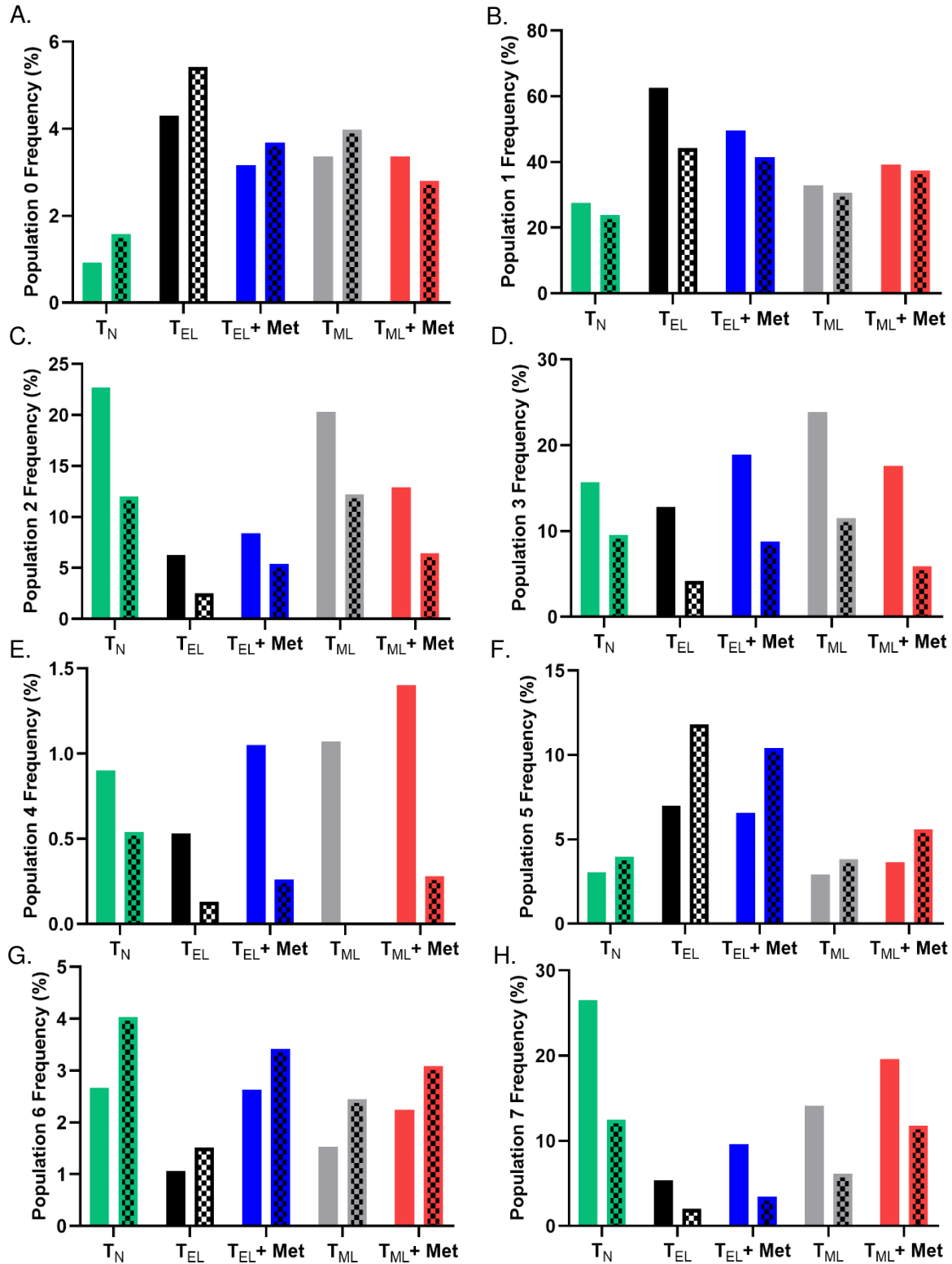| Population	Marker Expression
0	PD-1$^-$ KLRG-1$^-$ CD62L$^+$ CD44$^+$ CD127$^+$ CXCR3$^+$ CD25$^+$
1	KLRG-1$^-$ CD62L$^-$ CD44$^+$ CD127$^+$ CXCR3$^+$ CD25$^+$
2	PD-1$^-$ KLRG-1$^+$ CD62L$^-$ CD44$^+$ CXCR3$^+$ CD25$^+$
3	PD-1$^-$ KLRG-1$^-$ CD62L$^-$ CD44$^+$ CD127$^-$ CXCR3$^+$ CD25$^+$
4	PD-1$^+$ KLRG-1$^+$ CD62L$^-$ CD44$^+$ CD127$^-$ CXCR3$^-$ CD25$^-$
5	KLRG-1$^-$ CD62L$^-$ CD44$^+$ CD127$^+$ CD25$^-$
6	KLRG-1$^-$ CD62L$^-$ CD44$^+$ CD127$^-$ CD25$^-$
7	PD-1$^+$ KLRG-1$^-$ CD62L$^-$ CD44$^+$ CD127$^-$ CXCR3$^+$ CD25$^+$

Figure 4.9. FlowSOM versus manual gating of adoptively transferred T cell populations. (A-H)
Phenotypic characterization of ACT populations in the lung 30 days following Mtb infection. Graphs
represent the % cells in each population identified by either FlowSOM (solid) or manual gating
(checkered). Data represents analysis of one concatenated sample per group of N=5.

Discussion

The aim of this study was to determine whether metformin treated *in vitro* differentiated CD4+ T cells elicit superior protection against Mtb infection in comparison to untreated cells, *in vivo*. Earlier studies performed by our lab showed that metformin treatment alone, when administered prior to or concurrent with Mtb infection, reduced TB disease severity of Mtb infected guinea pigs. These results were associated with differences in T cell metabolic phenotypes between metformin treated and untreated animals, suggesting metformin's targeted effect on T cell metabolism, and potentially, T cell phenotype and function. *In vitro* analysis demonstrated that when differentiated in the presence of metformin, CD4+ T cells exhibited reduced properties of terminal differentiation compared to untreated cells. These non-terminally differentiated T cells displayed unique metabolic characteristics, which corresponded to improved survival and enhanced proliferation and IL-2 production in response to secondary antigen challenge.

To determine whether metformin treated *in vitro* differentiated CD4+ T cells also display enhanced function and protective properties against Mtb challenge *in vivo*, we adoptively transferred pre-differentiated Mtb Ag85b TCR transgenic p25 T cells into recipient mice. Mice were then subjected to Mtb aerosol infection and disease burden was assessed at acute timepoints following infection. In addition, properties of less differentiated T cells that typically correspond to increased protection against Mtb infection, including lung homing and surface marker expression were evaluated.

Prior to adoptive transfer, *in vitro* differentiated CD4+ T cells were confirmed to resemble cell phenotypes produced in chapter 3. Effector like CD4+ T cells (T_{EL}) were classified as CD62L⁻CCR7⁻CD44+ and T_{ML}s, CD62L+CCR7+CD44+. Consistent with previous findings, metformin resulted in reduced mitochondrial membrane potential and CD25 expression and increased expression of the migratory and tissue retention markers, CD44 and CD69, on T_{EL} cells. Because metformin treatment also corresponded to enhanced proliferation by T_{ML} cells following antigen

re-challenge, both untreated and metformin treated T_{ML} cells were also assessed in this study. Like T_{EL}s, CD25 and mitochondrial membrane potential were both decreased by metformin treatment of T_{ML} cells. In contrast, however, CD69 was dramatically decreased rather than increased and expression of CCR7 and CD62L were increased on T_{ML} cells. Though further studies are needed to confirm the reproducibility of this phenotype, these data suggest that metformin also modulates T_{ML} differentiation, which appear to further resemble decreased activation and differentiation phenotypes.

Also prior to adoptive transfer, T cell purity and the proportion of CD4+ versus CD8+ T cells present in each sample was evaluated following negative selection of live CD3+ cells. Viability ≥85% was confirmed for all samples and CD3 purity was confirmed to be >97%. Among these cells, most T lymphocytes were CD4+ (>70%) and only a small fraction (<11%) were CD8+; this was not significantly different between groups. These results were somewhat surprising since CD8+ T cells, in general, have a great propensity for survival and proliferation compared to their CD4+ counterparts [13]. One explanation for this is due to the expression of the Ag85b transgenic TCR on CD4+ T cells, which like other TCR transgenic T cells, may confer a lower threshold for cellular expansion and survival signals. Nonetheless, these data support the fact that *in vivo* effects observed in this study are predominantly mediated by CD4+ T cell populations, which remain similar between groups.

On 30 days following infection with the H37Rv strain of Mtb, we show that adoptive transfer of any one pre-differentiated CD4+ T cell phenotype did not significantly enhance protection against TB disease— measured by lung and spleen bacterial and lesion burden. These results were surprising considering that previous studies have demonstrated that *in vitro* differentiated, Mtb antigen specific Th1 CD4+ effector T cells decrease Mtb bacterial load in the lungs by approximately one log [14, 15]. Various explanations may explain these results. First, although our studies and others' both utilize Mtb-antigen specific engineered T cells, our studies were the first

to use Ag85b TCR Tg T cells. Due to TCR specificity, differential antigen availability over the course of infection and variable responses to each different antigen may explain these differences [16, 17]. In addition, different methodologies used between experiments to derive Th1 polarized CD4 T cells likely generates T cells with varying degrees of "effectorness", which can ultimately impact cellular survival, recruitment, and response to antigen challenge [18].

Other reasons that adoptively transferred T cells may have failed to reduce CFUs and lesion burden are due to the low numbers of transferred cells, cell survival, the timing of infection relative to cell transfer, and the relatively short infection period. Though studies demonstrate that 1×10^6 T cells are sufficient to reduce lung CFUs, greater reductions in bacterial burden are achieved with higher cell numbers [6, 14]. In addition, competition for survival niches and nutrients between transferred cells and host-derived populations may decrease their capacity to survive and expand over extended periods of time [6, 19]. Lymphopenic hosts may be used in future experiments to facilitate the homing and survival of adoptively transferred cells. Furthermore, acute timepoints were evaluated in these studies to increase the likelihood of recovering transferred cells. This short time period, however, may not be adequate to observe disease reductions that occur as a consequence of resolution rather than immediate protection. Moreover, the timing of cell transfer relative to infection may not have yielded the appropriate response to assess the direct impact of T cell differentiation on protective efficacy. Recent literature suggests that while highly differentiated effector T cells produce higher levels of cytokines and respond well to early infection, they proliferate poorly, quickly die following antigen encounter, or become anergic and lose their ability to respond to infection [3, 11, 20, 21]. Alternatively, less differentiated phenotypes, such as memory T cells, provide long term protection by continuously cycling through a pool of cells that migrate to the site of infection, proliferate, and produce cytokines [10, 21, 22, 23, 24]. Reduced T cell differentiation by metformin leads us to believe that rather than providing an immediate and robust response, these cells may generate a pool of cells with high plasticity that

provide sustained response during chronic infection. This hypothesis is supported by our guinea pig data given that decreased disease burden was not observed until chronic stages of infection. Future studies will take this into account by transferring cells following the onset of infection rather than prior to it as well as assessing local lymphoid organs for the storage and maintenance of such populations.

In addition to resistance against TB disease, we measured the differential homing capacity of *in vitro* differentiated T cell subsets, treated with or without metformin, within the vasculature versus lung parenchyma on days 15 and 30 following Mtb infection. Previous studies show that the level of T cell differentiation is associated with their homing and migratory capacity, which in turn, corresponds to their protective efficacy against infection [7, 8]. Highly differentiated CD4$^+$ T cells, including those that express the terminal differentiation marker KLRG1, are more commonly found in the vasculature compared to non-terminally differentiated subsets and correspond to decreased protection against disease following adoptive transfer [6]. Characterization of metformin exposed T_{EL} and T_{ML} subsets found lower expression of the terminal differentiation markers KLRG1 and Blimp-1 and increased levels of the cell adhesion and migration marker, CD44, and the tissue retention molecule, CD69, in comparison to T_{EL} cells. Based on these data we hypothesized that metformin treated T_{EL} and T_{ML} cells would preferentially home to the lung parenchyma while terminally differentiated T_{EL} would reside in the vasculature. Surprisingly, no significant differences in the proportion of lung tissue versus vasculature homing T cells were found among cellular phenotypes at neither 15 nor 30 days following infection. Although not significant, the greatest proportion of lung to vasculature homing cells were recovered from animals that received T_{EL} cells, which contrasts with our hypothesis. It is unknown why this occurred but may be due to the preferential homing of less differentiated T cells to other organs, such as the spleen or lymph nodes. This would make sense given the sustained expression of

lymphoid homing receptors CCR7 and CD62L on T_{ML} cells but requires further investigation to draw definitive conclusions.

Surface marker expression of adoptively transferred T cells was evaluated on CD4^{+} cells isolated from the lungs of Mtb infected mice on day 30 post infection. Markers were specifically chosen based on their relationship to longevity, migration, and differentiation status and included PD-1, KLRG-1, CD62L, CD44, CD127, CXCR3, and CD25 [6, 25, 26, 27]. Interestingly, although surface marker expression was highly variable among phenotypes prior to their transfer, only subtle differences in marker expression were observed following infection. Metformin treatment did not significantly alter the expression of any one marker between either T_{EL} or T_{ML} treated and untreated cells. The percent cells that positively expressed the IL-7 receptor CD127, most commonly expressed on naïve and memory T cell subsets and which promotes cell survival, was significantly increased on T_{EL} subsets, with or without metformin, in comparison to T_{ML} and T_N cells [28, 29]. It is important to note that while T_{EL} cells do in fact have increased expression of terminal differentiation features, the population as a whole is heterogenous and is likely comprised of both short-lived effectors, previously described as KLRG-1^{hi}CD127^{lo}, and long-lived effectors, KLRG-1^{lo}CD127^{hi} [19]. Therefore, selective survival and expansion of the latter may account for increased CD127 expression within T_{EL} populations.

To expand our phenotypic analysis, we also applied an unbiased clustering algorithm, FlowSOM, to all samples [30]. Eight unique populations were identified based on their similar expression of surface markers, which comprised anywhere from <1% to >60% of all CD4^{+} T cells. Most notably, FlowSOM identified populations are more evenly distributed among less differentiated phenotypes while T_{EL} cells preferentially clustered into one population of KLRG-1^{-} CD62L^{-} CD44^{+} CD127^{+} CD25^{-} expressing cells—accounting for greater than 50% of all CD4^{+} T cells. Without observed differences in the response to infection it is difficult to decipher the relevance of differential surface marker expression between populations. The adoption of similar

profiles in response to Mtb infection *in vivo*, however, may help explain the lack of variable protection among cell phenotypes.

Finally, it is difficult to make definitive conclusions from these data without reproducing this experiment; however, our data suggest that reduced levels of $CD4^+$ T cell differentiation by metformin do not enhance protection against early Mtb infection and acute TB disease. Our thorough assessment of the potential pitfalls of this experiment will aide in the design of future experiments to more accurately assess the impact that these cells have on chronic Mtb infection. Importantly, regardless of the outcome, these results contribute to our current understanding of the immune response against Mtb and bring to light the importance of the kinetics of TB disease regarding vaccine and treatment design.

REFERENCES

1.   Pearce, E.L. *et al.* Enhancing CD8 T Cell Memory by Modulating Fatty Acid Metabolism. *Nature* **460**, 103-107 (2009).

2.   Crotty, S., Johnston, R.J. & Schoenberger, S.P. Effectors and memories: Bcl-6 and Blimp-1 in T and B lymphocyte differentiation. *Nat Immunol* **11**, 114-120 (2010).

3.   Rutishauser, R.L. *et al.* Transcriptional repressor Blimp-1 promotes CD8(+) T cell terminal differentiation and represses the acquisition of central memory T cell properties. *Immunity* **31**, 296-308 (2009).

4.   van der Windt, G.J. *et al.* CD8 memory T cells have a bioenergetic advantage that underlies their rapid recall ability. *Proc Natl Acad Sci U S A* **110**, 14336-14341 (2013).

5.   van der Windt, G.J. *et al.* Mitochondrial respiratory capacity is a critical regulator of CD8+ T cell memory development. *Immunity* **36**, 68-78 (2012).

6.   Sallin, M.A. *et al.* Th1 Differentiation Drives the Accumulation of Intravascular, Non-protective CD4 T Cells during Tuberculosis. *Cell Rep* **18**, 3091-3104 (2017).

7.   Sakai, S. *et al.* Control of Mycobacterium tuberculosis infection by a subset of lung parenchyma homing CD4 T cells. *J Immunol* **192**, 2965-2969 (2014).

8.   Cyktor, J.C. *et al.* Killer cell lectin-like receptor G1 deficiency significantly enhances survival after Mycobacterium tuberculosis infection. *Infect Immun* **81**, 1090-1099 (2013).

9.   Gattinoni, L. *et al.* Acquisition of full effector function in vitro paradoxically impairs the in vivo antitumor efficacy of adoptively transferred CD8+ T cells. *J Clin Invest* **115**, 1616-1626 (2005).

10.   Lyadova, I. & Nikitina, I. Cell Differentiation Degree as a Factor Determining the Role for Different T-Helper Populations in Tuberculosis Protection. *Front Immunol* **10**, 972 (2019).

11.   Nikitina, I.Y. *et al.* Mtb-specific CD27low CD4 T cells as markers of lung tissue destruction during pulmonary tuberculosis in humans. *PLoS One* **7**, e43733 (2012).

12.   Anderson, K.G. *et al.* Intravascular staining for discrimination of vascular and tissue leukocytes. *Nat Protoc* **9**, 209-222 (2014).

13. Ferreira, C., Barthlott, T., Garcia, S., Zamoyska, R. & Stockinger, B. Differential Survival of Naive CD4 and CD8 T Cells. *J Immunol* **165**, 3689-3694 (2000).

14. Wangoo, A. *et al.* Contribution of Th1 and Th2 cells to protection and pathology in experimental models of granulomatous lung disease. *J Immunol* **166**, 3432-3439 (2001).

15. Gallegos, A.M., Pamer, E.G. & Glickman, M.S. Delayed protection by ESAT-6–specific effector CD4+ T cells after airborne M. tuberculosis infection. *J Exp Med* **205**, 2359-2368 (2008).

16. Moguche, A.O. *et al.* Antigen Availability Shapes T Cell Differentiation and Function during Tuberculosis. *Cell Host Microbe* **21**, 695-706.e695 (2017).

17. Miskov-Zivanov, N., Turner, M.S., Kane, L.P., Morel, P.A. & Faeder, J.R. The duration of T cell stimulation is a critical determinant of cell fate and plasticity. *Sci Signal* **6**, ra97 (2013).

18. Cano-Gamez, E. *et al.* Single-cell transcriptomics identifies an effectorness gradient shaping the response of CD4+ T cells to cytokines. *Nat Commun* **11**, 1801 (2020).

19. Kurtulus, S., Tripathi, P. & Hildeman, D.A. Protecting and rescuing the effectors: roles of differentiation and survival in the control of memory T cell development. *Front Immunol* **3** (2012).

20. Sande, O.J. *et al.* Mannose-Capped Lipoarabinomannan from Mycobacterium tuberculosis Induces CD4+ T Cell Anergy via GRAIL. *J Immunol* **196**, 691-702 (2016).

21. Reiley, W.W. *et al.* Distinct functions of antigen-specific CD4 T cells during murine Mycobacterium tuberculosis infection. *Proc Natl Acad Sci U S A* **107**, 19408-19413 (2010).

22. Gattinoni, L. *et al.* A human memory T cell subset with stem cell-like properties. *Nat Med* **17**, 1290-1297 (2011).

23. Lugli, E. *et al.* Superior T memory stem cell persistence supports long-lived T cell memory. *J Clin Invest* **123**, 594-599 (2013).

24. Moguche, A.O. *et al.* ICOS and Bcl6-dependent pathways maintain a CD4 T cell population with memory-like properties during tuberculosis. *J Exp Med* **212**, 715-728 (2015).

25.   Bull, N.C. *et al.* Enhanced protection conferred by mucosal BCG vaccination associates with presence of antigen-specific lung tissue-resident PD-1(+) KLRG1(-) CD4(+) T cells. *Mucosal Immunol* **12**, 555-564 (2018).

26.   Tezera, L.B. *et al.* Anti-PD-1 immunotherapy leads to tuberculosis reactivation via dysregulation of TNF-alpha. *Elife* **9** (2020).

27.   Mpande, C.A.M. *et al.* Functional, Antigen-Specific Stem Cell Memory (TSCM) CD4(+) T Cells Are Induced by Human Mycobacterium tuberculosis Infection. *Front Immunol* **9**, 324 (2018).

28.   Rathmell, J.C., Farkash, E.A., Gao, W. & Thompson, C.B. IL-7 Enhances the Survival and Maintains the Size of Naive T Cells. *J Immunol* **167**, 6869-6876 (2001).

29.   Kaech, S.M. *et al.* Selective expression of the interleukin 7 receptor identifies effector CD8 T cells that give rise to long-lived memory cells. *Nat Immunol* **4**, 1191-1198 (2003).

30.   S, V.G. *et al.* FlowSOM: Using self-organizing maps for visualization and interpretation of cytometry data. *Cytometry. Part A : the journal of the International Society for Analytical Cytology* **87** (2015).

CONCLUSIONS

The goals of these studies were to 1. evaluate whether treatment with the anti-diabetic drug metformin improves the clinical outcome of tuberculosis (TB) disease and 2. determine the mechanisms by which metformin modulates the host response to disease. The outcomes of these studies were intended to increase our understanding of the pathogenesis of TB as well as identify novel markers that are predictive of host resistance against disease. The use of a metformin allowed us to evaluate the impact of both systemic and cellular metabolism on TB pathogenesis, and importantly, was used as a tool to better understand how immunomodulation through metabolic targeting could lead to a more desirable immune response against *Mycobacterium tuberculosis* (Mtb).

Metformin enhances host-mediated protection against Mtb infection.

The first aim of this study was to evaluate whether metformin treatment of Mtb infected guinea pigs could improve clinical TB disease outcome. We conclude that, when initiated prior to or concurrent with Mtb infection, metformin does indeed improve TB disease severity during the chronic stages of infection. This was demonstrated by a significant reduction in lung CFUs and percent lesion burden in metformin treated compared to untreated animals. Of note, improved disease outcome in the lungs did not translate to increased survival of metformin treated animals. Assessment of disease in secondary organs, including the spleen and liver, showed that despite decreased disease in the lungs, CFUs and lesion burden were unchanged between treated and untreated animals, which may explain the lack of improved survival by metformin.

The outcome from this aim suggests that while metformin may not be a practical therapeutic for the treatment of TB, it is a useful tool for studying host-derived protective responses against disease. In addition, metformin treatment may have added therapeutic value when combined with other host-directed therapies or antimicrobials.

In vivo systemic and cellular metabolism are altered in response to Mtb infection and metformin treatment.

In aim 1, we hypothesized that reduced TB disease by metformin treatment would be due to the maintenance of hemostatic blood glucose concentrations through normalization of insulin sensitivity and glucose tolerance, both of which are altered over the course of Mtb infection. Consistent with previous results, we found that guinea pigs in our study developed insulin resistance and glucose intolerance in response to Mtb infection. Treatment of Mtb infected animals with metformin resulted in restoration of insulin sensitivity compared to uninfected animals, yet despite these results, it was unable to restore homeostatic glucose tolerance. From these results we concluded that the protective effects of metformin were not due to the maintenance of systemic metabolism, but rather due to other host-directed mechanisms.

Because metformin is also known to directly target cellular metabolism, we hypothesized that by modulating immune cell metabolism, metformin could influence immune response to Mtb infection that result in a more favorable disease outcome. Immunometabolism, or the link between cell metabolism and function, has recently emerged as a novel area of research to help explain the implications of disease on immune function as well as identify unique targets for the development of immune-mediated therapeutics. Evaluating immune cell metabolism was therefore, not only logical approach to identify the underlying mechanisms of metformin's protection against TB, but also a widely unexplored area in TB research that could be used to aide in our current understanding of the immune response to disease.

In our studies, we found that infection with Mtb alone increases PBMC metabolic rates, which correspond to heightened levels of inflammation over the course of disease and ultimately, disease progression. Treatment with metformin, however, maintained metabolic homeostasis that was associated with reduced lesion burden and CFUs during chronic infection. Additionally, significantly reduced levels of pro-inflammatory cytokines were measured in the lungs of

metformin treated compared to untreated Mtb infected animals, further supporting reduced inflammation by metformin. We concluded that metformin elicits host-mediated protection against Mtb by directly modulating immune cell metabolism resulting in decreased inflammation.

From this study it was not clear exactly what cell type was responsible for this increased protection, however, evidence of altered T cell metabolism highly suggested that T cells are likely responsible for these results. Furthermore, it is not well understood whether normalized metabolism of T cell derived PBMCs is a result of disease resolution from some other mechanism or if altered T cell function is directly responsible for the observed disease reduction. In support of the latter, data from our study show that T cell metabolism, specifically mitochondrial membrane potential, was significantly impacted by metformin treatment prior to chronic infection, which suggests the direct effect of metformin on cellular metabolism prior to disease resolution.

Metformin prevents premature CD4$^+$ T cell terminal differentiation.

The results from the first aim of this dissertation led us to hypothesize that metabolic targeting of T cells by metformin promotes the formation of memory T cells. Using an *in vitro* model of T cell differentiation, we showed that while metformin does not result in the increased generation of CD4$^+$ memory T cells, it does dramatically modulate the expression of surface markers associated with activation, migration, and tissue homing. Furthermore, metformin significantly reduced expression of the terminal differentiation marker KLRG1 and transcription factor Blimp-1. Like the results observed in our *in vivo* studies in aim 1, we found that T cells differentiated in the presence of metformin *in vitro* had significantly lower mitochondrial membrane potential and produced significantly less pro-inflammatory cytokines in comparison to untreated T cells. Furthermore, antigen re-stimulation of CD4$^+$ T cells differentiated in the presence of metformin resulted in more robust cell proliferation, increased survival, and increased IL-2 production.

The overall conclusion from this portion of the dissertation is that metformin impacts T cell function by preventing terminal differentiation of effector T cells. Consequently, the reduced level

185

of differentiation yields antigen-specific T cells that have enhanced survival and recall to secondary antigen challenge. Based off these findings, we hypothesize that metformin also prevents T cell terminal differentiation of T cells responding to Mtb infection, resulting in a pool of antigen-specific T cells that maintain plasticity, have increased survival and proliferative potential, and effectively migrate to the site of infection throughout the course of disease. While aim 3 was performed to address whether T cells that were exposed to metformin during differentiation do in fact have these properties and provide increased protection against TB disease, limited conclusions can be drawn from this study. As previously discussed, nutrient competition by other T cells of an immunocompetent host, the timing of transfer relative to infection, and the duration of infection may all impact the outcome of adoptive transfer experiments.

Future studies will need to evaluate whether *in vivo* treatment with metformin yields similar alterations to T cell development and function in response to Mtb infection. Furthermore, future studies will address concerns about the study design for aim 3 and thereby, provide more conclusive evidence as to whether T cell immune phenotypes elicited by metformin improve T cell mediated protection against Mtb infection.

Metformin modulates T cell metabolism.

Finally, one of the last goals of this dissertation was to evaluate the mechanisms by which metformin modulates T cell metabolism to identify and describe metabolic properties of T cell function and phenotype. Major findings from this portion of ours studies show that metformin preserves mitochondrial function by increasing glycolysis to maintain energy demands and induces properties of memory T cell metabolism including increased mitochondrial spare respiratory capacity and decreased mitochondrial membrane potential.

Increased glycolytic dependency was surprising in that T cells with less-differentiated phenotypes generally display upregulated reliance on oxidative rather than glycolytic metabolism. However, the reduction in mitochondrial membrane potential and corresponding decrease in the ratio of NAD to NADH provides strong evidence that metformin promotes glycolysis by inhibiting

the electron transport chain. Increased glucose uptake and fulfillment of cellular energy demands, as demonstrated by maintenance of ADP ATP ratios, further demonstrate that glycolysis is sufficient to maintain energy production for survival and maintenance of metformin treated cells. Therefore, we conclude that by increasing glycolysis through electron transport chain inhibition, glycolysis is utilized as the primary pathway for energy production by metformin treated T_{EL} cells.

In addition, metabolic characterization revealed that although metformin reduces mitochondrial metabolism, it increases mitochondrial spare respiratory capacity, a hallmark feature of memory T cells. While we did not find that metformin promoted the differentiation of memory T cells, these results describe a unique metabolic phenotype that may equip these cells to better respond to secondary challenge, which is observed in our recall experiments. Additionally, though our studies did not directly assess the cause of increased spare respiratory capacity by metformin, increased fatty acid uptake along with decreased capacity to perform fatty acid oxidization suggest that metformin may promote fatty acid storage, which has been previously demonstrated to be linked to SRC. Moreover, endogenous fatty acid synthesis and storage are shown to be upregulated among T cells that possess memory like characteristics, including long term survival and increased proliferative capacity. It is, therefore, possible that metformin "primes" T cell metabolism to enhance the recall response by diverting biosynthetic intermediates away from mitochondrial metabolism and into anabolic pathways in which intermediates are synthesized and stored for future cell growth and proliferation.

Concluding remarks.

Taken together, we describe a non-terminally differentiated CD4^{+} effector T cell phenotype with unique metabolic properties that are associated with enhanced survival and recall capacity in response to metformin treatment. While we were unable to determine whether these cells play a direct role in the enhanced response to chronic Mtb infection— that is observed *in vivo* by metformin— we have defined a novel cell subset that will aide in the understanding of pathogenesis and immune-mediated protection against multiple diseases that benefit from

metformin treatment. In the future, our goal is to translate these findings into immune protection against Mtb in order to describe biomarkers of protection and help guide the development of novel vaccines and immunotherapeutics.